DEVELOPMENT OF A HYBRID RECURRENT NEURAL NETWORK BASED INTELLIGENT DECISION SUPPORT SYSTEM WITH REVERSE MAPPING FOR CNC MACHINING

Thesis

Submitted in partial fulfilment of the requirements for the degree of

DOCTOR OF PHILOSOPHY

by

RASHMI LAXMIKANT MALGHAN

DEPARTMENT OF MECHANICAL ENGINEERING

NATIONAL INSTITUTE OF TECHNOLOGY KARNATAKA,

SURATHKAL, MANGALORE -575025

December, 2017

Dedicated to

My Parents, Brother, Husband, In-Laws and Gurus

DECLARATION

By the Ph. D. Research Scholar

I hereby declare that the Research Thesis entitled **"*DEVELOPMENT OF A HYBRID RECURRENT NEURAL NETWORK BASED INTELLIGENT DECISION SUPPORT SYSTEM WITH REVERSE MAPPING FOR CNC MACHINING*"** which is being submitted to **National Institute of Technology Karnataka, Surathkal** in partial fulfillment of the requirements of award of the degree **Doctor of Philosophy** in **Department of Mechanical Engineering** *is a bonafide report of the research work carried out by me.* The material contained in this Research Thesis has not been submitted to any University or Institution for the award of any degree.

Register Number : 123026ME12F07

Name of the Research Scholar : Rashmi L Malghan

Signature of the Research Scholar :

Department of Mechanical Engineering

Place: NITK- Surathkal
Date:

CERTIFICATE

This is to certify that the Research Thesis entitled "***DEVELOPMENT OF A HYBRID RECURRENT NEURAL NETWORK BASED INTELLIGENT DECISION SUPPORT SYSTEM WITH REVERSE MAPPING FOR CNC MACHINING***" submitted by **Mrs. Rashmi L Malghan (Reg. No. 123026ME12F07)** as the record of the research work carried out by her, is accepted as the Research Thesis submission in partial fulfillment of the requirements for the award of the degree of **Doctor of Philosophy.**

Prof. Shrikantha S. Rao
Research Guide
Date:

Prof. R J D'Souza
Research Guide
Date:

Chairman DRPC
Date:

ACKNOWLEDGEMENT

This thesis embodies the results of the last couple years' work whereby I have been accompanied and supported by many people. It is an honor and a very pleasant opportunity to be able to express my gratitude to all of them.

It has been indeed a great honor for me to work under the guidance of my advisors **Prof. Shrikantha S. Rao and Prof. R J D'Souza** Department of Mechanical Engineering, Department of Mathematics and Computational Science NITK Surathkal. With deep sense of gratitude and humility, I express my sincere thanks to them for their valuable guidance, untiring perseverance and unending patience which made the research not merely educational but also enjoyable. I also take this opportunity to thank the Director, NITK Surathkal and Head of Mechanical Engineering Department, NITK Surathkal for allowing me to carry out my doctoral studies.

I sincerely thank the Research Progress Assessment Committee consisting of **Dr.T. Laxminidhi** (Electronics and Communication Engineering Department), **Dr. Naveen Karanth P** (Mechanical Engineering Department), and Dr. Shrikantha Rao, Dr. R J D'Souza and **Dr. Mervin Herbert** for their valuable comments and constructive criticism which have helped the enrichment of this doctoral work. I owe my deepest gratitude to Dr. Akshay Nigalye, Dr.Arunkumar Shettigar for their valuable suggestions and constant support during my research work. I am indeed extremely indebted to all of them. I extend my sincere thanks to **Mr.karthik Rao M C** for kind help in carrying out experiments and providing me continuous motivation and support.

My sincere thanks to my co-research colleague Mr. Conel Rodrigues and Dr. Akshay Nigalye and **Dr.Arunkumar** for rendering their advice in coding for the ANN and RNN models. I am immensely indebted to the unending help and support I received from my co-research colleagues Mr. Karthik Rao, Ms. Roopa Swamy, Ms. Charitha Rao, Mr. Subramanya, Mr. Shrivathsa T V, Mr. Venkatesh G, Mr.Shivaya, Dr. Vignesh, Dr. Manjunatha, Dr. Manjaihia, Dr. Murali , Dr. Nagraj Shetty and Dr. Mrunali Sona during the course of my research work. I also thank **Mr. Jaya Devadiga, Mr. Mahesh B.K and Mr. B Gangadhar,** Assistant Executive Engineer, Department of Mechanical Engineering who provided me continuous

support during my research work. My sincere thanks to **Mr. Guruprasad, Mr. Pradeep and Sudhakar Naik R** for extending their help while conducting the experiments.

I am indebted to my parents **Mr. Laxmikant Malaghan and Mrs. Maitra Malaghan** for inculcating in me the right values and virtues. I am extremely grateful to my brother **Mr. PavanKumar L Malaghan, Mrs. Sanvi Pavankumar Malaghan and My husband Mr. Karthik Rao M C, Mrs. Chinnamma Sonwalkar, Mr Veerana Hosur, Mrs. Sunitha Hosur, Mr. Shivu V Hosur, Ms. Shravani V Hosur, Mr. Chandarshekar Rao, Mrs. Surekha C Rao, Mrs. Rashmi Revenkar, Mr.Kiran Revenkar, and Mr. Aryan K R** for providing continuous encouragement and financial support. I wish to express my special thanks Mrs. Saishyama V G, **Mr.Vinayak Manoji**, to all my family members and friends who were a constant source of motivation and encouragement during the entire course of my doctoral work.

I am indebted to all my friends of Department of Mechanical Engineering NITK Surathkal for their constant help and encouragement during the entire this research work. The list goes on and there are many others I should mention. There are people who helped me all the way and provided me support when I didn't even realize i needed it, or needed it now, or needed it constantly. Listing all of them would fill a book itself, so I merely will have to limit myself to a few words: I THANK YOU ALL...!

Praise to the Almighty who bestows success and guides our destiny. I fall to find words to express my thankfulness and gratitude for the blessings and for bestowing ever pervading illumination and perseverance in accomplishing the uphill task.

_____

Rashmi L Malghan

ABSTRACT

The growth of consumer demands for better quality metal cutting related products has motivated the metal cutting industry to continuously enhance quality control of metal cutting processes. Of the several processes, the face-milling is one of the most fundamental metal removal operations used. It is affected by machining process parameters like cutting force, ambient conditions, coolant type, tool parameters and material properties. Nowadays, diverse types of materials have been used based on the condition requirements like strength, weight, corrosion resistance, etc. Metal reinforced composites have tailorable properties which widen their applications. Machining of composite materials is difficult to carry out due to the anisotropic and non-homogeneous structure of composites and the high abrasiveness of their reinforcing constituents. In this study on milling of AA6061 and AA6061-4.5%Cu-5%SiCp composite, formation of unwanted scratches on the surface of the material were witnessed due to presence of hard particles, resulting in increased surface roughness. Design of experiment is used to analyse the machining process parameters. Taguchi orthogonal array design is used to analyse the levels of the experiment. The Analysis of Variance (ANOVA) is also used to evaluate the contribution of process parameters on milling process output variables for both alloys and composites. The mathematical models for cutting force, surface roughness and power consumption are developed using response surface methodology(RSM).

Under utilization of machine capacity limits the efficient use of machines and is presently continually being run at sub-optimal conditions. In this study, a novel technique is introduced wherein the desired depth of cut is achieved with lesser number of passes, lesser time and also by consuming lesser power. Planning a strategy for better machine utilization based on power constraint in machining using PID logic.

Further, prediction of responses of milling process are carried out using artificial neural network (ANN) with feed forward architecture using error back propagation learning algorithm. A reverse mapping neural network (NN) has been implemented as a novel architecture, which can derive the input responses, based on the desired system outputs. Reverse mapping approach can be treated as advisory system in absence of human experts, can predict the settings of various process parameters in a milling process to achieve the desired responses as per the requirements of end user. Further this model can be implemented to adjust the process parameters in on-line control of the milling quality. The validity of the

models is established. The ANN models formulated for cutting force, surface roughness and power consumption are found to predict the corresponding responses quite accurately, within the acceptable limits of prediction errors.

To explore the dynamic learning capacity of Elman Simple Recurrent Neural Network as advancement over ANN model, the corresponding RNN model was developed. The convergence problem of RNN model was overcome by an innovative way by using Hybrid Recurrent Neural Network (HRNN). The biases and weights are borrowed in a HRNN model with feedback connections, from a partially trained ANN model having similar architecture. The HRNN formulated using this methodology is able to predict the relationship between input and output data and a good correlation is achieved. With reduced learning time, it is observed that an HRNN modelled from a partially trained ANN has equivalent prediction capability and is superior to ANN in terms of computational time.

It is noteworthy that, prediction helps the investigator to determine the outputs as well as inputs, but since it fails to estimate the global extreme values of the response responsible for the best product quality (minimum defects). Identifying the extreme values for the conflicting outputs poses difficulties. Traditional methods (DOE, RSM, Grey Relational Analysis and Classical engineering approach) might fail to determine the global optimum values as searches are carried out in single direction. Evolutionary algorithms (Particle Swarm Optimization(PSO)) through their heuristic search mechanisms determine the global solutions at many distinct locations in multi-dimensional space, simultaneously. The lower and upper levels of machining parameters were opted as constraints. The optimized results were cross verified with experiments and found to have good agreement with the experimental values. PSO outperforms Grey Relational Analysis and RSM thus can be utilized as a tool to optimize and predict results during machining of AA6061 and AA6061-4.5%CU-5%SiCp.

Graphical user interface (GUI) has been designed using available API libraries which include two main modules, namely, Prediction (both forward and reverse mapping) and Optimization. Each model has the sub components for prediction of cutting force, surface roughness and power consumption. There is provision to obtain outputs by manually feeding the inputs as well for plotting bar graphs by varying one parameter at a time, keeping others constant.

Keywords: Artificial Neural Network, Forward Mapping, Reverse Mapping, Hybrid Recurrent Neural Network, Particle Swarm Optimization.

CONTENTS

List of Tables

List of Tables

NOMENCLATURE

Ra	: Surface Roughness
FX	: Cutting Force
SEM	: Scanning Electron Microscope
EDAX	: Energy Dispersive X-Ray Analysis
OA	: Orthogonal Array
DOE	: Design of Experiments
RSM	: Response Surface Methodology
CCRD	: Central composite rotatable design
ANOVA	: Analysis of Variance
ANOM	: Analysis of Mean
SS	: Sequential sum of squares
SG	: Servo Guide
Adj. SS	: Adjusted Sum Of Squares
MS	: Mean Square
F	: F-Ratio Value
P	: Percentage of Contribution
EA	: Evolutionary Algorithm
GA	: Genetic Algorithm
GRA	: Grey Relation Analysis
GRG	: Grey Relation Grade
PSO	: Particle Swarm Optimization
ANN	: Artificial Neural Networks
BPNN	: Back Propagation Neural Network
RNN	: Recurrent Neural Network

CHAPTER 1

INTRODUCTION

1.1 GENERAL BACKGROUND

The challenge of modern machining industries is mainly focused on the achievement of high quality, in terms of work piece dimensional accuracy, surface finish, production rate, and lesser wear on the cutting tools, economy of machining and reduced environmental impact. Several mathematical models have been proposed to focus on this wider objective so far.

Now days, Metal Matrix Composites (MMCs) play a vital and effective role in the field of aerospace, marine and automotive industries. For important applications, MMCs have functional properties such as higher strength to weight ratio, enhanced elastic modulus, improved strength at elevated temperature, higher wear resistance, attractive electrical and thermal conductivity and low coefficient of thermal expansion compared to the conventional metals and alloys (Necat et al. 2006, Bayraktar et al. 2008). The focus is mainly on discontinuously reinforced aluminium alloys (DRA) based MMCs, due to their better strength to weight ratio, high stiffness, high modulus, better thermal stability and their isotropic nature. The demand for Al based composites for use as structural material is growing day by day due to its attractive light weight and high strength to weight ratio (Joardar et al.2014, Degischer et al. 2001). The limitation in achieving excellent permutation of strength, toughness, density and stiffness in monolithic materials has led to the invention of new generation of material known as composite material. (Nair et al. 1985, Hashim et al 1999, Bandyopadhyay et al. 2007) Composite materials are the most promising materials and are in boom due to their tailorable properties. (Previtali et al. 2008, Bandyopadhyay et al. 2007).In recent era, different types of composites have come in to being namely, fibre reinforced composite and particulate reinforced composite, etc. (ASTM, Composites). Such sort of composite are known as polymer matrix composite, metal matrix composite and ceramic matrix composites. (Karl 2006)Metal

Matrix Composites have emerged as futuristic material in the engineering field due to their superior mechanical properties, and alterable thermal and electrical properties (Ashok and Murugan 2014, Bayraktar et al. 2008). These materials possess significant advantages in terms of strength to weight ratio, stiffness and wear resistance.

Under utilization of machine capacity limits the efficient use of machines and is continually being run at sub-optimal conditions. In this study, a novel technique is introduced wherein the desired depth of cut is achieved with lesser number of passes, lesser time and also by consuming lesser power. Even though the total power for a specific pass is higher in the present approach, overall there is a 40 % decrease in the power consumption and that too in a shorter time interval.

The present study explores to increase the machine capacity utilization and hence increasing the machine availability without affecting the quality performance of the machine, inturn increasing the productivity. Hence, to exploit the full capabilities, power consumption is the desirable metric which is used as maximum capacity utilization criterion of CNC (Computer Numerical Control) machine. With this approach, for the given depth of cut, the total power consumption and the time required to perform the entire job is reduced and hence enhancing the utilization capacity of the machine.

Since it is difficult to identify the process parameters to obtain the desired responses by conducting individual experiments, statistical modelling approaches have been utilized like Taguchi Orthogonal array, Response Surface Method, Grey Relation Analysis. An attempt has been made to develop the forward and reverse process models for the milling process models using the neural network based approaches (i.e. ANN and RNN). In this study, neural networks based approaches (i.e ANN and RNN) has been applied to milling process for prediction of its three responses based on three machining parameters namely spindle speed, feed rate and depth of cut through forward mapping. Using a reverse mapping method, based on the end user's requirements for the desired values of various responses, the optimal settings of milling process parameters were also predicted. It has been observed that the ANN

and RNN predicted results closely corroborate with the experimental and test case results which prove the capability of neural network based approaches as an effective tool for developing such prediction models to cater the needs of both the operators and the end users. It can also be extended further for modeling other complex machining processes with a large number of control parameters and responses. It is to be noted that the results of the reverse modelling are considered to be more useful for the end user to achieve the desired output. In addition, the developed methodology can be implemented to adjust the process parameters in on-line control of the milling quality. This model for reverse mapping is also trained using the test cases and is subsequently used for prediction of the tentative settings of the milling process parameters based on a set of desired response characteristics. It can also be treated as an advisory system in absence of human experts, can predict the settings of various process parameters in a milling process in order to achieve the desired responses according to the requirements of the end users.

The ANN and RNN concepts are implemented to predict responses of AA6061 and AA6061-4.5%Cu-5%SiCp via forward and reverse mapping in milling process. Very few research has been done on the prediction of the process parameters by reverse mapping technique in casting process (Manjunath Patel et al. 2014). In this process, the desired response of the system is fed in to the system and input process parameters are generated. So far, this system is used only for predicting the best input parameters but very few research works are addressed towards reverse mapping to develop control logic of machining process. Further, this system can be used in the development of feedback system to control the machining process.

One of the main objectives in any system is to optimize the multiple responses of the process parameters. The recent focus has been towards the multi-objective optimization of machined surfaces to reduce the cost of the machining operation. One of the techniques used in statistical tools is desirability approach. This approach gives satisfactory result but further minimization of error can be obtained by particle swarm optimisation. Particle swarm optimization searches the minimum global optimization from the entire population. PSO is a computational method that optimizes the issues

by iteratively training to improve a candidate solution with regards to quality. Such methods are commonly known as metaheuristics as they make few or no assumptions about the issue being optimized and can search very large space. PSO can handle mixed integer nonlinear optimization problems with only concise program. But, hardly any work has been carried out regarding the development of a control strategy for improving the machine utilization and availability to increase productivity. So, the present study focuses on development of control strategy through an intelligent software system.

This system utilizes empirical formulae (as discussed in chapter 4) to measure the cutting forces and each time these forces are compared with the machine working capacity. If the machine working capacity is below the maximum level of machine capacity, then it will increase the rotational speed or feed rate to maximize the power consumption. Such a novel strategy has been implemented here.

1.2 PROPOSED STUDY OUTCOME

This thesis is an effort to develop ANN models which can predict the responses of AA6061 alloy and AAT061-4.5%Cu-5%SiCp composite, and to establish a relationship between the input parameters and the desired responses. Further the predictions made by the ANN models are validated by conducting the validation experiment within the range of data used for training the ANN models. The predictions made by the models are then analysed with respect to the training as well as validation data to assess the suitability of the ANNs to model the AA6061alloy and AA6061-4.5%Cu-5%SiCp composite in milling process.

Recurrent neural networks (RNN) are known for better convergence characteristics (Elman 1990). However, the use of Elman Simple recurrent network as well as extended Elman network (Kremer 1995, Song et al. 2008, Gruning 2006) using back propagation training algorithm led to network getting stuck in local minima. The problem of convergence has also been noticed while modelling the process of mushy state rolling using Elman and extended Elman recurrent neural networks, to predict the grain sizes, hardness, wear and tensile properties. Various strategies were tried out

to overcome the problem of Elman extended recurrent neural network which led to the formulation of a Hybrid Recurrent Neural Network (HRNN). The predictions of the HRNNs formulated are shown to be statistically equivalent to the predictions done by using ANN model. Further, the predictions made by HRNNs modelled for milling of AA6061 alloy and AA6061-4.5%Cu-5%SiCp composite are analysed with those obtained using ANN models. The assessment of the performance of HRNN models with the ANN models provides the decision to accept the HRNN model as an alternative tool for predictions and input - output mappings, with the added advantage of faster convergence.

To introduce higher level of generality, two materials (AA6061 and AA6061-4.5% Cu-5% SiCp) have been taken in to consideration. Inorder to predict the process parameters of these materials usually different models need to be integrated. This issue has been overcome in the present study by developing a common prediction model. The developed model will identify and predict the common best process parameters that hold good for different types of materials.

The present research delineates a new comprehensive approach for selecting optimal cutting parameters for machining. The approach is based on ideal optimization methods such as Response Surface Methodology (RSM) and Particle Swarm Optimization. Development of ANN and RNN models by Forward and Reverse Mapping simulate the relationship of milling process parameters and their influence on cutting force, surface roughness and power consumption.

The developed models were tried out on the above mentioned materials so as to prove their generality. Secondly, the study was more concentrated in developing a model that behaves and performs in a better way by providing the desired output. A Graphical User Interface (GUI) environment is developed to enable the user in using the system more comfortably.

1.3 LAYOUT OF THE THESIS

In the present work, a systematic study is carried out to elucidate the machining performance of AA6061 and AA6061-5%SiCp composite materials. The effect of the machining parameters involved in the milling of AA6061 and AA6061-5%SiCp have been studied. In addition, a detailed analysis of experiment is performed by using Orthogonal Array (OA) technique and later on the prediction of the model is carried by RSM, ANN and RNN techniques. Further on, the optimization was implemented by Desirability approach, Grey Relation Analysis and PSO. The various stages of the investigations were carried out and these investigations were divided into six chapters. The summary of discussions carried out chapter wise is detailed below.

Chapter 1 presents the historical background and the challenges faced and motivation to take up the present work. An overview of proposed research work is enunciated in this chapter.

Chapter 2 presents a comprehensive survey of literature on milling process, application and the influencing process variable. The chapter also makes a critical review of the current knowledge in the area of neural network techniques as a tool for mapping input and output relationships right from the historical inventions of artificial neuron till the current literature regarding convergence in recurrent neural networks. The aims and objectives of the present thesis have been set based on the gaps identified through a detailed literature survey. The application of Taguchi DOE, ANOVA, RSM, Grey Relational Analysis, Desirability approach, ANN, RNN and PSO, summary of literature review, problem statement, objectives of the study, scope and plan of work also have been addressed in this chapter.

Chapter 3 elucidates the selection of raw materials for conducting the experiments for validation of the model and also it deals with description of the experimental procedures adopted for AA6061 and AA6061-5%SiCp machining.

Chapter 4 deals with description of the methodology for calculating the cutting force via indirect approach.

Chapter 5 The Taguchi parameter design has been incorporated to identify the number of experiments need to be carried out and also deals with the investigation on the effect of machining parameters on the responses such as surface roughness, cutting force and power consumption.

Chapter 6 illustrates the formulation of prediction model (both conventional and non-conventional techniques, i.e RSM, ANN, RNN, HRNN) for the selection of major influencing factors affecting the responses, to develop mathematical model (response equation) for analysis and prediction of cutting parameters, for development of single response prediction model using RSM, and confirmation test (validation) was performed by conducting the experiments.

The chapter deals with the formulation of ANN model for prediction of responses of AA6061 alloy and AA6061-4.5%Cu-5%SiCp composite in milling condition. The chapter presents the analysis of variation of responses with their respective responses in case of forward and reverse mapping to highlight on the development of multi objective prediction models using ANN for both forward and reverse Mapping.

It presents the formulation of an RNN model as a tool that could be used as an improvement over the ANN model. The chapter highlights the problems encountered in formulation of an RNN model to map the input – output data and the strategies to overcome this problem. The formulation of HRNN models for prediction responses of cutting force and surface roughness and power consumption of milling of AA6061 and AA6061-4.5% Cu-5%SiCp composite have also been included here.

It deals with the performance (validation) of HRNN models with the corresponding ANN models has also been discussed, establishing the use of HRNN models as prediction tools having capabilities equivalent to ANN models in terms of predictions but being better than ANN models in terms of convergence characteristics.

- Development of multi objective prediction models using ANN and RNN for both forward and reverse Mapping.

- Confirmation experimental verification was performed for various process combinations for forward and reverse mapping.

The chapter also addresses the performance of RNN model with corresponding ANN model, establishing the use of RNN models as prediction tools having equivalent capabilities to ANN models in terms of predictions but being better than ANN models in terms of convergence characteristics.

The chapter deals with development of Graphical User Interface (GUI), encompassing the above mentioned prediction/optimization functionalities and to enable the user in using the system more comfortably.

Chapter 7 discusses the formulation of optimization models to identify the optimum parameters of the desired responses.

- Development of multi objective optimization models (Grey Relational Analysis, Desirability approach) and particle swarm optimization approach.
- Confirmation experimental verification was performed for optimized process combinations.

The chapter also addresses the performance of PSO model with corresponding statistical methods.

Chapter 8 discusses the development of control strategy. The section discusses the modeling and simulation of control strategies in process of milling using software tool (Labview). The feedback control logic using PID (Proportional, Integral and Derivative) to control the power utilization with comparative to power capacity of the machine. Based on the power error attained the spindle speed or feed rate is compensated. In the concept process parameter controls one or more of controlled parameters to achieve desired output/result. The foresaid concept is developed to minimize machining time.

Chapter 9 presents the overall summary and the objective conclusions derived from the present research work. The further direction of research work is also stated in this chapter.

CHAPTER 2

LITERATURE SURVEY

2.1 INTRODUCTION

During milling process, insert hits hard agglomerated particles which lead to breakages. If a system is developed with an adaptive control technique, it will identify the change in the response and based on the change in the response, necessary action will be taken to avoid the failure. For example, the adaptive control system immediately senses difference in hardness and immediately sends the command signal to feed drive to slow down the feed rate until the tool is passed through the hard region. Even if there are no unexpected agglomerated particles in the metal, the hardness of cast component has variation upto 300 percent, and the adaptive control system will adjust feedrate to handle those variations. The application of adaptive control systems can be found in aerospace industries like— General Electric and Pratt & Whitney. They machine metals so hard that tools can get dull on a single cut. When that happens, the tool might break during machining, causing scrap or rework. Meanwhile, with adaptive control system, the feedrate slows down and allows the dulled tool to finish the machining process (Hariharan and Narayan 1974, (Volos et al. 2015), Yang sheng et al. 1994). The following section elucidates on effect of machining process parameters and prediction.

- Cutting force measurements
    - Direct method
    - Indirect method
- Cutting force prediction and optimization model
    - Statistical tool
    - Neural Network Methods

- Cutting force controller
    - Using Direct method of measuring cutting force
    - Using Indirect method of measuring cutting force
- Surface roughness prediction and optimization model
    - Statistical model
    - AI based models

2.2 CUTTING FORCE

Cutting force is one of the important characteristic variables to be monitored during the machining process. Tool breakage, tool wear, and work piece deflection are mainly due to abnormal cutting force developed during the machining process (Zhang and Zheng 2005). Cutting forces of the tool point are measured by specially designed dynamometers. Early researchers used a variety of hydraulic, pneumatic and strain gage instruments. However, piezoelectric dynamometers employing quartz load measuring elements are most commonly used for cutting force measurement. The dynamometers are mounted between the tool or workpiece and non-rotating part of the machine tool structure. A coordinate system can be used to resolve the cutting forces into directional components. In the milling process, force components are related to the axes of motion of the machine tool. Three resolved components of the force are in-feed force, cross-feed force and thrust force. The in-feed force acts tangent to the rotating tool and acts in the x direction of the machine tool, cross-feed force acts normal to the rotating tool and acts in the y direction of the machine tool and thrust force acts parallel to the axis of the tool and acts in the z direction of the machine tool as shown in Figure 2.1. The literature survey pertaining to the work of other researchers is indicated below.

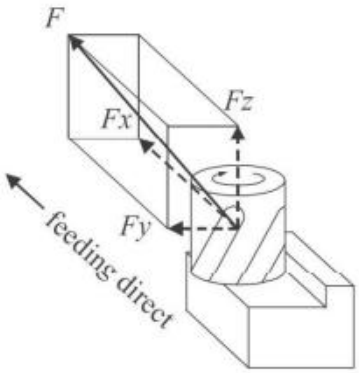

Figure 2.1: Cutting forces in end milling

(Ding et al. 2010) (Y. Li and Liang 1999) (Li et al. 2004) displayed a generalized cutting force model in terms of material properties, tool geometry, cutting parameters and process configuration. The model indicates the association among the workpiece and numerous cutters, flutes by the convolution of front line geometry work with a prepare of motivations having the period comparable to tooth dividing. The creators led tests over different cutting conditions and acquired the outcomes to check the model loyalty. Lai (2000) clarified the impact of dynamic radii; feed rate, radial and axial depths of cut on cutting forces. The author clarified that when radial and axial depths of cut increment, the cutting forces likewise increment since the engaged flute lengths are expanded. Tandon (2001) employed neural system to foresee cutting force regarding machining parameters for example tool diameter, spindle speed, feed rate, number of flutes, rake angle, clearance angle, axial and radial depth of cut. The creators presumed that this model can anticipate precisely the cutting forces in three ways. Lin et al. (2003) utilized neural system (radial basis function) and numerous relapse investigations to predict machining forces–tool wear relationship in machining of aluminium metal matrix composites. Other than process parameters, feed and cutting forces were utilized to estimate tool wear. The creators got better correlation of tool wear with feed force data than with cutting force.

Kovacic et al. (2004) proposed demonstrating of cutting forces with genetic programming, which mirrors the standards of living creatures. Estimations were produced using two materials (aluminium alloy and steel) and two distinct sorts of

processing (conventional milling and STEP milling). For every material and sort of processing parameters, tensile strength and hardness of work piece, tool diameter, cutting depth, spindle speed, feeding and type of milling were monitored, and cutting forces were measured for every combination of milling parameters. On the premise of the test information, distinctive models for cutting forces prediction were acquired by genetic programming (Palanisam et al. 2007) built up a cutting force model to anticipate the tangential and thrust cutting force in end milling of AISI 1020 steel. Li et al. (2004) exhibited an exploratory investigation on cutting force variations at last processing of Inconel 718 with coated carbide inserts. The cutting force variation along with tool wear propagation was analyzed. Haci et al. (2006) developed a model to ascertain the different segments of cutting forces and analyzed the impact of machining parameters and tool geometry on cutting force. Omar et al. (2007) acquainted a technique with all the while predict the conventional cutting forces alongside 3D surface topography amide side processing. The model joins the impacts of tool runout, tool deflection, system dynamics, flank face wear, and the tool tilting on the surface roughness.

Astakhov et al. (2007) examined the influence of the cutting feed, depth of cut, and workpiece diameter on the tool wear rate. The outcome demonstrated that the impact of the cutting feed on the tool wear rate was distinctive at various cutting speeds and the depth of cut on the tool wear rate was irrelevantly little if the machining was completed at the ideal cutting regime. Ganesh et al. (2017) employed response surface strategy to build up a scientific model to foresee cutting forces in terms of depth of cut, feed, cutting speed and immersion angle by utilizing response surface methodology in end processing of composite material. The authors dissected direct and collaboration impacts of the machining parameter with cutting forces. Huang et al. (2007) examined a logical cutting force model for miniaturizd scale end milling. The cutting force model, which considered the edge radius of the smaller scale end mill, was reproduced. They found that the expanding of thrust force influences the feed direction cutting force in micro end milling with a very small feed per tooth. Patwari and Anayet (2011) examined the advancement of the first and second request models for predicting the tangential cutting force delivered in end-milling operation

of medium carbon steel. The author found that expansion in either the feed or the axial depth of cut expands the cutting force, while an expansion in the cutting speed diminishes the cutting force. Ozturk and Budak (2009) exhibited models for 5-axis milling process geometry, cutting force and stability. The use of the models in determination of essential parameters was additionally illustrated. A practical method, produced for the extraction of cutting geometry, was utilized as a part of recreation of a total 5-axis cycle. Ding et al. (2010) tentatively researched the impacts of machining parameters on cutting forces and surface roughness in hard milling of AISI H13 steel with coated carbide tools. In view of Taguchi's technique, four-factor (cutting speed, feed, radial depth of cut, and axial depth of cut) four-level orthogonal tests were employed. Three cutting force components and roughness of machined surface were measured, and then range analysis and ANOVA are performed. It is discovered that the axial depth of cut and the feed are the two overwhelming elements influencing the cutting forces. The legitimacy of the model was demonstrated through cutting experiment, and model was used to predict the machined surface roughness from the data on the cutting parameters. Zhang et al. (2007) analyzed the tool wear and the cutting force amid high-speed end-milling Ti-6Al-4V alloy. The exploratory outcomes demonstrated the major tool wear mechanisms in high-speed end milling of Ti-6Al-4V alloy with uncoated cemented tungsten carbide tools are bond and diffusion at the crater wear along with adhesion and abrasion at the flank wear. Peng and Xu (2017) investigated the qualities of rapid speed machining dynamic milling forces of Titanium alloy by use of polycrystalline diamond tools. They found that amplitudes increment with the expansion of cutting velocity and tool wear level, which could be connected to the checking of the cutting process. Hector Siller et al. (2006) proposed a mechanistic approach to deal with cycle time prediction of high speed milling for sculptured surfaces with high feed rates. Errors amongst modified and actual feed rates were assessed. Looking at the two cases illustrated, the proposed display was fit for predicting process duration with a most extreme error of 5-22%. Abou-El-Hossein et al. (2007) examined the improvement of the first and second order models for predicting the cutting force produced in end milling using RSM to contemplate the impact of cutting parameters on cutting force. It was discovered that the collaboration feed with axial depth was extremely strong and the interaction of

feed with radial depth of cut was seen to be noteworthy. The predictive models delivered estimations of the machining force near to those readings recorded tentatively with 95% sure interim. Felho et al. (2015) presented the aftereffects of a progression of tests performed to analyze the legitimacy of a hypothetical model for assessment of cutting forces and machining error in ball end milling of curved surfaces. Cutting force diminished with an expansion in milling position angle, while two force components are not really influenced by processing position angle. The machining error for the most part diminished with an expansion in milling position angle. Hypothetical and test comes about demonstrated sensibly great efficiency.

2.3 CUTTING FORCE MEASUREMENTS

During cutting operation, cutting forces include lot of information on dependent variables in machining, which will help to decide how to improve or minimize the sudden change due to that specific process parameter. For example during cutting, if there is a sudden increase in the cutting force it tends to indicate possible tool wear condition or if cutting force suddenly drops to zero, indicates that the tool in air or the tool is broken. This information can be implemented to increase the production rate and optimization. The slight changes in the cutting force information can be used as an input to the adaptive control system to control the specific process parameters.

2.3.1 Direct Method Of Cutting Force Measurement

In their research, (Kim et al. 1999), focused on the cutting forces in face milling operation and procedure was presented for the simulation of static and dynamic cutting forces in face milling operation. For the static model, the initial position error of the inserts and eccentricity of the spindle were taken into consideration as the major factors affecting the variation of the chip cross section. The structural dynamic model for the multi tooth oblique cutting operation is assumed as a multi- degree of freedom spatial system. From the relative displacement of the system, based on the double modulation principle, the dynamic cutting force were derived and simulated. The simulated forces were subsequently compared to measured cutting force in the time and frequency domain.

Abou- El- Hossein et al. (2008), have presented Finite element (FEA) method and response surface method (RSM) to find the effect of milling parameters on cutting force when milling Hastelloy C-HS. Optimized cutting force values are subsequently obtained from model equations. FEA model showed distribution of cutting force.

Seeman et al. (2010), dealt with the goal of concentrate the effects of cutting parameters on the variations of cutting forces during end milling operation of Al SiC metal matrix composite material. Cutting forces were measured for various feed rates. The average cutting forces were resolved at various feed rates in tangential, radial, and axial directions per tooth period by keeping immersion and axial depth of cut as constant. A correlation between response surface modeling and experiment was presented. In their research, (Fadhel et al. 2008), have observed that, Cutting forces produce deformations along cutting tool which is one of the mechanical machining errors.

2.3.2 Indirect Method Of Cutting Force Measurement

In their research, (X. Li 2001), discussed about the feed cutting force measurement using an inexpensive current sensor installed on the a.c. servo motor of a CNC turning centre. The factors that affect a feed drive system are analyzed in detail, and a neuro-fuzzy model of the feed drive system for estimating feed cutting force has been presented. Experimental results demonstrate that this method can accurately estimate feed cutting force within an error of 5%.

2.4. CUTTING FORCE PREDICTION AND OPTIMIZATION MODEL

Ogedengbe (2011) modified the feed rate or spindle speed to avoid chatter incorporating acoustic signals. Tsai et al. (2010), proposed an innovative control loop, in view of Spindle Speed Compensation Strategy (SSCS) by utilizing Acoustic Chatter Signal Index (ACSI), to counteract event of milling chatter. Acoustic Chatter Signal Index (ACSI) and Spindle Speed Compensation Strategy (SSCS) were used to measure the acoustic signal and effectively tune the spindle speed individually. By changing over the acoustic feedback signal into ACSI, a suitable Spindle Speed

Compensation Rate (SSCR) can be dictated by SSCS based in view of continuous chatter level or ACSI. In like manner, the pay summon, alluded to as to as Added-On Voltage (AOV), is connected to build/diminish the sindle motor speed.

The milling force prediction model was implemented and compared using regression and ANN models (Radhakrishnan and Nandan 2005). Regression analysis is a statistical techinque used for developing a relationship between dependent and independent variables.The analysis was carried out to predict the force and the obtained result is (94.2 %) accurate. The back propogation neural network algorithm was used to train and predict the cutting forces and the obtained value is (95.3 %) acccurate and concluded that back progation model is better.In addition to the cutting force model, a neural network and fuzzy logic model was developed to predict the material removal rate for composites (Pallavi et al. 2012). The fuzzy logic model has the ability of predict the future based on membership function of input and output variables From the developed , It has been concluded that BPN is better than fuzzy logic model, in their work.

In their research, (T. Y. Kim et al. 1999) (T. Y. Kim and Kim 1996), exhibited the indirect cutting force estimation method in contour NC milling processes by using current signals of servo motors. They recommended a simulated neural system and Kalman filter unsettling influence spectator. A Kalman filter disturbance observer has actualized by utilizing the dynamic model of the feed drive servo system and each of the outer load torques to the x and y-axis servo motors of a horizontal machining centre are evaluated. An ANN framework has additionally been actualized with a training set of experimental cutting data to gauge cutting force indirectly. The input variables of the ANN framework are the motor currents and the feed rates of x and y-axis servo motors, and output variable has the cutting force of each axis. A progression of experimental works on the circular interpolated contour milling process with the path of a complete circle has been performed. It is presumed that by looking at the Kalman filter disturbance observer and the ANN system with a dynamometer measuring cutting force directly, the ANN framework has superior execution.

Table 2.1: Papers Referred On Cutting Force

Author	Year	Operation & Parameters	Prediction Model	Conclusion	Future
Chao Wang et al.	2014	Lathe Speed, Feedrate DOC. Kistler dynamometer	SAW-based smart cutting tool and the	Machining the dual-material, hybrid dissimilar workpiece has provided an excellent method of triggering an adaptive control event during the machining process; emulating an abrupt change in material properties.	SAW-based cutting tool for force measurement in adaptive machining
Giuseppe Ingarao et al.	2014	Milling Feed rate step down	CNC milling AMINO Six axes ROBOT	Machine Tool Efficiency, considering Total energy demand Robot provides best solution.	
Hae-Sung Yoon et al.	2014	Milling Cutting force Current Power monitoring (Indirect)	Response surface methodology (RSM)	The power consumption of the machine tool increased with the cutting load. The material-removal power was found to consist of ~7.6% of the total power consumption The material-removal power increased with the feed, spindle rotational speed, and depth of cut	performed in measurement and standardization of energy consumption at various scales with various types of machine tools
Ulrich Schneider et al.	2014	Milling Geometric parameters.	Piezo-actuated compensation mechanism	The system performance is evaluated in extensive machining experiments. It is shown that the proposed approach to machining offers significantly higher accuracy , up to eight times improvement for milling in steel	

Author	Year	Operation & Parameters	Prediction Model	Conclusion	Future
X. Li et al.	2014	Turning Feed, cutting force, speed	Neuro-Fuzzy Technique	The error between the actual and the estimated force is within 5%, which validates the accuracy and feasibility of the suggested approach	
KiousMech eriet al	2014	Milling Cutting force, vibrations	Neural network	Estimate the flank wear from the cutting Force measurement and the cutting conditions.	Data base of many inserts
Dohyun Kim et al.	2011	Milling Current ,feed	FLC	FLC was successful in maintaining a reference cutting force in real time in both numerical simulation, and experiments for two-flute end milling of aluminium work pieces when the tool dynamometer was used.	The tool wear, another important variable in the process control, could be estimated intermittently using the Spindle motor current.
Tunde Isaac Ogedengbe et al.	2011	Micro(Face) Milling DOC, Feed, Speed	Fast Fourier Transform (FFT)	spindle and feed motor current signals as to their ability for sensing and monitoring tool wear progression on a micro milling machine.	Establish an effective tool condition monitoring system for micro milling using spindle and feed motor current signals

Author	Year	Operation & Parameters	Prediction Model	Conclusion	Future
Tzeng-Yih-Fong	2009	Milling speed, feed, feed per tooth, rake angle and helix angle.	GA, Hybrid GA, PSO, Simulated annealing and Threshold acceptance algorithm to compare the result between up milling and down milling	A regression equation is developed involving tool wear for upward milling and downward milling. In case of down milling tool wear is minimum as compare to up milling so we can conclude that with down milling long tool life is possible.	
Tae-Yong Kim et al.	1999	Milling (Indirect) Current, Feed rate	Kalman Filter disturbance and ANN method comparison.	The ANN system has a better performance compared to kalman Filter.	

2.5 CUTTING FORCE CONTROLLER

Kim et al. (1996) presented an adaptive cutting force controller for the milling process, which can be embedded to commercial machining centres in a particular way. The cutting forces along x, y and z axes were measured indirectly from the use of current drawn by a.c. feed-drive servo motors. They have developed a typical model for feed drive control system of horizontal machining center to analyze cutting force measurement from the drive motor. The pulsating milling force can be measured indirectly within the bandwidth of the current feedback control loop of the feed drive system. From its study, the measured cutting force from the dynamometer and the measured cutting force from the current signal are same. This relation was used to develop adaptive controller for cutting force regulation.

2.5.1 Cutting Force Controller Using ANN

In the last few decades, neural networks are extensively used for prediction of nonlinear relation between the input and the output. It also has been applied successfully to speech recognition, image analysis and adaptive control, in order to construct software agents (in computer and video games) or autonomous robots. Most of the currently employed artificial neural network models are based on statistical estimation, optimization and control theory. Research has been carried out in implementing Artificial Neural Network models to control the cutting parameters .The main purpose of the constant cutting force controller is to increase the metal removal rate and avoid the tool breakage. In a similar way Shiuh-Jer et al., 1996 used adaptive resonance theory 2(ART) to control the feed rate system. The ART neural network structure was used to learn and sort the appropriate system parameters. The contour error in multi-dimensional end milling operation was studied by (Luo et al. 1999). The work consisted of two sets of neural networks for controling the avearge resultant cutting force of the feed axis in x and y direction. . In addition, the application of perception-type neural networks to tool-state classification during a metal-milling operation has been studied by (Dimla 2002). They investigated both single-layer networks and multi-layer networks and found that the multi-layer networks had better performance than the single-layer tool-state classification. The

milling force prediction model was implemented and compared using Regression and ANN models (Radhakrishnan and Nandan 2005). The analysis was carried out to predict the force with an accuracy of 94.2 %. The back propagation neural network algorithm was used to train and predict the Fx to an accuracy of 95.3 %, better than the regression model.

2.5.2 Controller For Machining Parameters

Several researches have been done on the adaptive control system using cutting force as input parameters to override the feed rate of the control system. Cutting forces can be measured using direct (Fadhel et al. 2008) and indirect method (Kaya et al. 2011, X. Li et al. 2000). T Kim et al. (1996) , developed adaptive cutting force controller for a machining centre. The cutting forces along x, y and z axes were measured indirectly from the use of currents drawn by a.c. feed-drive servo motors. The pulsating milling forces can be measured indirectly within the bandwidth of the current feedback control loop of the feed-drive system. It is demonstrated that indirectly measured cutting force signals can be utilized as a part of the adaptive controller for cutting force regulation.

2.6 SURFACE ROUGHNESS

Surface roughness is a quantifiable trademark in light of the roughness deviations as characterized in the preceding. Surface finish is a more subjective term signifying smoothness and general nature of a surface. The most usually utilized measure of surface texture will be surface roughness. Concerning Figure 2.2, the surface roughness can be characterized as the average of the vertical deviations from the nominal surface over a predefined surface length.

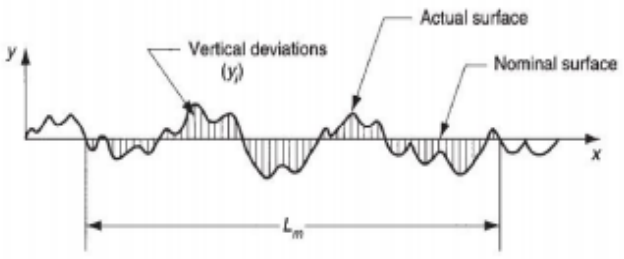

Figure 2.2: Deviations from the nominal surface used in the two definitions of surface roughness

An Arithmetic Average (AA) is generally used, based on the absolute values of the deviations, and this roughness value is referred by the name average roughness. In Equation form (2.1) .

$$R_a = \int_0^{L_m} \frac{|y|}{L_m}\, d_x \quad (2.1)$$

where R_a = arithmetic mean value of roughness, m (µm); y = the vertical deviation from nominal surface (converted to absolute value),m(µm); and L_m=the specified distance over which the surface deviations are measured. The AA method is the most widely used averaging method for surface roughness today.

Alauddin (1995) built up a surface-roughness model for the end milling of 190 BHN steel. They recognized that feed rate is an extremely overwhelming element in both first and second order model and an increment in either the feed rate or axial depth of cut increases the surface roughness, whilst an increase in cutting speed diminishes the surface roughness. Ma et al. (2016), Lou et al. (1999) explored another approach for surface finish prediction in end-milling operations. Through experimentation, the framework demonstrated fit for predicting the surface roughness (Ra) with around 90% accuracy. The author concluded feed rate was the most critical machining parameter used to anticipate the surface roughness in the various regression models.

Ming and Changyun (2012) investigated the influence of machining parameters such as the cutting speed, feed, depth of cut, concavity and axial relief angles of the cutting edge of the end mill on surface roughness in the slot end milling of aluminium alloy. Predictive surface roughness models were worked by applying response surface methodology for both dry and coolant cutting conditions. They reasoned that the significant factors affecting the dry-cut model were the cutting speed, feed, concavity and axial relief angles and for the coolant model, the feed and concavity angle.

Ghani et al. (2004) applied Taguchi optimization method to optimize cutting parameters in end milling when machining hardened steel AISI H13 with TiN Coated

P10 carbide insert tool under semi-finishing and finishing conditions of high-speed cutting. The milling parameters assessed was cutting speed, feed rate and depth of cut. An orthogonal array, signal-to noise ratio and Pareto analysis of variance were utilized to analyze the effect of these milling parameters. The investigation of the outcome demonstrated that the ideal blend for low resultant cutting force and good surface finish were high cutting speed, low feed rate and low depth of cut.

Selaimia et al. (2017) , Ficko et al. (2004) proposed genetic programming way to deal with predict the surface roughness in end milling. Cutting parameters for example spindle speed, feed, and depth of cut and also vibration amongst tool and work piece, were utilized to predict surface roughness. The authors found that the proposed model that involves all these variables predict the surface roughness precisely.

Gupta et al. (2015), Ozcelik et al. (2005) set up a first and second order statistical model to predict surface roughness for high-speed flat end milling process under wet cutting conditions by utilizing rotatable central composite design.

Bagci et al. (2006) used Taguchi strategy for examining the impacts of cutting parameters on the surface roughness value in the face milling. The milling parameters assessed were feed rate, cutting speed and depth of cut.

Erzurumlu et al. (2007)focused on the advancement of a powerful strategy to decide the ideal machining conditions prompting least surface roughness in the milling of mold surfaces by coupling response surface methodology (RSM) with a developed genetic algorithm. Ramanujam et al. (2014), Jenarthanan and Jeyapaul (2013), Nee et al. (2012), Zhang et al. (2007) a connected the Taguchi strategy to optimize the machining parameters such as spindle speed, feed rate and depth of cut for surface roughness. They reasoned that the impact of spindle speed and feed rate on the surface were larger than the depth of cut for milling operation. Sadasiva et al. (2012), Haque and Sudhakar (2002) developed a multiple regression model to predict surface roughness in end milling process by relating with spindle speed, cutting feed rate and

depth of cut. The impacts of spindle speed, feed rate and depth of cut on surface roughness were examined.

Michalik et al. (2014), Kadirgama et al. (2007) built up the surface roughness prediction models, with the guide of statistical methods, for Hastelloy C-22HS .These forecast models were then contrasted and the outcomes acquired tentatively. By utilizing RSM, first order models were created with 95% confidence level.The surface roughness models were produced regarding cutting speed, feed rate and axial depth utilizing RSM as a tool of DoE. In general, the outcomes acquired from mathematical models were in great concurrence with those obtained from the machining experiments.

Ramesh et al. (2013) employed both Taguchi and response surface methodologies for minimizing the surface roughness in machining glass fiber reinforced plastics with a polycrystalline diamond tool. The cutting parameters used were cutting speed, feed and depth of cut. The impact of cutting parameters on surface roughness was evaluated and the optimum cutting condition for minimizing the surface roughness was determined.

Yusup et al. (2012), Prakasvudhisarn et al. (2009) process parameters of CNC end milling were chosen for example, feed rate, spindle speed, and depth of cut to find the minimum surface roughness. Support vector machine was proposed to capture qualities of roughness and its factors. PSO system is then utilized to discover combination of optimal process parameters The outcomes demonstrated that cooperation between the two strategies can accomplish the desired surface roughness and furthermore maximize productivity simultaneously (Shunmugam 2015).

Turnad et al. (2009) employed central composite response surface methodology to build up an analytical model for surface roughness in terms of cutting parameters such as cutting speed, axial depth of cut, and feed per tooth. Software tool (Design Expert) was used to build up the first order and the second order mathematical model. The sufficiency of the predictive model was verified using analysis of variance.

Routara et al. (2009) led tests for three distinctive work piece materials to see the influence of work piece material variation in this respect. Five parameters, viz., center line average roughness, root mean square roughness, skewness, kurtosis and mean line peak spacing were considered. The second-order mathematical models, as far as the cutting parameters, were created for each of these five roughness parameters prediction using RSM on the premise of experimental results. The roughness models and additionally the significance of the machining parameters were approved with ANOVA. It was discovered that the response surface models for various roughness parameters were particular to work piece materials. An endeavour was additionally made to acquire optimum cutting conditions as for each of the five roughness parameters using a response optimization technique.

In the examination by (Zain et al. 2010) the three parameters of end milling were considered for minimizing surface roughness. From the analyses, it was prescribed that prcedure parameters should be set at the highest cutting speed, lowest feed and highest radial rake angle in order to accomplish the minimum surface roughness. Demir and Gündüz (2009) built up numerical model of the surface roughness to research the impacts of cutting tool geometry parameters and found the ideal estimation of geometry parameters, the quadratic model of response surface methodology was utilized. The creator has indicated that the tool nose radius was the dominant factor on the surface roughness. Kadirgama et al. (2012) developed a surface roughness model to optimize machining conditions of aluminium alloys with carbide coated inserts by design of experiments method and response surface methodology. Patel (2012) investigated the influence of various machining parameters like tool speed, tool feed, depth of cut and tool diameter. In their study, experiments were conducted on AL 6351 –T6 material with four factors and five levels. Ahmet (2013) determined the effects of process parameter on surface roughness and the factor levels with minimum surface roughness in pocket machining. The author found that that surface roughness correlates negatively with cutting speed and positively with feed rate and cutting depth. Moshat et al. (2010) indicated optimization of CNC milling process parameters utilizing PCA- based Taguchi

method that had filled the need of advancement however not synchronous enhancement of surface roughness and the material removal rate in the investigation. Routara et al. (2010) had given the blueprint of the soft material milling parameters in their examinations on advancement of CNC end-milling of UNS C34000 medium-leaded brass with various-surface roughness characteristics. A single-response study provided base in deciding the parameters that were considered. The contextual analyse led at the research center have prompted for the real-time studies and to discover the answer for the manufacturing firms around the place. Mustafa and Ali (2006) analyzed the effect of the length and diameter of work piece, depth-of-cut and feed while the cutting speed, which is an imperative machining parameter, was kept consistent. Taguchi strategy was utilized as part of this work with a specific end goal to obtain more reliable and ideal outcomes.

2.6.1 Prediction Of Surface Roughness

Nimase and Khodke (2015) discused on joining of Taguchi and the impact of paremeters on surface roughness of Al-7075 in end milling. From the outcomes, it was inferred that spindle speed and feed rate are the most noteworthy elements. Sukumar et al. (2014), Saurav Datta et al. (2010) covered on optimization of CNC end milling process parameters to give good surface finish and in addition as high material removal rate (MRR). The surface finish and material removal rate have been distinguished as quality ascribes and are thought to be straight forwardly identified with profitability. An endeavour has been made to optimize previously mentioned quality traits in a way that these multi-rules could be satisfied all the while up to desired level. This invites a multi-target optimization issue which has been settled by PCA based Taguchi method. To meet the essential supposition Taguchi method; in their work, singular response correlations have been disposed of first by methods for Principal Component Analysis (PCA). Associated responses have been changed in to uncorrelated or autonomous quality indices called vital segments. The vital segments, imposing most noteworthy responsibility extent, have been dealt with as single target work for streamlining (multi-response execution list). Finally Taguchi method has been adjusted tot ake care of this optimization problem. The aforementioned approach has been discovered productive in the situations where concurrent streamlining of

immense number of reactions is required. Yu-Hsuan et al. (1999) developed an in-process surface acknowledgement framework utilizing accelerometer, proximity sensor and ANN model to predict surface roughness of machined parts in end milling. It was observed that ANN surface recognition model is sparing, proficient and able to produce a high accuracy rate of 96-99% predicting accuracy for assortment of blends of machining conditions.

In their exploration, D. Baji et al. (2010), exhibited an investigation on the influence of cutting parameters on surface roughness of steel work-piece in face milling operation. The response surface method (RSM) in view of the rotatable central composite design (RCCD) has been utilized together with an analysis of variance (ANOVA) and regression analysis (RA). To get the minimal value of surface roughness, the surface roughness equation has been optimized by finding the partial derivations and solving the system of equations. A comparison of results obtained by means of the Taguchi method with the regression model was carried out. The Taguchi method, in view of orthogonal arrays, has utilized likewise to determine the impact specific machining parameters.

In their research, Ab. Rashid M et al. (2009), displayed the improvement of numerical model for surface roughness prediction before milling process in keeping in mind the end goal to assess the fitness of machining parameters; spindle speed, feed rate and depth of cut. 84 samples were run in this study by using CNC Milling machine. The specimens were arbitrarily separated in to two data sets- the training sets (m=60) and testing sets (m=24). ANOVA analysis showed that at least one of the population regression coefficients was not zero. Multiple Regression Method is used to determine the correlation between a criterion variable and a combination of predictor variables. It was established that the surface roughness is most influenced by the feed rate. By using Multiple Regression Method equation, the average percentage deviation of the testing set was 9.8% and 9.7% for training data set. This showed that the statistical model could predict the surface roughness with about 90.2% accuracy of the testing data set and 90.3% accuracy of the training data set.

In their research Nurul Amin et al. (2007), H.C.D. Mohd Radzi et al. (2009), have focused on developing an effective methodology to determine the performance of uncoated WC-Co inserts in predicting minimum surface roughness in end milling of titanium alloys Ti-6Al-4V under dry conditions. Central composite design of response surface methodology is employed to create an efficient analytical model for surface roughness in terms of cutting parameters: cutting speed, axial depth of cut, and feed per tooth. Design of expert package was applied to establish the first order and the second order model and develop the contours. The adequacy of the predictive model was verified using analysis of variance.

In their research, Kareem Saad et.al (2007) reported on statistical package for social sciences (SPSS), to predict surface roughness. Two independent data sets were obtained on the basis of measurement such as training data set and testing data set. Spindle speed, feed rate, and depth of cut are used as independent input variables (parameters) while surface roughness as dependent output variable. The multiple regression models by using SPSS could predict the surface roughness (Ra) with average percentage deviation of 7.8%, or 92.2%, accuracy from training data, and from testing data set that was not included in the multiple regression analysis with average percentage deviation of 11.95%, or accuracy of 88%, for 4-Flute end mill.

In their research, Zhang et al. (2007), reported on the Taguchi design application to optimize surface quality in a CNC face milling operation. The Taguchi design is an efficient and effective experimental method in which a response variable can be optimized, given various control and noise factors, using fewer resources than a factorial design. Confirmation tests verified that the Taguchi design was successful in optimizing milling parameters for surface roughness. Paulo Davim and Muthukrishnana (2009) studied the influence of cutting conditions on tool wear while turning metal matrix composites. Taguchi's design of experiment was followed and an orthogonal array and ANOVA were used to investigate the cutting parameters. These correlations were obtained by multiple linear regressions and finally confirmation tests were performed to compare the results of experiments and correlations. Janez Kopac et al. (2002) determined optimal cutting conditions for

achieving desired surface roughness with a minimal number of experimental runs. The results revealed the fact that the majority of machining processes are performed outside the optimal cutting conditions, which has an essential impact on the process efficiency and the direct costs of machining.

Baji et al. (2009) presented a study on the influence of cutting parameters on surface roughness of steel work-piece in face milling operation. The RSM based on the rotatable central composite design (RCCD) has been used together with an analysis of variance (ANOVA) and regression analysis. To obtain the minimal value of surface roughness, the surface roughness equation has been optimized by finding the partial derivatives and solving the system of equations. A comparison of results obtained by means of the Taguchi method with the regression model was carried out. Hae-Sung Yoon et al. (2014) used RSM technique in face milling operation and concluded that material-removal power increased with the feed rate, spindle speed, and depth of cut. The material-removal power was found to consist of ~7.6% of the total power consumption. A model for surface roughness prediction using the RSM by combining its methodology with factorial design of experiments has been developed by (Choudhury et al.1997).

Asif Iqbal et al. (2007) focused on the enhancement of tool life and surface finish using ANOVA, optimization module and prediction module. The proposed expert system could able to recommend helix angle of the tool, milling orientation and also could predict tool life, surface roughness and cutting force for a high speed milling operation. Optimization module provided the selection of milling parameters according to the desired objective while the prediction module provided the prediction of performance measures for the combination of parameters finalized by the optimization module. Julie et al. (2007) presented Taguchi design to optimize surface quality in a CNC face milling operation. The authors conducted experiments based on orthogonal array design and analyzed using ANOVA and finally verified by conducting the confirmation tests that the Taguchi design was successful in optimization for surface roughness. Oguz Colak et al. (2007) used Gene Expression Programming (GEP) method for predicting surface roughness of milling surface with

cutting parameters. The author claimed 91 % predicting accuracy level of the proposed GEP method over the method of experimental data. Omar et al. (2007) introduced a generic and improved model to simultaneously predict the cutting force and the surface quality during side milling operation. The authors incorporate the effects of tool run out, tool deflection, system dynamics, flank wear and the tool tilting on the surface roughness. They also presented a technique to calculate the instantaneous chip thickness and finally found that the prediction model agreed well with the experimental results.

Hun-Keun Chang et al. (2007) proposed a real time surface roughness prediction method using a sensor system. Surface roughness was measured based on the relative motion between tool and work piece using Cylindrical Capacitive Displacement Sensor (CCDS). A simple linear regression model was developed to predict surface roughness using the measured signals. The close relation between the machined surface and the roughness predicted was found to be about 95%. Ghassan et al. (2007) proposed machine vision-based topography for surface roughness measurement and compared the same with the stylus-based measurements. Results showed that intensity-topography compatible model gives more superior results compared to the light-diffuse model with close values to the traditional stylus-based data.

Babur Ozcelik et al. (2005) developed a statistical model based on RSM for surface roughness estimation in a high-speed flat end milling process. The author found that the estimation capability of the first and second order models developed using experimental results were observed to be in good fit with the actual measured values.
Suresh Kumar et al. (2005) investigated the role of solid lubricant assisted machining on surface quality and cutting forces. ANOVA has been performed to find the influence of different factors on surface finish. The results indicated that there is a considerable improvement in the process performance with solid lubricant to that of machining with cutting fluids. Palani Kumar et al. (2013) assessed the influence of machining parameters on the machining of glass-reinforced polymer composite material. Full factorial design was used for experimentation and assessed using

response table, response graph, normal probability plot, interaction graphs and ANOVA technique. Cheng et al. (2008) presented a theoretical and experimental analysis of nano-surface generation in ultra-precision raster milling. An optimization system was established for optimizing the cutting conditions and a series of experiments were also conducted. The results show that the theoretical model has predicted well the trend of variation of surface roughness under various cutting condition and cutting strategies. Sahoo et al. (2008) developed fractal dimension models for the surface topography in CNC end milling of three different material using RSM. The investigation indicated that the cutting parameters and their interactions influence the surface topography. The other attempt was to estimate optimum machining conditions for producing best possible surface with minimum fractal dimension which greatly depends on specific tool-work piece material combination.

Paulo Davim et al. (2004) studied the influence of cutting parameters on surface roughness in Medium Density Fibreboard (MDF) milling. The milling tests showed the importance of cutting speed on the evolution of the surface roughness as a function of Material Removal Rate (MRR). Yung-Kuang et al. (2007) applied design of experiments to optimize parameters in end milling high-purity graphite under dry machining. Dimensional accuracy and surface roughness were studied. Mathematical predictive model was developed using regression analysis. The feed rate was found to be the most significant factor and for a low feed rate, it increased the flank wear of the tool but improved surface quality.

Ghani et al. (2004) used orthogonal array, signal-to-noise ratio and Pareto ANOVA to analyze the effect of milling parameters on surface finish and cutting force. The study proved that the Taguchi method is suitable to solve the stated problem with minimum number of trails as compared to full factorial design. Lamikiz et al. (2004) proposed a model to estimate the cutting forces in inclined surfaces machined both up milling and down milling on aluminium alloy and tool steel. Validation tests were carried out on different slopes and machining conditions. The results provided errors below 10% and both the value and shape of the predicted forces matched with the measured cutting

force. Ming-Yung Wang et al. (2004) analyzed the influence of cutting condition and tool geometry on surface roughness in slot end milling. Surface roughness models for both dry and coolant cutting were built using RSM and experiments. Surface roughness generally increases with increase in feed, concavity and axial relief angles, while concavity angle is more than 2.5.

Tongchao et al. (2010) established empirical models for cutting force and surface roughness in milling using four factor-four level orthogonal experiments. The results of ANOVA indicated that the linear model best fits the variation of cutting force while the quadratic model best described the variation of surface roughness. Surface roughness under some cutting parameters is less than 0.25 μm which showed that finish milling is an alternative to grinding process in die and mold industry. Franco et al. (2008) studied the influence of back cutting on the surface finish obtained by face milling operations. The surface roughness was modeled from the perspective of tool run outs and height deviations which affects the surface marks provoked by back cutting. The author claimed to obtain good results when experimental observations were compared with the theoretical model predictions.

2.6.2 Prediction Of Surface Roughness Using Artificial Neural Network

Patricia et al. (2009), implemented different artificial neural network models (ANN) for the prediction of surface roughness (Ra) values in Al alloy 7075-T7351 for face milling machining process. The radial base (RBNN), feed forward (FFNN), and generalized regression (GRNN) networks were selected, and the data used for training these networks were derived from experiments conducted using a high-speed milling machine. From this study, the performance of each ANN used in this research was measured with the mean square error percentage and it was observed that FFNN achieved the best results. Also the Pearson correlation coefficient was calculated to analyze the correlation between the five inputs (cutting speed, feed per tooth, axial depth of cut, chip width, and chip thickness) selected for the network with the selected output (surface roughness). Results showed a strong correlation between the chip thickness and the surface roughness followed by the cutting speed. In Alam et al. (2010), machining process parameters of NC milling such as speed, feed rate, and

depth of cut were used to predict surface roughness. In the paper, the quadratic prediction model was coupled with GA to optimize the machining process parameters for minimum surface roughness. Chandrasekaran et al (2010). reviewed the application of soft computing tools such as neural networks, fuzzy sets, genetic algorithms, simulated annealing, ant colony optimization, and PSO to various machining processes like turning, milling, drilling, and grinding. The authors highlighted the progress made in this area and discussed the issues that need to be addressed. Del Prete et al. (2010) developed a prediction model for surface roughness in flat end mill operation using RSM. ANN was used to predict surface roughness and GA was employed to optimize the surface roughness model. By coupling developed an RS model with GA, the optimization methodology is effective and can be effective if the developed RS model is accurate. (Benardos et al. 2010) presented NN modeling approach for the prediction of surface roughness in CNC face milling. ANN based procedure predicted the surface roughness with a mean error of 1.86% and was found to be consistent throughout the entire range of values. Kadirgama and Noor et. al. (2008) highlighted the optimization of the surface roughness when milling aluminium alloys (AA6061-T6) with carbide coated inserts using response surface method (RSM) and Radian Basis Function Network (RBFN) to predict thrust force and surface roughness. Kechagias (2011) brought out the influence of cutter geometry and cutting parameters during end-milling on the surface texture of aluminium alloy.

Baji et al.(2008), presented influence of cutting parameters on surface roughness in face milling. Cutting speed, feed rate and depth of cut have been taken into consideration as the influential factors. In order to obtain mathematical models that are able to predict surface roughness two different modelling approaches, namely regression analysis and neural networks, have been applied to experimentally determined data. Obtained results have been compared and neural network model gives better explanation of the observed physical system. GA optimization technique was used by Palanisamy et al. (2007) to find the most optimal process parameters of end milling machining such as cutting speed, depth of cut and feed rate. The objective function considered in this study was machining time.

In their research, H. S. Lu et al. (2008), focused on optimal cutting in side milling. The fuzzy logics tools were applied to perform the optimization procedure with complicated multiple performance characteristics. Using this approach combined with the grey-relational analysis, the design algorithm is transformed into optimization of a single and simple grey-fuzzy reasoning grade rather than multiple performance characteristics. The Taguchi method was also adopted to search for an optimal combination of cutting parameters for this rough cutting process in side milling. The improvement of tool life and metal removal rate from the initial cutting parameters to the optimal cutting parameters were 54% and 9.7%.

Oktem et al. (2005) focused on the development of an effective methodology to determine the optimum cutting conditions leading to minimum surface roughness in the milling of mold surfaces by coupling Response Surface Methodology (RSM) with a developed Genetic Algorithm (GA). An effective fourth order Response Surface (RS) model is developed involving parameters namely feed, cutting speed, axial depth of cut, radial depth of cut and machining tolerance. RS model is further interfaced with the GA to optimize the cutting conditions for desired surface roughness.

In their research, Ship-Peng Lo et al. (2003), presented an adaptive-network based fuzzy inference system (ANFIS) used to predict the workpiece surface roughness after the end milling process. Three milling parameters that have a major impact on the surface roughness, including spindle speed, feed rate and depth of cut, were analyzed. The predicted surface roughness values derived from ANFIS were compared with experimental data. The comparison indicates that the adoption of both triangular and trapezoidal membership functions in ANFIS achieved very satisfactory accuracy. Yu Hsuan et al. (1999) developed an in-process based surface recognition system to predict the surface roughness in the end milling process. A back propagation artificial neural network model was developed by using spindle speed, feed rate, depth of cut, and the vibration average per revolution as four input neurons to predict surface roughness. Babur et al. (2005) employed feed forward artificial neural network to predict surface roughness in terms of cutting parameters such as cutting speed, feed

rate, depth of cut and material removal rate and further optimized to obtain minimum surface roughness by genetic algorithm.

In their research, P.G. Benardos and G.C. Vosniakosa, et al. (2002), presented a neural network model approach for the prediction of surface roughness (Ra) in CNC face milling. The factors considered in the experiment were the depth of cut, the feed rate per tooth, the cutting speed, the engagement and wear of the cutting tool, the use of cutting fluid and the three components of the cutting force. Using feed forward artificial neural networks (ANNs) trained with the Levenberg Marquardt algorithm, the most influential of the factors were determined.

In their research, Lee and Chen (2003), highlighted on artificial neural networks (OSRR-ANN) using a sensing technique to monitor the effect of vibration produced by the motions of the cutting tool and work piece during the cutting process. It was an on-line surface recognition system. In their research, Choudhury and Bartarya (2003) focused on design of experiments and the neural network for prediction of tool wear. The input parameters were cutting speed, feed and depth of cut; flank wear, surface finish and cutting zone temperature were selected as outputs.

Yongjin et al. (2002) used fuzzy adaptive modeling technique to predict surface roughness. The approach completely eliminated the expensive and time consuming experimental data and also avoided empirical equations, as they are sensitive to specific domain applications. Shinn-Ying et al. (2005) proposed ANFIS to establish the relationship between the surface image and the actual surface roughness. Based on this approach, surface roughness can be predicted using the optimal cutting parameters. Experimental results showed that the proposed ANFIS-based method outperforms the existing polynomial network-based method in terms of modeling and prediction accuracy. Risbood et al. (2003) explored the possibility of predicting surface finish and dimensional deviation by measuring forces and vibration using neural networks. Benardos et al. (2003) presented the various methodologies and practices employed for the prediction surface roughness. Each approach with its merits and demerits were outlined. The present and the future trends were also discussed. The approaches were discussed based on machining theory, experimental

investigations, design of experiments and AI. In this study, surprisingly, a combined effort of both AI and analytical modeling to validate the theoretical models was not found in the literature. Tandon et al. (2002) implemented PSO to optimize machining parameters of milling accompanied by ANN for predicting cutting forces. Both feed and speed were considered during optimization but depth of cut was not considered in the optimization problem. Jorge et al. (2002) estimated the forces developed during milling using two supervised neural networks. Verification experiments were conducted to evaluate these two models. Radial basis network is shown to be superior than back propagation networks. Ship-Peng Lo (2003) presented an Adaptive Network based Fuzzy Inference System (ANFIS) for predicting surface roughness in end milling process. While comparing with the experimental data, the author found that the prediction accuracy reached as high as 96%.

Brezoenik et al. (2004) proposed Genetic programming to predict surface roughness in end milling. Prediction accuracy of surface roughness by the developed model was very good for both the training and tested data set. Hasan Oktem et al. (2005) coupled RSM with GA to determine the optimum cutting conditions to get minimum surface roughness in milling of mold surfaces. The proposed GA was able to reduce the roughness value in the mold cavity from 0.412 µm to 0.375 µm. Hasan Oktem et al. (2005) determined best cutting parameters to minimize surface roughness in end milling by coupling design of experiments, NN and GA. Erzurumlu et al. (2007) developed RSM and ANN model to predict surface roughness on mold surfaces. The RSM model and ANN are compared based on computational cost, cutting forces, tool life and dimensional accuracy and it is found that the maximum test errors were 2.05% and 1.48% respectively. El-Sonbaty et al. (2008) developed an ANN model for the analysis and prediction of cutting conditions for achieving specific surface roughness profile. The input parameters are the rotational speed, feed, depth of cut, pre-tool flank wear and vibration level. The predicted profiles exhibited more details than the actual measured roughness profiles. Vedat Savas and Cetin et al. (2008), presented GA for optimization of cutting parameters leading to minimum surface roughness in the milling process. It is concluded that GA prediction has errors in the measurement regions between 2-7%. Vimal et al. [79] realized the need for

personalized products in satisfying the ever-growing needs of the consumer. This research provided a predictive model using design of experiments strategy to obtain optimized machining parameters using GA for a specific surface roughness in ball-end machining of polypropylene, with an accuracy of 91.57%. Chen Lu (2008) reviewed the advantages and disadvantages of various methodologies that were employed to predict surface roughness. The author revealed that the main advantages of AI approaches were that the models created seem to be the most realistic and accurate and further added the dominance of ANN as a powerful tool, easy to use and have a good prospect for the future application.

Zain et al. (2010) applied GA to find optimal cutting conditions for obtaining minimum surface roughness. The analysis of the study proved that GA technique performed better than experimental sample data, regression modeling and RSM. Wen-Hsien et al. (2009) used ANFIS with GA to predict the surface roughness in end milling process. The authors have also used Hybrid Taguchi-Genetic Learning Algorithm (HTGLA) in ANFIS to determine optimal parameters to minimize error. Experimental results showed that the prediction error of the HTGLA based ANFIS approach is 4.06%, which outperformed the prediction error 4.17% from ANFIS method given in the Matlab toolbox. Eyup Sabri [87] discovered the role of step over ratio in surface roughness prediction studies of end milling operations. Experiments were conducted and two ANN structures were constructed; one with considering step over ratio and the other without considering step over ratio. Average RMS error of the ANN model considering step over ratio is 0.04 and without considering is 0.26. Devi Kalla et al. (2010) studied the machining of carbon fiber reinforced polymers in a helical end mill and developed a methodology for predicting the cutting forces by transforming specific cutting energies from orthogonal to oblique cutting. Predictions were in good agreement with the experimental data in unidirectional laminate but lesser agreement in multidirectional laminate. Ilhan Asilturk (2011) implemented full factorial design of experiment to increase the confidence limit and reliability of the experimental data during turning. The authors compared the multiple regressions and neural network based models with the statistical methods and found that ANN model could estimate with higher accuracy when compared to the other methods. Azlan Zain

et al. (2010) discussed the utilization of ANN for predicting the surface roughness in the milling process. Based on the experiments conducted, the author concluded that the use of high speed and low feed and rake angle is highly recommended for better surface finish. The authors have suggested that AI approaches have the potential to be applied for optimization problems. Lou and Chen (1999) developed an in-process surface recognition system that measures surface roughness during end-milling. The framework of the system is based on an intelligent hybrid software-fuzzy-nets as well as an hardware components consisting of a sensor tested, which assesses the real-time surface of a work piece with which information on the achievement of quality standard could be met.

Oktem et al. (2006) reported an approach to determining the best cutting parameters, leading to minimum surface roughness in end-milling mould surfaces of an Ortiz part, which is commonly used in biomedical applications by coupling neural network and genetic algorithm. These two artificial intelligence techniques were then fused to design of experiments for optimization purposes. Experimental data and more extensive data were utilized to validate the work. It was concluded by the authors that experimental data predicted values agreed.

2.6.3 Neural Networks V/S Statistical Techniques

As a forecasting tool, ANN can be compared to Autoregressive moving Average (ARMA) class of models. ARMA methods, since ages have been used to model time series. In general, similarities do exist between the ANN and statistical techniques. An FFNN can be termed as a form of non-liner regression (Ripley 1994, Potzinger et al. 2000). A multiple linear regression scheme, a standard statistical tool, can be thought of as a simple ANN node. For example, for a linear equation of the type, $y = w_0 + w_1x_1 + w_2x_2 + \ldots\ldots\ldots + w_nx_n$, the x_i can be taken to represent the inputs to the node, wi can be taken as the corresponding weights and w0 can be the threshold function.

While fitting the ARMA type of model to a time series, the data has to be stationary and must exhibit normal distribution. If indeed, that is not the case, then techniques have to be used to induce stationary data and normally distribute the data. In case of

ANN, the statistical variation of data is immaterial, as the hidden neurons account for non stationarities in the data (Reddy 2004). An ANN also possesses another advantage over ARMA type models as it is a non-linear model, though some non-linear ARMA type models are witnessed in literature in statistics. ANNs are most ideally suited for mapping complex relationships between input-output and where the relationships are not clearly understood, either due to no proper relationship being there or inadequate data. Furthermore, ANN can make an n-step ahead forecast directly without any recursive procedure. Due to its inherent robustness in design which can be attributed to massive parallel processing, the ANNs are good modelling tools for real life problems, in which data may be inadequate, may be available with a lot of noise, and there could be distortions in data.

The ANNs have been rigorously compared with statistical methods for applications pertaining to classification and prediction (Ripley 1994). Effectiveness of ANN in time series forecasting have been examined. Lapedes and Farber (1988) have shown that in two time series prediction problems, neural networks are clearly superior to statistical methods.

Sharada and Patil (1994) analysed 75 different time series problems and inferred that the ANN and Box-Jekins forecasting system performed equally. Interestingly, it has been observed that the memory of a time series has some bearing on the performance. ANN performs slightly better than Box_Jekins model for time series with short memory while reverse is true for time series with long memory.

One of the major demerits of the artificial neural network is that unlike the statistical methods wherein the entire functioning of the model is transparent, the working of an ANN is opaque. What exactly happens inside the hidden layers is not visible although the output of the model is obviously useful. In artificial neural nets the functioning of the hidden neurons once they are trained is not clearly understood (Fraser 2000). Which of the neuron fires or why it fires is as mysterious as it was in the early days of research in neural computations. Moreover, a trained ANN serves a model for a particular problem, while there are set procedures or frameworks for selection of a

fitment model in statistical techniques. Some disadvantages of ANN have been highlighted by Maier and Dandy (1999). First of all, the architecture, learning rate parameter (η) and momentum factor (α), which are functional parameters of an ANN are dependent on the problem at hand. There are no guidelines as to what architecture or what learning rate and momentum factor should be used for a particular problem. Each problem attempted by ANN is unique and all the function parameters are likely to be unique for that problem. The entire training process is a trial and error process with different combinations of number of hidden layers, number of neurons in each hidden layer, learning rate parameter and momentum factor. Another problem with ANN is that many a times, the data available to train the network isn't sufficient enough to be able to bring the generalisation of the model. Also in a system which is quite responsive to changes in the environment, ANN modelling may not be appropriate as the network may not be able to cope up to the changes taking place. For example, the networks when trained on static (past data) data may not be able to lend results for future, unless the weight matrices are updated or adjusted with suitable learning, to understand the new changes in the system.

A lot of study has been done on artificial neural networks and the regression methods to determine the suitability of these models for pattern mappings (Kim et al. 1993, Patuwo et al. 1993, Subramanian et al. 1993, Yoon et al. 1993 and Potts 2000).

Thus it can be summarised that

- ANN can learn the relationship between input-output patterns and can generalise the relationship.
- They can handle a wide variety of data.
- They are universal approximators.
- No assumptions are required to be made in understanding relationships.
- The type or in general, the details of the process need not be known to frame an ANN model.
- Rigorous mathematical treatment is not required

All things put together, in actual practical situations, a trained ANN model has proved to be a success, complementing human brain decision making.

2.6.4 Optimization Of Parameters Based On AI

Abellan et al. (2008) have proposed new methodology based on AI techniques. The overall desirability function has increased up to 0.520. He mentioned the improvement is due to two effects: (1) the ANN process models deal with non-linearity so these models are more accurate than response surface models for modelling high quality machining operations; (2) the on-line nature of the methodology lets adapt the cutting parameters every cutting pass so the system is more flexible to adapt any change in the objective function during the cutting-tool life-cycle. Rodolfo et al. (1996) presented an intelligent supervisory system from a model-based approach. They applied their system as a case study for predicting tool wear in machining processes. Rodolfo et al. (2007) represented Fuzzy logic-based torque control system for milling process optimization. Shaw Wong et al. (2003) investigated the feasibility of using a neural network to represent machinability data. In order to predict optimum machining parameters under different cutting conditions, they used the feed forward neural network. They developed and implemented an object-oriented neural network-handling library in the milling process.

García-Plaza et al. (2013) studied the contribution of cutting force, mechanical vibration and emission acoustic signals for the on-line monitoring and diagnosis of the surface finish (Ra) in automated taper turning operations. Systems design was based on predictive models obtained from regression analysis and artificial neural networks, involving numerical parameters that characterize cutting force signals, mechanical vibration, and acoustic emission. Cutting force (Fx, Fy, Fz) signals were the most significant, and were the primary means for estimating the arithmetic mean roughness (Ra). The models based on these signals provided the best fit and highest predictions, with the lowest mean relative prediction errors. In comparison, the machine vibration signals, and the acoustic emission signal had little influence on the Ra roughness parameter, and failed to provide relevant data on their own; notwithstanding, these signals can slightly improve the performance of predictive models when combined with cutting force signals.

2.7 SELECTION OF OPTIMAL MACHINING PARAMETERS

Baskar et al. (2005) implemented various operations research techniques such as GA, Tabu search (TS) algorithm, ACO and PSO for optimizing machining parameters of multi-milling operation. The authors concluded that PSO algorithm always yields best result when compared to other algorithms and handbook recommendations. Wang et al. [26] presented a hybrid of SA and GA optimization technique to select the optimal machining parameter for multi-pass milling operations. This approach used the strengths of SA and GA and overcame their weakness. It is evident from the results that this hybrid approach was more effective than conventional methods. Indrajit Mukherjee et al. (2006) appraised the application potential of several modeling such as statistical regression technique, ANN, Response Surface Methodology (RSM) etc., and optimization techniques such as SA, GA and TS algorithm in metal cutting processes. Ramon et al. (2006) used GA for optimizing cutting parameters and made a remark on the advantages of multi-objective optimization approach over single objective function. An application sample was developed and its results were analyzed for different machining conditions. Tansel et al. (2006) proposed Genetically Optimized Neural Network System (GONNS) for the selection of optimal cutting condition in machining. Optimal operating conditions were calculated to obtain the best possible compromise between roughness of machined surface and the duration. Baskar et al. (2006) developed GA, Hill Climbing Algorithm (HCA) and Memetic Algorithm (MA) to find optimum cutting parameters for multi-tool milling operations like face milling, corner milling, pocket milling and slot milling. Significant improvement was observed in using these techniques when compared to handbook recommendations and method of feasible direction.

Franci Cus et al. (2003) proposed ANN to optimize cutting parameters for machining operation. The objective was to increase the productivity and reduce the production cost. Raid Al-Aomar et al. (2006) used GA to determine near optimal settings to both machining and production process parameters so that the overall per order production cost is minimized. The experimental results and the sensitivity analysis showed the robustness of the proposed GA. Suresh et al. (2002) dealt with the study and

development of surface roughness prediction model for machining mild steel using RSM. GA was used to give minimum and maximum values of surface roughness and their respective optimal machining conditions.

Zarei et al. (2009) presented a Harmony Search (HS) algorithm to determine optimum cutting parameter for multi-pass face milling. GA was used to solve the same problem. Comparison of results revealed that the HS algorithm could obtain optimum solution with higher accuracy when compared to GA. Venkata Rao et al. (2010) applied Artificial Bee Colony (ABC), PSO and SA algorithm for parameter optimization of a multi pass milling process. Minimization of production time was the objective considered subjected to various constraints. The accuracy and quick convergence to global optimum solution of ABC and PSO were very high as compared to SA algorithm.

Zain et al. (2009) have incorporated Genetic Algorithm (GA) to find the optimal cutting conditions for acquiring better surface finish in milling process and concluded that good surface finish can be obtained at high speed, high rake angle and low feed rate. Benardos et al. (2002) have included the ANN technique in the study to predict surface roughness value. The authors concluded that the mean error of 1.86% obtained by using ANN seemed to be consistent throughout the range of values. In their research, Ab. Rashid et al. (2009), presented the development of mathematical model for surface roughness prediction for the milling process in order to evaluate the fitness of machining parameters namely spindle speed, feed rate and depth of cut.

2.8 PARTICLE SWARM OPTIMIZATION

This approach is a meta-heuristic method and evolutionary computational algorithm. PSO has been adopted by many researchers in different engineering problems all around the world. The main advantage of this technique is very simple. Easy to apply, less time consuming compared to other computational algorithms with high efficiency. PSO was first introduced by Eberhart and Kennedy in the year 1995 (Yu et al. 2004). PSO is applied to optimize the thermally assisted machining process parameters. Sarah et al. (2010) used PSO technique in the pulp industry to get

optimal solution in terms of resource utilization and wastage of the finished paper. The experimental results were compared with both genetic algorithm (GA) and PSO. PSO gave the better computational efficiency with less time than GA. Lee and Ponnambalam (2012) performed PSO and GA multi objective optimization of turning process. These two techniques show similar trend in pareto optimal fronts but PSO produced optimal solution with less time compared to GA. Ciurana et al. (2009) performed the experiments on Nd: YAG laser system on AISI H13 hardened tool steel for making mould cavities and implemented a model for volume error, machining time and surface roughness by using ANN and PSO techniques and concluded that PSO is suitable to identify the optimum process parameters.

Zuperl et al. (2007) employed PSO to optimize process parameters of milling machining. A predictive model was developed using ANN to predict the cutting forces during machining and PSO was used later to obtain optimal process parameters of milling machining such as cutting speed and feed rates. The results were compared with other evolutionary techniques such as GA and SA and proved that the proposed technique improved the quality of the solution while speeding up the convergence process. A new technique has been proposed by Huang et al. (2002) by using the combination of wavelet neural network (WNN) algorithm and modified PSO for solving tool wear detection and estimation. By using the Daubechies-wavelet, the cutting power signal is decomposed into approximation and details. The energy and square-error of the signals in the detail levels is used as characters which indicate tool wear. The characters are input to the trained WNN to estimate the tool wear. The results of the experiments were compared with BP neutral network, conventional WNN and GA-based WNN. The results showed a faster convergence and more accurate estimation of tool wear. The process parameters of milling operation such as spindle speed and feed rate were considered to be optimized in the study (Li et al. 2008). The considered machining performances were cutting force, tool-life, surface roughness and cutting power. An algorithm for process parameters optimization known as cutting parameters optimization (CPO) was introduced and PSO technique was employed to optimize the process parameters. From the experimental results, the authors concluded that PSO in optimizing process parameters can converge quickly to

a consistent combination of spindle speed and feed rate. The optimization of process parameters for constant cutting force was discussed based-on virtual machining (Zhao et al. 2008). PSO was employed to find the optimal process parameters (spindle speed and feed rate). The framework of virtual machining based cutting parameters optimization was established.

Prakasvudhisarn et al. (2009) illustrated with process parameters of CNC end milling namely feed rate, spindle speed, and depth of cut to find the minimum surface roughness. Support vector machine (SVM) was proposed to capture characteristics of roughness and its factors. PSO technique is then employed to find the combination of optimal process parameters. The results showed that cooperation between both the techniques can achieve the desired surface roughness and also maximize productivity simultaneously. Razfar et al. (2010) proposed a PSO-based neural network to create a predictive model for the surface roughness level that is based on experimental data collected on face milling X20Cr13 stainless steel. The optimization problem is then solved using a PSO-based neural network for optimization system (PSONNOS). A good agreement is observed between the predicted surface roughness values and those obtained in experimental measurements performed using the predicted optimal machine settings. The PSONNOS is compared to the GA optimized neural network system (GONNS). Farahnakian et al. (2011) considered the effect of process parameters of high speed steel end mill such as spindle speed and feed rate. Nanoclay (NC) content on machinability properties of polyamide-6/nanoclay (PA-6/NC) nanocomposites was studied for modeling cutting forces and surface roughness by using PSO-based neural network (PSONN). The obtained results for modeling cutting forces and surface roughness also showed a remarkable training capacity of the proposed algorithm compared to the conventional neural network. Yang et.al (2011a) proposed a methodology called fuzzy PSO (FPSO) algorithm to distribute the total stock removal in each of the rough passes and the final finish pass based on fuzzy velocity updating strategy to optimize the machining parameters implemented for multi-pass face milling. The optimum value of machining parameters including number of passes, depth of cut in each pass, speed, and feed are obtained to achieve minimum production cost. The proposed methodology for distribution of the total

stock removal in each of the passes is effective, and the proposed FPSO algorithm does not have any difficulty in converging towards the true optimum. From the given results, the proposed schemes may be a promising tool for the optimization of machining process parameters. Also in Yang et al. (2011b) the researchers proposed fuzzy global and personal best-mechanism-based multi-objective PSO (F-MOPSO) to optimize the machining parameters in multipass face milling. It was found that the F-MOPSO does not have any difficulty in achieving well-spread Pareto optimal solutions with good convergence Chandrasekaran et al. (2011) have given the overall history and the application of soft computing technique in machining performance prediction and optimization.

Table 2.2: Papers Referred On PSO Techniques

SL. NO	Authors	Input Parameters	Operation	Output Parameters	Remarks/ Conclusion
1	Farahnakian et al. (2011)	Cutting speed, feed depth of cut	End milling	Cutting forces and surface roughness	A very good training capacity of the proposed PSONN algorithm
2	Yang et al.(2011a)	Number of passes, depth of cut in each pass, speed, and feed	Multi-face milling	Production cost	The proposed schemes may be a promising tool for the optimization of machining process parameters.
3	Yang et al.(2011b)	Number of passes, depth of cut in each pass, speed, and feed	Multi-pass face milling	Production cost	The F-MOPSO does not have any difficulty in achieving well-spread Pareto optimal solutions with good convergence to true Pareto optimal front for multiobjective optimization problems.
4	Razfar et al.(2010)	Cutting speed, feeddepth of cut, engagement	Face milling	Surface roughness	A good agreement is observed between the values predicted by the PSONNOS algorithm and experimental measurements.
5	Rao and Pawar (2010b)	Number of passes, depth of cut, cutting speed and feed	Multi-pass milling	Production time	The results are compared with the previously published results obtained by using other optimization techniques.

SL. NO	Authors	Input Parameters	Operation	Output Parameters	Remarks/ Conclusion
6	Escamilla et al. (2009)	Speed, feed and depth of cut	End milling	Surface roughness	PSO optimization it can be successfully applied to multiobjective optimization of titanium's machining process.
7	Prakasvudhisarn et al. (2009)	Speed, feed and depth of cut	CNC end millling	Surface roughness	Both techniques can achieve the desired surface roughness and also maximize productivity simultaneously.
8	Li et al. (2008)	Spindle speed, feed rate	Milling	Cutting force, tool-life, surface roughness and cutting power.	PSO in optimizing process parameters can converge quickly to a consistent combination of spindle speed and feed rate.
9	Zhao et al. (2008)	Spindle speed and feed rate.	Milling	Cutting forces	The machining process with constant cutting force can be achieved via process parameters optimization based on virtual machining.
10	Zuperl et al. (2007)	Cutting speeds and feed rates	Milling	Cutting forces	Compared with GA and SA the proposed algorithm can improve the quality of the solution while speeding up the convergence process.

SL. NO	Authors	Input Parameters	Operation	Output Parameters	Remarks/ Conclusion
11	Huang et al. (2007)	Spindle, Feed rate, width	End milling	Tool wear	Tool wear
12	Rashmi et al. (2016)	Spindle speed, Feed rate and Depth of cut	Face Milling	Cutting force, surface roughness and power consumption	Compared with RSM, Desirability approach and the proposed PSO algorithm attained the effective results. PSO optimization it can be successfully applied to multiobjective optimization of AA6061-4.5%Cu-5%SiCp machining process.
13	Z.G. Wang et al.	Cutting speed (m/min) Feed rate (mm/rev) machining time (min)	multi-pass milling.	Four typical runs at different depth of cut	PGSA is shown to be more suitable and efficient for optimizing the cutting parameters for milling operation than GPCDP and PGA.
14	S.Bharathi Raja et al. (2010)	Cutting speed (rev/min), Feed (mm/min), Depth of cut(mm), Machining time	Face Milling	Desired Surface Roughness in minimum machining time	It has been found that the predicted roughness using PSO is in good agreement with the actual roughness.

SL. NO	Authors	Input Parameters	Operation	Output Parameters	Remarks/ Conclusion
15	F. Cus et al. (2008)	Cutting Speed and Fee Rate	End Milling	Optimum Cutting Speed and Feed Rate and Cutting Force	The simulation results show that compared with genetic algorithms (GA) and simulated annealing (SA), the proposed algorithm can improve the quality of the solution while speeding up the convergence process. PSO is proved to be an efficient optimization algorithm.
16	F. Cus et al. (2003)	Cutting Speed and Fee Rate	End Milling	Surface Roughness and MRR	PSO is proved to be an efficient optimization algorithm. The experimental results show that the MRR is improved by 28%. Machining time reductions of up to 20% are observed.
17	Prakasvudhisarn et al. (2009)	Cutting speed, Feed Rate, Depth of cut	End Milling	Surface Roughness	SVMs and PSO techniques were implemented. The cooperation between both techniques can achieve the desired surface roughness and also maximize productivity simultaneously.

SL. NO	Authors	Input Parameters	Operation	Output Parameters	Remarks/ Conclusion
18	Tandon, V et al. (2008)	Cutting Speed and Fee Rate	End Milling	Optimum Cutting Speed and Feed Rate and Cutting Force	ANN was implemented to predict cutting force and PSO to identify optimum speed and feed rate. Machining time reductions of up to 35% are observed. In addition, the new technique is found to be efficient and robust.
19	R. Venkata Rao et al. (2010b)	Number of passes, depth of cut for each pass, cutting speed, and feed.	Milling	Minimization of Production Time	ABC, PSO and SA are implemented. The comparison between these 3 techniques have been made and concluded that ABC and PSO perform better compared to SA.
20	M.Chandrasekaran et al. (2010)	N/A	Milling, Turning, Grinding.	Machining Performance prediction and optimization	Discussed the overall history of the application of soft computing technique in machining performance prediction and optimization.

Table 2.3: Papers Referred On Surface Roughness

Author	Year	Operation and parameter	Prediction model	% Of Prediction
Dong-Hyeon	2014	Laser assisted milling of Inconel 718 and AISI 1045 Steel. Speed, feed and depth of cut.	Box-Behnken (RSM)	6% error
AntoniWibowo	2012	End mill with 3 type of tool. Speed, feed and radial rake angle	KPCA based regression	43 % improve in the surface roughness
Luis Rubio	2013	Milling operation, 7 modules are used to select optimum cutting parameters.	Modular expert rule-based system in order to automatically select cutting parameters in milling operations.	Optimization
S. Ramesh	2012	Milling, material Ti–6Al–4V (grade-5)	Taguchi's orthogonal array to design the experiment and RSM is used to analyse the experiment and prediction.	The most influencing parameter was identified as the feed.
ZahiaHessainia	2013	Cutting speed, Feed rate, Depth of cut and tool vibration in radial and in main cutting force directions.	RSM	Only a small number of experiments are required to generate helpful information exploited for predicting roughness equations.
EtoryMadrilles Arruda	2014	The input parameters were the radial depth of cut, feed rate, and contact angle.	Taguchi method	feed rate can have a significant influence on the finishing.

Author	Year	Operation and parameter	Prediction model	% Of Prediction
TurgayKıvak	2014	The cutting tool, cutting speed and feed rate were selected as machining parameters	Linear and quadratic regression analyses were applied to predict the outcomes of the experiment	The feed rate was the most significant parameter for surface roughness with a percentage contribution of 82.38% and that the cutting speed was the most significant parameter for flank wear with a percentage Contribution of 49.33%.
K. Venkata Rao	2014	Milling operation, Speed feed doc and vibration signals	Feed forward 4 layered NN	4.59% error and The neural network can help in selection of proper cutting parameters to reduce tool vibration and tool wear and reduce Surface roughness.
NilrudraMandal	2013	Milling, Cutting speed, Feed, DoC	RSM design called central composite design (CCD).	Direct effect of cutting speed, depth of cut & cutting speed2 has maximum influence on the surface roughness.
P.G. Benardos	2002	depth of cut, the feed rate per tooth, the cutting speed, the engagement and wear of the cutting tool, the use of cutting fluid and the three components of the cutting force	Feedforward artificial neural networks (ANNs) trained with the Levenberg Marquardt algorithm	predict the surface roughness with a mean squared error equal to 1.86% and to be consistent throughout the entire range of values.

Author	Year	Operation and parameter	Prediction model	% Of Prediction
S. Bharathi Raja	2012	Face milling, cutting speed, feed, and depth of cut	ParticleSwarm Optimization (PSO)	In milling, use of higher cutting speed, lower feed rate and lower depth of cut are recommended to obtain better surface roughness for the given material. Feed rate has greater influence on surface roughness when compared to speed and depth of cut.
Fabrício José Pontes	2012	Turning	Radial Basis Function neural network	Results obtained show that RBF ANNs trained with only 30 examples can present mean value S. D. Ratio equal to 0.016409, for the worst case corresponding to a training set.

2.9 SUMMARY OF THE LITERATURE REVIEW AND RESEARCH GAP

The survey of literature on neural networks reveals the use of artificial neural networks in various applications ranging from speech recognition and image processing to robotics and material science. Moreover, the author has come across very few applications of recurrent neural networks and their variations in machining process. The FFNN presents a powerful tool for generalisation of relationships between inputs and outputs of a metallurgical process without a need to understand the intricacies of the process. A dedicated approach therefore needs to be undertaken to improve the usefulness of the research work carried out in milling (processing of composites). Further, the possibility of use of recurrent neural networks in processing of composites needs to be explored. In the present study neural network approach, inclusive of FFNN modelling and RNN modelling, towards process/system generalisation has been demonstrated. Moreover, the author has not come across the concept of reverse mapping in machining process for prediction of responses using neural network based approaches i.e (ANN and RNN).

From the literature review it can be inferred that

1. Numerous works have been carried out on modeling, considering cutting force, surface roughness and power consumption in CNC end milling process for various Aluminium alloys. But no work has been reported for the prediction and optimization of cutting force, surface roughness and power consumption in the case of AA6061 and AA6061-4.5%Cu-5%SiCp.
2. The model for predicting cutting force, surface roughness and power consumption has been evolved by most researchers based on machining parameters But fetching of cutting force via indirect approach and development of combination of both prediction and optimization models has not been addressed so far. The present study focuses on the development of ANN and RNN model by Forward and Reverse Mapping to simulate the relationship of milling process parameters and their influence on cutting force, surface roughness and power consumption. Even the optimization techniques

namely PSO, Grey relation analysis and Desirability approach have been incorporated in the study, for comparative study.

3. Applications of intelligent optimization technique like PSO to optimize process parameters namely, cutting force, surface roughness and power consumption have been tried out, as very little work is available. In the present work the comparison study has been made on the intelligent optimization technique and statistical techniques namely grey relation analysis and RSM techniques.

A lot of research articles are available on determining the optimal machining parameters using the evolutionary techniques such as GA, Fuzzy Logic and ANN. But most of the researchers concentrated on ANN to predict surface roughness by using different algorithms. But, very limited work has been carried out to predict the multi objectives (responses or output), comprising of cutting force, surface roughness, power consumption, material removal rate etc. In the present work, the PSO technique has been included to overcome the issues of the performance measures based on the multi-objective optimization in face milling or end milling operation.

The selected machining parameters play an imperative role in determining the product quality, reducing machining cost and increasing productivity. However, many of the techniques are not proficient in determining the global optimum solution. Inorder to overcome the issue of determining the global optimum solution the PSO optimization technique has been developed. Hence the PSO technique has been incorporated in the present study for optimizing the machining parameters.

Thus, in this study the PSO and Desirability approach are used to identify the machining parameters to obtain desired responses such as cutting force (FX), surface roughness (Ra) and power consumption. At the end of the study, the comprised model is validated with the help of the confirmatory experimental results.

Hence, in the present work both regression ,RSM, ANN and RNN models were developed to predict cutting force, surface roughness and power consumption in CNC face milling of AA6061 and AA6061-4.5%Cu-5%SiCp. A comparison has been made

between them to identify the best model for prediction. Using regression model, optimization of process parameters was carried out by applying optimization techniques like PSO. The results obtained from this PSO technique were compared with statistical techniques (Grey Relation and Desirability approach) and the best algorithm that can be used to get accurate result was identified. In the current work, surface topography AA6061 and AA6061-4.5%Cu-5%SiCp studies were carried out on the specimens to study the effects of process parameters like spindle speed , fee rate and depth of cut when they are kept at the minimum and maximum levels. Implementation of control strategy (Power and Force Control System by PID logic) for decreasing machining time and increasing productivity was achieved using software tool (LABVIEW). The idea behind selecting the different materials is to identify whether the developed model and the developed strategy work well with different materials thus enabling the decision support system to be more generic in application.

2.10 OBJECTIVES

Following objectives have been identified, as part of the development of an intelligent decision support system:

1. Comparative Study of various soft computing techniques for optimized prediction in CNC machining application, to identify the best suited technique.
2. Development of Hybrid Recurrent Neural Network model from an extended RNN (SRN) model for mimicking the process of milling of AA6061 and AA6061-4.5%Cu-5%SiCp composite to predict the responses and comparing the performance of HRNN model with reference to ANN models for its effectiveness.
3. Development of Reverse mapped neural network system for prediction of input parameters for CNC machining based on desired output measure using ANN and RNN.
4. Development of a GUI for integrated platform of task management, like prediction, material library, optimization etc…
5. Planning a strategy for better machine utilization based on power constraint in machining.

CHAPTER 3

EXPERIMENTAL METHODOLOGY

3.1 CONCEPT OF MACHINE UTILIZATION

The main concept in the present study is to increase the utilization of machine capacity. In the present scenario, even though machine has higher capacity to perform the machining operations, due to operator's lack of knowledge, the machines are run at sub-optimal conditions. Hence, it is desired to know the optimal machine capacity utilization based on the power consumption. For example, 5mm depth of cut can be achieved by removing material at spindle speed of 1000 rpm, feed rate of 300 mm/min and depth of cut 1 mm. The power consumed for each 1mm per pass is 0.6 kW and time required is 1minute. Therefore, 5 passes are required to achieve the desired depth of cut (5mm). Hence, the total power consumption required by all the 5 passes is 3 kW and the time required is 5minutes as depicted in Figure 3.1 (a-b).

Proposed research concept is, rather than removing 1 mm per (single) pass, 5mm material can be removed at each single pass as depicted in Figure 3.2. By using this concept the number of passes and the time required to remove the desired depth of cut (5mm) will be reduced with the power consumption being 1.8 kW. The total power consumption required to remove 5mm is 1.8 kW. The number of passes required is 1 pass and the time required is 1 minute to achieve the desired depth of cut of 5mm. Thus the total power consumed for specific pass might be more, but the total power consumption and the time required to perform the entire job is reduced i.e. 1.8kW(1 pass, 1minute, 5mm) in contrast to 3kW (5 passes, 5 minutes, 5mm). Thus the power consumed is 1.8 kW (For 1 pass) is lesser in contrast to 1mm depth of cut (For 10 passes, i.e. 3 kW).

In the present study, power consumption response is used as maximum capacity utilization criterion of CNC (Computer Numerical Control) machine (Fig 1(a-b)). The main objective of using this strategy is to minimize the machining time without affecting the quality performance of the machine, inturn bringing down the machining

cost. Few researchers concentrated only on the optimal process parameters without considering the maximum capacity utilization of the CNC machine. The power consumption relates to cutting forces required to remove the material and forces required to move the component against the tool for each pass. The power required to move the component against the tool for each pass remains constant without the effect of depth of cut.

Steps: (No of passes)

1)

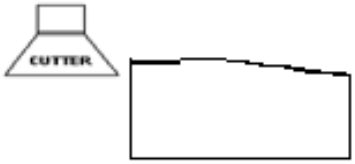

Conditions: (Present Scenario)

- Rough cut
- Required depth of cut is 5 mm
- Removing 1mm material per pass
- Machining Rated Capacity = 3.5 kW

Figure 3.1 (a): Present Concept of Power Utilization (For Initial/Single Pass)

(Without Cut): Power utilization for 1 pass = 0.3 kW

(With Cut): Power utilization for 1 pass = Cutting Power + Power Required to move the bed

= 0.6 kW

For first pass: Total Power Consumption = 0.6 kW, Time Required: 1 min

2)

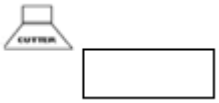

3)

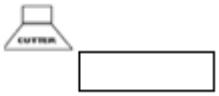

4)

5)

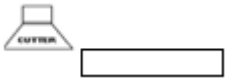

Figure 3.1 (b) Present Concept of Power Utilization (For Multiple/Next passes)

For second pass: Total Power Consumption = 1.2 kW, Time Required: 2 min.

For third pass: Total Power Consumption = 1.8 kW, Time Required: 3 min.

For forth pass: Total Power Consumption = 2.4 kW, Time Required: 4 min.

For fifth pass: Total Power Consumption = 3.0kW, Time Required: 5 min.

Steps: (No of passes)

1)

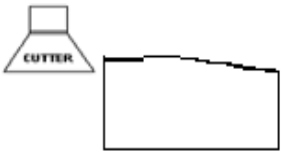

Conditions:(Proposed Research Concept)

- Rough cut
- Required depth of cut is 5 mm
- Removing 5mm material per pass
- Machining Rated Capacity = 3.5 kW

Figure 3.2: Proposed Research Concept for Maximum Machine Utilization

(Without Cut): Power utilization for 1 pass = 0.3 KW,

(With Cut): Power utilization for 1 pass = Cutting Power + Power Required to move the bed

= 0.3 + 1.5 KW

For single pass: Total Power Consumption = 1.8 kW, Time Required: 1 min

From this we can conclude that the total power required to remove the material for single pass in research concept might be more (i.e 1.8kW) compared to present scenario (i.e. 0.6kW), but the number of passes and the time required to remove the desired (5mm) material is less. So this concept is effective compared to the present scenario concept. The research concept is implemented using nueral network based techniques (ANN, HRNN) using both forward and reverse mapping approaches. Reverse mapping approach can also be treated as an advisory system in the absence of human experts, can predict the settings of various process parameters in a milling process parameters in order to achieve the desired responses according to the requirements of the end users. One of the main objectives in any system is to optimize the multiple responses of the process parameters, so the mutli objective optimization technique like desirability and particel swarm optimization (PSO) has been implemented.

The aim of this work is to develop an offline prediction model using neural network architectures via both forward and reverse mapping concept. The experiments were designed and conducted based on the design and analysis of experiment. In Design of Experiment (DOE), Response Surface Method (RSM) with three factors of cutting parameters and three levels have been considered. The cutting force of each axis is measured indirectly through measuring the current drawn by the feed motors. There

are two sets of experiment conducted such as without cutting and with cutting for two different hard materials (AA6061 and AA6061 4.5%Cu SiCp).

3.1.1 Experimental Setup

The machining experiments have been carried out on a CNC Milling Machine (Spark DTC 250) as shown in Figure 3.3(a). It is having drum type tool changer. The maximum number of tools that can be accommodated in this machine is 12. Proximate sensors are provided to sense the tool position. The movement of the axis are achieved by the servo motor. The Servo motor of the Z axis is selected in such a manner that it supports the power required for clamping and de-clamping of the tool also. During the tool change the Z axis servo motor draws 160% of current. Servomotor supplies the torque required to move the table in each direction. Therefore the cutting force of each axis is calculated by current drawn by the each axis servo motor. Tool holder type is BT 30. The total power required is 15KW. 24 volts is required for machine control box.

In this experimental study, the structural parameters for the machine tool are constant for every experiment in as much as all of the experiments have been completed on the same machine tool. Similarly, cutting tool parameters are constant because all of the cutting tools used have the same characteristics, and, in order to minimize the effect of tool wear, which could affect surface quality, the inserts were changed fairly often. Also the cutting parameters have been reduced to three to simplify matters. In this context, 61 different cutting conditions have been considered and for more accurate results, every experiment has been repeated two times. For this purpose, 122 samples have been prepared. The specimen used was 100 mm×60 mm in size as shown in Figure 3.3(b). All of the parts have been machined for dry run under the same cutting conditions as represented in Table 1. The cutting force was fetched through Ethernet cable via indirect approach (the details of calculating cutting force are discussed in chapter 4). Every specimen machined was subsequently kept protected so that their surfaces were not damaged.

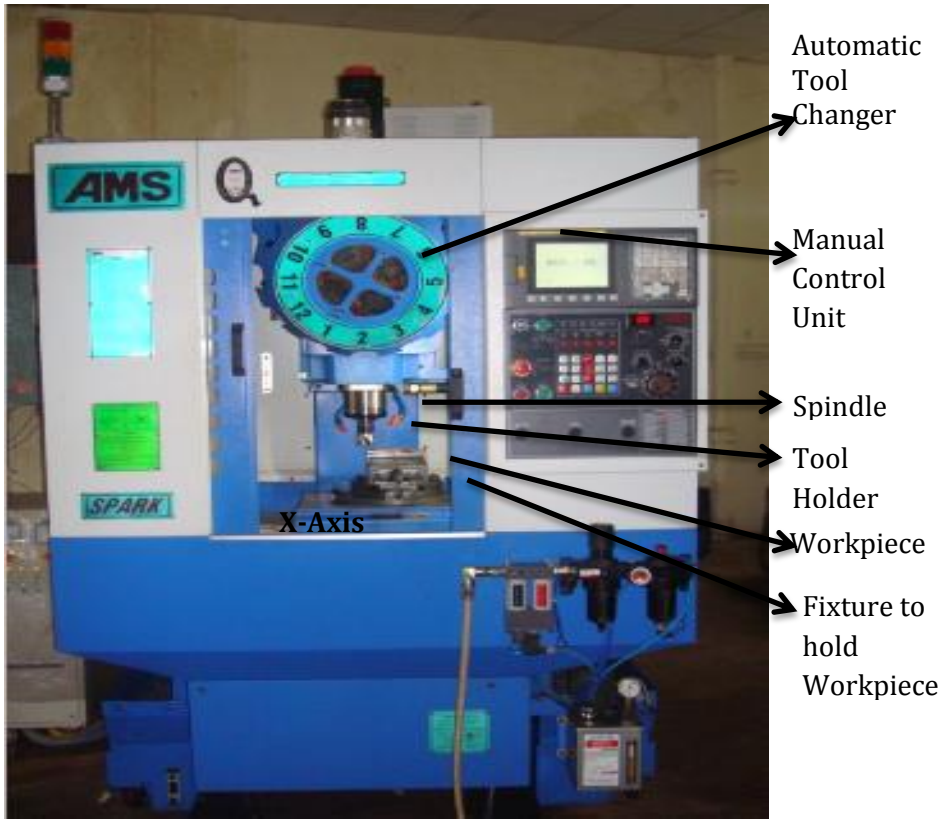

Figure 3.3 (a): Experimental Setup CNC Vertical Milling Machine (Spark DTC 250)

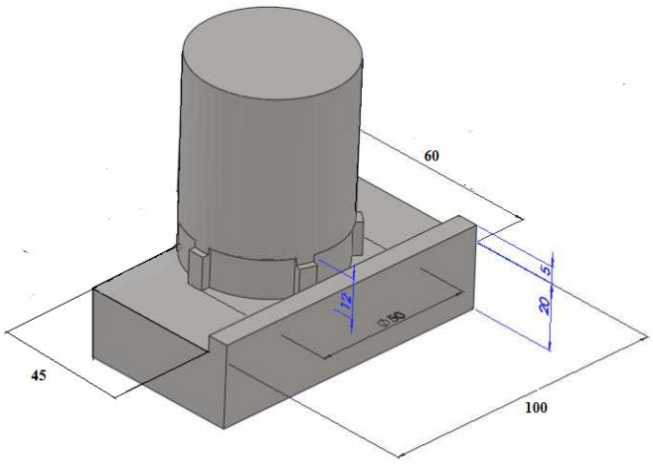

Figure 3.3 (b): Workpiece Tool Interface

3.2 MACHINE SPECIFICATION

DTC- 250/Spark [Drill Tap Machining Center, Vertical]

- Max working Stroke (**Z Axis):** 250 mm.
- Max working Stroke **(Y axis):** 300 mm.
- Max working Stroke (**X axis):** 250 mm.
- Speed Range **:** 60 to 6000rpm as std, 80 to 8000 rpm as optional
- Constant Power Range **:** 5.5 kW max at 30 min. of Continuous Running, 3.7 kW Continuous Running.

3.3 WORK MATERIAL

In the present study two materials were used. The two opted materials are of different categories, The first one is Aluminium material AA6061which falls in to a category of soft material. The second material is Metal Matrix Composite AA6061-4.5%Cu-5%SiCp. The chemical composition of AA6061 and AA6061-4.5%Cu-5%SiCp were obtained using an optical emission vacuum spectrometer. The attained chemical composition is listed in Table 3.1.

The aluminium material **AA6061** was opted as it is structural material, having high strength to weight ratio and hence used widely in aircraft industries.

The Metal Matrix Composite material **AA6061 4.5%Cu 5%SiCp** was selected. Now a days, Metal Matrix Composites (MMCs) play a vital and effective role in the field of aerospace, marine and automotive industries. For important applications, MMCs have functional properties such as higher strength to weight ratio, enhanced elastic modulus, improved strength at elevated temperature, higher wear resistance, attractive electrical and thermal conductivity and low coefficient of thermal expansion compared to the conventional metals and alloys (Necat et al. 2006, Bayraktar et al. 2008). The focus is mainly on discontinuously reinforced aluminium alloys (DRA) based MMCs, due to their better strength to weight ratio, high stiffness, high modulus, better thermal stability and their isotropic nature.

The idea behind selecting different materials is to test the generic nature of the decision support system proposed here in this study. Secondly, the study was more

concentrated in developing a model that behaves and performs in a better way by providing the desired output.

Table 3.1 : Composition of AA6061

Element	**Al**	**Si**	**Cu**	**Mg**	**Cr**
Weight %	97.9	0.60	4.5	1.0	0.20

3.4 CUTTING TOOL

The machining parameters are selected based on the recommended range supplied by the tool manufacturer and maximum spindle speed and feed rate of machine. Several experiments had been conducted within the a foresaid range to identify the desired range of process parameters which leads to end up with feasible machining parameters as depicted in Table 3.4.

Carbide tooling is used for the operation ISCAR Supplied tool holder as depicted in Figure 3.4 (a) and inserts for the operation. We are analysing the cutting force and surface roughness of the AA6061 and AA6061-4.5%Cu-5%SiCP material during the face milling operation. The tool holder selected is having the BT 30 taper type.

Square type insert as depicted in Figure 3.4 (b) with following specifications side clearance angle 15°, tolerance 0.08 mm, type T, cutting edge length 12 mm, thickness 5 mm, type of mount 90°, lead 15°, radius of nose 0.4 mm, direction of cutting Right rotation, machining condition is medium , and IC 910 grade is used.

The Tool Specifications are as follows:

1) Cutting Speed (Vc) = 100 - 600 m/min. **2)** Feed Per Tooth (fz) = 0.080 - 0.15 mm/tooth.

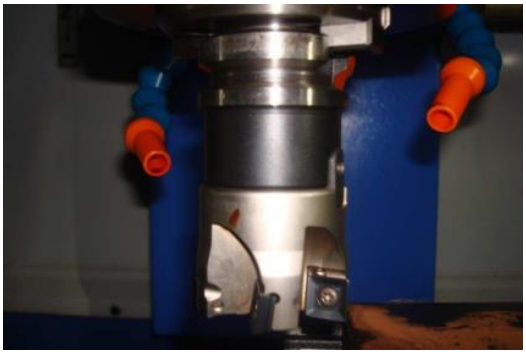

Figure 3.4 (a): Tool holder F90SD D50 ,22,12

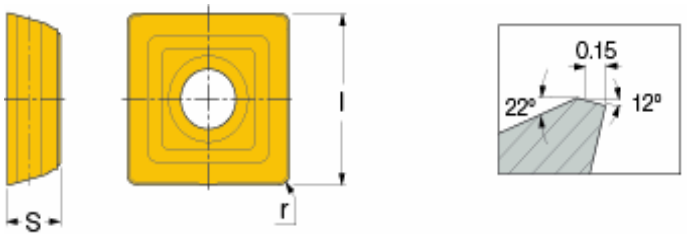

Figure 3.4 (b): Insert Nomenclature

3.5 EXPERIMENTAL DESIGN AND METHODOLOGY

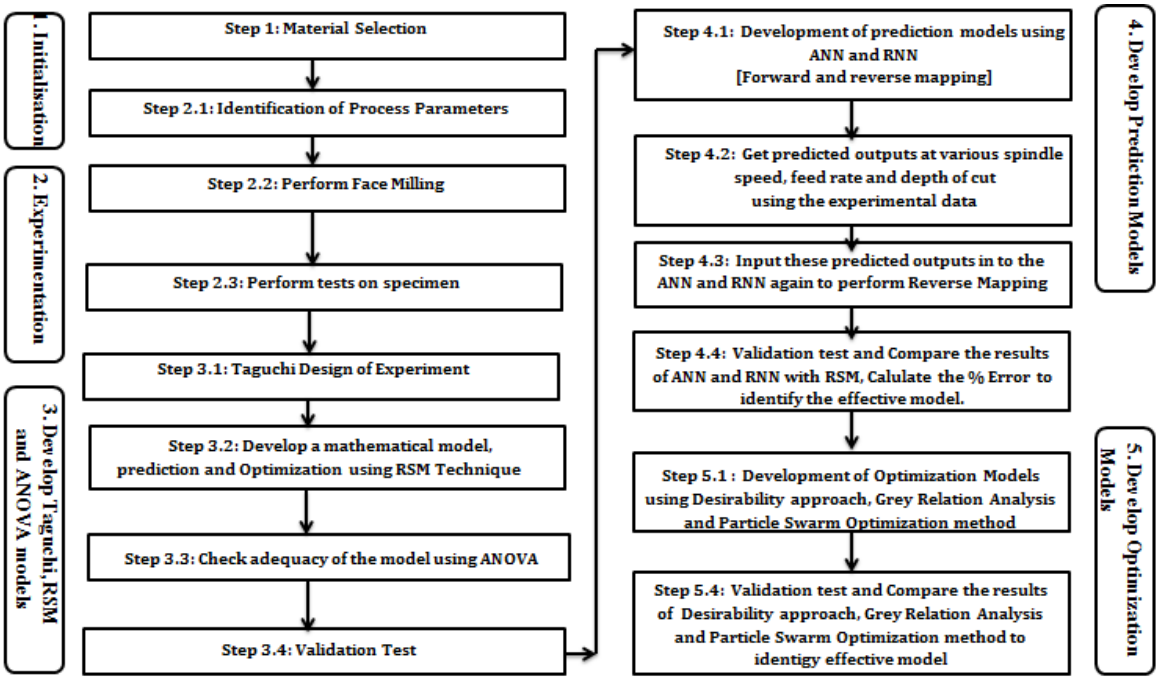

Figure 3.5 (a): Flow of work

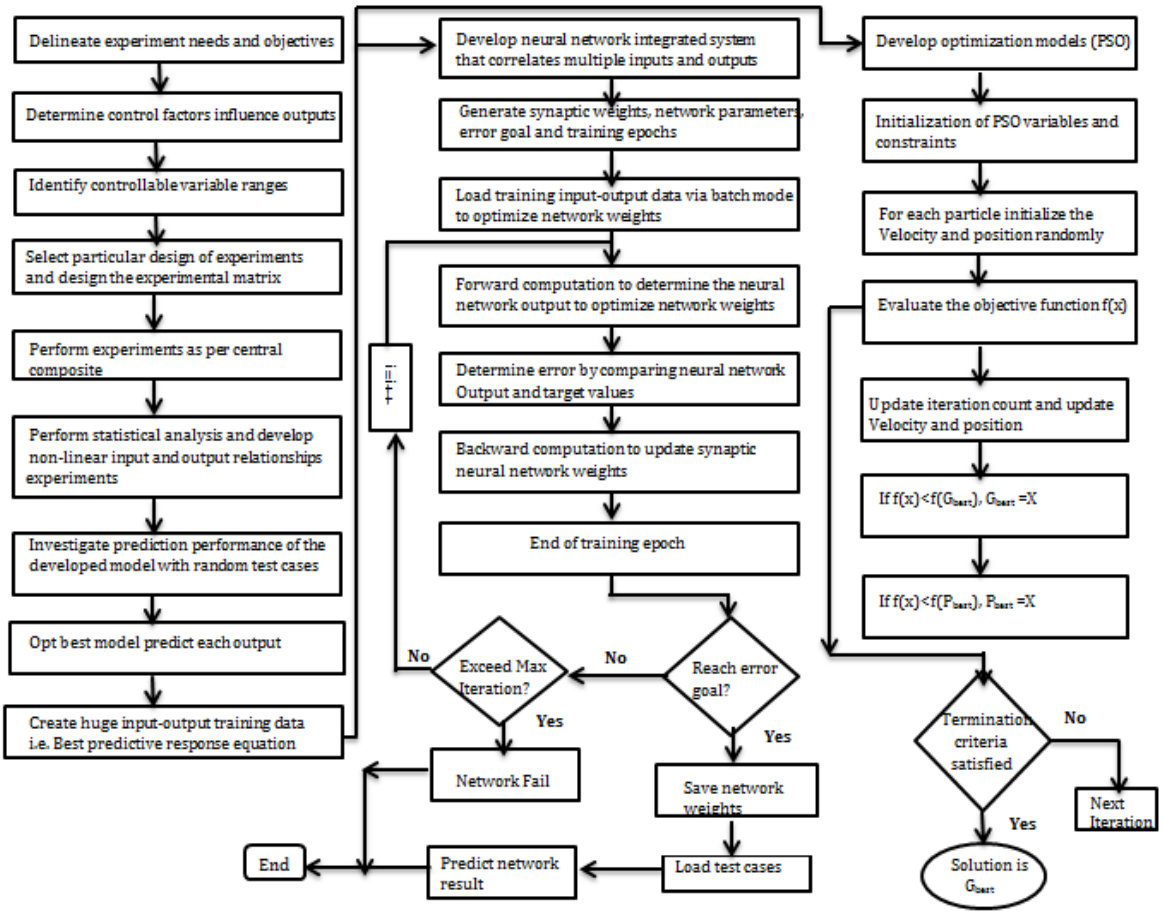

Figure 3.5(b): Detail ANN and PSO algorithm

Design of experiments (DOE) is essential to minimize and to perform the experiments productively. Generally, most of the problems in research observation of the system at work require experimentation to elucidate information regarding why and how it works. However, experimental procedures are generally expensive and time consuming. So it is necessary to carry out the work with minimum number of experiments, as it is a precise way to satisfy the desired objectives. Generally well designed experiments lead to a model of system performance and the experimentally determined models are named as empirical model (Montogomery). In the late 1920's R.A. Fisher in England addressed the design of experiments. It is a statistical tool to study the effect of multiple factors at the same instance (Ranjith Roy 2001). This technique has been more utilized and incorporated in academic field to provide a solution for engineering applications in the production floor. Dr. Genechi Taguchi in the year 1940 carried out a remarkable research with DOE techniques. The effort was

put forth to present the experimental technique in simple and uncomplicated way. The same was applied in the manufacturing field to improve the product quality. Dr. Taguchi's standard version of DOE, widely known as Taguchi approach or Taguchi method is applied to determine the optimum settings of the design parameters for performance and cost. The designer can easily adopt this systematic and efficient approach for experimentation. For Engineering analysis, Taguchi technique is popularly used. The experimental plan and analysis of results flow chart is shown in Figure 3.5 (a-b)

3.6 TAGUCHI EXPERIMENTAL DESIGN

Taguchi approach consists of set of experimental plans for obtaining experimental results in a controlled manner. This technique involves laying out the experimental conditions using specially designed tables known as 'orthogonal arrays'. By using orthogonal arrays considerably decreases the number of experimental configuration to be studied. In the current study, in order to determine the influence of process parameters and their effects on the machining characteristics of AA6061 and AA6061-4.5%Cu-5%SiCp, Taguchi technique for three parameters at three different levels are determined. The orthogonal array criteria was selected based on the degrees of freedom for the orthogonal array, which must be greater than or equal to sum of process parameters. From the list of experimental designs Taguchi L_{27} orthogonal array was selected. The design consists of 13 columns and 27 rows is shown in Table 3.6 . From the considered orthogonal array, the individual and interaction effects of the input parameters on the output parameters can be studied. Thus it is utilized for investigation of 3 factors at 3 levels. The effect of noise were tried to reduce by performing the specific experiment. By using this orthogonal array the individual as well as interaction effects of the process parameters on the responses can be studied. Therefore, it is best suitable for the conditions being investigated, 4 parameters each at 3 levels (3^4) along with the interaction effects. Taguchi method is basically incorporated to identify the most significant and influencing process parameters to attain the desired response (Ross, 1996 and Phadke, 1989). The main motive to carry out orthogonal experiments is to find out the optimum levels for all the involved parameters by analysis of means (ANOM). To find out the comparative significance

of individual parameter on the proposed performance characteristics, analysis of variance (ANOVA) was used. Taguchi address signal to noise ratio (S/N) as the objective function for matrix experiments (Ross, 1996 and Phadke,1989). Objective function categorized in to three sectors namely smaller the better, nominal the best and larger the better. In the present study, the cutting forces, power consumption responses need to be maximized. So larger is better option was opted. Similarly, surface roughness need to be minimized thus smaller the better is selected.

3.7 PARAMETERS AND THEIR LEVELS

The process parameters and their levels for milling operation considered in the study are shown in Table.3.2 for Taguchi L27 orthogonal array experiments. The parameter ranges were set based on the trial experiments and cutting tool specifications.

Table 3.2: The Machining Parameters and their levels

Spindle Speed (rpm)	Feed Rate (mm/min)	Depth of Cut (mm)
1000	300	1
2000	400	2
3000	500	3

3.8 RESPONSE SURFACE METHODOLOGY

Response surface methodology (RSM) is a collection of both statistical and mathematical techniques utilized for modeling, analysis and design of experiments, in which a response of interest is influenced by several variables and the objective, is to optimize this response. This technique is helpful for modeling and analysis of parameters, in which response of interest is affected by several variables and the purpose is to optimize this response. In this study, RSM based central composite rotatable design experiments of all possible combination of levels of the spindle speed, feed rate and depth of cut were investigated. It is a dynamic and foremost important tool of design of experiment, wherein the relationship between responses of a process with its input decision variables is mapped to achieve the objective of maximization or minimization of the response properties (Raymond & Douglas 2002).

The multiplicative model for the predicted surface roughness (response surface) in end milling in terms of the independent variable investigated can be expressed as,

$$R_a = C_o\, V_o^k\, f_z^1\, a^m \tag{3.1}$$

Where *Ra* is the predicted surface roughness (μm), V_o is the cutting speed (m/min), f_z is the feed per tooth (mm/tooth), and a is the axial depth of cut (mm). C_o, k, l, and m are model parameters to be estimated from experimental results. To determine the constants and exponents, this mathematical model can be linearized by employing a logarithmic transformation and equation (3.1) can be re-expressed as,

$$\ln R_a = \ln C + k \ln V + l \ln f_z + m \ln a \tag{3.2}$$

The linear model of equation (3.2) is,

$$y = \beta_0 x_0 + \beta_1 x_1 + \beta_2 x_2 + \beta_3 x_3 \tag{3.3}$$

Where y is the true response of surface roughness on a logarithmic scale $x_0 = 1$ (dummy variable), x_1, x_2, x_3 are logarithmic transformations of speed, feed, and depth of cut, respectively, while β_0, β_1, β_2, and β_3 are the parameters to be estimated. Equation (3.3) can be expressed as,

$$\widehat{y_1} = y - \varepsilon = b_0 x_0 + b_1 x_1 + b_2 x_2 + b_3 x_3 \tag{3.4}$$

Where $\widehat{y_1}$ is the estimated response and y the measured surface roughness on a logarithmic scale, ε the experimental error and the b values are estimates of the β parameters.

The second-order model can be extended from the first-order model's equation as:

$$\widehat{y_2} = y - \varepsilon = b_0 x_0 + b_1 x_1 + b_2 x_2 + b_3 x_3 + b_{11} x^2{}_1 + b_{22} x^2{}_2 + b_{33} x^2{}_3 + b_{12} x_1 x_2 + b_{23} x_2 x_3 + b_{13} x_1 x_3 \tag{3.5}$$

Where $\widehat{y_2}$ is the estimated response based on the second order model.

It is also called multiple regressions. In this, three-way interaction is carried out.

3.9 MEASUREMENT OF PERFORMANCE CHARACTERSTICS

In the present study, the considered responses are cutting force, surface roughness and power consumption. So, the upcoming section deals with the measurement of the response characteristics through various devices.

3.9.1 Cutting Force: Indirect method of measuring the Cutting forces

Measuring the cutting forces during machining is a very complicated task. The direct method of measuring the cutting force is having a lot of disadvantages like cost, mounting of sensors, constrains of cutting parameters and machine, and cutting condition. Therefore indirect method of measuring cutting forces is used. There are several techniques used to measure the cutting forces in indirect method. One technique is to tap the current signals of the feed servo motor from the MCU as shown in Figure 3.6. The current drawn by each axis is measured with and without cutting. The current drawn by the servomotor is nothing but the force required to move the table from the initial stage to the cutting stage. The current drawn during without cutting includes contributing factors like the friction force, preload torque, weight of the table and component, motor inertia, disturbance in the electrical and mechanical system. The current drawn during cutting includes these effects and cutting force required to remove the material during cutting. To calculate the cutting force, we have to subtract the without cutting current from cutting current. The torque can be calculated by multiplying the current with torque constant.

Torque of the motor T_m, = current drawn by the motor * RMS Torque constant. (3.6)

Each motor has its own torque constant which is specified in the motor specification table. We have

$$T_{m=\frac{FL\pi\eta}{1000}} \quad (3.7)$$

Where F= cutting force in N, L = lead in mm, η = efficiency of power transmission.

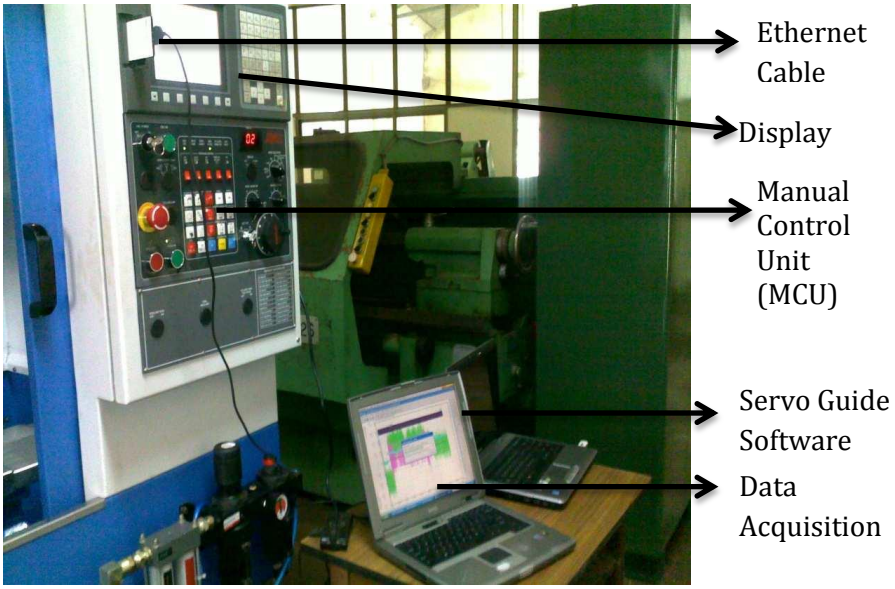

Figure 3.6: Data acquiring from SERVOGUIDE software

3.9.2 Surface Roughness Measurement

The surface roughness was measured by using 'MITUTOYO SURFTEST SJ-301 surface roughness tester as shown in Figure 3.7. The roughness tester uses a differential inductance method as direct technique. The tester consists of a hard needle shape stylus made of diamond. The stylus includes a tip radius of 2 µm and applies a force of 0.75 mN with a stylus speed of 0.25 mm/s to measure the surface roughness. Basically, the surface roughness (Ra) was measured at three different locations. Further on, the average was calculated and the average was considered as the response. While carrying out the measurement, the cut off length evaluation length was fixed as 0.8 mm and 4mm respectively. The Ra and Rz values of AA6061 and AA6061-4.5%Cu-5%SiCp machined surface were directly fetched using roughness tester.

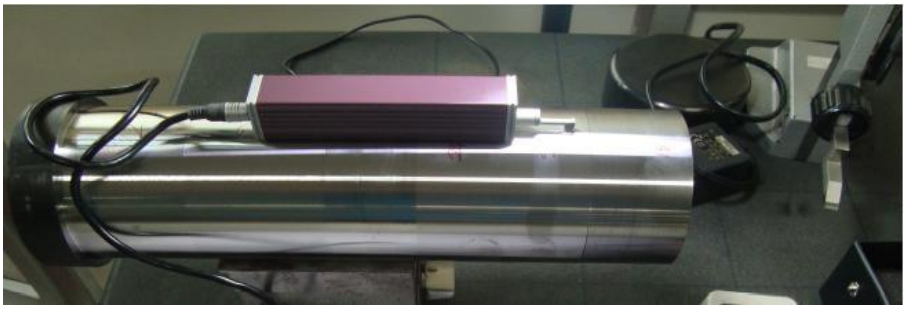

Figure 3.7: Surface roughness tester

3.9.3 Surface Topography

The topography of the AA6061 and AA6061-4.5%Cu-5%SiCp machined surface was examined using a 3D laser microscope by using Olympus LEST OLS4000 laser confocal microscope available at CMTI, Bangalore as shown in Figure 3.8. The microscope uses a laser scanning to measure the surface profile of the machined components. The microscope can measure surface texture more accurately due to low laser spot diameter of 0.4 µm

Figure 3.8: Laser optical confocal microscope

3.10 OPTIMIZATION OF PARAMETERS

3.10.1 Parametric Optimization Using Desirability Function

Desirability Function approach is a multiple-response optimization method. This approach was first introduced in 1980 by Suich and Deringer. The method finds operating conditions "targeted" which are the most desirable response value. The general approach is first converting each response x1 into an individual desirability function d_i that varies over the range $0 \leq d_i \leq 1$ (Deringer and Suich 1980, Baji et al.2010). The desirability functions are categorized into three sectors based on the response characteristics.

1. If the target for the response is a maximum value / "Higher is better".

$$\begin{cases} ri \leq r_{i*} & 0 \\ r_{i*} < r_i < r_i' & \left[\frac{ri - ri*}{ri' - ri*}\right]^a \\ & 1 \end{cases}$$

Where : r_{i*} is the minimum adequate value of r_i, r_i' is the maximum adequate value of r_i and a describes the shape function for desirability.

2. If the target for the response is a minimum value / "Lower is better".

$$\begin{cases} ri \le r_i'' & \\ r_i'' < r_i < r_i^* & \\ r_i \ge r_i^* & \end{cases} \qquad \begin{cases} 1 \\ \left[\frac{ri^*-ri}{ri^*-ri''}\right]^b \\ 0 \end{cases}$$

Where : r_i'' is the minimum value of r_i, r_i^* is the maximum adequate value of r_i and b describes the shape function for desirability.

3. If the target for the response is between lower and higher value / "Nominal is better".

$$\begin{cases} r_{i*} < r_i < O_i & \\ O_i < r_i < r_i^* & \\ r_i > r_i^* \text{ or } r_{i*} > r_i & \end{cases} \qquad \begin{cases} \left[\frac{ri-ri^*}{Oi-ri^*}\right]^c \\ \left[\frac{ri-ri^*}{Oi-ri^*}\right]^a \\ 0 \end{cases}$$

Where: O_i is the objective value, c and a describe the exponential parameters which verify the shape of the desirability function.

3.10.2 Hybrid Taguchi-Grey Relation Analysis

Taguchi design undertakes orthogonal arrays to reduce the number of experiments required to determine the optimal setting of process parameters. The effectiveness of the Taguchi method for improving quality in industry has extensively been verified. However, most of the Taguchi applications are concerned with the optimization of only one response, while most of the industrial problems are concerned with multiple responses (Deng 1989).Whereas, grey relational analysis (GRA), based on grey system theory is the solution for solving the problem of complicated interrelationships among the multi-responses. The term ‘Grey’ lies between ‘Black’ (symbols no information) and ‘White’ (symbols full information), and it symbolizes that the information is partially available. It is suitable to unascertained problems with poor and incomplete information. This method transforms multiple quality characteristics into single grey relational grades (Chen et al. 2000, Balasubramanian et al. 2011, Lin et al. 2004). By comparing the computed grey relational grades, the arrays of respective quality characteristics are obtained in accordance with response grades to select an optimal set of process parameters.

3.10.3 Optimal Machining Parameters: Particle Swarm Optimization (PSO)

The optimal process parameters are achieved by employing the PSO and desirability approach. The PSO was implemented using MATLAB and the Desirability approach was carried out using Minitab software. The working conditions for the PSO model are illustrated in the algorithm. The projected model and the parameters that play a vital role in obtaining finer convergence characteristics of PSO are discussed in (Optimization Chapter 7). If the number of parameters increases, the learning rate increases in turn the number of iteration increases in the search space. The outcome leads to probability of getting global optimum solution and leading the convergence to be accomplished in a smaller number of iterations. Therefore there is a boundary on maximum velocity to be attained by the particles.

The above criterion indicates the abandoned increase in velocity of particles, so it is necessary to make the search algorithm to be limited boundary range. The direction of the velocity gets altered in opposite direction if the velocity of the particles surpasses ahead of the specified range. This results in converging quickly towards its global optimum solution.

A) Proposed Methodology: PSO

Based on the literature survey, the PSO technique yields good result as compared to the rest of the techniques. So the PSO technique is incorporated in this present study. PSO is stochastic optimization technique which is a population based optimization technique, PSO technique was implemented (Eberhart et al.in 1995). The PSO technique was implemented by taking an inspiration of birds flocking. In the PSO algorithm the particles are estimated by the fitness function to be optimized and have velocities for the particles. The PSO has two important values which are termed as pbest and gbest. The pbest value is the best solution achieved so far among the particle, gbest value is the best solution obtained so far in the population. Once these two values i.e pbest and gbest are acquired, the particles are upgraded with their velocity and positions using the equation (3.8). PSO incorporates various parameters such as number of particles, range of particles, global vs local values, dimension of particles, learning factor. The information mechanism sharing in PSO is entirely

diverse as compared to the rest of the techniques. The information sharing in PSO is one way sharing mechanism. In PSO, the gbest has the right to share the information with others. As the evolution glances only for the best solution, all the particles present intend to converge towards the best solution as quickly as possible in most of the cases. The PSO algorithm mainly consists of three different factors as follows: 1) Social 2) Cognitive 3) Inertia (Eberhart et al.in 1995, Munish et al.2015). All these three constraints concentrate mainly on accelerating the particle towards the best position. The best position is the one which is so far followed by all the neighbouring swarm; this position is considered to be the global best (gbest) position. The Cognitive constraint concentrates on accelerating the individual particle towards its best position (pbest), the position (pbest) which is accomplished by the individual particles so far. The inertia constraint plays an vital role in maintaining the stability between the gbest and pbest investigation competence among the search space. If the fitness values of gbest and pbest values are compared among each other, if the pbest value is found to be better than the gbest value, then the value of the gbest changes

The equations (3.8 - 3.10) are incorporated to vary the position of the individual particles to reach global optimum solution in search space.

$$v_i^{r+1} = w.v_i^r + c1.Q1.(pbest_i - y_i^r) + c2.Q2.(gbest - y_i^r) \quad (3.8)$$

Where v_i^r = ' ith' particle momentum at 'rth' iteration; w = inertia weight; c1,c2=learning factors which varies in the range of 1 to 4; Q1,Q2= random numbers between 0 to 1; $pbest_i$= *pbest* location of ' ith' particle or *pbest* value is the best solution achieved so far among the particle; *gbest=gbest* location of swarm; y_i^r = $[y_{i1}^r, y_{i2}^r, y_{i3}^r, \ldots\ldots\ldots\ldots\ldots y_{iN}^r]$, "ith" particle current position at "rth" iteration in N-dimensional search space or *gbest* value is the best solution obtained so far in the population.

After calculating the momentum, the next position of the rth particle is calculated as follows:

$$y_i^{r+1} = y_i^r + v_i^{r+1} \quad (3.9)$$

Inertia weight can be determined by using the equation (3.10) or the Inertia weight can be chosen to be any random value. This determined inertia weight can be substituted in equation (3.9)

$$W = w_{max} - \frac{[(W_{max} - w_{min}) * iter_{curr}]}{iter_{total}} \quad (3.10)$$

Where W_{max} = maximum inertia weight; W_{min} = minimum inertia weight; $iter_{curr}$= current iteration; $iter_{total}$=total number of iteration.

B) PSO OPTIMIZATION OF PROCESS PARAMETERS

PSO coding structure is to be defined and the initial population is distinct. The computation with particle swarm with particle swam intelligent operators is used to evaluate fitness with respect to the objective function. General flow chart of PSO algorithm is shown in Figure 3.9.

Terminologies used in PSO algorithm:

- **Particle:** Individual in the group of swarms. A potential solution is represented each swarm in the problem.

- **Swarm:** Population of the algorithm.

- **Personal best (pbest):** Personal best position of a given particle, so far. That is, the position of the particle that has provided the greatest success, pbest in equation (3.8) represents best position (pbest) individual until iteration k.

- **Global best (gbest):** Position of the best particle of the entire swarm, gbest in equation (3.8) represents best position of the group until iteration k.

- **Leader:** Particle that is used to guide another particle towards better regions of the search space.

- **Velocity (vector):** This vector drives the optimization process, that is, it determines the direction in which a particle needs to "fly" (move), in order to improve its current position.

- **Inertia weight (w):** It is employed to control the impact of the previous history of velocities on the current velocity of a given particle and denoted by w.

- **Learning factor:** Represents the attraction that a particle has towards either its own success or that of its neighbours. Two learning factors used: C1 and C2, where C1 is the cognitive learning factor and it represents the attraction that a particle has towards its own success and C2 is the social learning factor and represents the attraction that a particle has toward the success of its neighbours. Both, C1 and C2 are constants (Malghan et al. 2016, González et al. 2012).

C) PSO Algorithm : (Malghan 2016, Eberhart et al.in 1995)

1. Initialize the population of n particles randomly.
2. For each particle, the fitness value is calculated.
3. If the obtained fitness value of the particle is better than the best fitness value (P_{best}) in history, than the present value is assigned as new best fitness value (new P_{best}).
4. Choose the particle with the best fitness value of all the particles which are considered so far as the global best (gbest).
5. The velocity and position of each particle need to be calculated.
6. Each particle velocities are secured to a maximum velocity. If the sum of the acceleration will cause the velocity on that dimension to surpass ahead of the specified range set by the user, then the velocity need to be limited.
7. Terminate if minimum error condition is reached or when the maximum iteration is reached else go to step 2.

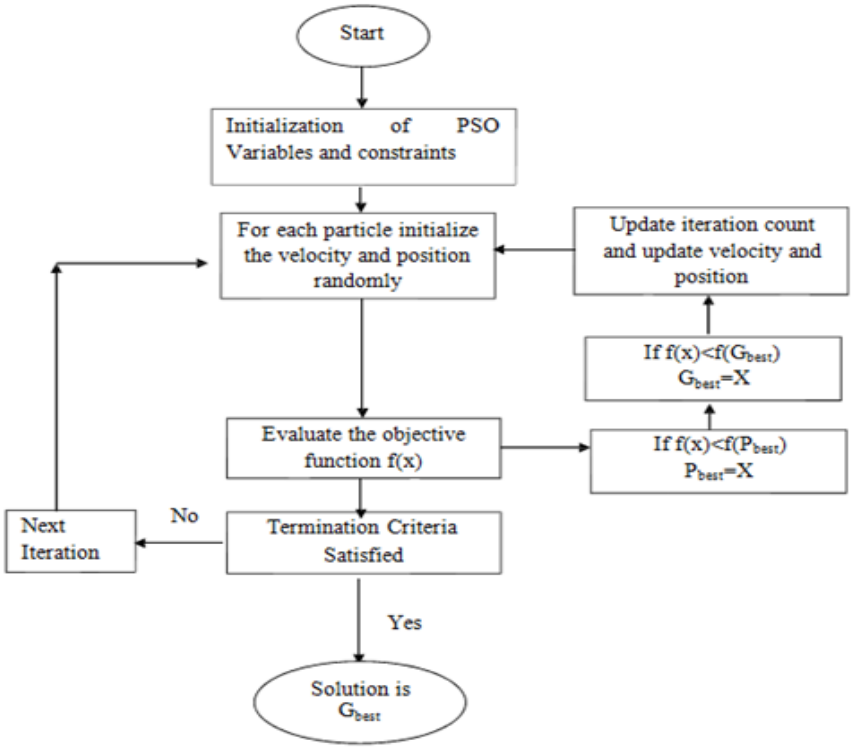

Figure 3.9: Illustrates the PSO flow chart to optimize the process parameters: cutting force, surface roughness and power consumption as objective functions.

3.11 PREDICTION TECHNIQUE: NEURAL NETWORK MODEL

The goal of the work is to construct a neural network model in order to predict the surface roughness, cutting force and power consumption during milling operation. Two models were developed for prediction, namely, Recurrent Multilayer Perceptron (RMLP) and Multilayer Perceptron (MLP). The learning algorithm incorporated in both the models RMLP and MLP is Error back propagated Gradient Decent method. The following section will focus on the architecture and training methods used in the present work.

3.11.1 Architecture Of Multi-Layer Perceptron Model- ANN

The intricate and disruptive engineering problems have been effectively solved by using the Multilayer perceptron (MLP) models.Error back propagation method has been adopted to consecutively solve these problem. In order to resolve the errors occurring during learning process various learning algorithms exist such as the

Gradient Decent learning rule, Adaptive Filtering or Least Mean Square algorithm. The architecture encompasses three different types of layers namely input layer, hidden layer, and output layer. The flow of signal is named as Feed Forward Neural Network as the signal moves in a forward direction, from input layer to hidden layer and then from hidden layer to the output layer. The data being processed in the network will bypass several layers without any existence of feedback connections. Figure 3.13 shows schematic representation of input and output parameters in Multi-Layer Perceptron feed forward neural network. The neural network has to behave in a way that the set of inputs should determine anticipated result. The weights are assigned primarily in two ways. One way is to use the learning rule to learn the output pattern by providing the trained data. Another way is to assign the weights based on the prior knowledge. The back propagation algorithm for given epoch of training data executes in two different ways namely the sequential mode or batch mode. Basically the disparity among these two ways is that in sequential mode, the weights of neurons are entirely dependent on the pattern basis. While in the case of batch mode, the weights and the bias of neurons are entirely on the epoch basis. Generally, the sequential mode is widely used in back-propagation learning. Usually, the network needs to be trained in a way that it leads to minimal error. The error is calculated based on the difference between the desired error and actual error. Basically there are two methods to specify the error, either by specifying the number of epochs or by specifying the error value. The variation among these two ways is that if number of epochs is specified, then the training data will execute until it reaches the specified epoch number; later on the testing of the data is carried out. In epoch specification, the training data will run up to the specified number of epoch and once it reaches the specified value; the testing of the data is carried out. In the other way, the training will iterate till the specified value of error is reached. In the present study, Multi-Layer Feed Forward Neural Network (MLFFNN) architecture is adopted for training and predicting the mechanical properties of the AA6061 and AA6061 4.5%Cu SiCp material. The input parameters are rotational speed, feed rate, and depth of cut. The predicted response parameters are surface roughness (Ra) and cutting force (FX).

3.11.2 Architecture Of Recurrent Multi-Layer Perceptron Model

The elementary feature of Recurrent neural networks (RNN) is that the network at least includes one feedback connection and is used to perform the sequential processing. The presence of feedback connection indicates that activations can flow around in the loop, thus leading the network to perform temporal processing and even to learn the sequences. The feedback may be identity-feedback or it may be from one layer to another layer. The dynamic properties of the network play a key role and acts contrary to feed-forward networks. The stable state is achieved by the network when the activated values do not illustrate any diverging results as the activated values reach to relaxation mode.

Recurrent neural network architecture can be of different forms. One common form consists of Multi-Layer perceptron (MLP) with appended loops. There are abundant other neural network architectures available such as Elman networks, adaptive resonance theory (ART), Competitive network etc. RNN has various training approaches such as the Back propagation through time (BPTT), Extended Kalman Filter, Real time recurrent learning etc. Figure 3.15 shows the schematic representation of Recurrent Multi-Layer Perceptron Model. In the present study, RNN architecture is used to train and predict the responses of the AA6061 and AA60614.5%-Cu5%-SiCp material. The input parameters are rotational speed, feed rate, and depth of cut. The predicted response parameters are surface roughness (Ra) and cutting force (FX).

3.12 PROCEDURE INVOLVED IN ANN MODEL DEVELOPMENT

The development of an ANN model involves various processes and functions. To develop an ANN model one needs to know the best representative input parameters for the given output(s). The preparation of the model would require sufficient amount of training data so that network can learn. The selection of the type and amount of data is often a matter of in depth knowledge and experience about the process considered for modelling. The model developer should be in a position to determine the data which is most representative of the input-output population. Thus data generation becomes an important task in model development. Next, the input as well

as output data needs to be scaled so that data is grouped in a pre-decided range. Also, the methods for weight initialisation to be used, determination of biases, deciding on the architecture etc. are not readily available and require good amount of attention during model development. The model developer should be aware that a neural network does not have any information about the metallurgical process that is being modelled. In order that the network understands the underlying relationships for the process, the network needs to be trained. Hence, neural network training is the heart of the entire ANN model development. The model developer should be sure that the data that is being used for training is authentic, devoid of any significant measurement errors. Any erroneous data used for training can lead to a situation similar to teaching wrong things thereby, resulting in wrong learning. Wrong learning will automatically lead to erroneous outputs from the model.

3.13 VARIOUS STEPS IN DEVELOPING A NEURAL NETWORK

3.13.1 Data Preparation

Generally the data for an NN model arrives from a variety of sources. The NN is able to process the data in a certain structured form. The network learning is affected by the form in which the data is presented to the network. Hence the right coding scheme for the data needs to be decided before hand, so that the network can learn and can perform the given task. Therefore, the coding scheme for the data has to be in place before the data collection task is taken up. Design of data coding system should be decided before data collection as one should be aware as to what he is going to do with that data. The process of data preparation involves the following steps.

3.13.2 Data Collection and Generation

The primary step in the ANN model development is deciding on the input and output data required. After these have been identified, the metallurgical system/process data needs to be generated. There are usually, two sources available for data generation/collection. One can get data from the hand books or data books in metallurgy and secondly from experiments. Actually, data generation means use of a data generator which will give an output for each chosen sample. The total numbers of samples are so chosen that the final model represents the actual metallurgical

problem on hand accurately. The type of data generator selected, generally depends upon the type of problem being modelled.

3.13.3 Identification of input variable

The input variables are significant for modelling output variable(s) under study and are selected by suitable variable selection procedures. The most important parameters are spindle speed, feedrate, depth of cut for predicting the cutting force, surface roughness and power consumption.

3.13.4 Range and Distribution of Samples [Formation of training and validation sets]

The data set is classified in to three distinct set such as training set, testing set, validation set. Training data is used for training the network, that is, to update the weights as the network learns from the test samples being presented to it during training. The validation data performs the function of monitoring the quality of training and helps in decision making as regards to terminating the training process. The test data is used to check the final performance of the trained model.

The neural network applies the training set successively to gain knowledge of the patterns and the training set is deemed to be the prime set. In order to assess the generalisation ability of the trained network, a testing set is functional to the trained network. The performance of the network is verified by applying the validation dataset to the trained network. In total, 27 sets of experiments were conducted for AA6061 material and 27 sets of experiment were conducted for AA6061 4.5%Cu SiCp. Out of that, 22 data sets from each of the AA6061 and AA6061 4.5%Cu SiCp materials were used for the training the networks, 3 data sets are used for testing the network and finally for validation 2 data sets are utilized.

3.13.5 Pre-Processing and Post-Processing of Data

The pre-processing of data is carried out to convert the data and the specific signals in to data representation which indeed is suitable to an application through the series of operations. The main aim behind using the data pre-processing is to attain a smoother relationship, size reduction of the input space, feature extraction, noise reduction and data normalization.

The brief description of the terms mentioned in pre-processing data sections are defined as follows:

- **Smoother Relationships:** The problem transformation is the commonly used type of Pre-Processing. It implies that the problem is basically transformed in to simple problem. After implying this type of pre-processing, the associated mappings become quite smoother. Usually the transformations can be obtained from instinct about the problem.
- **Feature Extraction:** The feature extractions are usually contingent on the domain-specific knowledge. The input data is a pattern itself. From the data, if the key attributes are extracted then the encountered problem is solved automatically.
- **Noise Reduction: The** series of data may involve inconsistent data, useful data and noisy data. So inorder to filter out the inconsistent and noisy data from data, the Pre-Processing is carried out. Thus Pre-Processing helps in recovering of the corrupted data and helps in reducing the unwanted data from the data.
- **Normalization:** In most of the problems, the units incorporated to measure each of the input variables can skew the data, inturn making the range of values along some axes much larger than others. Hence resulting in unnecessarily complex relationships by making the nature of mapping along some dimensions much different from others. Such issues can be overcome by scaling (normalization) each of the input effect, thus increasing the accuracy and performance of the neural network model or neural network system.

The last step to be performed in the Pre-Processing is the Normalization of data. Usually the Normalisation is applied to both the input and the output values. The main aim of the Normalization is to uniformly distribute across the data range. The Normalization of data must be carried out, in such the values of input and output range should not cross the range of the summing of the neuron or the device. However, for the current study the scaling is within the range of 0.1 to 0.9.The following Normalization function is used in the study.

$$x_n = \frac{(x - x_{min}) * 0.8}{(x_{max} - x_{min})} + 0.1 \quad (3.11)$$

Where x_n refers to the normalised value, x_{min} is the minimum and x_{max} is the maximum value in the range (Negalye et al. 2012).

The training of the network is carried out until it attains the required degree of performance. Once the degree of performance is attained, the network provides the expected output values that are understood by the end user. Inorder to achieve the desired outputs, the Post-processing of data is carried out as it assesses the network performance. In this step, the outputs of the network in the normalised form are de-normalised using the following equation (Negalye et al. 2012).

$$x = \frac{(x_{max} - x_{min}) * (x_n - 0.1)}{0.8} + x_{min} \quad (3.12)$$

There are several algorithms for data Pre-Processing such as data normalization(Min-Max Normalization, Zscore Normalization, Sigmoidal Normalization) data values averaging, input space reduction (Principal Component Analysis (PCA)). The input space consists of more than one variable. Each of the input for the data collected may have different range. Similarly, the number of outputs may be more than one and each may have a different range. Hence each of the inputs and the outputs needs to be normalised by its own normalising factors. Hence there is a need for pre-processing of the raw input and output data or else the network will not perform satisfactorily. This is a critical phase in the overall model design and development. Pre-Processing improves the efficiency of neural network training. The Post-Processing enables assessing and detailed analysis of the network performance.

3.13.6 Hidden layers

The hidden layer has the capability to generalize the network. Hidden layers consist of the neurons or they may be called as the inter-neurons that neither seen or act upon the outside world directly, these inter-neurons communicate only with the other neurons. The sufficient amount of the hidden neurons in the single hidden layer will enable approximation of the continuous function. In the present study, two hidden layers were opted for the networks.

3.13.7 Hidden nodes

The network attains the desired output only when the optimal number of hidden layers, as well as nodes in each hidden layer is incorporated in the network. The integration of the optimal hidden layers will make the trained network generalize well and minimize the error. If too few nodes are opted in the hidden layer, then it leads to high training and high generalization error for the system as the predictive factors might be too complex for a small number of nodes to capture. In either way if too many nodes are opted in the hidden layer, then it leads to overfit of the training data and trained network will not generalize well as there is high variance. So to overcome this issue to some extent, few thumb rules are adopted. Some of few thumb rules anticipated by the experts are as follows, **a)** The hidden layer size is selected somewhere between the input and output layer size (Blum, 1992). **b)** The general rule to calculate the number of hidden nodes is [(number of inputs + number of outputs) * 2/3]. **c)** The hidden layer should never be more than the twice as large as the input layer (Berry etc, 1997). **d)** Hidden nodes are considered as the principal components, which are needed to capture about 70-90% of the variance of the input data set (Boger etc ,1997). The number of hidden neurons with n inputs and m output neurons for the three layer neural network is obtained by the minimum square root of (n*m) neurons. Therefore, at first hidden layer stared from 4 neurons and best results were obtained at 7 neurons. Similarly, the second hidden layer showed best results at 4 neurons. From the graph, it is observed that the mean square error increases as the number of neurons increases. Figure 3.10 represents the mean square error versus number of neurons .

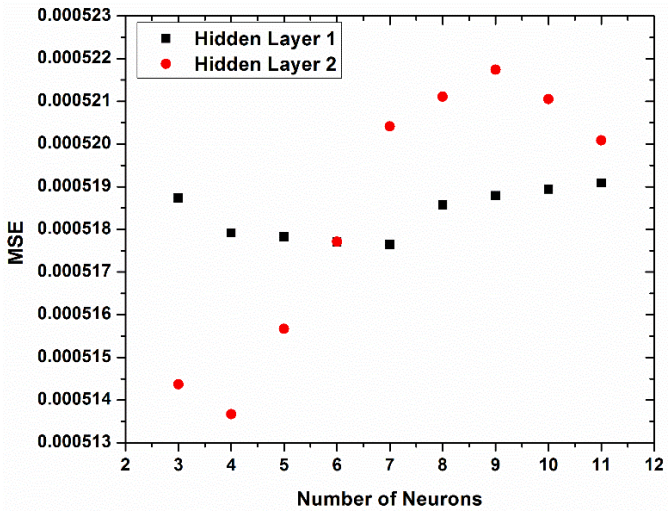

Figure 3.10: Number of neurons in hidden layer 1 and 2 verses mean square error

3.13.8 Output nodes

The network performance drops down due to the broad spacing of the outputs with multiple outputs in the network as when compared to a network with single output. The output parameters are surface roughness and cutting force.

3.13.9 Concept of Activation function

Activation functions it is a decision making function that helps in determining the presence of particular feature. Generally activation functions are needed for transforming the input to different domain where they may be easily separable or bound a model. Inorder to make the incoming data non-linear we use non-linear mapping called as the activation functions. Activation functions are mathematical formulae that decide the output of a processing node. The process of an ANN is to sum up the product of the associated weight and the input signal and produce an output or activation function. Neural network uses various kinds of activation functions such as the binary step function, binary sigmoid functions and bipolar sigmoid functions.

In the present study the sigmoidal activation function is used due to its nature of reducing the saddle of the complication present in the training phase. The selection of sigmoidal activation function is due to its features of nonlinearity and being

continuously differentiable, which is unipolar continuous. The sigmoid function is given below (Negalye et al. 2012).

$$f(x) = \frac{1}{1+e^{-x}} \tag{3.13}$$

Based on the suitability of the distribution of the target values, the activation functions are integrated for the outputs. In the study the logistic function is incorporated, which is a sigmoid function between 0 and 1. It indicates that the output values vary from 0 to 1 or binary.

3.13.10 Initial Weights

Typically the weights of the network are initialised at small random values. The weight initialisation has a strong bearing on the way the network learns. If the network is trained even after reaching the area of stability then it results in drifting of the assigned weights thus leading to poor performance of the network. Even it increases the error value, in turn leading the network to suffer with poor mapping quality of network. To conquer this, it is advisable to commence with a new set of random weights.

3.13.11 Learning Rate

The Learning rate (η) factor usually identifies at which rate the network needs to be converged and even it helps in determining the quantum of weight needed to be adjusted at each step. Learning rate parameter decides the quantum of weight adjustment done at each step and is responsible for the rate at which the convergence of the network takes place. A poor choice of this parameter can lead to convergence problems. The selection of proper value of learning rate coefficient determines the effectiveness of the use of back propagation algorithm. There is no proper or exact method to select the learning rate value since as the learning rate solely depends on the relation that exists in the data sets (Reddy et al. 2005).Thus, there is no unique learning rate available which can hold good for all of the models, so the learning rate always decided based on the trial and error. The learning rate and the rate of convergence both are directly proportional to each other. The use of high learning rate parameter will lead to higher non convergence or the network starts oscillating. Similarly the too low learning rate parameter value leads the network to converge at

very slower rate. Rumelhart and McClelland 1986, reported that a value of η = 0.25 and α = 0.9 give good results for most of the computations. Usually η being the quantum of weight adjustment for each step or iteration, its value always lies down between 0.1 and 0.9. Here, it is found that for the current study the learning rate of 0.3 yields better results.

3.13.12 Momentum Factor

The core of back propagation algorithm is the assessment of the contribution of each weight to the error output. The objective function in NN training is a incessantly differentiable function of the weights. There is always a possibility that the training may get trapped in local minimum and might not shift out this plane. In order to overcome these issues, the momentum factor is introduced. It accelerates the network convergence in an FFNN method. The enhancement of the present weight adjustments are done basically with a fraction of the weight adjustment in the previous time step. The current weight adjustment then takes the form shown below (Negalye et al. 2012).

$$\Delta w(t) = -\mu \nabla E(t) + \alpha \Delta w(t-1) \qquad (3.14)$$

The parameters Δw is current weight, ∇E is error, t and (t-1) in the above equation specify the existing and the most recent preceding training step. The variable α is described as the momentum factor. The basic role of the momentum factor is that it gives an added momentum to the descending descent movement. The process indeed helps the network to ascend beyond local minima and travel further downwards towards the slope of error profile. The momentum term is proportional to the proportion of divergence. Hence it can be stated that, larger the momentum factor, the faster will be the convergence. Usually α is in the extremities of 0.1 to 0.9. During the training process, in most of the cases α value will be significantly varied between the range of 0.1 to 0.9. In the current study, it is found that in case of Feed Forward Neural Network, the momentum factor of 0.2 and 0.5 for AA6061 and AA6061 4.5%Cu SiCp materials yield satisfactory results.

In the present study, the two materials have been taken in to consideration, such as AA6061 and AA6061 4.5% Cu SiCp. Two different materials are chosen to ascertain the generality of the NN model developed. The developed ANN and RNN model will identify and predict the common best process parameters that hold good for two different types of materials.

3.14 FORWARD AND REVERSE MAPPING MODEL

An attempt has been made to develop the forward and reverse process models for the milling process models using the neural network based approaches (i.e. ANN and RNN). In this study, neural networks based approaches (i.e ANN and RNN) has been applied to milling process for prediction of its three responses based on three machining parameters namely spindle speed, feed rate and depth of cut through forward mapping as shown in Figure 3.12. Using a reverse mapping method, based on the end user's requirements for the desired values of various responses, the optimal settings of milling process parameters were also predicted. It has been observed that the ANN and RNN predicted results closely corroborate with the experimental and test case results which prove the capability of neural network based approaches as an effective tool for developing such prediction models to cater the needs of both the operators and the end users. It can also be extended further for modeling other complex machining processes with a large number of control parameters and responses. It is to be noted that the results of the reverse modelling are considered to be more useful for the end user to achieve the desired output. In addition, the developed methodology can be implemented to adjust the process parameters in on-line control of the milling quality. This model for reverse mapping is also trained using the test cases and is subsequently used for prediction of the tentative settings of the milling process parameters based on a set of desired response characteristics. It can also be treated as an advisory system in absence of human experts, can predict the settings of various process parameters in a milling process parameters in a milling set up in order to achieve the desired responses according to the requirements of the end users.

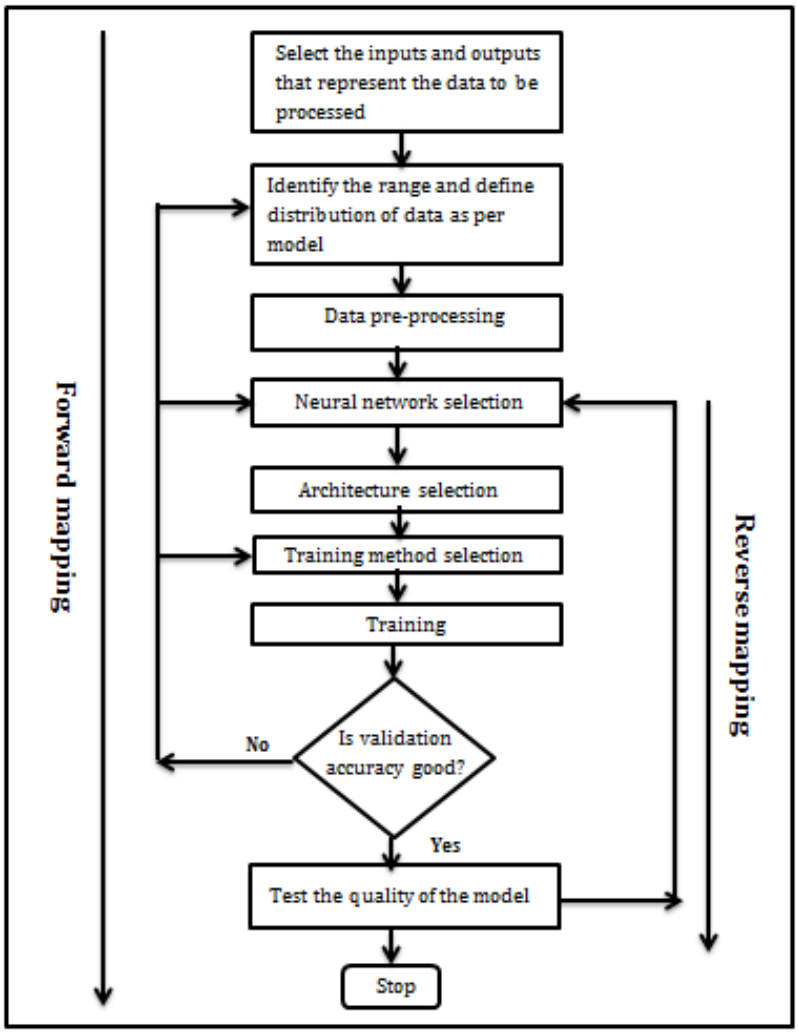

Figure 3.11: Steps in Developing Neural Network

The working and procedure involved in ANN Model Development are discussed in section 3.12 and Figure 3.11.The prediction carried out by the Reverse Mapping can be compared with the Neural Network based approaches such as Genetic Algorithm Neural Network (GA-NN) ,Back Propagation Neural Network (BPNN) . Reverse Mapping was used in order to predict the process parameters for the desired responses. Figure 3.13 shows the structure of a neural network used in reverse mapping. The responses namely: surface roughness(Ra), cutting force (Fx) and power consumption were treated as an input to NN, whereas process parameters such as spindle speed, feed rate and depth of cut were considered as output in reverse mapping. Hence, the NN structure in reverse mapping consists of two neurons for the input layer and three neurons in output layer.

Since ANN can represent the relationship between the input and output, the reverse mapping can be used as one of the strategies for controlling the output parameters of CNC machine. This can be carried out by simulating the dynamic nature of the CNC machine. This can mimic or behave similar to that of the CNC machine. This will help in establishing an intelligent decision support system for any manufacturing industry.

3.14.1 Artificial Neural Network (ANN) Modeling: Forward And Reverse Mapping For AA6061 and AA6061-4.5%Cu- 5%SiCp

The prediction carried out by the Reverse Mapping can be compared with the Neural Network based approach: BPNN. Reverse Mapping was used in order to predict the process parameters for the desired responses. The vital goal of Reverse Mapping is to identify the set of input process parameters, corresponding to a set of desired output parameters. The statistical methods fail to achieve the condition of reverse mapping because of invertible nature of the matrix transformation. Thus to overcome the issues, the ANN and RNN techniques are incorporated as these techniques handle the reverse mapping method in an significant manner.

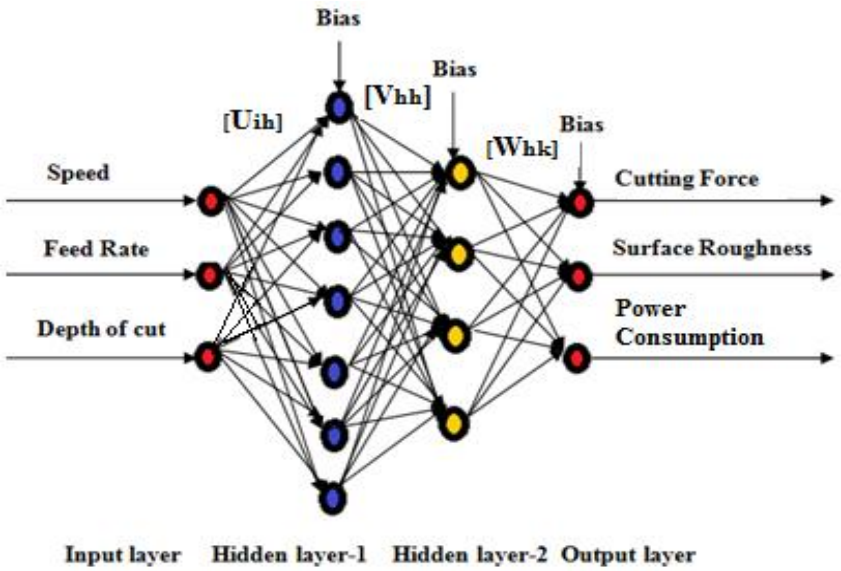

Figure 3.12 : ANN - Neural Network Structure used in case of Forward Mapping

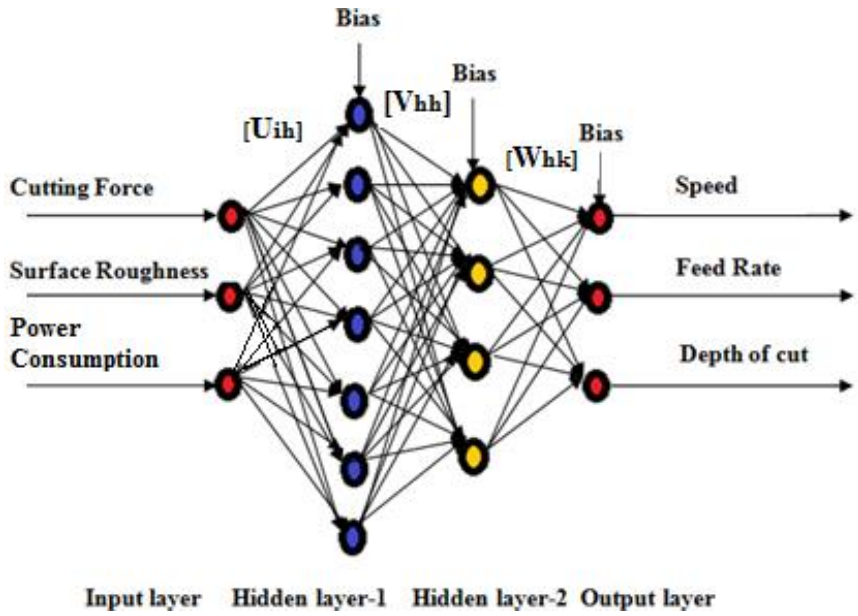

Figure 3.13: ANN - Neural Network Structure used in case of Reverse Mapping.

The neural network architecture in case of forward mapping and reverse mapping of ANN technique are shown in Figure 3.12 and 3.13 respectively. Figure 3.13 presents the structure of a neural network used in reverse mapping. The responses namely surface roughness, cutting force in X direction (X axis) are treated as input to NN, whereas process parameters such as spindle speed, feed rate and depth of cut are considered as output in reverse mapping. Hence, the NN structure in reverse mapping consists of three neurons for the input layer and three neurons in output layer.

3.14.2 Recurrent Neural Network (RNN) Modeling: Forward And Reverse Mapping

The Elman Network (Elman 1990) is used as the ANN model for prediction of Fx , SR and power Consumption. The Elman RNN network has 3 input neurons, 7 neurons for hidden layer 1, 4 neurons for hidden layer 2 and 3 neurons for output layer, The hunt for these number of hidden layer neurons is to be continued till one obtains minimum generalization error. Generally in the RNN technique, the feedback connections may be inter linked either from layer to other layer or the feedback connections may be self-feedback (Negalye 2013). Figures 3.14 and 3.15 represent the schematic representation of RNN technique opted to train and predict the

responses. The input parameters assigned for training process in case of forward mapping are spindle speed, feed rate and depth of cut. The predicted responses are Fx , SR and power consumption. Similarly in the case of reverse mapping, the input parameters considered are Fx , SR and power consumption, and the predicted responses are spindle speed, feed rate and depth of cut. The neural network architecture in the case of forward mapping and reverse mapping of RNN technique are shown in Figure 3.14 and 3.15 respectively.

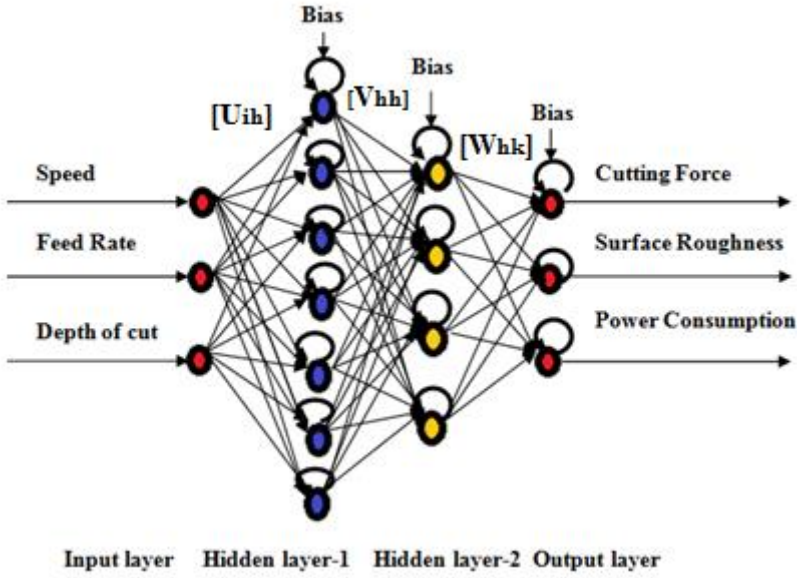

Figure 3.14: RNN - Neural Network Structure used in case of Forward Mapping

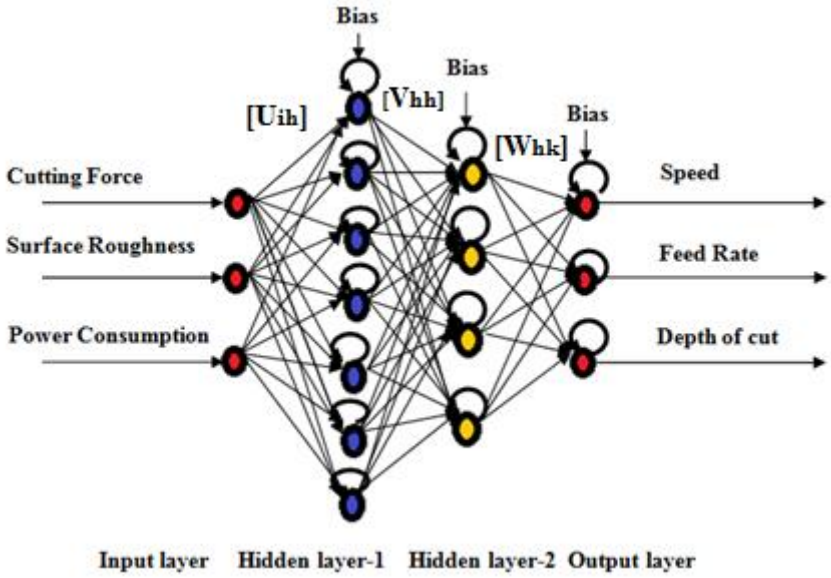

Figure 3.15: RNN - Neural Network Structure used in case of Reverse Mapping .

3.15 GRAPHICAL USER INTERFACE DESIGN

The medium of graphics has revolutionised the user interface design. If used appropriately, it can harness the information assimilation, processing and dissemination capabilities of the user and allow for faster interaction with computer system. Graphical User Interface (GUI) has brought about a marked change in the world of computing in terms of use of computer systems across professions. A well designed GUI will help the user to interact with the system comfortably, in the sense, that it is easier to learn, more effective to use and does not cause vision fatigue when used for long periods. The fact that they are easy to use does not imply that they are easy to design. In fact the designing medium for GUIs in modern days is so rich with so many different options of architectures, colour combinations, facilities, metaphors, patterns available that one can create an excellent GUI for a given application. However, with so much flexibility available in terms of choices in design, there is every possibility of the designer going overboard and coming out with a mediocre, lacklustre design of GUI. Therefore designing a good GUI is a challenging task.

3.15.1 Objectives Of Graphical User Interface Design

The user interface is a part of the computer system which connects the user with the internal system of the computer. While the user operates on a GUI, has no access to what is happening inside the computer system. The system will work in the background based on the information provided by the user in the input section and provide him/her with the processed outputs. Therefore the user is more concerned with the interface, rather than what is happening in the background. Hence the objective of the GUI design is to make it as user friendly as possible, by increasing its usability.

3.16 INTRODUCTION FOR DEVELOPING CONTROL STRATEGY USING SOFTWARE TOOL (LABVIEW).

Adaptive control system is an appendage of a machine's control that enables the machine to cope with the variables that software cannot tackle. Adaptive control (AC) is designed specifically to handle conditions safely such as variations in material hardness, uneven dimensions and surfaces of the workpiece, tool wear, and temperature variations during cutting and fixture instability while maximizing metal removal (Mathias 1968, Bedini et al. 1976, Huber et al.1968). The use of computer numerical control (CNC) machining centres has expanded rapidly through the years. A great advantage of the CNC machining center is that it reduces the skill requirements of machine operators. However, a common drawback of CNC end milling is that its operating parameter such as spindle speed or feedrate is prescribed conservatively either by a part programmer or by a relatively static database in order to preserve the tool. As a result, many CNC systems run under inefficient operating conditions sometimes. For this reason, a CNC machine tool control system, which provides on-line adjustment of the operating parameters, is being studied with interest.

These systems can be classified into three types: a geometric adaptive compensation (GAC) system; an adaptive control optimization (ACO) system; and an adaptive control constraints (ACC) system. GAC systems enhance part precision by applying real time geometric error compensation for imprecision caused by varying machine temperature, imprecise machine geometry, tool wear and other factors (Yoram Koren 1989). However, due to the difficulty in on-line measurement of tool wear and machine tool temperature, there are no commercial GAC systems available. ACO systems and ACC systems enhance productivity by applying an adaptive control technique to vary then machining variables in real time (Porter et al.1969, Peklenik 1970). ACO systems set up the most effective cutting condition for the present cutting environment. For this purpose, ACO systems require on-line measurement of tool wear unfortunately; adaptive control alone cannot effectively control cutting forces. There is no controller that can respond quickly enough to sudden changes in the cut geometry to eliminate large spikes in cutting forces. Therefore, an on-line adaptive

control in conjunction with off-line optimization is attempted here. In our AC system, the feedrate and spindle speed is adjusted on-line and off-line based on the power constraint using PID logic in milling to increase machine utilization and to maintain a constant cutting force in spite of variations in cutting conditions.

CHAPTER 4

CONCEPT OF MEASURING CUTTING FORCE:

INDIRECT METHOD

4.1 INDIRECT METHOD OF MEASURING THE CUTTING FORCES

Measuring the cutting forces during machining is a very complicated task. The direct method of measuring the cutting force is having a lot of disadvantages like cost, mounting of sensors, constrains of cutting parameters and machine and cutting condition. Therefore indirect method of measuring cutting forces is used. There are several techniques used to measure the cutting forces in indirect method. One method is to mount the current sensor at the place where the power goes to the servo motor and other technique is to take the current signals of the feed servo motor from the MCU as depicted in Figure 3.5 (Chapter 3, In section 3.9). The current drawn by each axis is measured with and without cutting. The current drawn by the servomotor is nothing but the force required to move the table from the initial stage to the cutting stage. The current drawn during without cutting includes contributing factors like the friction force, preload torque, weight of the table and component, motor inertia, disturbance in the electrical and mechanical system. The current drawn during cutting includes these effects and cutting force required to remove the material during cutting. To calculate the cutting force, we have to subtract the cutting without current from cutting current. The torque can be calculated by multiplying the current with torque constant as in equation (4.1).

Torque of the motor T_m, = current drawn by the motor * RMS Torque constant.

Each motor has its own torque constant which is specified in the motor specification table. We have

$$T_m = \frac{F\,L\,\pi\eta}{1000} \tag{4.1}$$

Where F= cutting force in N, L = lead in mm, η = efficiency of power transmission

4.2 SERVOGUIDE (SG)

SERVOGUIDE software from FANUC system is used for tuning and performance check of the CNC machine. It provides communication interface between the CNC machine and personal computer. This software is developed by FANUC motor tuning, program upload and download feed and speed commands, measurements of power consumed by the spindle motor, torque and current drawn by the each axis of the servomotor, spindle motor etc. The connection between Servoguide and the CNC system is established through Ethernet cable.

4.3TESTING METHODS FOR THE CUTTING FORCE

Machining process is dynamic, nonlinear, random and coupling. The cutting force mainly varies with these factors, including work piece materials, cutter materials, cutter geometric shapes, cutting angle, cutting speed, cutting depth, cutting fluids, feed at which work piece advances, type of chip and so on. Therefore the accurate measurement of cutting force has been a difficult problem in the manufacturing industry for a long time.

The traditional measurement of cutting force can be classified into two groups. One of them is using formulae. There are usually versatile formulae corresponding to different machining operations. The formulae are simple and convenient to be used and are widely used in manufacturing. But there are many factors, such as work piece materials, cutter materials, cutter geometric shapes and other factors, which are not given enough consideration in these formulae. So the result from this method is imprecise and can only be used as reference.

In the other method, force measuring sensors and control signal have been used to measure the forces induced during cutting. The accuracy of force sensor mainly depends upon accuracy of the sensor and the testing methodology adapted to measure the forces. There are different types of force measuring sensors, especially the resistance strain measurement system and the piezoelectric crystal measurement system which are commonly used in measuring cutting forces. The resistance strain

measure system is also divided into two types, static and dynamic measurement. They differ mainly in the core element. The cutting force is typically random and changes with the machining time and cutting conditions. Thus we can only adopt the dynamic resistance strain measurement to measure the cutting force.

The dynamic resistance strain measurement is quite common to measure the cutting force. In the machining, the strain area and magnitude are varied with the different cutting edges and directions. According to this, the strain element should be differently placed. Currently, the dynamic resistance strain measurement is successfully used to measure the cutting force of milling, grinding and lathe operations. When testing the cutting force of the milling machines in face milling processing, it is difficult to fix the sensor on the cutter, so it is fixed on the work piece. In the process, because of the shape and size of workpiece keeps changing, the stress distribution caused by the cutting force is changing over time. Therefore, it is difficult to attain the value of cutting force simply by measuring the response in milling process. And the resistance strain measure system has lower precision to measure the cutting force. In the control system, the controller sends the current signal to the servo driver, where this signal gets amplified to drive the servo motor at a specified feed rate. A tacho generator generates a signal according to the feed of the table. This signal is sent back to the machine control unit(MCU) for comparison between the actual feed of the servo motor and the desired feed, if there is an any error, it is corrected by MCU and adjusted feed rate signal is sent to the servo driver. The comparison of the dynamometer measured cutting force and the indirect method of measuring the current signal of the controller has been done by (Kim et al. 1995, and Wang et al. 2006).

Several current measuring sensors have been developed to measure the current consumed during the process. A system controlled current signal was used, which is sent to driver during the cutting. The drives then amplify this signal according to the servo motor requirements. For communication purpose, Servoguide diagnostic software which is developed by the FANUC was used.

4.4 MATHEMATICAL METHOD TO MEASURE THE CURRENT IN THE CONTROL SYSTEM

The linear transfer function between the variation of the feed rate command Vco and the variation of the actual feed rate Vao , for the x-axis feed-drive system is determined as:

$$\frac{Vco}{Vao} = \frac{\omega_{co}}{\omega_{ao}} = \frac{K_0 K_{i1t1} \; K_{t1} \; e^{-st1}}{J_e L_{ao} S_1^3 + J_e \left(R_a + KHK_{i1p1}\right) S_1^2 + K_{t1}\left(K_{p1}K_{i1p1} + K_{bo}\right) S_1 + K_{i1}K_{t1}K_{i1p1}} \qquad (4.2)$$

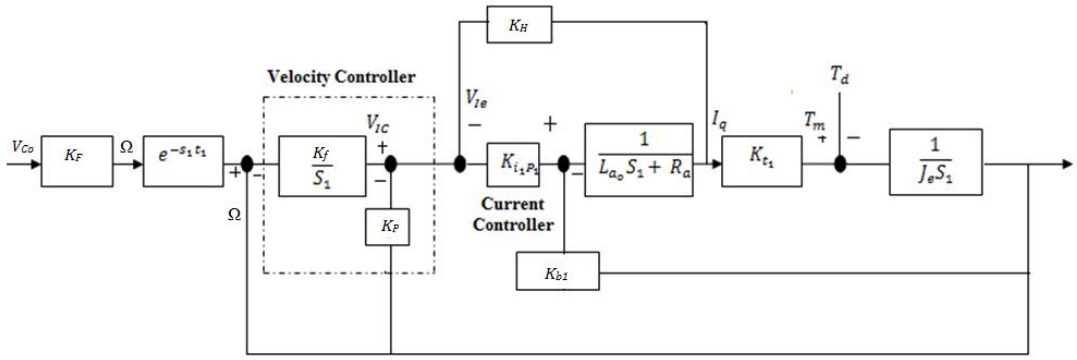

Figure 4.1: Control system diagram of CNC machine (courtesy Tae-Yong Kim et al. 1995)

As shown in the Figure 4.1 the motor drive torque T_m is exerted in accelerating the equivalent feed-drive inertia J_e, and in overcoming the disturbance torque T_d. The disturbance torque T_d consists of the friction torque in the drive T_f and the cutting torque T_c reflected on the motor shaft.

V_{Co}	Feedrate command [mm/min]	Ω	Actual ang. Vel. [rad/min]
Ω	Ang.vel command [rad/min]	K_F	Angular Velocity gain [(rad/sec)/(mm/min)]
K_f	Velocity integral gain [V/(Rad/sec)]	V_{1e}	Feedback current [V]
K_p	Velocity propotional gain [V/(rad/sec)]	Ki_1p_1	Current proportional gain [-]
V_{1c}	Current command [V]	L_{ao}	Armature coil inductance [mH]
K_H	Current feedback gain [V/A]	I_q	Actual current [A]
Ra	Armature coil resistance [ohms]	K_{b1}	Back EMF constant [V/(rad/sec)]
Kt	Torque constant [kgf.m/A]	T_d	Disturbance torque [kgf.m]
T_m	Motor drive torque [kgf.m]	Ω	Angular velocity of motor shaft [rad/sec]
J_e	Equivalent feed drive inertia [kgf.m.sec^2]		

Mechanical equation for torque is given by;

$$T_m = J_e \frac{d\Omega}{dt} + T_d \tag{4.3}$$

$$Td = sign(\Omega)\, T_f + T_c \tag{4.4}$$

Electrical equation for torque

$$T_m = K_t I \tag{4.5}$$

4.5 THE RELATIONS BETWEEN THE CURRENT OF THE SERVOMOTOR AND THE CUTTING FORCE

4.5.1 The Servo Drive System of the CNC Machine Tool

The servomotor is widely used in NC machine tools, processing centres, industrial robots, printing machinery and other high-performance electromechanical equipment's, because of the characteristics of good control performance, the simple structure, the smooth low-speed operation and the high precision positioning. A

servomechanism is a closed-loop control system in which the mechanism position or motion will be precisely controlled. So in the NC machine tool, the servomechanism is usually adopted to the feed control. Figure 4.2 shows the sketch of a servomechanism of NC machine tools. In Figure 4.2, the servomotor generates electromagnetic torque Tm and drives precision ball screw assembly which serves to transform rotary motion into linear motion to move the workbench. Thus, the machining process can be approximately divided into three sequential processes: the formation of cutting force, the transfer of cutting force and the conversion from mechanism to electricity. When the servomotor works in the stable state, the electromagnetic torque of the servomotor should be equal to the load torque which consists of the friction torque T_f, the additional friction torques T_o and the cutting torque T_c. So the torque balance equation of the servo drive system is:

$$T_m = T_f + T_c + T_o \tag{4.6}$$

Where,

T_m—electromagnetic torque;

T_f —equivalent friction torque;

T_c—cutting torque;

T_o—equivalent additional friction torque with the preload.

$$T_o = \frac{F_0 L_0}{2\pi\eta}$$

$$T_f = \frac{F_{p0} L_0 (1 - \eta_0^2)}{2\pi\eta}$$

$$T_o = \frac{F_c L_0}{2\pi\eta}$$

F_0 —the friction force of guides;

L_0 —the ball screw pitch; [length/rotation]

η —the overall efficiency of the transmission chains;

F_{p0} —the pro-load of the ball screw;

η_0 —the efficiency of the ball screw without the pro-load;

F_c—the feed cutting force.

Substituting the above term in equation in 4.6;

$$T_m = \frac{L_o}{2\pi\eta}\left[F_o + F_{po}(1-\eta_0^2) + F_c\right] \tag{4.7}$$

Equation (4.7) is the mathematical model relating the cutting force to the electromagnetic torque of the servomotor. When the cutting force increases, the electromagnetic torque of the servomotor should show a follow-up increase. According to the control theory of the electromagnetic torque of the motor, the current of the servomotor will also augment. So, relation can be established between the current and the milling force. Therefore, the indirect measurement of the cutting force is feasible through measuring the current signal of the servomotor.

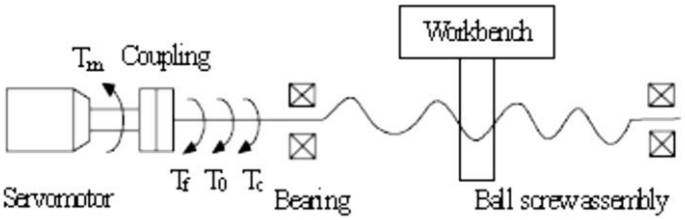

Figure 4.2:The sketch of a servomechanism of the CNC machine tools (Na Wang 2006)

4.5.2 Characteristics Of The Drive motor

In the CNC machine, permanent magnetism synchronous motor (PMSM) is widely used to drive the machine tool. Next, we use vector conversion technology to illustrate the relation between the testing current and the electromagnetic torque of the PMSM. The vector conversion technology is used to analyze the motor current in the rule of forming the same rotary magnetic field. According to this, the three-phase electrical current of the servomotor can be equalled to two-phase electrical current to establish the d-q coordinate system as shown in Figure 4.3. Thus we can control the servomotor just like controlling the DC motor through the vector conversion control. Three-phase stator currents of the PMSM generate the rotary magnetic field, but the permanent magnetism poles of the rotor generate sinusoid magnetic field which is located on the rotor. So the rotor magnetic potential is attracted to rotate by the stator

magnetic potential. In the coordinate rotation system, we take the rotor magnetic field as axis d, thus the three-phase stator currents of the PMSM (iu, iv, iw) can be decoupled as Fig. 4.3 In the d-q coordinate system, the three-phase alternating current can be expressed as shown in equations (4.8), (4.9) and (4.10).

$$i_u = I\,cos\theta \tag{4.8}$$

$$i_v = I\,cos\left(\frac{\theta + 2\pi}{3}\right) \tag{4.9}$$

$$i_w = I\,cos\left(\frac{\theta - 2\pi}{3}\right) \tag{4.10}$$

Where,

I – the amplitude of the stator current;

θ – the Phase angle of the armature current

The u and v phase stator currents, i_u and i_v, respectively cane be measured with Hall sensors.

The w phase stator current can be calculated from the following relationship:

$$i_u + i_v + i_w = 0$$

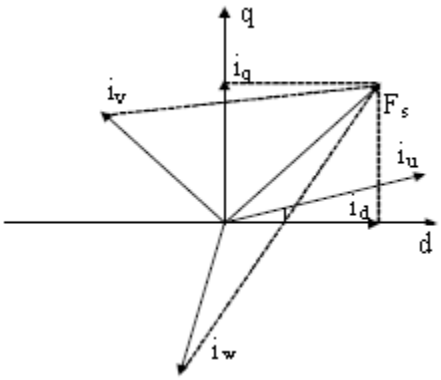

Figure 4.3: The vector conversion technology

Through the vector conversion, the two-phase electrical current on the d-q coordinate system can be denoted as:

$$\begin{bmatrix} i_d \\ i_q \end{bmatrix} = \sqrt{\frac{2}{3}} \begin{bmatrix} \cos\theta & \cos\left(\theta + \frac{2\pi}{3}\right) & \cos\left(\theta - \frac{2\pi}{3}\right) \\ \sin\theta & \sin\left(\theta + \frac{2\pi}{3}\right) & \sin\left(\theta - \frac{2\pi}{3}\right) \end{bmatrix} \begin{bmatrix} i_u \\ i_v \\ i_w \end{bmatrix} \tag{4.11}$$

Apparently, the current i_d and i_q can be calculated using two phase current of the servomotor stator current in actual control. The equation (4.11) of the electromagnetism torque of the PMSM can be expressed as follows,

$$T_m = \frac{3}{2}P\left[\lambda_m i_q + i_d i_q\left(L_d - L_q\right)\right] \quad (4.12)$$

Where

P = the pole of the motor

λ_m = the amplitude of the rotor magnetic chain,

L_d , L_q = the stator equivalent inductance of axis d and q.

On the principle of the maximum of the ratio of the torque and current equation above, we often adopt i_d=0. Then the electromagnetism torque can be simplified as,

$$T_m = \frac{3}{2}P\lambda_m i_q \quad (4.13)$$

When the gas magnetic field of the motor is distributed as sine wave, the λ_m is constant, so T_m is proportional to the armature current i_q. Therefore, the current measurement of the PMSM can reflect the variety of the electromagnetic torque of the motor. Each motor has its own torque constant. Then equation 4.13 can be simplified as

$$T_m = T_t i_q \quad (4.14)$$

Where, T_t = torque constant in Nm/A.

4.6 CNC PART PROGRAMING FOR MACHINING

The following program is used to run the machine. The description of the each code is given in the appendix.

O2701/* Program Name

N001 G21 G94 G54; /*Metric system, Feed rate in mm/min and Work Zero

N002 G91 G28 Z0; /* Incremental Dimension and go to Z Home Position

N003 G28 X0 Y0; /* Go to X and Y Home Position

N004 M06 T08; /*Tool Change and Select Tool Number 8

N005 M03 S1000; /* Spindle Rotation in Clockwise Direction and Speed is 1000 rpm

N006 G90 G00 X-50 Y+50 Z5; /* Linear Interpolation, Absolute Dimension and Go to Work Position Dimensions

N007 G01 X-50 Y50 F300; /*Feed Rate

N008 G01 Z-1; /*Z-axis Depth of Cut 1mm

N009 G01 X110; /*X-axis Traverse

N0010 G01 Z5; /*Z-axis Movement 5mm Above the Surface

N0011 G28 Z0; /*Go to Z Home Position

N0012 G28 X0 Y0; /* Go to X and Y Home Position

N0013 M05; /*Spindle Stop

N0014 M30; /* Machine Stop

4.7 INSTANTANEOUS CURRENT DRAWN BY EACH AXIS

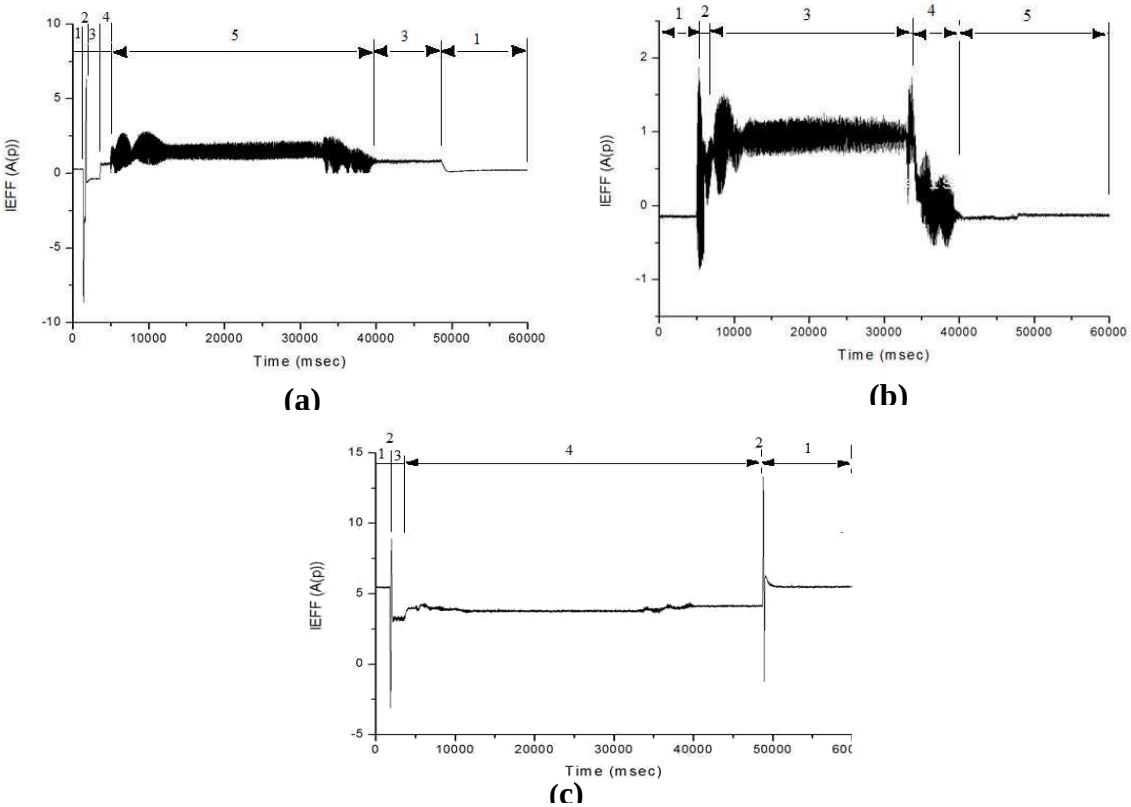

FIGURE 4.4: Instantaneous Current Drawn by (a) X-axis (b) Y-axis (c) Z-axis

The Figure 4.4 (a) shows the instantaneous current drawn by the feed servo motor in the X direction during the execution of the program. Initially, it draws some current to hold the table in position. It is nothing but holding current. This region marked as 1. Sudden rise and sudden fall in the current marked as 2 is the current required for moving the table from undetermined position to home position. Region designated 3 corresponds to tool change and moving the table to work position. Region 4 corresponds to tool movement from X 0 to up to tool and material engages. Region 5 corresponds to cutting action. During this time the current is suddenly raised in the beginning and falls suddenly, when the cutter moves away from the workpiece.

The Figure 4.4 (b) shows the instantaneous current drawn by the Y axis feed table during the execution of the program. In Y axis of the table there is no movement at all. Therefore it requires force to remain in the position. Hence, holding current before and after the cutting execution is required. This is named as number 1 and 5 in the figure 4.4 (b). The number 2 corresponds to the tool movement from home position to work position. The number 3 is cutting region. From the Figure 4.4(b) it ca be observed that at region 3 there is a sudden raise and sudden fall in the graph. It indicates that entry and exit of the tool, cutting and exit of the tool. The number 4 corresponds to without cut region.

The Figure 4.4 (c) shows the instantaneous current drawn by the servo motor in the Z axis direction of the feed table during the program execution. Initially it requires a high amount of current (5 Amps). It means that the Z axis in vertical direction and requires the power to hold the spindle assembly in position to perform machining process which is indicated as number 1in Figure 4.4 (c). After that there is a sudden rise and fall in the current on the both sides. It corresponds to the tool movement in the vertical direction at rapid traverse marked as number 2. In between this peak somewhat constant current is required to hold the cutter in position during the execution of cutting process which is numbered as 4. The number 3 region represents the tool movement in the z direction from 5 mm to -0.5 mm.

4.8 CALCULATION OF CUTTING FORCE

The calculations were performed using formulas as discussed in upcoming section (4.10) inorder to find out the maximum and minimum range of the spindle speed and feed rate. Thus with the help of the tool specifications, literature and preliminary experiments the operating ranges of the rotational speed and feed rate were derived.

During machining, the data acquisition was carried out using FANUC LAN cable. The data related to the current drawn by each axis was captured under two varying cases one "With Cut" and "Without Cut". Later the surface roughness values of (Ra) have been measured with a Mitutoyo Surface Roughness Tester.

In "without cutting" method, the tool was in air and the program was executed. The current drawn by the each axis is measured. This current is nothing but the current required to move the table at specified feed rate to overcome the friction, electrical disturbances and mechanical disturbances.

In "with cutting" method, the tool is engaged with the material by a specified depth of cut and current drawn by the servomotor is measured. This current includes the current required to remove the material and also the current required to move the table, overcome the friction, electrical and mechanical disturbances.

Now by separating the "with cut current" with "without cut current" results in the current required to remove material from the surface of the specimen. This current value, when multiplied by the torque constant gives the cutting force required to cut the material.

The current drawn by the servomotor was measured through a diagnostic system (Ethernet cable) which was interfaced to the CNC system. It has a feature of direct interface between the CNC machine and computer system through the LAN cable.

Thus the experiments have been carried out to cover the face milling on CNC milling machine, with AA6061 and AA6061 4.5%Cu 5%SiCp as work materials.

4.8.1 Indirect Method for Calculating Cutting Force

For the experimental instance of : spindle speed = 2000 rpm, feedrate = 400 mm/min and depth of cut = 1mm.

Instantaneous current drawn by the servo motor while with cutting $\mathbf{I_{XW}}$ = 0.74199

Instantaneous current drawn by the servo motor while without cutting $\mathbf{I_{XO}}$ = 0.540392

Current required for cutting

$\mathbf{I_X = I_{XW} - I_{XO}}$ = 0.2015978 A

Torque constant **TCC = 1.16 Nm/A**

Torque = Torque constant * Instantaneous current.

$\mathbf{T_{XW} = T_{CC} * I_{XW}}$ $\mathbf{T_{XO} = T_{CC} * I_{XO}}$

$\mathbf{= 1.16 * 0.74199}$ $\mathbf{= 1.16 * 0.540392}$

$\mathbf{T_{XW} = 0.860708\ N\text{-}m}$ $\mathbf{T_{XO} = 0.6268548\ N\text{-}m}$

Instantaneous torque produced while with cutting $\mathbf{T_{XW} = 0.860708\ N\text{-}m}$

Instantaneous torque produced while without cutting $\mathbf{T_{XO} = 0.6268548\ N\text{-}m}$

$\mathbf{F_X = T*2*\pi*\eta / L}$ Where η is efficiency of power transmission = 90 %, **L=** Lead of the ball screw = 12mm for X and Y axis, 10mm for Z axis.

Instantaneous cutting force with cutting $\mathbf{F_{XW} = \frac{0.860708 * 2 * \pi * 0.9 * 1000}{12}\ N}$

$\mathbf{F_{XW} = 405.6518\ N}$

Instantaneous cutting force without cutting $\mathbf{F_{XO} = \frac{0.6268548 * 2 * \pi * 0.9 * 1000}{12}\ N}$

$\mathbf{F_{XO} = 295.437\ N}$

Cutting force required to remove the material is **Fx** is obtained by,

$\mathbf{F_X}$ = Instantaneous cutting force with cutting - Instantaneous cutting force without cutting.

F_X = 405.6518 - 295.437 = 110.22 N, Similarly,

The **F_Y , F_Z** are calculated , **F_Y = 56.03444 N; F_Z = 32.642 N.**

The vertical (Z-direction) force component was negligible and hence it was not recorded. In Y axis of the table there is no movement at all. Hence inorder to retain the table in position some amount of power is required, it is negligible and hence it was not recorded. It was seen that the milling force component transverse to the feed direction (along X-axis) was consistently significant and changed appreciably with change in cutting conditions. This force component was therefore focused upon for analysis and the mean value of this X-direction force (henceforth referred to as force) was used for this study (T.Radhakrishnan et.al). So in this study the Fy and Fz forces are negligible.

4.9 ANALYSIS OF VARIATION IN FEED DRIVE CURRENT TO RELATE RESULTING CUTTING FORCE VARIATION

Attempt has been done to analyze the variation in surface finish with the cutting force variation, because it has been proved that the variation in cutting force affects the dynamic stiffness of the machine tool which is responsible for the variation in surface finish. For effective automation, where the process takes place without human interference, continuous monitoring of the milling process is necessary. Most frequently, this has been made possible by measuring the cutting force characteristics by which it is possible to assess the changes of the quality of the surface finish.

The adaptive system of control, which controls the cutting force and maintains constant roughness of the machined surface during milling by continuous dynamic adjustment of the cutting parameters, is an important development in the field of machining. The model based on forces measured using Kistler or similar dynamometers have rigidity, loading capacity and economic limitations as the actual forces developed during machining of component mounted directly on the fixture is

much more as compared to the forces measured by, mounting the force sensor on the workpiece.

The objective of the proposed system is to relate the cutting force variation with surface roughness, on similar lines as been attempted by using the current measured online though servo guide software, on FANUC - OM controlled ACE machining centre model - Spark DTC 250. The data of instantaneous current drawn by the servomotor of the axes have been converted by using the physical equations to determine the torque developed by each motor and the cutting forces have been calculated using the servo guide software. The plot of the cutting force variation is compared with plot of current variation of servomotors and observed that there is lot of similarity and hence calculated cutting force plot can be directly used to reflect variation in surface roughness of the machined work piece, on similar trend.

4.10 SUMMARY

In this chapter, indirect method of calculating cutting force using current consumed by each axis of the motor is discussed. The measured cutting forces are used to infer the knowledge of the machine to correlate the surface roughness and power consumption.

- The data of instantaneous current drawn by the servomotor of the axes have been converted by using the empirical equations to determine the torque developed by each motor and the cutting forces have been calculated using the servo guide software.
- The plot of the cutting force variation is compared with plot of current variation of servomotors and observed that there is lot of similarity and hence calculated cutting force plot can be directly compared with variation in surface roughness of the machined work piece.

Related Article: Rashmi Malghan, Karthik Rao, Arun Shettigar, Shrikantha Rao and D'Souza (2017)." Investigation of Cutting Force via Indirect Approach and Evaluation of machining characteristics of AA6061", *Materials and Manufacturing Processes*, https://doi.org/10.1080/10426914.2017.1388520

CHAPTER 5

RESULTS AND DISCUSSION (PART 1)

DESIGN OF EXPERIMENT: TAGUCHI METHOD

5.1 INTRODUCTION

The influence of machining parameters on performance measures, namely cutting force (FX), surface roughness (Ra) and Power consumption are discussed in the subsequent section. The input parameters and their respective levels used for the current study are listed in Table 5.1. The selections of these parameters are based on the survey of literature and by preliminary investigations. L_{27} Taguchi orthogonal array (OA) of experiments was opted to further carry out the experiments and to analyze the involved process parameters,

5.2 EXPERIMENTAL RESULTS

The machining experiments were carried out on the CNC milling machine to identify and to study the effect of process parameters on the output characteristics such as FX, Ra and Power consumption with their respective S/N ratio values, as exhibited in Table 5.2, 5.3 and 5.4 for AA6061 & AA6061-4.5%Cu-5%SiCp materials.

In the present study all the plots, designs and analysis have been incorporated using Design Expert software. The main criteria to use S/N ratio is to measure responses to identify, develop products and processes insensitive to noise factor (Cochran and Cox 1962). Usually from this the predictable outputs of either product or processes in the existence of noise factor can be identified. The process parameter with greater S/N ratio will yield optimum value with minimum variance. The S/N ratio values used in the present study are as follows, for FX larger the better characteristic, for Ra smaller the better characteristic, and for Power consumption larger the better characteristic.

Table 5.1: Experimental Design using L_{27} orthogonal array for AA6061, AA6061-4.5%Cu-5%SiCp

Trial. No	Levels of Process Parameters Settings					
	AA6061 , AA6061-4.5%Cu-5%SiCp					
	Coded Form			Un Coded Form		
	Spindle Speed (rpm)	Feed Rate (mm/min)	Depth of Cut (mm)	Spindle Speed (rpm)	Feed Rate (mm/min)	Depth of Cut (mm)
1	1	1	1	1000	300	1
2	1	1	2	1000	300	2
3	1	1	3	1000	300	3
4	1	2	1	1000	400	1
5	1	2	2	1000	400	2
6	1	2	3	1000	400	3
7	1	3	1	1000	500	1
8	1	3	2	1000	500	2
9	1	3	3	1000	500	3
10	2	1	1	2000	300	1
11	2	1	2	2000	300	2
12	2	1	3	2000	300	3
13	2	2	1	2000	400	1
14	2	2	2	2000	400	2
15	2	2	3	2000	400	3
16	2	3	1	2000	500	1
17	2	3	2	2000	500	2
18	2	3	3	2000	500	3
19	3	1	1	3000	300	1
20	3	1	2	3000	300	2
21	3	1	3	3000	300	3
22	3	2	1	3000	400	1
23	3	2	2	3000	400	2
24	3	2	3	3000	400	3
25	3	3	1	3000	500	1
26	3	3	2	3000	500	2
27	3	3	3	3000	500	3

Table 5.2: Experimental results of FX for AA6061 & AA6061-4.5%Cu-5%SiCp

Trial. No	Cutting Force FX (N)			
	AA6061		AA6061- 4.5%Cu-5% SiCp	
	FX	S/N ratio	FX	S/N ratio
1	45.50	33.16	71.28	37.06
2	50.31	34.03	78.03	37.85
3	56.69	35.07	87.64	38.85
4	58.72	35.38	90.37	39.12
5	63.42	36.05	109.45	40.78
6	72.60	37.22	115.33	41.24
7	73.27	37.30	120.39	41.61
8	79.05	37.96	134.79	42.59
9	83.56	38.44	139.53	42.89
10	93.58	39.42	144.91	43.22
11	100.01	40.00	155.12	43.81
12	107.23	40.61	176.66	44.94
13	110.22	40.84	179.40	45.08
14	115.02	41.22	182.50	45.23
15	119.84	41.57	185.55	45.37
16	126.74	42.06	187.34	45.45
17	134.22	42.56	190.09	45.58
18	141.48	43.01	194.46	45.78
19	143.30	43.12	232.49	47.33
20	148.55	43.44	241.82	47.67
21	150.52	43.55	245.12	47.79
22	152.58	43.67	247.98	47.89
23	153.29	43.71	249.63	47.95
24	155.15	43.82	250.16	47.96
25	158.30	43.99	254.03	48.10
26	159.82	44.07	257.86	48.23
27	164.21	44.31	259.00	48.27

Table 5.3: Experimental results of Ra for AA6061 & AA6061-4.5%Cu-5%SiCp

Trial. No	Surface Roughness Ra (μm)			
	AA6061		AA6061- 4.5%Cu-5% SiCp	
	Ra	S/N ratio	Ra	S/N ratio
1	0.70	3.10	3.24	-10.21
2	0.64	3.88	2.99	-9.51
3	0.63	4.01	2.35	-7.42
4	0.86	1.31	3.81	-11.62
5	0.76	2.38	3.39	-10.60
6	0.67	3.48	2.70	-8.63
7	0.96	0.35	4.35	-12.77
8	0.86	1.31	3.99	-12.02
9	0.68	3.35	3.06	-9.71
10	0.63	4.01	2.00	-6.02
11	0.61	4.29	2.07	-6.32
12	0.62	4.15	1.77	-4.96
13	0.73	2.73	2.44	-7.75
14	0.66	3.61	2.29	-7.20
15	0.62	4.15	1.74	-4.81
16	0.85	1.41	2.82	-9.00
17	0.71	2.97	2.58	-8.23
18	0.60	4.44	1.94	-5.76
19	0.52	5.68	1.20	-1.58
20	0.55	5.19	1.40	-2.92
21	0.56	5.04	1.30	-2.28
22	0.66	3.61	1.21	-1.66
23	0.58	4.73	1.34	-2.54
24	0.55	5.19	1.14	-1.14
25	0.71	2.97	1.45	-3.23
26	0.56	5.04	1.35	-2.61
27	0.48	6.38	1.00	0.00

Table 5.4: Experimental results of Power Consumption for AA6061 & AA6061-4.5%Cu-5%SiCp

Trial . No	Power Consumption (kW)			
	AA6061		AA6061- 4.5%Cu-5% SiCp	
	Power	S/N ratio	Power	S/N ratio
1	0.04	-28.53	0.06	-24.50
2	0.04	-27.48	0.07	-23.17
3	0.05	-26.33	0.08	-22.06
4	0.07	-23.42	0.11	-19.25
5	0.07	-22.65	0.13	-17.74
6	0.08	-21.47	0.14	-17.07
7	0.11	-19.32	0.18	-14.81
8	0.12	-18.64	0.20	-13.84
9	0.13	-18.03	0.21	-13.45
10	0.08	-21.61	0.15	-16.67
11	0.09	-20.90	0.15	-16.20
12	0.10	-20.29	0.17	-15.37
13	0.13	-17.46	0.23	-12.73
14	0.14	-17.03	0.24	-12.48
15	0.15	-16.62	0.24	-12.22
16	0.19	-14.26	0.31	-10.07
17	0.20	-13.78	0.32	-9.87
18	0.22	-13.31	0.33	-9.56
19	0.13	-17.59	0.24	-12.40
20	0.14	-17.29	0.25	-12.10
21	0.14	-17.16	0.25	-11.89
22	0.19	-14.56	0.33	-9.61
23	0.19	-14.39	0.34	-9.42
24	0.20	-14.20	0.35	-9.24
25	0.25	-12.06	0.44	-7.20
26	0.25	-11.88	0.44	-7.05
27	0.26	-11.64	0.45	-6.95

5.3 EFFECT OF PROCESS PARAMETERS ON FX, RA AND POWER CONSUMPTION -ANOVA

5.3.1 Effect of Process Parameters on FX, Ra and Power Consumption AA6061

The effect of process parameters on the responses FX, Ra, and Power Consumption were analysed using the L_{27} OA as represented in Table 5.1.The implication, significance of the process parameters on the responses and even the contribution percentage on the responses were identified by implementing the Analysis of variance (ANOVA) computational technique (Phadke, 1989 and Ross, 1996). ANOVA complies of sum of squares, degrees of freedom, mean square, F-value and P value. Table 5.5 - 5.7 shows the Analysis of variance for AA6061material. From the Table 5.5 - 5.7 it can be observed that the Speed, Feed Rate and Depth of cut are significant parameters and have significance on the Ra, FX and Power Consumption responses. The significance of the parameter is concluded based on the P value, if the P value attained is less than 0.05 then the parameters are assigned to be significant parameters. The percentage of contribution for individual process parameter along with the interaction of the process parameter percentage contribution is calculated to identify the major contribution complied by the process parameters on the responses.

From the Table 5.5, it can be observed that Speed has major contribution of 90.76 % on FX, followed by Feed Rate 7.08 % and Depth of cut 1.11 %. The interaction of Speed * Feed Rate 0.85 %, Speed * Depth of cut 0.12 % and Feed Rate * Depth of cut 0.01 % have lesser contribution on FX.

From the Table 5.6, it can be observed that Speed has major contribution of 41.22 % on Ra, followed by Depth of cut 23.97% and The Feed Rate 15.20 %. The interaction of Feed Rate * Depth of cut 12.69%, Speed * Feed Rate 4.44 % and Speed * Depth of cut 1.63 % have minor contribution on Ra.

From the Table 5.7, it can be observed that Speed has major contribution of 54.59 % on Power Consumption, followed by Feed Rate 42.90%. Similarly the interaction of, Speed * Feed Rate 1.68 %, Depth of cut 0.74 %, Speed * Depth of cut 0.04 % and Feed Rate * Depth of cut 0.04% have minor contribution on Power Consumption.

From Table 5.5 - 5.7, it can be concluded that Speed has major contribution on all responses Ra, FX and Power Consumption.

Table 5.5: Analysis of Variance for FX of AA6061

Source	DF	Seq SS	Adj MS	F	P	Remarks	P (%)
Speed	2	36089	18044.5	8001.49	0.000	Significant	90.76
Feed Rate	2	2815.3	1407.7	624.2	0.000	Significant	7.08
DOC	2	441.5	220.7	97.89	0.000	Significant	1.11
Speed*Feed Rate	4	340.4	85.1	37.74	0.000	Significant	0.85
Speed*DOC	4	50.2	12.5	5.56	0.019	Significant	0.12
Feed Rate*DOC	4	4.6	1.2	0.51	0.73	Insignificant	0.01
Residual Error	8	18	2.3				
Total	26	39759.1					

F - F_{test}, P- Percentage of contribution, 95% of confidence

Table 5.6: Analysis of Variance for Ra of AA6061

Source	DF	Seq SS	Adj MS	F	P	Remarks	P (%)
Speed	2	0.141	0.070	200.56	0.000	Significant	41.22
Feed Rate	2	0.052	0.026	73.97	0.000	Significant	15.20
DOC	2	0.082	0.041	116.65	0.000	Significant	23.97
Speed*Feed Rate	4	0.015	0.004	10.82	0.003	Significant	4.44
Speed*DOC	4	0.006	0.001	3.97	0.046	Significant	1.63
Feed Rate*DOC	4	0.043	0.011	30.88	0.000	Significant	12.69
Residual Error	8	0.003	0.000				
Total	26	0.341					

F- F_{test}, P - Percentage of contribution, 95% of confidence

Table 5.7: Analysis of Variance for Power Consumption of AA6061

Source	DF	Seq SS	Adj MS	F	P	Remarks	P (%)
Speed	2	0.061	0.030	19236.72	0.000	Significant	54.59
Feed Rate	2	0.048	0.024	15115.49	0.000	Significant	42.90
DOC	2	0.001	0.000	261.59	0.000	Significant	0.74
Speed*Feed Rate	4	0.002	0.000	296.07	0.000	Significant	1.68
Speed*DOC	4	0.000	0.000	7.57	0.008	Significant	0.04
Feed Rate*DOC	4	0.000	0.000	6.4	0.013	Significant	0.04
Residual Error	8	0.000	0.000				
Total	26	0.111					

F - F_{test}, P- Percentage of contribution, 95% of confidence

Main Effects Plot for Means for FX, Ra and Power Consumption of AA6061

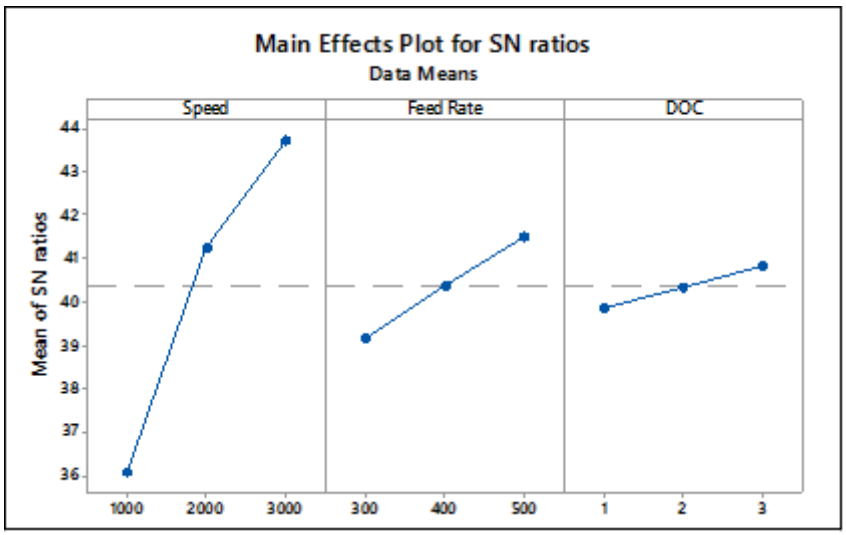

Figure 5.1: Effect of process Parameters on Cutting Force (FX) of AA6061

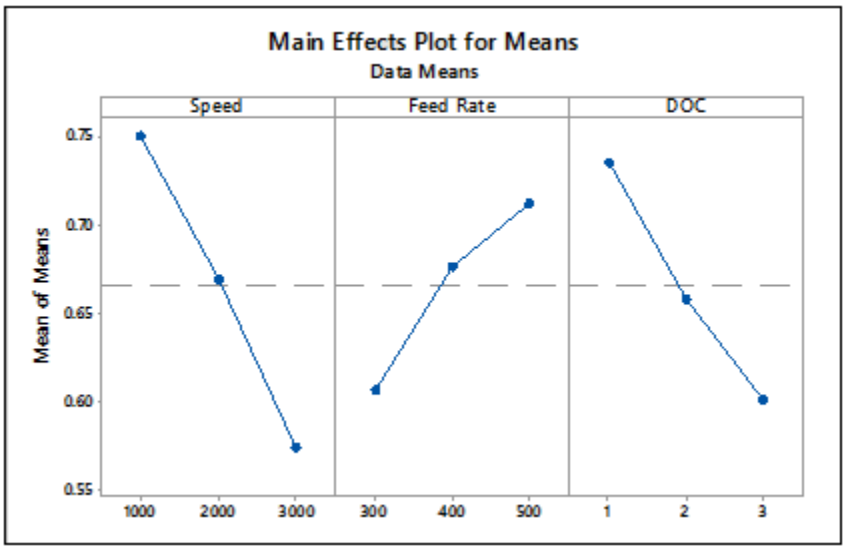

Figure 5.2: Effect of process Parameters on Surface Roughness (Ra) of AA6061

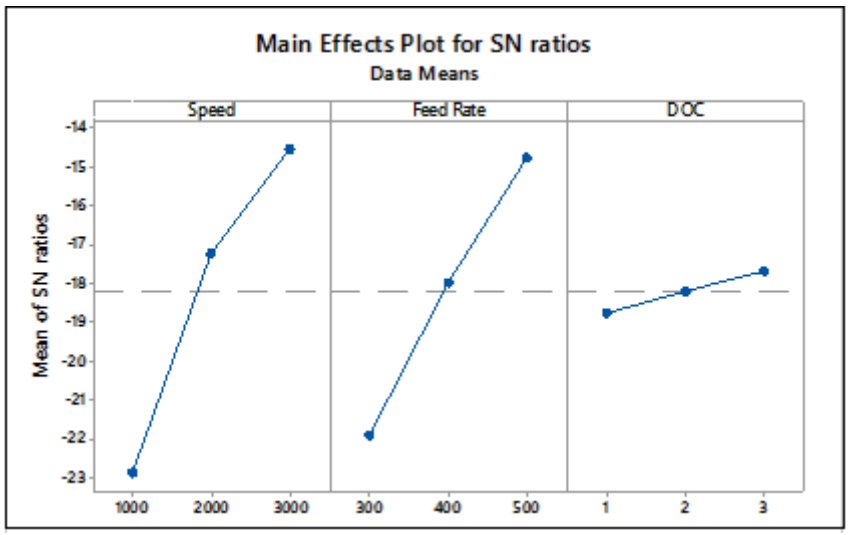

Figure 5.3: Effect of process Parameters on Power Consumption of AA6061

The Figure 5.1 - 5.3 represents the main effect plots for Ra, FX and Power Consumption of AA6061 material. Figure 5.2 exhibits that as the spindle rotational speed increases the value of the Ra decreases due to the built up edge which is formed at the tip of the cutting edges vanishing and hence resulting in better surface finish. As the feed rate increases the Ra value increases. This is due to the axial movement of the cutting tool being larger which results in shifting of the tool to new position on the workpiece surface without completely removing the material .As the depth of cut increases Ra decreases. This is due to increase in the rigidity of the machine during machining process. Further, increases in depth of cut will detroit the surface finish due to the chattering and vibration effect of the machine. The cutting force and the power consumption have shown direct proportional relationship, Figures 5.1 and 5.3 exhibits that as the spindle speed, feed rate and depth of cut increase, the cutting force (FX) indeed increases due to increased area of the chip-tool contact.

5.3.2 Effect of Process Parameters on FX, Ra and Power Consumption -ANOVA for AA6061-4.5%cu-5%SiCp

Similar trend like that for AA6061 materials in terms of the effect of process parameters on FX, Ra and power consumption is observed here also, as can be seen from tables 5.8-5.10.

Table 5.8: Analysis of Variance for FX of AA6061-4.5%cu-5%SiCp

Source	DF	Seq SS	Adj MS	F	P	Remarks	P (%)
Speed	2	92635	46317.7	1942.04	0.000	Significant	92.447
Feed Rate	2	5195	2597.6	108.91	0.000	Significant	5.184
DOC	2	877	438.5	18.38	0.001	Significant	0.875
Speed*Feed Rate	4	1026	256.4	10.75	0.003	Significant	1.024
Speed*DOC	4	172	43	1.8	0.221	Insignificant	0.172
Feed Rate*DOC	4	107	26.7	1.12	0.412	Insignificant	0.107
Residual Error	8	191	23.8				
Total	26	100203					

F - F_{test}, P- Percentage of contribution, 95% of confidence

Table 5.9: Analysis of Variance for Ra of AA6061-4.5%cu-5%SiCp

Source	DF	Seq SS	Adj MS	F	P	Remarks	P (%)
Speed	2	19.065	9.533	3033.360	0.000	Significant	80.782
Feed Rate	2	1.000	0.500	159.020	0.000	Significant	4.235
DOC	2	1.892	0.946	301.030	0.000	Significant	8.017
Speed*Feed Rate	4	0.713	0.178	56.740	0.000	Significant	3.022
Speed*DOC	4	0.691	0.173	54.930	0.000	Significant	2.926
Feed Rate*DOC	4	0.215	0.054	17.120	0.001	significant	0.912
Residual Error	8	0.025	0.003				
Total	26	23.601					

F - F_{test}, P- Percentage of contribution, 95% of confidence

Table 5.10: Analysis of Variance for Power Consumption of AA6061-4.5%Cu-5%SiCp

Source	DF	Seq SS	Adj MS	F	P	Remarks	P (%)
Speed	2	0.201	0.100	10165.98	0.000	Significant	61.471
Feed Rate	2	0.121	0.060	6101.92	0.000	Significant	36.897
DOC	2	0.002	0.001	90.31	0.000	Significant	0.546
Speed*Feed Rate	4	0.003	0.001	83.29	0.000	Significant	1.007
Speed*DOC	4	0.000	0.000	4.27	0.039	Significant	0.052
Feed Rate*DOC	4	0.000	0.000	0.24	0.908	Insignificant	0.003
Residual Error	8	0.000	0.000				
Total	26	0.327					

F - F_{test}, P- Percentage of contribution, 95% of confidence

Main Effects Plot for Means for FX, Ra and Power Consumption of AA6061-4.5%cu-5%SiCp

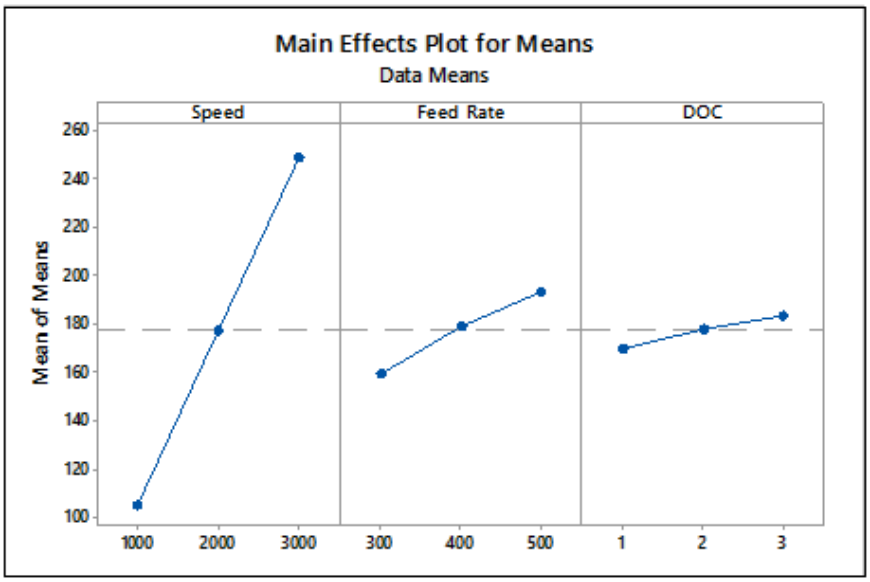

Figure 5.4: Effect of process Parameters on Cutting Force (FX) of AA6061-4.5%cu-5%SiCp

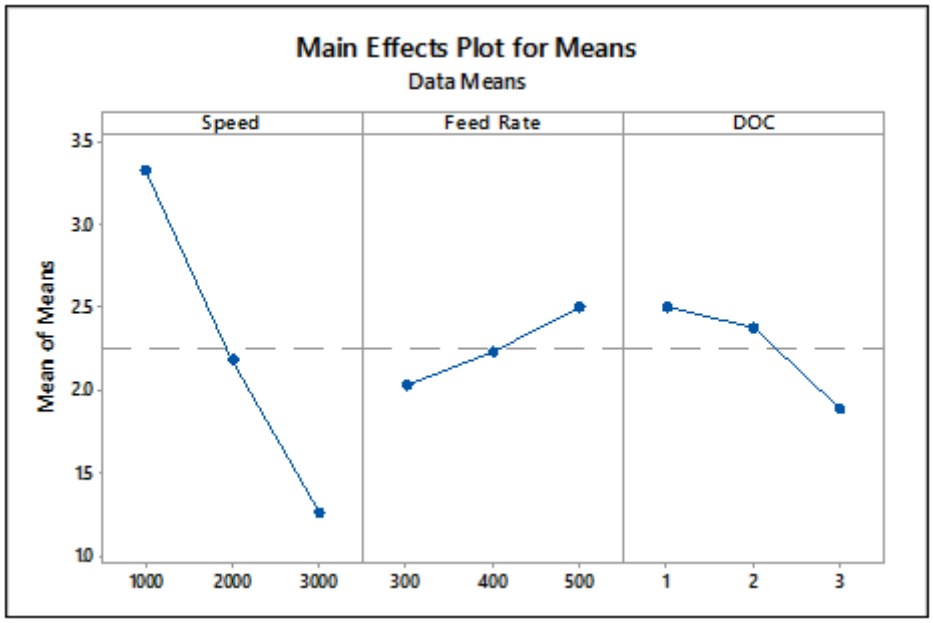

Figure 5.5: Effect of process Parameters on Surface Roughness (Ra) of AA6061-4.5%cu-5%SiCp

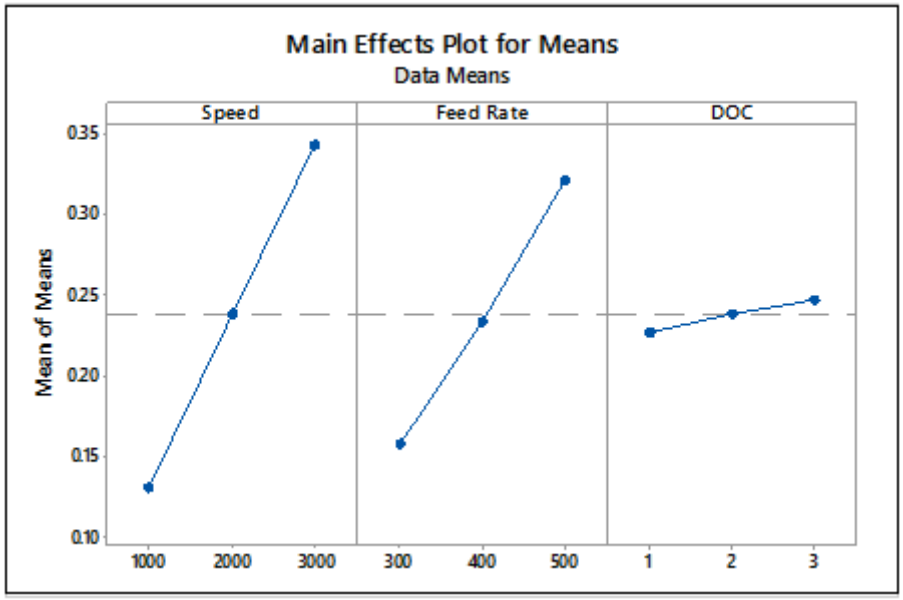

Figure 5.6: Effect of process Parameters on Power Consumption of AA6061-4.5%cu-5%SiCp

Figure 5.4 - 5.6 represents the variation of cutting force, surface roughness and power consumption respectively w.r.t spindle speed, feed rate and depth of cut. There trends are similar to those observed in the section 5.3.

5.4 SUMMARY

The Taguchi parameter design has been incorporated to identify the number of experiments need to be carried out and also deals with the investigation on the effect of machining parameters on the responses such as surface roughness, cutting force and power consumption. The main effect plot of Taguchi for Signal-to-Noise (S/N) ratio is employed to evaluate the effect of process parameters on milling process output variables. The Analysis of Variance (ANOVA) is also used to evaluate the contribution of process parameters on milling process output variables. To identify the interaction between the process parameters, contribution of each parameter and significance of the parameters Response Surface Methodology (RSM) is incorporated in the next chapter. The interaction effect of process parameters on milling process output variables is analyzed using perturbation plots of RSM.

CHAPTER 6

RESULTS AND DISCUSSION (PART 2)

RSM MODELLING FOR PREDICTION

6.1 RSM FOR AA6061

The Central Composite Design (CCD) was used to implement the response prediction using RSM. A total of 20 experiments were performed, which incorporates of 8 cube points, 6 center points in cube, 6 Axial points and alpha value is 1. The range of the process parameters were set by taking into consideration the tool or insert specification and even by performing the trial experiments inorder to achieve the desired responses. In the present work, CCFCD is used for establishing the relationship between the empirical process parameters and the milling process output variables of three different materials i.e. AA6061, AA6061-4.5%Cu-5%SiCp. The final obtained mathematical regression equations are listed in Table 6.4.

Later on the model performance was validated with the help of analysis of variance (ANOVA) (Tables 6.1- 6.3). The significance of the model is identified by this method. If the model satisfies the condition of Prob>f is less than 0.0500 then the model is significant. Since all the proposed models satisfies the condition of Prob>f is less than 0.0500, hence it can be concluded that all the proposed models are significant. The adequacy of the fitted regression model was identified using the R^2correlation coefficient, the value of R^2 need to be close to unity. For all the responses the “Pre R-squared” are in reasonable accidence with the “Adj R-Squared” values. The precision ratio of all the developed models (ratio >4 is desirable) shows the adequacy of incorporating the proposed model.

From the Table 6.1 it can be observed that Speed has major contribution of 91.18 % on FX, followed by Feed Rate 6.29 %. The Depth of cut 0.89 %, Speed * Speed 0.79 % , Speed * Feed Rate 0.38 % have lesser contribution on FX.

From the Table 6.2 it can be observed that Speed has major contribution of 40.52 % on Ra, followed by Depth of cut 22.10%, Feed Rate * Depth of cut 15.2%, Feed Rate 14.21 % contribution respectively. The Speed * Feed Rate 2.63 % and Speed * Depth of cut 1.68 % has minor contribution on Ra.

From the Table 6.3 it can be observed that Speed has major contribution of 55.73 % on Power Consumption, followed by Feed Rate 40.93%. Similarly the, Speed * Feed Rate 1.77 %, Depth of cut 0.61 %, Speed * Speed 0.41 % and Feed Rate * Feed Rate 0.21 % have minor contribution on Power Consumption. From Table 6.1 – 6.3 it can be concluded that Speed has major contribution on all responses Ra, FX and Power Consumption.

Table 6.1: Analysis of Variance for FX of AA6061 using RSM Method

Source	Sum of Squares	DF	Mean Square	F Value	p-value Prob> F	Percentage Contribution	Remarks
Model	21831.5	5	4366.3	630.33	< 0.0001		significant
Speed	19995.2	1	19995.2	2886.5	< 0.0001	91.18%	significant
Feed Rate	1381.45	1	1381.45	199.43	< 0.0001	6.29%	significant
DOC	195.75	1	195.75	28.26	0.0001	0.89%	significant
Speed * Feed Rate	84.2	1	84.2	12.16	0.0036	0.38%	significant
Speed * Speed	174.95	1	174.95	25.26	0.0002	0.79%	significant
Residual	96.98	14	6.93				
Lack of Fit	93.64	9	10.4	15.61	0.0037		significant
Pure Error	3.33	5	0.67				
Cor Total	21928.5	19					

Table 6.2: Analysis of Variance for Ra of AA6061 using RSM Method

Source	Sum of Squares	DF	Mean Square	F Value	p-value Prob> F	Percentage Contribution	Remarks
Model	0.18	6	0.031	225.54	< 0.0001		significant
Speed	0.077	1	0.077	570.38	< 0.0001	40.52%	significant
Feed Rate	0.027	1	0.027	199.16	< 0.0001	14.21%	significant
DOC	0.042	1	0.042	311.19	< 0.0001	22.10%	significant
Speed * Feed Rate	5.00E-03	1	5.00E-03	36.83	< 0.0001	2.63%	significant
Speed * DOC	3.20E-03	1	3.20E-03	23.57	0.0003	1.68%	significant
Feed Rate * DOC	0.029	1	0.029	212.12	< 0.0001	15.20%	significant
Residual	1.77E-03	13	1.36E-04				
Lack of Fit	1.57E-03	8	1.96E-04	4.89	0.0485		significant
Pure Error	2.00E-04	5	4.00E-05				
Total	0.19	19					

Table 6.3: Analysis of Variance for Power Consumption of AA6061 using RSM Method

Source	Sum of Squares	DF	Mean Square	F Value	p-value Prob> F	Percentage Contribution	Remarks
Model	0.061	6	0.01	749.4	< 0.0001		significant
Speed	0.034	1	0.034	2492.41	< 0.0001	55.73%	significant
Feed Rate	0.025	1	0.025	1877.39	< 0.0001	40.93%	significant
DOC	3.72E-04	1	3.72E-04	27.6	0.0002	0.61%	significant
Speed * Feed Rate	1.08E-03	1	1.08E-03	79.78	< 0.0001	1.77%	significant
Speed * Speed	2.55E-04	1	2.55E-04	18.88	0.0008	0.41%	significant
Feed Rate * Feed Rate	1.28E-04	1	1.28E-04	9.46	0.0088	0.21%	significant
Residual	1.75E-04	13	1.35E-05				
Lack of Fit	1.55E-04	8	1.94E-05	4.87	0.0489		significant
Pure Error	1.99E-05	5	3.99E-06				
Cor Total	0.061	19					

6.1.1 Regression Analysis For AA6061

The regression analysis is opted to obtain the correlation between the process parameters and the responses. In the current study the quadratic method is used in order to fit the model and to further carry out the analysis of the experimental data. The regression was implemented for responses FX, Ra and Power Consumption for 2 different materials. The regression equations obtained for AA6061 are listed in Table 6.4

Table 6.4: Regression Equations of FX, Ra and Power Consumption.

SL.No	Responses	Regression equation
1	**FX**	-79.78776 + 0.081353*Vc + 0.18242*f + 4.42441*d - 3.24420E-005*Vc*f - 5.91517E-006*Vc*Vc
2	**R_a**	0.15850 - 2.80000E-005*Vc + 2.22000E-003*f + 0.13500*d - 2.50000E-007*Vc*f + 2.00000E-005*Vc*d - 6.00000E-004*f*d
3	**Power**	-0.030842 + 4.72657E-005*Vc - 2.33913E-004*f + 6.10045E-003*d + 1.15949E-007*Vc*f - 8.91940E-009*Vc*Vc + 6.31394E-007*f*f

Table 6.5 exhibits Comparison of FX, Ra and Power Consumption predicted by RSM Model, with the experimentally obtained FX, Ra and Power Consumption of AA6061material. From the data presented in Table 6.5, the maximum error obtained for surface roughness is 3.95 % at rotational speed of 2000 rpm, feed rate of 400 mm/min and depth of cut of 3 mm which indicates good prediction is possible by the quadratic terms and interaction terms. Similarly the minimum percentage of relative error is -3.02 % at rotational speed of 3000 rpm, feed rate of 500 mm/min and depth of cut 3 mm. Similarly, the maximum error obtained for cutting force is 5.47 % at rotational speed of 2000 rpm, feed rate of 500 mm/min and depth of cut of 2 mm which indicates good prediction is possible by the quadratic terms and interaction terms. Similarly the minimum percentage of relative error is -3.35 % at rotational speed of 2000 rpm, feed rate of 300 mm/min and depth of cut 2 mm. The maximum error obtained for power consumption response is 6.44 % at rotational speed of 1000 rpm, feed rate of 300 mm/min and depth of cut of 1 mm which indicates good prediction is possible by the quadratic terms and interaction terms. Similarly the minimum percentage of relative error is -6.92 % at rotational speed of 2000 rpm, feed rate of 300 mm/min and depth of cut 2 mm.

Table 6.5: Comparison of FX, Ra and Power Consumption predicted by RSM Model, with the experimentally obtained FX, Ra and Power Consumption of AA6061

Experimental				RSM - Prediction			Error (%)		
Expt. No	FX (N)	Ra (µm)	Power (kW)	FX (N)	Ra (µm)	Power (kW)	FX (N)	Ra (µm)	Power (kW)
1	45.5	0.7	0.04	45.07	0.7	0.04	0.94	0.5	6.44
2	143.3	0.52	0.13	140.99	0.53	0.13	1.61	-2.02	3.18
3	73.27	0.96	0.11	75.06	0.97	0.11	-2.45	-1.09	-4.04
4	158.3	0.71	0.25	158.01	0.7	0.25	0.18	0.77	-0.9
5	56.69	0.63	0.05	53.92	0.65	0.05	4.9	-2.62	2.04
6	150.52	0.56	0.14	149.84	0.56	0.14	0.45	-0.09	-0.98
7	83.56	0.68	0.13	83.91	0.68	0.12	-0.42	-0.07	0.65
8	164.21	0.48	0.26	166.85	0.49	0.26	-1.61	-3.02	-0.7
9	63.42	0.76	0.07	64.49	0.75	0.07	-1.68	1.51	0.22
10	153.29	0.58	0.19	153.92	0.57	0.19	-0.41	1.29	0.65
11	100.01	0.61	0.09	103.37	0.61	0.1	-3.35	0.25	-6.92
12	134.22	0.71	0.2	126.87	0.71	0.2	5.47	-0.35	3.74
13	110.22	0.73	0.13	110.7	0.73	0.13	-0.44	0.62	-0.3
14	119.84	0.62	0.15	119.55	0.6	0.15	0.25	3.95	0.69
15	115.02	0.66	0.14	115.12	0.66	0.14	-0.09	-0.08	0.22
16	115.02	0.66	0.14	115.12	0.66	0.14	-0.09	-0.08	0.22
17	114.82	0.65	0.14	115.12	0.66	0.14	-0.26	-1.62	-1.39
18	113.02	0.66	0.14	115.12	0.66	0.14	-1.86	-0.08	1.62
19	115.02	0.67	0.14	115.12	0.66	0.14	-0.09	1.42	0.22
20	114.02	0.66	0.14	115.12	0.66	0.14	-0.97	-0.08	-2.45

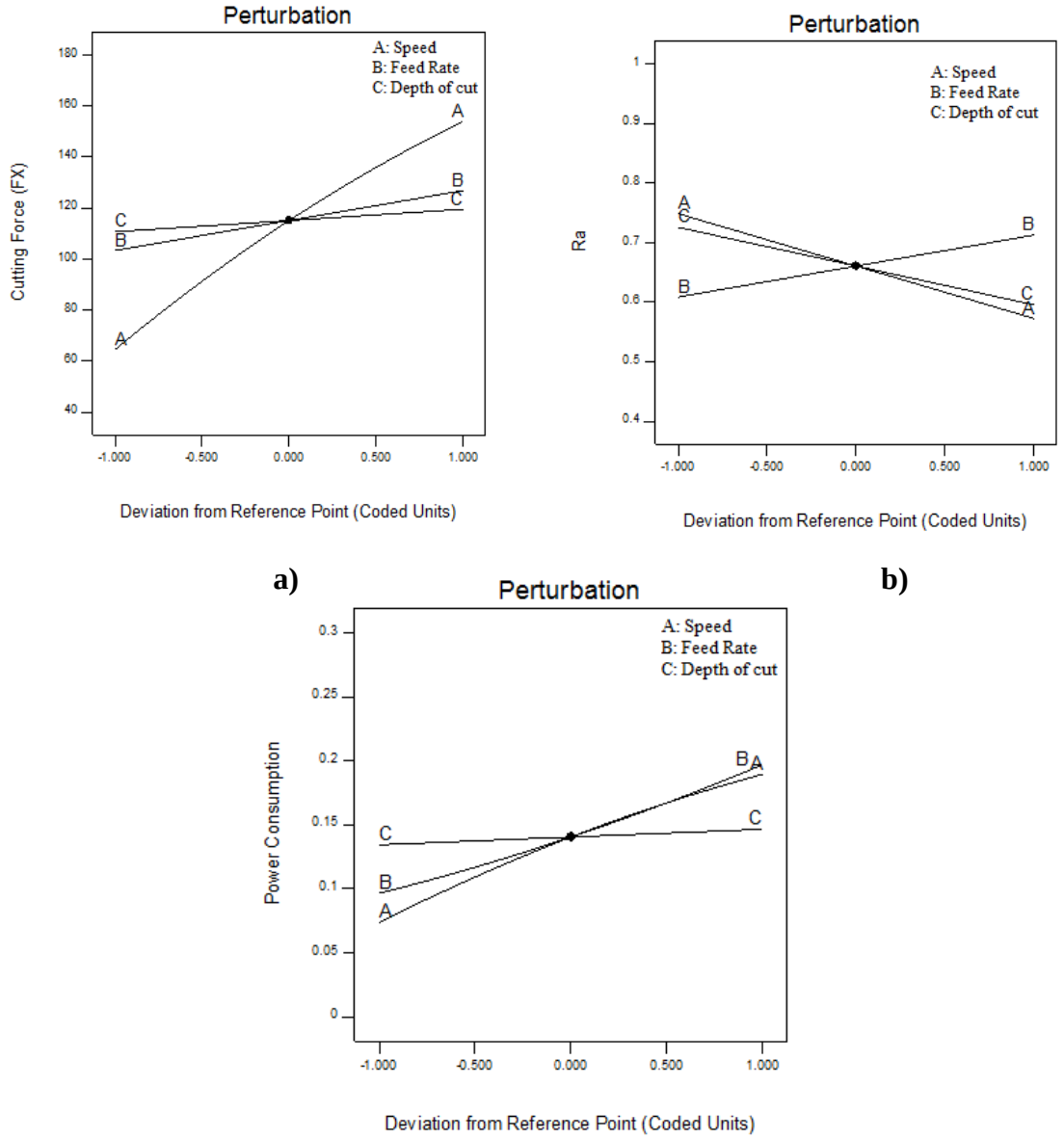

Figure 6.1: Effect of cutting parameters on (a) Cutting Force (b) Surface roughness (c) Power Consumption.

Figure 6.1 (a), (b) and (c) depict the variation of cutting force, surface roughness and power consumption respectively, w.r.t spindle speed, feed rate and depth of cut. These trends are similar to those observed by the ANOVA analysis in section 5.3.2.

6.1.2 RSM For AA6061 4.5%Cu-5%SiCp

Tables 6.6 – 6.8 show the Analysis of variance (ANOVA) for AA6061-4.5%cu-5%SiCp material. From the Table 6.6 it can be observed that Speed has major contribution of 92.45 % on FX, followed by Feed Rate 5.35 %. The interactions of Speed * Feed Rate 0.98 %, Depth of cut 0.64 %, Feed Rate * Feed Rate 0.35% and Speed * Depth of cut 0.07 %, have lesser contribution on FX.

Table 6.7 it can be observed that Speed has major contribution of 79.43 % on Ra, followed by Depth of cut 8.09 %. The Feed Rate 4.04 %, Speed * Feed Rate 3.42 % and Speed * Depth of cut 3.27, Feed Rate * Depth of cut 0.85 %, Speed * Speed 0.20 %, Depth of cut * Depth of cut 0.67 % Feed Rate * Feed Rate 0.07 % has minor contribution on Ra.

Similarly from the Table 6.8 it can be observed that Speed has major contribution of 61.11 % on Power Consumption, followed by Feed Rate 36.66 %. Similarly the, Speed * Feed Rate 1.28 %, Depth of cut 0.46 % have minor contribution on Power Consumption. From Table 6.6 – 6.8 it can be concluded that Speed has major contribution on all responses Ra, FX and Power Consumption.

Table 6.6: Analysis of Variance for FX of AA6061-4.5%cu-5%SiCp using RSM Method

Source	Sum of Square	DF	Mean Square	F Value	p-value Prob> F	Percentage contribution	Remarks
Model	54750.09	6	9125.02	1519.36	< 0.0001		Significant
Speed	50690.95	1	50690.95	8440.3	< 0.0001	92.45%	Significant
Feed Rate	2937.52	1	2937.52	489.11	< 0.0001	5.35%	Significant
DOC	350.98	1	350.98	58.44	< 0.0001	0.64%	Significant
Speed * Feed Rate	537.53	1	537.53	89.5	< 0.0001	0.98%	Significant
Speed * DOC	40.05	1	40.05	6.67	0.0228	0.07%	Significant
Feed Rate * Feed Rate	193.07	1	193.07	32.15	< 0.0001	0.35%	Significant
Residual	78.08	13	6.01				
Lack of Fit	72.44	8	9.06	8.04	0.0172		Significant
Pure Error	5.63	5	1.13				
Cor Total	54828.17	19					

Table 6.7: Analysis of Variance for Ra of AA6061-4.5%cu-5%SiCp using RSM Method

Source	Sum of Squares	DF	Mean Square	F Value	p-value Prob> F	Percentage Contribution	Remarks
Model	12.82	9	1.42	927.76	< 0.0001		
Speed	10.2	1	10.2	6642.55	< 0.0001	79.43%	Significant
Feed Rate	0.52	1	0.52	338.5	< 0.0001	4.04%	Significant
DOC	1.04	1	1.04	679.36	< 0.0001	8.09%	Significant
Speed * Feed Rate	0.44	1	0.44	284.63	< 0.0001	3.42%	Significant
Speed * DOC	0.42	1	0.42	272.59	< 0.0001	3.27%	Significant
Feed Rate * DOC	0.11	1	0.11	73.46	< 0.0001	0.85%	Significant
Speed * Speed	0.026	1	0.026	16.94	0.0021	0.20%	Significant
Feed Rate * Feed Rate	9.02E-03	1	9.02E-03	5.87	0.0358	0.07%	Significant
DOC * DOC	0.087	1	0.087	56.56	< 0.0001	0.67%	Significant
Residual	0.015	10	1.54E-03				
Lack of Fit	7.02E-03	5	1.41E-03	0.84	0.5721		
Pure Error	8.33E-03	5	1.67E-03				
Cor Total	12.84	19					

Table 6.8: Analysis of Variance for Power Consumption of AA6061-4.5%cu-5%SiCp using RSM Method

Source	Sum of Squares	DF	Mean Square	F Value	P-Value Prob>F	Percentage contribution	Remarks
Model	0.18	4	0.045	1578.72	< 0.0001		
Speed	0.11	1	0.11	3891.85	< 0.0001	61.11%	Significant
Feed Rate	0.066	1	0.066	2313.52	< 0.0001	36.66%	Significant
DOC	8.29E-04	1	8.29E-04	28.97	< 0.0001	0.46%	Significant
Speed * Feed Rate	2.31E-03	1	2.31E-03	80.56	< 0.0001	1.28%	Significant
Residual	4.29E-04	15	2.86E-05				
Lack of Fit	1.77E-04	10	1.77E-05	0.35	0.9249		
Pure Error	2.52E-04	5	5.04E-05				
Cor Total	0.18	19					

6.1.3 Regression Analysis for AA6061-4.5%Cu-5%SiCp

The regression equations obtained for AA6061-4.5%Cu-5%SiCp are listed in Table 5.19

Table 6.9 Regression Equations of FX, Ra and Power Consumption

SL. No	Responses	Regression equation
1	FX	-215.06991+ 0.10846*Vc + 0.83246*f + 10.39903*d - 8.19703E-005*Vc*f - 2.23735E-003*Vc*d - 6.21407E-004*f*f
2	R_a	2.71064 - 9.21591E-004*Vc + 4.74818E-003*f + 0.40541*d - 2.33750E-006*Vc*f + 2.28750E-004*Vc*d - 1.18750E-003*f*d + 9.72727E-008*Vc*Vc + 5.72727E-006*f*f - 0.17773*d*d
3	Power	-0.18139+ 3.7262467E-005*Vc + 4.74091E-004*f + 9.10346E-003*d+ 1.69738E-007*Vc*f

Table 6.10: Comparison of FX, Ra and Power Consumption predicted by RSM Model, with the experimentally obtained FX, Ra and Power Consumption of AA6061-4.5%Cu-5%SiCp

Experimental				RSM - Prediction			Error (%)		
Expt. No	FX (N)	Ra (µm)	Power (kW)	FX (N)	Ra (µm)	Power (kW)	FX (N)	Ra (µm)	Power (kW)
1	71.2	3.24	0.06	70.8	3.2	0.1	0.71	0.46	0.02
2	232.	1.20	0.24	234.	1.2	0.2	-0.67	-1.26	0.02
3	120.	4.35	0.18	121.	4.4	0.2	-0.87	-0.83	-0.03
4	254.	1.45	0.44	251.	1.4	0.4	0.83	0.61	0.01
5	87.6	2.35	0.08	87.1	2.4	0.1	0.62	-0.39	0.03
6	245.	1.30	0.25	241.	1.3	0.3	1.51	2.76	0.01
7	139.	3.06	0.21	137.	3.0	0.2	1.26	0.49	0.03
8	259.	1.00	0.45	259.	1.0	0.4	-0.11	-1.51	0.00
9	109.	3.39	0.13	110.	3.4	0.1	-0.95	0.46	-0.01
10	249.	1.34	0.34	252.	1.4	0.3	-1.30	-1.07	-0.01
11	155.	2.07	0.15	158.	2.1	0.1	-2.07	-1.27	0.65
12	190.	2.58	0.32	192.	2.6	0.3	-1.33	1.07	0.01
13	179.	2.44	0.23	175.	2.4	0.2	2.03	1.13	0.01
14	185.	1.74	0.24	187.	1.8	0.2	-1.11	-1.51	0.00
15	182.	2.29	0.24	181.	2.3	0.2	0.45	1.00	0.00
16	183.	2.29	0.23	181.	2.3	0.2	0.99	1.00	-0.03
17	182.	2.29	0.24	181.	2.3	0.2	0.45	1.00	0.00
18	180.	2.29	0.24	181.	2.3	0.2	-0.65	1.00	0.00
19	182.	2.25	0.25	181.	2.3	0.2	0.45	-0.76	0.04
20	181.	2.19	0.23	181.	2.3	0.2	-0.21	-3.52	-0.04

The Table 6.10 exhibits the ability of RSM in predicting the responses of required surface roughness (Ra), cutting force (FX), Power (Power) for the given input process parameters. Table 6.10 exhibits Comparison of FX, Ra and Power Consumption predicted by RSM Model, with the experimentally obtained FX, Ra and Power Consumption of AA6061material. From the data presented in Table 6.10, the maximum error obtained for surface roughness is 2.76 % at rotational speed of 2000 rpm, feed rate of 400 mm/min and depth of cut of 3 mm which indicates good prediction is possible by the quadratic terms and interaction terms. Similarly the minimum percentage of relative error is -3.52 % at rotational speed of 3000 rpm, feed rate of 500 mm/min and depth of cut 3 mm.

Similarly, the maximum error obtained for cutting force is 2.03% at rotational speed of 2000 rpm, feed rate of 500 mm/min and depth of cut of 2 mm which indicates good prediction is possible by the quadratic terms and interaction terms. Similarly the minimum percentage of relative error is -2.07 % at rotational speed of 2000 rpm, feed rate of 300 mm/min and depth of cut 2 mm.

The maximum error obtained for power consumption response is 6.44 % at rotational speed of 1000 rpm, feed rate of 300 mm/min and depth of cut of 1 mm which indicates good prediction is possible by the quadratic terms and interaction terms. Similarly the minimum percentage of relative error is -6.92 % at rotational speed of 2000 rpm, feed rate of 300 mm/min and depth of cut 2 mm.

6.1.4 Validation Experiments Considered For AA6061 And AA6061-4.5%Cu-5%SiCp

Table 6.11: Validation Experiments

Expt. No	Spindle Speed (rpm)	Feed Rate (mm/min)	Depth of Cut (mm)
1	1200	340	1.2
2	1800	340	1.8
3	2400	340	2.6
4	1200	390	1.2
5	1800	390	1.8
6	2400	390	2.6
7	1200	460	1.2
8	1800	460	1.8
9	2400	460	2.6
10	2800	340	1.2
11	2800	390	1.8
12	2800	460	2.6

Table 6.12: RSM Experimented V/S Predicted (Validation of Experiments)

Experimental				RSM Predicted			Error (%)		
Expt. No	FX (N)	Ra (µm)	Power (kW)	FX (N)	Ra (µm)	Power (kW)	FX (N)	Ra (µm)	Power (kW)
1	101.04	3.16	0.106	102.1	3.14	0.1	-1.0461	0.537	0.896
2	153.26	2.35	0.17	152.66	2.38	0.17	0.3894	-1.325	1.798
3	204.09	1.7	0.229	202.62	1.66	0.23	0.7181	2.445	-1.055
4	114.86	3.4	0.14	116.12	3.38	0.14	-1.0974	0.648	1.02
5	168.62	2.47	0.211	164.23	2.51	0.21	2.6049	-1.633	2.316
6	208.91	1.69	0.27	211.73	1.67	0.28	-1.3497	1.183	-2.029
7	132.23	3.85	0.19	130.53	3.76	0.19	1.2831	2.467	2.143
8	175.77	2.69	0.26	175.2	2.74	0.26	0.3255	-1.834	-0.263
9	217.86	1.77	0.35	219.26	1.73	0.34	-0.6413	2.015	3.663
10	228.64	1.44	0.26	226.75	1.46	0.26	0.8286	-1.293	1.288
11	232.76	1.52	0.31	236.69	1.54	0.31	-1.6893	-1.074	0.171
12	248.89	1.4	0.39	245.23	1.38	0.38	1.4698	1.727	1.713

Table 6.11 depicts the experimented conditions for validation of the RSM technique. Table 6.12 shows the deviation among the experiments conducted and predicted using RSM technique.

6.1.5 Summary

The effect of process parameters of AA6061 and AA6061-4.5% Cu- 5% SiCp on cutting force, surface roughness and Power consumption of machined components for milling have been investigated experimentally. The experiments were carried out as per L_{27} OA inorder to identify the effects of input parameters such as Spindle speed, Feed Rate and Depth of cut on the performance attributes.

- RSM modeling developed has produced quite satisfactory predictions for the output of milling operation, which is indicated again by the validation experiments.
- RSM technique leads in predicting the single response individually thus reducing the importance of the other responses. Hence a multi objective optimization is advisable in case of more than one response.

Further, the same data is used for prediction of the responses using artificial neural network (ANN) and recurrent neural network (RNN). These neural network based approaches have been incorporated in the study, as few literatures suggest that neural network (NN) techniques are well suited to predict the non-linear behaviour of the system.

ANN MODELLING FOR PREDICTION

6.2 ANN MODEL DEVELOPMENT TO PREDICT RESPONSES OF AA6061, A6061-4.5%Cu-5%SiCp

Intelligent methods of a prediction system for the face milling operation using Neural Network technology are in this section. Machining is carried out at different rotational speed, feed rate and depth of cut. The model is trained with 82% of data collected from experimentation and remaining data are used to test and validate the model. The mean square error was fixed as 6×10^{-6}. The network converged to the specified error upon reaching 10000000 epochs. The formulation of ANN and HRNN model for prediction of cutting force, surface roughness and power consumption of AA6061 and AA6061-4.5%Cu-5%SiCp has been discussed in this chapter. The study also presents the results of the experiments on AA6061 alloy and AA6061-4.5%Cu-5%SiCp composite performed to validate the ANN model for cutting force, surface roughness and power consumption and compares them with the cutting force, surface roughness and power consumption predicted by the model. The values of the responses predicted by ANN are compared with the corresponding experimentally obtained values as represented in Table 6.1 and 6.2, to check the suitability of the model within the purview of experimentation. Further, the model is checked for its capability to extrapolate and interpolate the responses with the outcome of validation experiments.

A. Scope

In this section, it is proposed to formulate a Neural Network based approaches (ANN and RNN) with Feed Forward architecture to predict the responses of AA6061 and AA6061-4.5%Cu-5%SiCp with the input parameters being spindle speed, feed rate and depth of cut.

B. Data Collection

The data for training the ANN and RNN network proposed for response prediction in AA6061 and AA6061-4.5%Cu-5%SiCp is collected from the experiments carried out on milling. This data is listed in Table 6.1.

C. **Neural Network Training**

In any FFNN application even today, the exact architecture to be used needs to be found (Reddy et al. 2005). More often than not, this is a trial and error exercise, as regards to the selection of a number of hidden layers and neurons in each of these layers. In this application, training was started with two hidden layers from 2 to 12 neurons in each hidden layer. The minimum mean squared error (MSE) was set as 0.00001 and the number of iterations to be executed as 1500000. Initially, during training, the learning rate parameter and momentum factor were preferred as 0.5 each. The number of hidden neurons was fixed based on MSE and the mean error in prediction of training data (Etr). Single and two hidden layers were tried out to obtain the minimum MSE. It was observed that the network fails to converge with a single hidden layer when tried with a different number of nodes varying from 2 to 12 in the hidden layer. This probably happens due to the fact that the input-output relationship is quite complex and nonlinear. Therefore, training with single hidden layer was terminated and training was started with two hidden layers. Here the training was started with varying learning rates from 0.1 to 0.9 in steps of 0.05. The learning rate and the momentum parameters were initially taken as 0.3 and 0.9 respectiely for training. For all patterns, p, the global error function is expressed in terms of MSE (Yagnanarayana 2008) and is given by

$$E = \Sigma E_P = \left(1/p\right) \Sigma\Sigma \left(b_{kp} - S_{kp}^{0}\right)^2 \qquad (6.1)$$

Where, $b_{kp}$is the actual output and S_{kp}^{0} is the network output for the K^{th} output neuron for the p^{th} pattern.

The mean error in the output prediction is (Reddy et al. 2005)

$$E_{tr}(x) = 1/N \; S \; |(b_k(x) - P_k(x))| \qquad (6.2)$$

Where, $E_{tr}(x)$ is the mean error in prediction of training data set for output parameter x, N is the number of the data sets, $b_k(x)$ is the actual output and $P_k(x)$ is the predicted output.

The following sigmoid function was used as the activation function (Reddy et al. 2008, Mandal et al. 2009, Reddy et al. 2005, Li, Liu and Xiong 2002, Mousavi et al.2007, Haque and Sudhakar 2002).

$$F(x) = 1/ (1+\exp (-x)) \quad (6.3)$$

Back propagation algorithm was used for training the network. It was found after a lot of trial and error that convergence of the network was obtained with 2 hidden layers with 7 neurons in the first and 4 neurons in the second hidden layer. Figure 3.13 from chapter 3 shows the schematic diagram of the FFNN used for aforesaid response predictions. The learning rate parameter was increased from 0.1 to 0.9 in steps of 0.05 and the momentum term was decreased from 0.9 in steps of 0.05 to observe the network behavior with respect to MSE and number of epochs. Finally, the optimized architecture obtained with learning parameter $\eta = 0.85$ and momentum factor $\alpha = 0.65$ was found to converge excellently after 15 lakh epochs giving an MSE of 0.00023, to predict the responses.

As discussed in section 6.5, the ANN was modeled with FFNN architecture. Both single, as well as two hidden layers, were tried out. Before training the network, both the inputs as well as the output variables were normalized between values 0.1 to 0.9 using the normalizing function given in equation (3.11) of chapter 3. Once the network is trained, all the values acquire their original values provided by the de-normalising function stated at equation (3.12) in chapter 3. Back propagation algorithm was used for training the network. With single hidden layered network (i.e. three layered perceptron network), the network was trained with different values of learning rate parameter (η) and momentum factor (a). The learning was started with 5 hidden nodes, with an initial value of η as 0.1 and with a=0.9. The value of η was increased while that of a was decreased in steps of 0.05 in each subsequent iteration. The MSE which is an indicator of network convergence given by equation (6.1) was set at 0.0001 while the number of epochs (iterations) was fixed at 5 lakhs. With repeated trials involving different values of hidden nodes ranging from 2 to 9, different values of η and an as well as by changing the order of the input vector presentation to the network, the network failed to converge towards the set MSE. This probably is due to the nonlinear correlation between the input output relationships of data (Reddy et al. 2005).

The network was then tried with two hidden layers following the same procedure used for three layered perceptrons. The network converged satisfactorily with 5 nodes in the first hidden layer and 3 nodes in the second hidden layer with η=0.5 and a=0.5, with an MSE of 9.76 x 10^{-5} after 3.25 lakh iterations. The sigmoid function in equation (3.13) of chapter 3 used to train the ANN model for response predictions is reproduced below as the activation function for training the network.

Table 6.13: Comparison of FX, Ra, and Power Consumption predicted by ANN Model, with the experimentally obtained FX, Ra and Power Consumption of AA6061

Experimental				ANN – Prediction			Error (%)		
Expt. No	FX (N)	Ra (µm)	Power (kW)	FX (N)	Ra (µm)	Power (kW)	FX (N)	Ra (µm)	Power (kW)
1	45.5	0.7	0.04	46.22	0.71	0.04	-1.59	-1.44	-1.84
2	50.31	0.64	0.04	51.28	0.62	0.04	-1.93	3.12	-1.46
3	56.69	0.63	0.05	57.82	0.62	0.05	-1.99	1.74	2.05
4	58.72	0.86	0.07	58.43	0.84	0.07	0.49	2.1	-1.07
5	63.42	0.76	0.07	64.22	0.76	0.07	-1.25	-0.16	-0.95
6	72.6	0.67	0.08	71.49	0.68	0.08	1.53	-1.64	2.89
7	73.27	0.96	0.11	72.37	0.93	0.11	1.23	3.17	-2.36
8	79.05	0.86	0.12	77.11	0.85	0.12	2.45	1.25	-1.7
9	83.56	0.68	0.13	83.34	0.67	0.13	0.27	0.9	-1.67
10	93.58	0.63	0.08	97.67	0.62	0.09	-4.36	1.26	-3.34
11	100.01	0.61	0.09	103.29	0.6	0.09	-3.27	2.38	-1.94
12	107.23	0.62	0.1	108.9	0.63	0.1	-1.55	-1.58	-1.63
13	110.22	0.73	0.13	110.29	0.75	0.13	-0.07	-2.12	0.36
14	115.02	0.66	0.14	116.1	0.67	0.14	-0.94	-1.83	-0.3
15	119.84	0.62	0.15	121.88	0.61	0.15	-1.7	1.98	-1.02
16	126.74	0.85	0.19	124.57	0.87	0.19	1.71	-2.4	-0.09
17	134.22	0.71	0.2	130.56	0.72	0.2	2.73	-1.16	0.61
18	141.48	0.6	0.22	139.51	0.58	0.21	1.39	2.55	1.36
19	143.3	0.52	0.13	141.18	0.53	0.13	1.48	-1.4	-0.02
20	148.55	0.55	0.14	144.71	0.54	0.14	2.58	2.29	-0.03
21	150.52	0.56	0.14	149.15	0.54	0.14	0.91	3.27	-1.98
22	152.58	0.66	0.19	148.89	0.67	0.18	2.42	-2.11	1.24
23	153.29	0.58	0.19	153.39	0.59	0.19	-0.07	-2.2	0.32
24	155.15	0.55	0.2	157.8	0.54	0.2	-1.71	2.34	-0.18
25	158.3	0.71	0.25	160.94	0.72	0.25	-1.67	-1.64	0.07
26	159.82	0.56	0.25	160.41	0.55	0.26	-0.37	2.57	-0.24
27	164.21	0.48	0.26	163.78	0.49	0.26	0.26	-1.93	0.32

From the Table 6.13 it can be observed that, The maximum percentage of relative error of FX obtained for trained data is 2.73% at a rotational speed of 2000 rpm feed rate of 500mm/min and depth of cut 2 mm. The minimum percentage of relative error obtained for trained data is -4.36 % of FX at a rotational speed of 2000 rpm feed rate of 300mm/min and depth of cut 1 mm for FX. The maximum percentage of relative error obtained for trained data is 3.27 % of Ra at a rotational speed of 3000 rpm feed rate of 300mm/min and depth of cut 3 mm. The minimum percentage of relative error obtained for trained data is -2.40 % of Ra at a rotational speed of 2000 rpm feed rate of 500mm/min and depth of cut 1 mm for Ra. The maximum percentage of relative error obtained for trained data is 2.89 % of power consumption at a rotational speed of 1000 rpm feed rate of 400mm/min and depth of cut 3 mm. The minimum percentage of relative error obtained for trained data is -3.34 % of power consumption at a rotational speed of 2000 rpm feed rate of 300mm/min and depth of cut 1 mm for Power Consumption. The error obtained using ANN model is much lesser than that of the RSM prediction. Hence, this model gives better results as compared to RSM. The reason to attain better results through ANN is, In general, similarities do exist between the ANN and statistical techniques. An FFNN can be termed as a form of nonlinear regression (Ripley 1994, Potzinger et al. 2000) ANN can make an n-step ahead forecast directly without any recursive procedure. Due to its inherent robustness in design which can be attributed to massively parallel processing, the ANNs are good modeling tools for real life problems, in which data may be inadequate, may be available with a lot of noise, and there could be distortions in data. (Lapedes et al.1988) have shown that in two-time series prediction problems, neural networks are clearly superior to statistical methods.

Table 6.14: Comparison of FX, Ra, and Power Consumption predicted by ANN Model, with the experimentally obtained FX, Ra and Power Consumption of AA6061-4.5%Cu-5%SiCp

Experimental				ANN - Prediction			Error (%)		
Expt. No	FX (N)	Ra (µm)	Power (kW)	FX (N)	Ra (µm)	Power (kW)	FX (N)	Ra (µm)	Power (kW)
1	71.28	3.24	0.06	69.88	3.19	0.06	1.96	1.5	-0.9
2	78.03	2.99	0.07	80.01	3.04	0.07	-2.53	-1.58	-0.58
3	87.64	2.35	0.08	89.02	2.33	0.08	-1.58	0.87	-0.42
4	90.37	3.81	0.11	91.13	3.87	0.11	-0.85	-1.7	-3.81
5	109.45	3.39	0.13	107.3	3.36	0.13	1.96	1.02	0.34
6	115.33	2.7	0.14	116.88	2.75	0.14	-1.34	-1.94	-1.18
7	120.39	4.35	0.18	117.5	4.28	0.19	2.4	1.64	-2.43
8	134.79	3.99	0.2	131.86	3.96	0.2	2.18	0.66	1.96
9	139.53	3.06	0.21	139.57	3.07	0.21	-0.03	-0.18	0.39
10	144.91	2	0.15	147.25	2.01	0.15	-1.62	-0.63	-1.18
11	155.12	2.07	0.15	158.35	2.06	0.16	-2.09	0.39	-2.77
12	176.66	1.77	0.17	170.7	1.73	0.17	3.38	2.44	0.88
13	179.4	2.44	0.23	174.68	2.43	0.23	2.63	0.32	1.93
14	182.5	2.29	0.24	177.74	2.24	0.24	2.61	2.13	0.42
15	185.55	1.74	0.24	185.05	1.71	0.25	0.27	1.45	-0.54
16	187.34	2.82	0.31	187.86	2.77	0.31	-0.27	1.86	0.29
17	190.09	2.58	0.32	194.86	2.63	0.32	-2.51	-1.75	-0.5
18	194.46	1.94	0.33	198.14	1.98	0.33	-1.9	-1.86	0.39
19	232.49	1.2	0.24	235.83	1.21	0.24	-1.44	-1.03	0.49
20	241.82	1.4	0.25	240.3	1.37	0.25	0.63	2.04	0.76
21	245.12	1.3	0.25	244.05	1.33	0.25	0.44	-2.47	0.23
22	247.98	1.21	0.33	245.33	1.21	0.33	1.07	-0.35	-0.6
23	249.63	1.34	0.34	248.86	1.32	0.34	0.31	1.32	-0.67
24	250.16	1.14	0.35	251.74	1.13	0.35	-0.63	0.94	-0.45
25	254.03	1.45	0.44	254.93	1.49	0.44	-0.35	-2.44	0.06
26	257.86	1.35	0.44	257.59	1.38	0.44	0.11	-2.23	0.27
27	259	1	0.45	259.68	1.02	0.45	-0.26	-1.64	0.17

The responses are predicted using ANN model for AA6061-4.5%Cu-5%SiCp as tabulated in Table 6.14 using the ANN model.The maximum percentage of relative error attained for trained data is 3.38% of FX at a rotational speed of 2000 rpm feed rate of 500mm/min and depth of cut 1 mm. The minimum percentage of relative error obtained for trained data is -2.53 % of FX at a rotational speed of 1000 rpm feed rate of 300mm/min and depth of cut 2 mm for FX. The maximum percentage of relative error obtained for trained data is 2.44 % of Ra at a rotational speed of 2000 rpm feed rate of 300mm/min and depth of cut 3 mm. The minimum percentage of relative error obtained for trained data is -2.47 % of Ra at a rotational speed of 2000 rpm feed rate

of 300mm/min and depth of cut 3 mm for Ra. The maximum percentage of relative error obtained for trained data is 1.96 % of power consumption at a rotational speed of 1000 rpm feed rate of 500mm/min and depth of cut 2 mm. The minimum percentage of relative error obtained for trained data is -3.81 % of power consumption at a rotational speed of 1000 rpm feed rate of 400mm/min and depth of cut 1 mm for Power Consumption. The error obtained using ANN model is much lesser than that of the RSM prediction. Hence, this model gives better results as compared to RSM.

6.2.1 Summary

1. ANN modeling developed has produced quite satisfactory predictions for the output of milling operation, which is indicated again by the validation experiments.
2. ANN model has been successfully designed and validated to predict the responses namely cutting force , surface roughness and power consumption in cas of forward mapping with the experimental data carried out on face milling of AA6061 alloy and AA6061-45%Cu-5%SiCp being used for training.
3. ANN model has been successfully designed and validated to predict the responses namely spindle speed, feed rate and depth of cut in cas of forward mapping with the experimental data carried out on face milling of AA6061 alloy and AA6061-45%Cu-5%SiCp being used for training.

The upcoming section deals with another evolutionay prediction technique, i.e. development of hybrid recurrent neural network (HRNN) in case of forward mapping and reverse mapping.

RNN MODELLING FOR PREDICTION

6.3 INTRODUCTION

ANN as a prediction tool has been vastly discussed in chapters 6 in terms of formulation, training as well as predictions done by these trained networks to provide outputs like cutting force, surface roughness and power consumption respectively. An attempt has been made here to develop an improvised neural network solution over the feed forward neural networks (FFNN). The objective here may mean either better predictions with equal training time for the model or at least comparable predictions with a decrease in the time required for training the model. It is well known (Reddy et al. 2005, Selvakumar et al. 2007) that a major issue in use of multilayered perceptron or FFNN to be used as a mapping tool is the problem of the model getting stuck while training, on the gradient descent curve of MSE v/s weight planes, in areas of local minima. The momentum factor (α) helps the model to jump over the local cliffs and the training proceeds further, and disturbances are encountered and overcome, till the training has reached a stage where the neural network reaches the bottom of the bowl. At this point, the training is stopped and the MSE of the network is checked with the set error. If the set error is significantly smaller as compared to the FFNN mean squared error (MSE), the parameters of the network (η and α) are changed and the training is started all over again. The FFNN model is trained with various combinations of η and α and also with different architectures (i.e. number of hidden layers and number of nodes per hidden layer), till the near about of the set MSE is achieved. As seen in the case of FFNN training for cutting force prediction, the number of epochs required to obtain the set MSE were 500000. It would be therefore viable to attempt a reduction in this training time and make the prediction more efficient. Recurrent Neural Networks (RNN) has been proposed in the recent past as a mathematical tool to map the inputs with outputs. The underlying principle which differentiates it from FFNN is that unlike in case of FFNN, the outputs in case of RNN are fed back to itself as well as other neurons of the same and/or other layer. It is believed that corrected weights which had provided output at time (t-1) if fed to the neurons during the subsequent epoch along with the current output from neurons of previous layer at time t, would result in a better output and it would make the training

faster. A lot of research is going on in the field of convergence characteristics of Elman Simple NN known as Simple Recurrent Network (SRN) and it is being actively studied for varying conditions of input-output data relationships (Lang et al.1990, Narendra and Parthasarathy 1990, Guler et al. 2005). In this chapter, it is proposed to formulate RNN model for the various cases for which ANN was formulated in Chapters 4 through 7 considering the difficulties in convergence spotted in Elman's SRN for these applications and overcoming them. These problems related to Elman SRN for the applications under study are presented in section8.4.

A. SCOPE

It is proposed to model recurrent neural networks to predict cutting force, surface roughness and power consumption for which ANN models have been presented in Chapter 6. The inputs for the models are kept same as that for the corresponding ANN models. The current chapter is written with the following objectives:

1. To formulate Elman Simple Recurrent Network for cutting force prediction, surface roughness prediction and power consumption prediction from same data from which ANN models were formulated.
2. To highlight the problems faced by SRN model in mapping the input-output relationship for the applications under study.
3. To propose Hybrid Recurrent Neural Network (HRNN) as an improvement over SRN overcoming the convergence related problems faced by SRN.
4. Application of HRNN models to predict cutting force, surface roughness and power consumption.
5. Analysis of predictions done by HRNN and its comparison with FFNN and establishing the usefulness of HRNN as a prediction system.

6.3.1 ELMAN SIMPLE NEURAL NETWORK

In the recent past quite a few Recurrent Neural Network (RNN) architectures have been studied (Elman 1990, Lang et al. 1990, Frasconi et al. 1992, Giles et al. 1992, Tesauro et al. 1995). Recurrent networks are neural networks with one or more

feedback loops, in which the loops may be local or global. RNN can be divided into two broad categories depending on whether the states of the network are guaranteed and observable or not. Observable state is one in which the state of the network can be derived by observing only the inputs and outputs (Giles et al. 1992). A model which falls into this class was proposed by Narendra and Parthasarathy (1990) and had time delayed outputs as well as inputs fed to a Multi-Layer Perceptron (MLP) which computed the output using the recent state dynamics. However, network having hidden dynamic states are not observable (Giles et al. 1992). Single layered and multi layered recurrent networks are being extensively studied in recent times. A typical single layered RNN was the one proposed by Elman in 1990 (Elman 1990). In this network, the hidden layer is copied in a virtual or context layer and the feedback is given back to the same layer along with the next set of inputs in the next time step as seen in Figure 6.2.

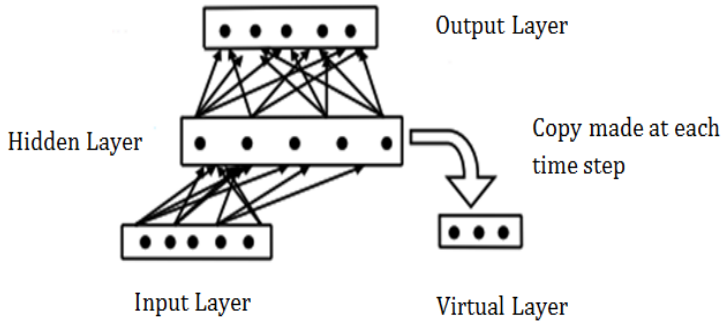

Figure 6.2 : A simple RNN proposed by Elman (1990)

The Elman network can be extended for a multilayered network with the temporal context layer providing feedback at each subsequent time step. Such a network is shown in Figure 6.3. The convergence of a Simple Elman Recurrent Neural Network (SRN) has been established. The computational power of Elman networks is as good as that of finite state machines (FSM) (Kremer 1995). In addition, it is reported that any network having additional layers between input and output layer than that of Elman network, possesses the same computational power exhibited by FSM (Kremer 1995). The convergence of RNN has been active subject of research in machine learning. An extended back propagation algorithm for Elman networks reported a

better convergence, faster training and better generalization (Song et al. 2009). In this algorithm, use is made of adaptive learning scheme coupled with adaptive dead zone to improve convergence speed.

In this study we try to develop a novel way of improving the convergence of Elman network (SRN) using the borrowed weights of a partially trained FFNN into an Elman network with single hidden layer or an extended Elman network having more than one hidden and context layer. The study further highlights the fact that the recurrent neural network so formulated performs the task of predictions comparable to that performed by the fully trained FFNN, from which the weights were borrowed to formulate the RNN, with better convergence.

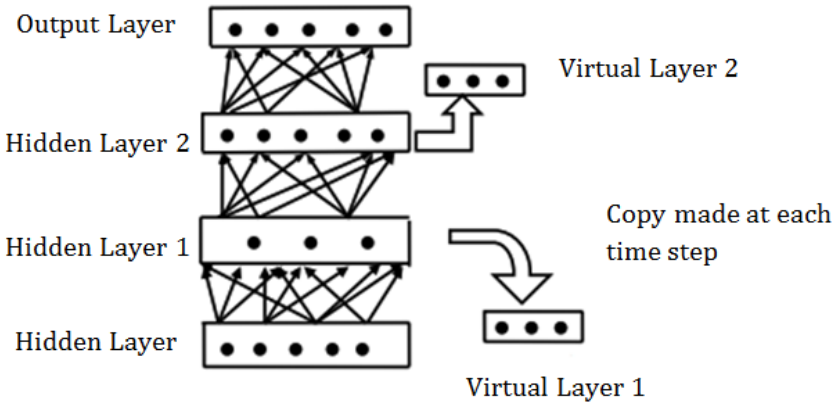

Figure 6.3: An extended simple RNN

6.3.2 RNN MODELLING

In this section, it is proposed to model the Elman Simple neural Network (SRN) to predict the cutting force, surface roughness and power consumption of AA6061 alloy and AA6061-4.5%Cu-5%SiCp composite for the data used for training the FFNN for cutting force, surface roughness and power consumption prediction shown at Table 6.13 and 6.14 respectively.

Elman Simple Recurrent Network (SRN) was modelled for cutting force as well as surface roughness predictions. The SRN with two context layers were tried with two hidden layer and with different combinations of number of neurons in each layer for

different combinations of η and a. The networks failed to converge for a variety of combinations mentioned above. The SRN with Elman architecture uses a context layer that contains the same number of neurons as that in the hidden layer. The output of each hidden neuron which is being copied in the context layer will contain neurons with exciting as well as inhibiting signals. These neurons then pass on the signals through weighted connections to each neuron in the current hidden layer in the next time step. Also these neurons receive signals from the neurons in the previous layer during this time step. Due to this, the previously excited neuron or the neuron which otherwise would have received a consistent excited signal from previous layer neurons may get inhibiting signals from the context layer neurons or vice versa. This probably, does not allow the network to move progressively along the path of negative gradient on the MSE weight plane. Such a phenomenon is likely to cause an oscillatory profile on the MSE synaptic weight plane, as witnessed while training the simple Elman recurrent network.

In order to overcome this shortcoming, various strategies discussed hereunder were tried:

a. The networks with single hidden layer were trained for the same architectures mentioned earlier with different combinations of η and a. During training, it was observed that the network does not converge. The system learns smoothly during initial phase. But as the training progresses, the network starts oscillating randomly. Further it is observed that the oscillations decrease and the network stops learning and MSE reaches a value much higher than the pre-set value which in our case is selected as 0.0001, thus indicating that the network has not been able to map the input output pattern.
b. In the next instance, the neural network model was modified with each neuron in the hidden layer giving feedback only to itself. The networks were modelled for each of the case with similar architectures discussed at (a) above with different combinations of η and a. It was observed that the networks still oscillate during training and fail to converge to the pre-set value, but a better convergence is seen as indicated by slightly lower MSE indicating that

learning capability of the network has slightly improved. But the convergence obtained is nowhere near the pre-set value of MSE. Hence, this strategy, though could not be discarded totally, was found to be ineffective.

c. In the modified model stated at (b) above, the weight vectors of a partially trained ANN with similar architecture were borrowed. The ANN network is partially trained till a steep negative gradient is identified on the MSE weights plane indicating the downward movement of MSE. The SNN with single context layer for second hidden layer, with each neuron giving feedback to itself in layer 2 is modeled with similar architecture as that of partially trained ANN. The weight vectors of the SNN from input layer to hidden layer 1, hidden layer1 to hidden layer 2 and from hidden layer 2 to output layer are replaced by the corresponding weight vectors of partially trained ANN. The biases for different layers except the context layers of the SNN are also replaced by the corresponding biases from the partially trained ANN. The weight vector from the context layer neurons to hidden layer neurons (each neuron to itself) is taken as a zero vector (unbiased). Once the architecture is finalized this way, the network is trained. Upon training with the same values of η and a as that used for partially trained ANN, the SNN so formulated is found to converge excellently. The convergence of SNNs so modeled is found to be better as compared to the parent ANNs from which these have been modelled. The performance of the SNNs modelled from the parent ANNs is demonstrated using the following cases. The SNN so developed has been named as Hybrid RNN (HRNN), since the RNN incorporates the weights from the partially trained FFNN for its processing. Figure 6.4 shows the block diagram for such an HRNN model formulation.

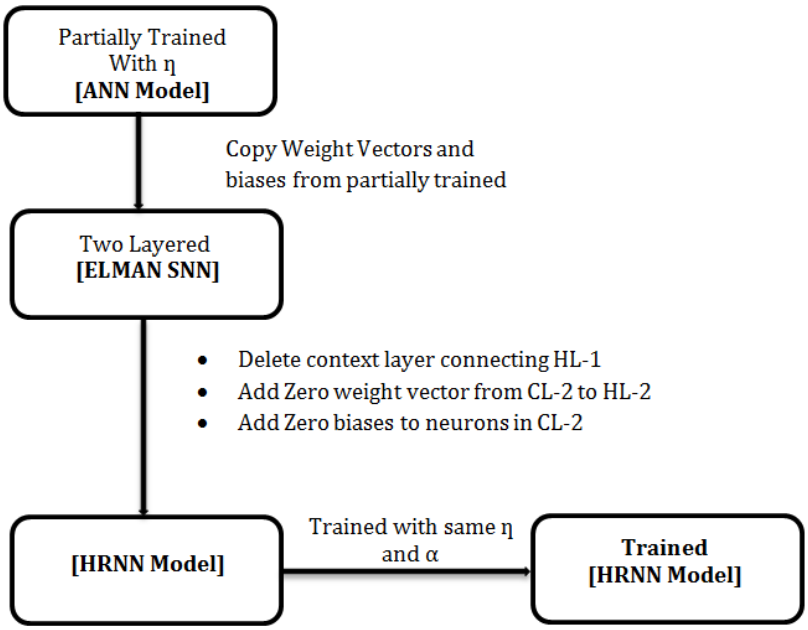

Figure 6.4: Formulation of HRNN model

6.3.3 FORMULATION OF HRNN

The formulation of a Hybrid Recurrent Neural Network (HRNN) is demonstrated in the following subsection by taking the example of a partially trained FFNN for AA6061 prediction of responses in milling condition. For this purpose, two Elman SRN architectures have been selected:

a) Elman SRN with 3 input neurons corresponding to Spindle speed, Feed rate, and Depth of Cut, 7 and 5 neurons in the first and second hidden layers, and 3 output neurons corresponding to cutting force, surface roughness and power consumption respectively. This architecture is denoted as 3-7-5-2 architecture.

b) The second architecture considered for demonstration of HRNN is the one containing 3 neurons in the input layer, 9 neurons in the first and 6 neurons second hidden layer and 5 neurons in the output layer. This architecture is denoted as 3-9-5-2 architecture.

6.3.4 HRNN With 3-7-5-2 Architecture:

The Elman RNN network opted involves 3 input neurons, 7 neurons in hidden layer1, 5 neurons in hidden layer 2 and 2 neurons in output layer and the sample data used for training is represented in Table 6.15. The network was trained with learning rate and momentum factor parameters with 0.82 and 0.62 values respectively. Initially the network is trained as an ANN network. Table 6.16, it delivers the information of the error in prediction in terms of MSE existing at various stages of network while carrying out the network training. The ANN network results in convergence to a MSE of 0.00029976 after 16 lakh epochs .Further to carry on and to attain the HRNN, the ANN will be trained until it reaches 50000 epochs. Later on, after training the ANN to 50000 epochs, the weights of the trained ANN are then borrowed and assigned in the input weights file for performing RNN training. After the transformation of weights the network is found to oscillate after it arrives at a MSE of 0.00217. This phenomenon is observed due to the fact that the ANN training up to 50000 epochs has not provided sufficient gradient descent on the MSE weights plane for the Hybrid RNN to further travel in the path of negative gradient. Later on, the ANN was trained up to100000 epochs and same foresaid process was carried, similarly at this stage the weights were again borrowed in the input weights file for RNN training. The results attained in this case were better than the first case, but the rate of convergence was found to be slow. Similarly the training was carried out for 150000 epochs, the MSE is found to be 0.0029. Hence in the next step the ANN is trained for 500000 epochs and subsequently, the weights are borrowed in the input file for RNN training. It was found that after training for around 235000 epochs, the network converged satisfactorily.

6.3.5 HRNN With 3-9-6-2 Architecture:

In this, the network is selected with 4 input neurons, 9 neurons in hidden layer1, 6 neurons in hidden layer 2 and 2 output neurons. Here the number of input patterns is taken as 270, just to emphasize that the number of input vectors has no great bearing on the convergence of Hybrid RNN. The ANN network is firs trained until 50000 epochs and then hybrid RNN is constructed by borrowing weights of trained ANN. The network is further trained for 85000 epochs as it gave the same MSE as that of parent ANN when trained to 325208 epochs.

Table 6.15: Experimental Data of AA6061-4.5%Cu-5%SiCp

SL. No	Spindle Speed (rpm)	Feed Rate (mm/min)	Depth of Cut (mm)	Cutting Force (N)	Surface Roughness (µm)
1	1000	300	1	71.27	3.24
2	1000	400	2	109.44	3.39
3	1000	500	3	139.52	3.06
4	2000	300	1	144.9	2.00
5	2000	400	2	182.49	2.29
6	2000	500	3	194.45	1.94
7	3000	300	1	232.48	1.20
8	3000	400	2	249.62	1.34
9	3000	500	3	258.99	1.00

Table 6.16: MSE Variation Based On Number Of Epochs

SL. No	Number of Epochs	MSE
1	1	0.478623
2	100000	0.00376582
3	200000	0.00263014
4	400000	0.0017198
5	600000	0.0013906
6	800000	0.00110638
7	1000000	0.00078334
8	1200000	0.00059087
9	1400000	0.00035691
10	1600000	0.00029976

6.3.6 Results And Discussion

A) HRNN with 3-7-5-2 architecture: Cutting Force and Surface Roughness Predictions

This section deals with a prediction comparison between the ANN and the HRNN network models. The prediction results attained after training ANN and HRNN model the results of the predictions attained between the ANN and HRNN network after 16 lakh and 2.58 lakh epochs respectively is represented in Table 6.17. The maximum error attained for AA6061-4.5%Cu-%SiCp in case of ANN is |0.59| % at spindle speed of rpm, feed rate of mm/min and depth of cut for the responses cutting force and surface roughness. However in the majority of the cases, the error attained by using hybrid RNN model is within |0.5|%.As discussed in prior sections, the HRNN is modelled after borrowing the weights from partially trained ANN after 5 lakh epochs. Further, the HRNN converged nicely to a MSE of 0.00029976. While in case of HRNN to attain the same convergence the HRNN consumed 776000 lesser epochs as compared to that of ANN. By this it can be concluded that the same degree of convergence was achieved by saving more than 50% of computational time. In other way, the better convergence can be achieved with lesser computational time. Furthermore, the error in predictions too is quite insignificant in comparison with the parent ANN predictions for the same data.

B) HRNN with 3-9-6-2 architecture: Cutting Force and Surface Roughness Predictions

The comparison of predictions between the parent ANN and Hybrid RNN is given in Table 6.18 below for a MSE of 0.00019 achieved by parent ANN after being trained using 325208 epochs. The total number of epochs of HRNN coupled with partially trained ANN works out to 128000 epochs, thus giving a saving in computation time in excess of 50%.It can be seen that the error in estimation with hybrid RNN with respect to Parent ANN falls within 6%, while in majority of the cases the error is within1%. Graphs represented in Figure 6.5 and Figure 6.6 depicts the comparison of predicted results attained through the ANN and HRNN for Al-4.5Cu-5%SiCp composite with various architectures Viz..(3-7-5-2, 3-9-6-2). From the Figure 6.5 and Figure 6.6, it can be concluded that ANN and HRNN not notably different in behavior and they follow each other very closely. Maximum deviation is observed in case of Ra prediction through ANN with 3-7-5-2 architecture. Similarly in

case of Figure 6.6 lighter deviation is observed for Ra with 3-9-6-2 as compared to 3-7-5-2 architecture. From the attained results it can be derived that, both the ANN and HRNN have comparable performance capabilities and both are almost identical notifying that the learning has been adequate and indicating that both the networks have generalized in a quite good way. But HRNN outperforms ANN as the involved computational time is lesser in HRNN to attain the desired responses.

C) Comparison of FX and Ra Prediction by ANN and HRNN with 3-7-5-2 architecture

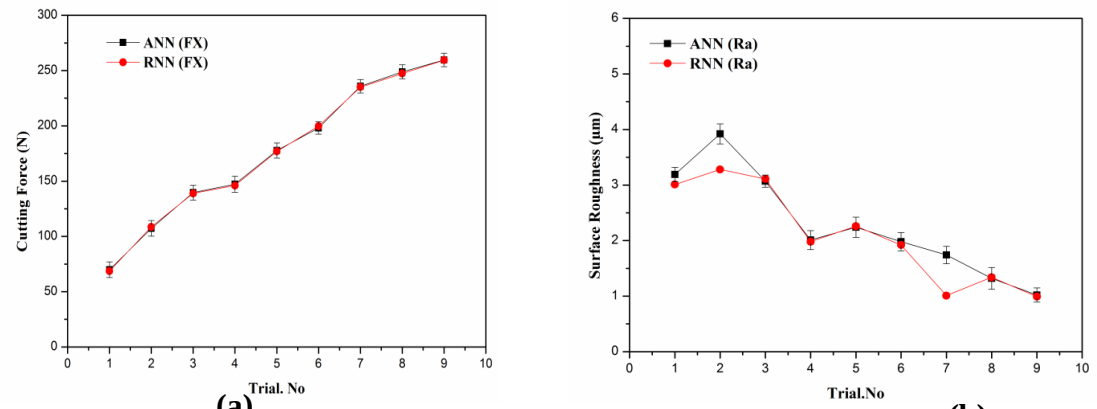

(a) **(b)**

Figure 6.5: (a) FX (b) Ra Prediction by ANN and HRNN with 3-7-5-2 architectures

D) Comparison of FX and Ra Prediction by ANN and HRNN with 3-9-6-2 architecture

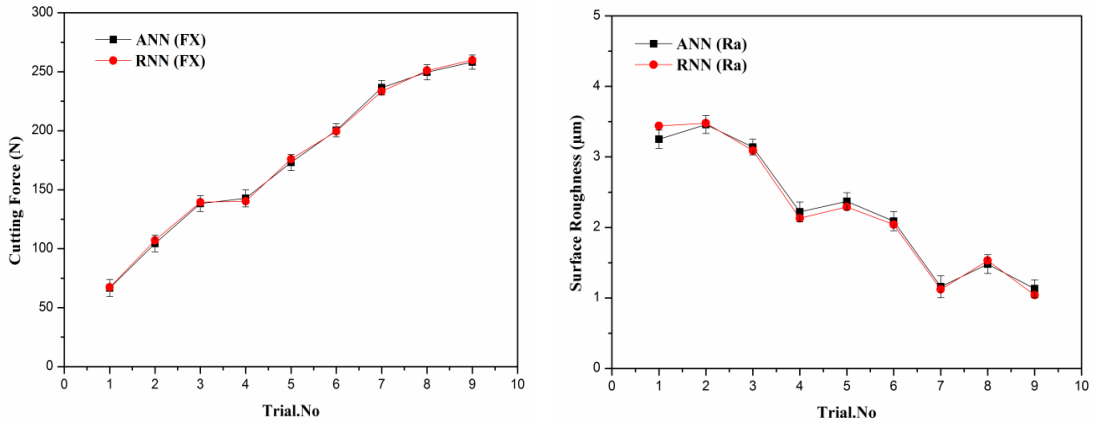

(a) **(b)**

Figure 6.6: (a) FX (b) Ra Prediction by ANN and HRNN with 3-9-6-2 architectures

Table 6.17: Comparison of FX and Ra Predicted by ANN, HRNN after 2.58 lakh epochs of HRNN and 16 lakh epochs of ANN

Input Parameters				Output Parameters					
SL. NO	Spindle Speed (rpm)	Feed Rate (mm/min)	Depth of Cut (mm)	FX (N)		% Difference Over ANN	Ra (µm)		% Difference Over ANN
				ANN	RNN		ANN	RNN	
1	1000	300	1	65.33	66.94	-1.61	3.13	3.17	-0.04
2	1000	400	2	105.38	106.12	-0.74	3.52	3.44	0.08
3	1000	500	3	135.02	134.48	0.54	3.31	2.72	0.59
4	2000	300	1	140.66	140.71	-0.05	2.26	2.2	0.06
5	2000	400	2	175.22	175.54	-0.32	2.39	2.31	0.08
6	2000	500	3	202.13	202.16	-0.03	2.01	2.08	-0.07
7	3000	300	1	234.51	234.28	0.23	1.12	1.19	-0.07
8	3000	400	2	250.75	251.29	-0.54	1.53	1.49	0.04
9	3000	500	3	256.17	257.37	-1.2	1.09	1.16	-0.07

Table 6.18: Comparison of FX and Ra Predicted by ANN Hybrid RNN after MSE = 0.00019

	Input Parameters			Output Parameters					
SL. NO	Spindle Speed (rpm)	Feed Rate (mm/min)	Depth of Cut (mm)	FX (N)		% Difference Over ANN	Ra (µm)		% Difference Over ANN
				ANN	RNN		ANN	RNN	
1	1000	300	1	59.22	60.09	-0.87	3.09	3.12	-0.03
2	1000	400	2	101.41	100.64	0.77	3.49	3.47	0.02
3	1000	500	3	129.13	129.14	-0.01	3.11	3.12	-0.01
4	2000	300	1	143.89	143.32	0.57	2.19	2.17	0.02
5	2000	400	2	169.36	170.09	-0.73	2.51	2.46	0.05
6	2000	500	3	204.17	202.94	1.23	2.07	2.08	-0.01
7	3000	300	1	228.08	228.18	-0.1	1.18	1.12	0.06
8	3000	400	2	246.75	246.29	0.46	1.53	1.34	0.19
9	3000	500	3	257.17	257.37	-0.2	1.07	1.09	-0.02

6.3.7 Summary

- Elman simple neural network (SRN) was found to have issues relating to convergence when trained for prediction of responses for application relating to face milling of AA6061 alloy and AA6061-4.5%Cu-5%SiCp composite. Three layered as well as four layered extended Elman recurrent networks were tried out with different combinations of neurons per hidden layer and learning rate parameter (η) and momentum term (a). The network was found to oscillate in local minimums and subsequently stopped learning with three

layered SRN. The four layered extended Elman recurrent neural network fared slightly better, but was unable to map the input output relationships, as there was no learning possible beyond a certain stage of training.

- The problem of convergence of extended Elman recurrent neural network was overcome by constructing a hybrid recurrent neural network (HRNN) by borrowing weights from a partially trained FFNN having same architecture as that of extended Elman recurrent neural network (minus context or temporal layers), when steep downward gradient is observed on the MSE v/s. Weights plane. Further training of such HRNN resulted in fast learning. The overall training time was found to reduce significantly.
- HRNN modeling developed has produced satisfactory predictions for the output of milling operation. The predictions of HRNN modelled for prediction of responses of AA6061 alloy and AA6061-4.5%Cu-5%SiCp composite matched the predictions done by ANN model and predicted results of the of ANN and HRNN are in good agreement desired results.
- The predicted responses of AA6061 alloy and AA6061-4.5%Cu-5%SiCp composite of face through HRNN and ANN were within an error of 5% in case of forward mapping and error within 10% in case of reverse mapping.
- This leads to an inference that HRNN models, being similar in performance to the ANN models in terms of prediction capabilities and the time required for training of HRNN being significantly reduced, they are superior to ANN models.

The further chapter deals with comparision study of statistical and evolutionary predition techniques for AA6061 alloy and AA6061-4.5%Cu-5%SiCp in case of forward and reverse mapping.

Related Airtcle: Rashmi L Malghan, Karthik Rao, Arun Shettigar, Shrikantha S Rao and R J D'Souza (2015). "Development of a Prediction Model for Optimized Surface Roughness in Face Milling Operation Using Recurrent Neural Network Technique." *International Journal of Applied Engineering Research*, 10(11), ISSN 0973-4562

COMPARISION OF PREDICTION RESULTS : FORWARD AND REVERSE MODELS

In this segment, the predicted results attained through the RSM (CCD), ANN and RNN methods have been discussed and compared.

6.4 FORWARD MAPPING OF AA6061

The BPNN and Elman network is developed to predict the responses for the respective process parameters namely spindle speed, feed rate and depth of cut of the milling process.

6.4.1 Selection Network Parameters for Forward Mapping – Back Propagation Neural Network (BPNN) Specification in AA6061 and AA6061-4.5%Cu-5%SiCp

In this segment, the parametric study was conducted to optimize the parameters of the network. The results of the considered parametric study are depicted in Figure 6.7 (a), (b), (c) and (d). The neural network consists of three input neurons corresponding to spindle speed, feed rate, and depth of cut, three response neurons corresponding to FX, Ra and power consumption. The training is carried out using normalized input values to obtain normalized output values. The optimal values attained for parameters such as a number of neurons in the hidden layer 1 and 2, learning rate factor value and the momentum factor value is mentioned below. Generally, there is no definite rule to identify the exact number of neurons to be fixed in specific layer [4-12,19]. Always trial and error method is incorporated. In order to compare the ANN and RNN models, the same architecture was considered in both neural network approaches. The minimum MSE is selected as the criteria to attain optimal neural network parameters. For example, in the case of Figure 6.7 (a), MSE has obtained 7 neurons in hidden layer 1. Thus the following parameters remain constant for both the neural network models.

- Number of neurons in hidden layer 1: 7
- Number of neurons in hidden layer 2: 4
- Learning rate factor value: 0.2
- Momentum factor value : 0.5

- Transfer Function used: Sigmoid
- Number of data used for training: 20
- Number of data used for testing: 15

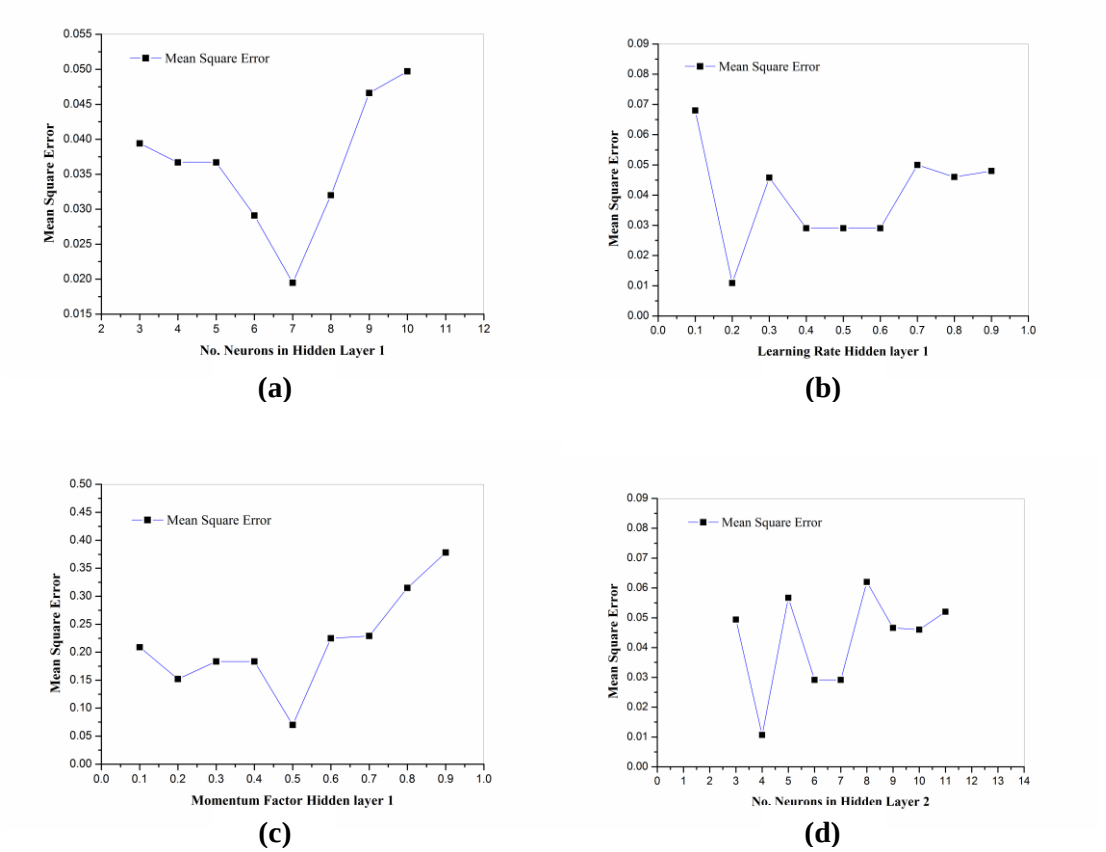

Figure 6.7: (a-d) Parametric studies to recognize optimal neural network parameters in case of forward mapping: a) Error v/s number of neurons in hidden layer 1. b) Error v/s learning rate in hidden layer 1 and 2 c) Error v/s momentum factor in hidden layer 1 and 2 d) Error v/s numbers of neurons in hidden layer 2.

6.4.2. Comparison of Statistical Model, ANN, and RNN for responses in Forward Mapping

Table 6.19: Summary of the Test Cases Results for the Response: FX

Test. No	Measured Fx (N)	RSM (CCD)		ANN		RNN	
		Predicted	% Deviation	Predicted	% Deviatio	Predicted	% Deviation
1	47.62	48.52	-1.89	48.01	-0.819	47.64	-0.04
2	103.28	102.66	0.6	101.26	1.956	102.49	0.76
3	108.44	110.58	-1.97	108.59	-0.138	110.87	-2.24
4	59.96	57.82	3.57	58.04	3.202	60.01	-0.08
5	114.38	116.39	-1.76	115.12	-0.647	114.39	-0.01
6	120.23	118.88	1.12	119.95	0.233	119.34	0.74
7	74.26	76.32	-2.77	73.28	1.32	74.28	-0.03
8	136.32	136.51	-0.14	135.44	0.646	137.99	-1.23
9	140.87	141.21	-0.24	140.92	-0.035	140.89	-0.01
10	144.22	151.86	-5.3	140.94	2.274	144.26	-0.03
11	152.93	151.36	1.03	153.01	-0.052	149.77	2.07
12	163.96	162.76	0.73	163.92	0.024	164.98	-0.62
13	52.27	53.04	-1.47	52.29	-0.038	52.28	-0.02
14	57.86	57.82	0.07	56.34	2.627	57.82	0.07
15	160.02	161.2	-0.74	159.76	0.162	160.08	-0.04

Table 6.20: Summary of the Test Cases Results for the Response: Ra

Test . No	Measured Ra (µm)	RSM (CCD)		ANN		RNN	
		Predicted	% Deviation	Predicted	% Deviation	Predicted	% Deviation
1	0.69	0.67	2.9	0.7	-1.45	0.71	-2.9
2	0.57	0.56	1.75	0.59	-3.51	0.58	-1.75
3	0.59	0.61	-3.39	0.6	-1.69	0.6	-1.69
4	0.88	0.9	-2.27	0.87	1.14	0.86	2.27
5	0.67	0.66	1.49	0.69	-2.99	0.66	1.49
6	0.63	0.64	-1.59	0.62	1.59	0.62	1.59
7	0.97	1	-3.09	0.98	-1.03	0.99	-2.06
8	0.72	0.71	1.39	0.71	1.39	0.73	-1.39
9	0.61	0.6	1.64	0.62	-1.64	0.61	0.33
10	0.51	0.49	3.92	0.5	1.96	0.51	-0.78
11	0.6	0.59	1.67	0.62	-3.33	0.6	-3.33
12	0.49	0.46	6.12	0.51	-4.08	0.5	-2.04
13	0.65	0.66	-1.54	0.66	-1.54	0.67	-3.08
14	0.87	0.82	5.75	0.86	1.15	0.9	-3.45
15	0.58	0.56	3.45	0.57	1.72	0.59	-1.72

Table 6.21: Summary of the Test Cases Results for the Response: Power Consumption

Test . No	Measured Power (kW)	RSM (CCD)		ANN		RNN	
		Predicted	% Deviation	Predicted	% Deviation	Predicted	% Deviation
1	0.04	0.04	-5.26	0.039	-2.63	0.04	0.26
2	0.09	0.09	1.1	0.094	-3.3	0.09	-2.2
3	0.1	0.1	-0.97	0.106	-2.91	0.11	-1.94
4	0.08	0.09	-3.66	0.085	-3.66	0.08	-2.44
5	0.14	0.13	7.14	0.139	0.71	0.14	0.71
6	0.15	0.15	-1.35	0.149	-0.68	0.15	-1.35
7	0.11	0.11	-0.92	0.106	2.75	0.11	-0.92
8	0.21	0.22	-4.76	0.214	-1.9	0.21	0.95
9	0.23	0.22	4.35	0.229	0.43	0.23	1.3
10	0.14	0.14	0.71	0.138	1.43	0.14	-2.86
11	0.18	0.18	0.56	0.181	-0.56	0.18	1.11
12	0.28	0.27	3.57	0.29	-3.57	0.27	2.14
13	0.04	0.04	-2.56	0.04	-2.56	0.04	2.56
14	0.07	0.07	-1.45	0.07	-1.45	0.07	-1.45
15	0.27	0.26	3.7	0.26	3.7	0.28	-2.22

The performance of the statistical model and the neural based approaches i.e. ANN and RNN were compared for the twenty test cases. The comparison carried out for all three techniques are summarized in Table 6.19-6.21. The results attained are represented in Figure 6.8 (a), (b), (c). Figure 6.8 (a), (b), (c) illustrates that the neural based approaches ANN and RNN techniques accomplished greater accuracy in prediction of responses FX, Ra, and Power Consumption. The values of % deviation for the response FX lie in the range of -5.3 to 3.57 for CCD, for ANN -0.819 to 3.202 and for RNN -2.24 to 2.07 as depicted in Table 6.19. Similarly, the values of % deviation for the response SR lie in the range of -3.39 to 6.12 for CCD, for ANN -4.08 to 1.96 and for RNN -3.45 to 2.27 as depicted in Table 6.20. Further on, the values of % deviation for the response Power consumption fall in the range of -5.26 to 7.14 for CCD, for ANN -3.66 to 3.70 and for RNN -2.86 to 2.56 as depicted in Table 6.21.

6.4.3 Test cases result in a comparison of CCD, ANN, and RNN techniques: Forward mapping for responses FX, Ra, and Power Consumption in terms of % deviation.

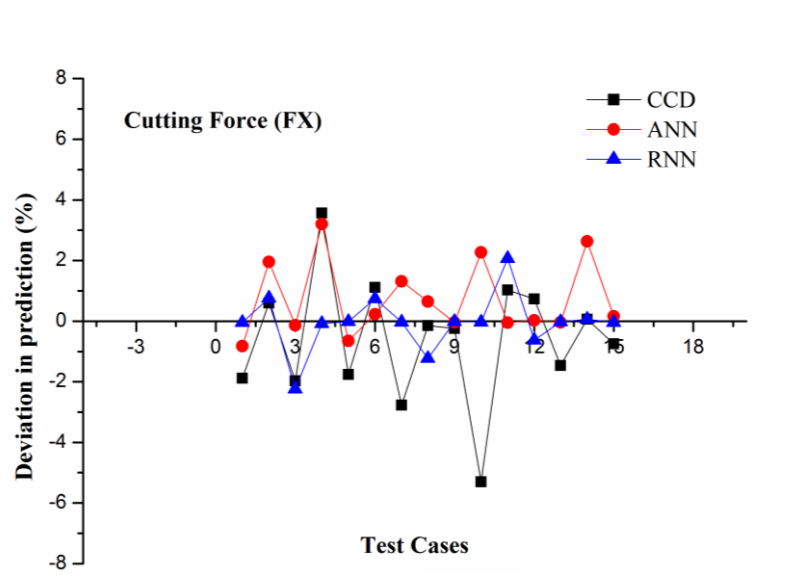

(a)

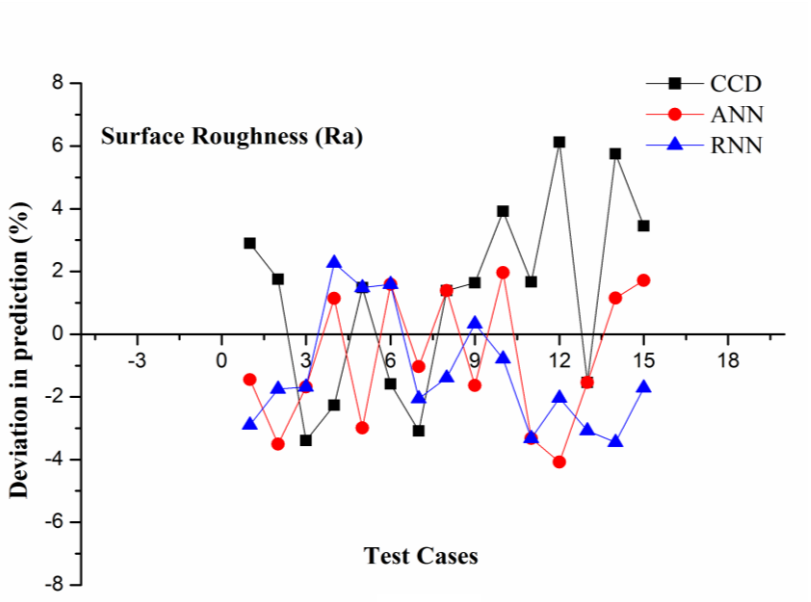

(b)

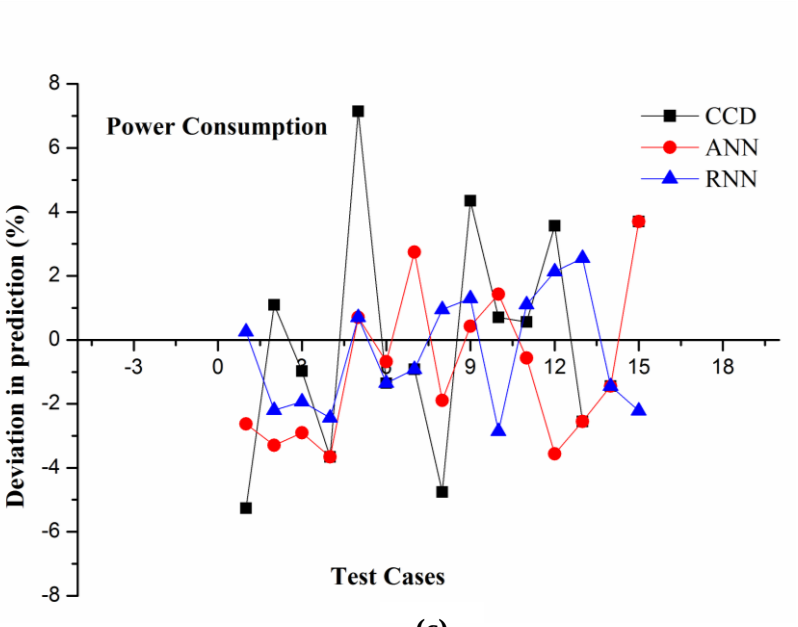

(c)

Figure 6.8: (a-c) Comparison of three models CCD, ANN, and RNN in the mode of % deviation in the prediction of responses to the test cases in case of forward mapping. (a) Prediction of response FX, (b) prediction of response Ra and (c) Prediction of response power consumption.

6.4.4 RESULTS OF REVERSE MAPPING

Reverse mapping has been implemented to predict process parameters such as the spindle speed, feed rate and depth of cut from the responses such as the Fx, Ra and Power Consumption. In the present study, the neural network architecture is maintained same as that of the forward mapping. However, while comparing to forward mapping the data provided in reverse mapping for training process changes i.e. in reverse mapping the training data considers the responses of the forward mapping data set as its input set of data and the process parameters of the forward mapping data sets as the output set of data. The parametric study similarly carried out as that of the forward mapping. The results attained by the parametric study of reverse mapping are same to that of the forward mapping as mention in Figure 6.7 (a), (b), (c) and (d).

In the case of the reverse mapping, twenty test cases were used and the further optimized network was used to pass these test cases through it. The percentage deviation was calculated for each of the predicted outcomes. The performance of the neural network based approaches i.e. ANN and RNN were compared for the twenty test cases. The comparison carried out for two techniques are summarized in Table 6.22-6.24. The results attained represented in Figure 6.9 (a), (b), (c). Figure 6.9 (a),(b),(c) illustrate that the neural based approaches ANN and RNN techniques accomplished greater accuracy in prediction of responses spindle speed, feed rate and depth of cut.

The values of % deviation for the response spindle speed lie in the range of -5.32 to 9.06, and RNN in the range of -4.14 to 7.23 as depicted in Table 6.22. Similarly, The values of % deviation for the response feed rate lie in the range of -2.12 to 9.37 in the case of ANN, for RNN lie in the range of -4.62 to 6.44 as shown in Table 6.23. Further on, the values of % deviation for the response depth of cut fall in the range of -1.82 to 10.0 in ANN, for RNN it is -1.90 to 8.33 as presented in Table 6.24.

6.4.5 Comparison of ANN, RNN for responses in Reverse Mapping for AA6061

Table 6.22: Summary of the Test Cases Results for the Response: Spindle Speed

Test Cases	Spindle Speed (rpm)	ANN		RNN	
		Predicted	% Deviation	Predicted	% Deviation
1	1050	1006.63	4.13	1022.41	2.63
2	1100	1158.47	-5.32	1123.69	-2.15
3	1200	1189.26	0.9	1249.72	-4.14
4	1300	1322.3	-1.72	1290.02	0.77
5	1400	1337.52	4.46	1440.33	-2.88
6	1500	1364.08	9.06	1467.15	2.19
7	1600	1457.14	8.93	1484.37	7.23
8	1700	1620.52	4.68	1644.06	3.29
9	1800	1845.98	-2.55	1872.64	-4.04
10	1900	1879.36	1.09	1924.27	-1.28
11	2050	1917.18	6.48	2079.36	-1.43
12	2100	1976.05	5.9	2096.11	0.19
13	2200	2119.37	3.67	2235.12	-1.6
14	2300	2182.24	5.12	2387.68	-3.81
15	2400	2322.85	3.21	2396.31	0.15
16	2500	2465.47	1.38	2528.44	-1.14
17	2600	2578.06	0.84	2661.69	-2.37
18	2700	2743.57	-1.61	2697.51	0.09
19	2800	2761.82	1.36	2899.36	-3.55
20	2900	2856.35	1.51	2926.34	-0.91

Table 6.23: Summary of the Test Cases Results for the Response: Feed Rate

Test Cases	Feed Rate (mm/min)	ANN		RNN	
		Predicted	% Deviation	Predicted	% Deviation
1	305	276.41	9.37	285.36	6.44
2	310	294.65	4.95	312.57	-0.83
3	320	312.73	2.27	317.08	0.91
4	330	334.68	-1.42	345.26	-4.62
5	340	339.09	0.27	347.66	-2.25
6	350	357.42	-2.12	354.37	-1.25
7	360	363.55	-0.99	357.96	0.57
8	370	369.42	0.16	368.96	0.28
9	380	383.86	-1.02	370.03	2.62
10	390	387.35	0.68	392.44	-0.63
11	405	396.09	2.2	403.97	0.25
12	410	400.67	2.28	410.89	-0.22
13	420	422.39	-0.57	419.14	0.2
14	430	426.81	0.74	421.01	2.09
15	440	441.36	-0.31	423.26	3.8
16	450	443.92	1.35	428.11	4.86
17	460	445.23	3.21	446.36	2.97
18	470	449.67	4.33	474.98	-1.06
19	480	476.28	0.78	477.36	0.55
20	490	494.07	-0.83	496.36	-1.3

Table 6.24: Summary of the Test Cases Results for the Response: Depth of Cut

Test Cases	Depth of Cut (mm)	ANN		RNN	
		Predicted	% Deviation	Predicted	% Deviation
1	1.05	1.01	3.81	1.03	1.9
2	1.1	1.07	2.73	1.06	3.64
3	1.2	1.08	10	1.1	8.33
4	1.3	1.32	-1.54	1.2	7.69
5	1.4	1.36	2.86	1.41	-0.71
6	1.5	1.42	5.33	1.46	2.67
7	1.6	1.53	4.38	1.62	-1.25
8	1.7	1.68	1.18	1.69	0.59
9	1.8	1.71	5	1.74	3.33
10	1.9	1.79	5.79	1.82	4.21
11	2.05	1.93	5.85	1.99	2.93
12	2.1	2	4.76	2.14	-1.9
13	2.2	2.24	-1.82	2.22	-0.91
14	2.3	2.28	0.87	2.27	1.3
15	2.4	2.31	3.75	2.42	-0.83
16	2.5	2.53	-1.2	2.48	0.8
17	2.6	2.58	0.77	2.63	-1.15
18	2.7	2.66	1.48	2.68	0.74
19	2.8	2.71	3.21	2.82	-0.71
20	2.9	2.79	3.79	2.86	1.38

6.4.6 Test cases results in comparison of ANN and RNN techniques: Reverse mappingfor responses spindle speed, feed rate and depth of cut in terms of % deviation.

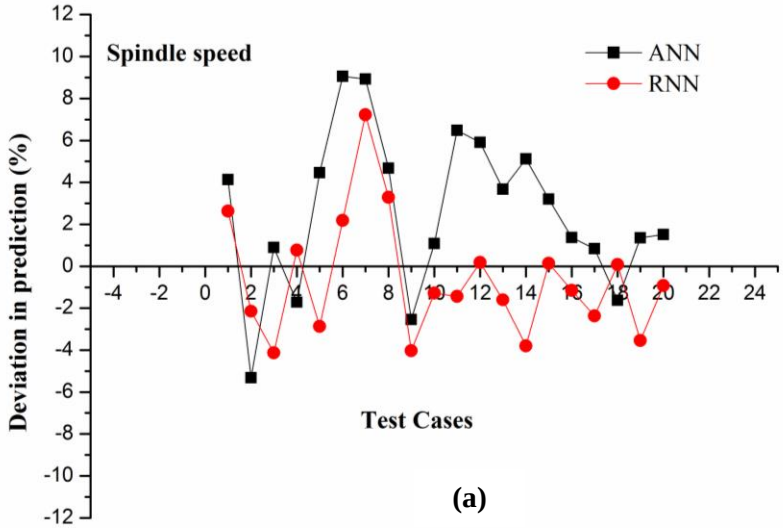

(a)

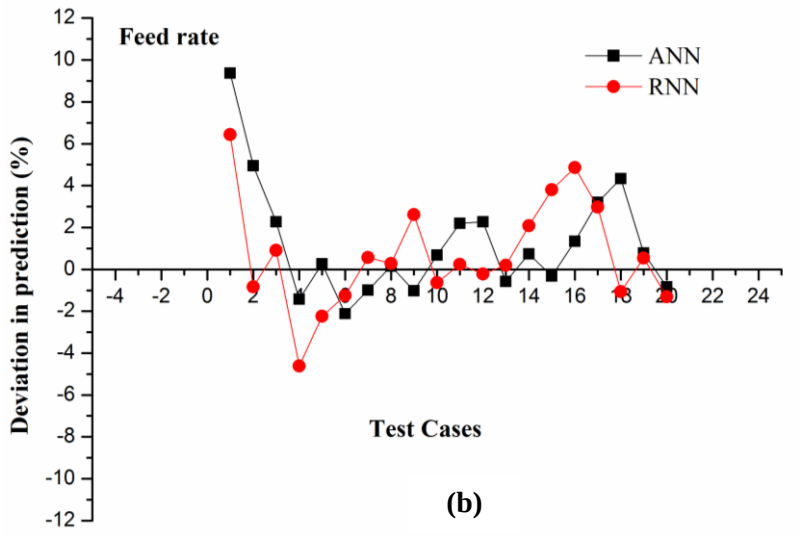

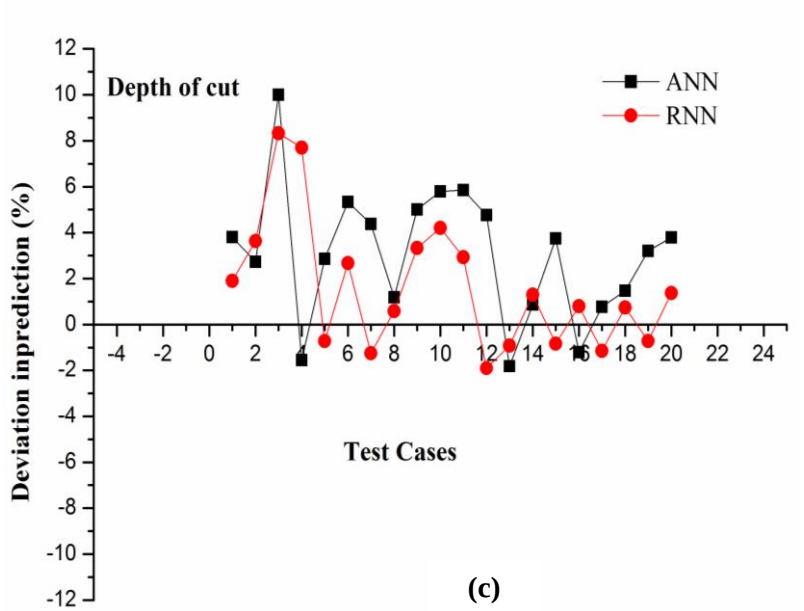

Figure 6.9: (a-c) Comparison of two models ANN and RNN in the mode of % deviation in the prediction of responses to the test cases in case of reverse mapping. (a) Prediction of response spindle speed, (b) prediction of response feed rate and (c) Prediction of response depth of cut.

6.4.7 Summarized results of Forward and Reverse Mapping techniques in terms of Deviation and Average absolute deviation % for AA6061

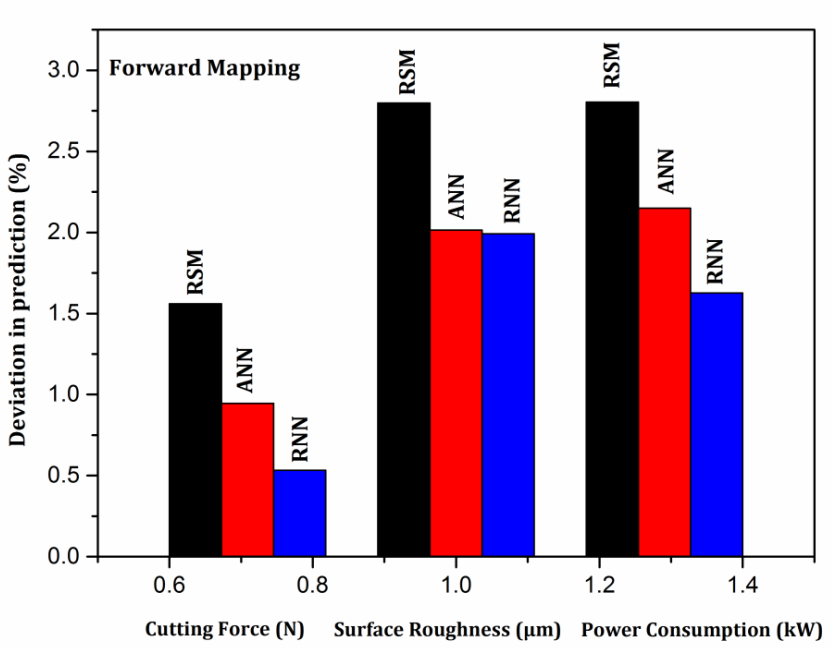

Figure 6.10: Forward Mapping: Comparison of RSM V/S ANN V/S RNN for AA6061

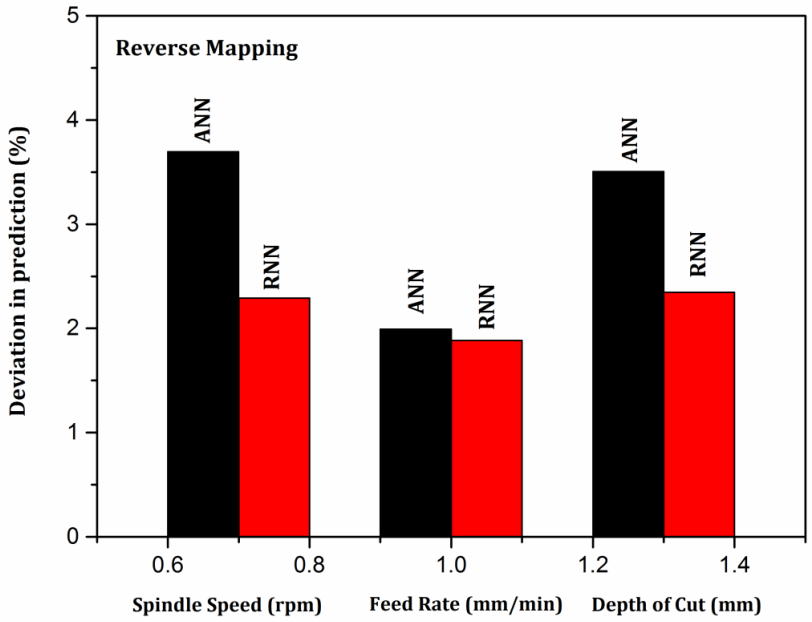

Figure 6.11: Reverse Mapping: Comparison of ANN V/S RNN for AA6061.

Figure 6.10 represents the comparision between the prediction models i.e. statistical method (RSM) with evolutionary prediction techniques (ANN, HRNN) for AA6061. From the Figure 6.10 it can be observed that the percentage of deviation attained through the RNN and ANN are within the range of ±5%. Thus indicate that the prediction accuracy is better compared to that of the RSM method.

From the Figure 6.11 represents the comparision between the ANN and RNN techniques in case of reverse mapping. From the Figure 6.11, it can be observed that the attained results through ANN and RNN are in well agreement with each other, the percentage of deviation lies within the acceptable range of ±10%. Thus indicate that the prediction accuracy is better compared to that of the RSM method.

Table 6.25, 6.26 summarizes the range of deviation % attained for CCD, ANN and RNN techniques in the mode of forward mapping. Similarly, in the mode of reverse mapping, the deviation % is achieved only through the neural network based approaches are indicated.

Further, Table 6.27, 6.28 infers the average absolute deviation % in neural network based approaches i.e. ANN and RNN. The results obtained from ANN and RNN infers that both the techniques show comparable results.

Table 6.25: Summary Results of Forward Mapping in terms of deviation %

SL. No	**Responses**	**Methods - (Deviation %)**					
		CCD		ANN		RNN	
		Min	Max	Min	Max	Min	Max
1	Fx	-5.30	3.57	-0.819	3.202	-2.24	2.07
2	Ra	-3.39	6.12	-4.08	1.96	-3.45	2.27
3	Power Consumption	-5.26	7.14	-3.66	3.70	-2.86	2.56

Table 6.26: Summary Results of Reverse Mapping in terms of deviation %

SL. No	Responses	Methods - (Deviation %)			
		ANN		RNN	
		Min	Max	Min	Max
1	Spindle Speed	-5.32	9.06	-4.14	7.23
2	Feed Rate	-2.12	9.37	-4.62	6.44
3	Depth of cut	-1.82	10.0	-1.90	8.33

Table 6.27: Summary Results of Forward Mapping in terms of Average absolute deviation %

SL. No	Responses	Methods - (Average Absolute Deviation %)	
		ANN	RNN
1	FX	0.94	0.53
2	Ra	2.01	1.99
3	Power Consumption	2.15	1.63

- Summation of Average deviation % in ANN = 5.105
- Summation of Average deviation % in RNN = 4.15
- Mean absolute deviation % in ANN = 1.70
- Mean absolute deviation % in RNN = 1.38

Table 6.28 Summary Results of Reverse Mapping in terms of Average absolute deviation %

SL. No	Responses	Methods - (Average absolute Deviation %)	
		ANN	RNN
1	Spindle speed	2.57	0.63
2	Feed Rate	1.27	0.67
3	Depth of cut	3.05	1.60

- Summation of Average deviation % in ANN = 6.89
- Summation of Average deviation % in RNN = 2.9
- Mean absolute deviation % in ANN = 2.29
- Mean absolute deviation % in RNN = 0.96

6.4.8 Comparison Of Statistical Model, ANN, And RNN For Responses In Forward Mapping Of AA6061-4.5%Cu-5%SiCp

Table 6.29: Summary of the Test Cases Results for the Response: FX

Test .No	Measured FX (N)	RSM (CCD)		ANN		RNN	
		Predicted	% Deviation	Predicted	% Deviation	Predicted	% Deviation
1	75.19	77.32	-2.83	75.12	0.09	75.17	0.03
2	104.63	103.72	0.87	106.58	-1.86	104.6	0.03
3	126.44	125.46	0.78	126.46	-0.02	128.43	-1.57
4	142.58	138.97	2.53	139.29	2.31	142.47	0.08
5	157.16	158.89	-1.1	157.11	0.03	157.17	-0.01
6	166.03	165.74	0.17	166.12	-0.05	166.06	-0.02
7	174.29	173.89	0.23	174.16	0.07	174.28	0.01
8	186.41	186.43	-0.01	184.39	1.08	186.72	-0.17
9	199.67	202.08	-1.21	199.58	0.05	199.68	-0.01
10	208.33	209.12	-0.38	208.35	-0.01	205.34	1.44
11	220.17	212.01	3.71	216.15	1.83	216.78	1.54
12	228.54	216.45	5.29	223.11	2.38	229.55	-0.44
13	236.03	236.09	-0.03	236.04	0.004	236.01	0.01
14	248.11	247.96	0.06	248.16	-0.02	248.14	-0.01
15	255.88	255.38	0.2	253.82	0.81	258.89	-1.18

Table 6.30: Summary of the Test Cases Results for the Response: Ra

Test . No	Measured Ra (µm)	RSM (CCD)		ANN		RNN	
		Predicted	% Deviation	Predicted	% Deviation	Predicted	% Deviation
1	3.07	3.12	-1.63	3.09	-0.65	3.06	0.33
2	3.52	3.49	0.85	3.6	-2.27	3.56	-1.14
3	4.03	3.98	1.24	3.98	1.24	4.01	0.5
4	1.96	1.94	1.02	1.95	0.51	1.94	1.02
5	2.12	2.07	2.36	2.13	-0.47	2.15	-1.42
6	1.68	1.7	-1.19	1.69	-0.6	1.67	0.6
7	2.36	2.33	1.27	2.37	-0.42	2.35	0.42
8	3.57	3.38	5.32	3.55	0.56	3.58	-0.28
9	2.09	2.1	-0.48	2.06	1.44	2.08	0.48
10	1.22	1.24	-1.64	1.21	0.82	1.23	-0.82
11	1.38	1.36	1.45	1.39	-0.72	1.37	0.72
12	1.41	1.42	-0.71	1.43	-1.42	1.39	1.42
13	1.66	1.64	1.2	1.64	1.2	1.68	-1.2
14	2.87	2.89	-0.7	2.86	0.35	2.88	-0.35
15	1.54	1.55	-0.65	1.53	0.65	1.53	0.65

Table 6.31: Summary of the Test Cases Results for the Response: Power Consumption

Test . No	Measured Power (kW)	RSM (CCD)		ANN		RNN	
		Predicted	% Deviation	Predicted	% Deviation	Predicted	% Deviation
1	0.07	0.073	-4.29	0.069	1.43	0.069	1.43
2	0.12	0.113	5.83	0.119	0.83	0.121	-0.83
3	0.19	0.191	-0.53	0.188	1.05	0.192	-1.05
4	0.14	0.139	0.71	0.142	-1.43	0.143	-2.14
5	0.16	0.157	1.88	0.159	0.63	0.161	-0.63
6	0.17	0.168	1.18	0.171	-0.59	0.172	-1.18
7	0.21	0.209	0.48	0.205	2.38	0.211	-0.48
8	0.22	0.218	0.91	0.223	-1.36	0.222	-0.91
9	0.34	0.349	-2.65	0.338	0.59	0.342	-0.59
10	0.26	0.257	1.15	0.261	-0.38	0.259	0.38
11	0.28	0.276	1.43	0.282	-0.71	0.278	0.71
12	0.3	0.312	-4	0.304	-1.33	0.302	-0.67
13	0.32	0.323	-0.94	0.321	-0.31	0.319	0.31
14	0.36	0.355	1.39	0.359	0.28	0.361	-0.28
15	0.43	0.427	0.7	0.432	-0.47	0.431	-0.23

The performance of the aforesaid models for considered fifteen test cases is summarized in Table 6.29 - 6.31. The results attained illustrates that the neural network based techniques predict the responses in greater accuracy compared to that of the statistical model, the achieved results are depicted in Figure 6.12 (a),(b),(c). The values of % deviation for the response FX lie in the range of -2.83 to 5.29 for CCD, for ANN -1.864 to 2.376 and for RNN -1.57 to 1.54 as depicted in Table 6.29. Similarly, The values of % deviation for the response Ra lie in the range of -1.64 to 5.32 for CCD, for ANN -2.27 to 1.44 and for RNN as -1.42 to 1.42 depicted in Table 6.30. Further on, the values of % deviation for the response Power consumption fall in the range of -4.29 to 5.83 for CCD, for ANN -1.43 to 2.38 and for RNN -2.14 to 1.43 as depicted in Table 6.31.

6.4.9 Test cases results in comparison of CCD, ANN, and RNN techniques: Forward mapping for responses FX, Ra, and Power Consumption in terms of % deviation for AA6061-4.5%Cu-5%SiCp

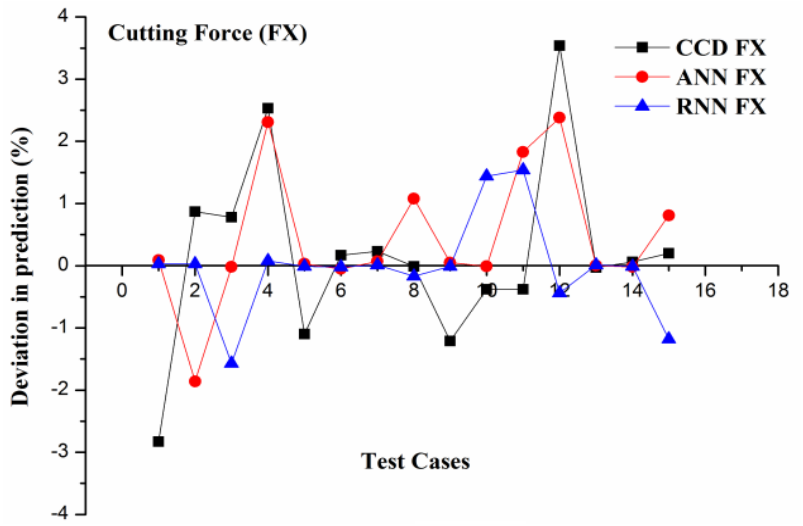

(a)

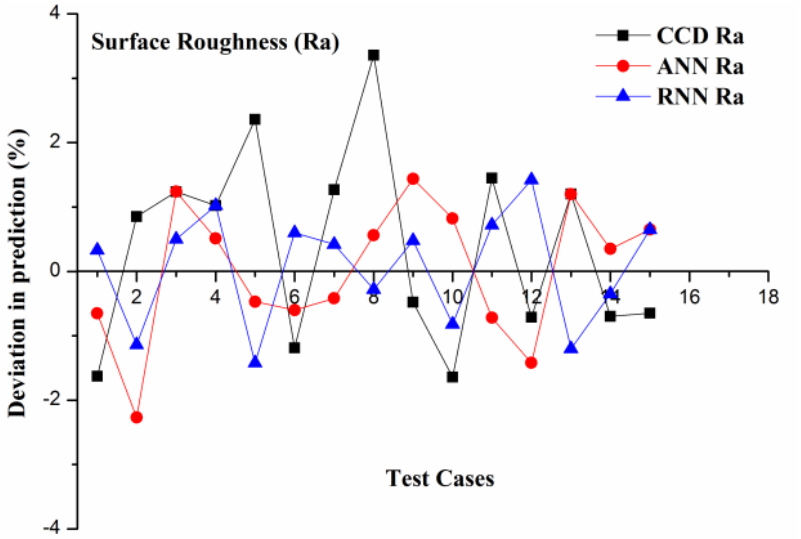

(b)

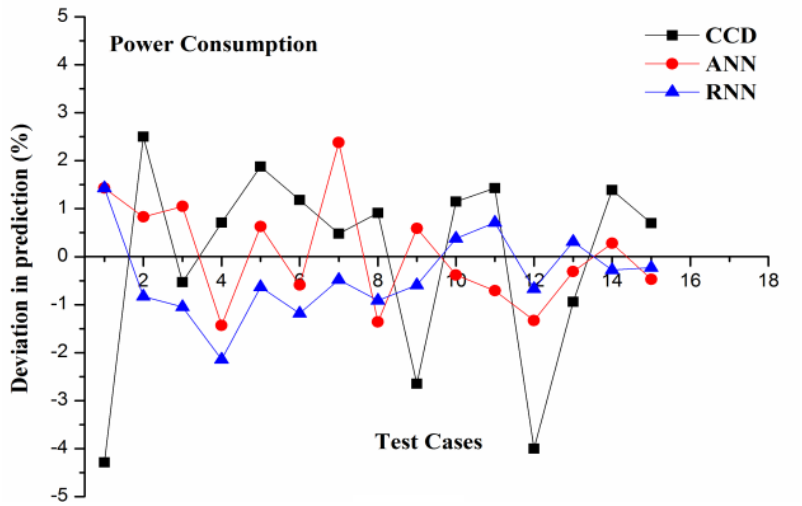

(c)

Figure 6.12 (a-c): Comparison of two models ANN and RNN in the mode of % deviation in the prediction of responses to the test cases in case of forward mapping. (a) Prediction of response cutting force (b) prediction of response surface roughness and (c) Prediction of response power consumption.

6.4.10 Results Of Reverse Mapping: AA6061-4.5%Cu-5%SiCp

In the case of the reverse mapping, twenty test cases were used. The percentage deviation was calculated for each of the predicted outcomes. The performance of the neural network based approaches i.e. ANN and RNN were compared for the twenty test cases. The comparison carried out for two techniques are summarized in Table 6.32 – 6.34. The results attained are represented in Figure 6.13 (a),(b),(c). Figure 6.13 (a),(b),(c) illustrates that the neural based approaches ANN and RNN techniques accomplished greater accuracy in prediction of responses spindle speed, feed rate and depth of cut. The values of % deviation for the response spindle speed lie in the range of -8.112 to 6.580, and RNN in the range of -7.44 to 5.39 as depicted in Table 6.32. Similarly, The values of % deviation for the response feed rate lie in the range of -2.067 to 8.125 in the case of ANN, for RNN lie in the range of -1.85 to 6.675 as shown in Table 6.33. Further on, the values of % deviation for the response depth of cut fall in the range of -3.333 to 9.231 in ANN, for RNN it is -3.913 to 8.667 as presented in Table 6.34.

6.4.11 Comparison of ANN, RNN for responses in Reverse Mapping for AA6061-4.5%Cu-5%SiCp

Table 6.32: Summary of the Test Cases Results for the Response: Spindle Speed

Test Cases	Spindle Speed (rpm)	ANN		RNN	
		Predicted	% Deviation	Predicted	% Deviation
1	1050	1046.38	0.345	1128.12	-7.44
2	1100	1189.23	-8.112	1150.74	-4.613
3	1200	1234.17	-2.848	1211.36	-0.947
4	1300	1302.04	-0.157	1258.18	3.217
5	1400	1375.12	1.777	1397.89	0.151
6	1500	1474.33	1.711	1483.06	1.129
7	1600	1502.45	6.097	1566.27	2.108
8	1700	1740.52	-2.384	1648.36	3.038
9	1800	1827.69	-1.538	1702.98	5.39
10	1900	1912.01	-0.632	1902.51	-0.132
11	2050	2038.24	0.574	2024.28	1.255
12	2100	2085.33	0.699	2095.33	0.222
13	2200	2169.76	1.375	2114.47	3.888
14	2300	2151.58	6.453	2267.09	1.431
15	2400	2373.22	1.116	2349.83	2.09
16	2500	2351.07	5.957	2498.96	0.042
17	2600	2428.93	6.58	2607.25	-0.279
18	2700	2714.75	-0.546	2699.08	0.034
19	2800	2728.42	2.556	2708.43	3.27
20	2900	2916.28	1.51	2832.11	2.341

Table 6.33: Summary of the Test Cases Results for the Response: Feed Rate

Test Cases	Feed Rate (mm/min)	ANN		RNN	
		Predicted	% Deviation	Predicted	% Deviation
1	305	280.22	8.125	294.36	3.489
2	310	296.13	4.474	296.07	4.494
3	320	310.22	3.056	298.64	6.675
4	330	323.48	1.976	318.19	3.579
5	340	330.61	2.762	345.28	-1.553
6	350	332.07	5.123	349.35	0.186
7	360	358.35	0.458	361.11	-0.308
8	370	363.24	1.827	362.23	2.1
9	380	384.86	-1.279	369.49	2.766
10	390	387.54	0.631	370.71	4.946
11	405	393.12	2.933	400.36	1.146
12	410	394.07	3.885	404.15	1.427
13	420	395.26	5.89	423.37	-0.802
14	430	432.35	-0.547	428.26	0.405
15	440	444.81	-1.093	430.74	2.105
16	450	447.13	0.638	449.82	0.04
17	460	448.39	2.524	468.51	-1.85
18	470	449.22	4.421	473.76	-0.8
19	480	473.86	1.279	484.23	-0.881
20	490	500.13	-2.067	495.57	-1.137

Table 6.34: Summary of the Test Cases Results for the Response: Depth of Cut

Test Cases	Depth of Cut (mm)	ANN		RNN	
		Predicted	% Deviation	Predicted	% Deviation
1	1.05	1.03	1.905	1.02	2.857
2	1.1	1.04	5.455	1.05	4.545
3	1.2	1.11	7.5	1.21	-0.833
4	1.3	1.18	9.231	1.23	5.385
5	1.4	1.36	2.857	1.28	8.571
6	1.5	1.39	7.333	1.37	8.667
7	1.6	1.61	-0.625	1.47	8.125
8	1.7	1.63	4.118	1.59	6.471
9	1.8	1.65	8.333	1.83	-1.667
10	1.9	1.84	3.158	1.89	0.526
11	2.05	2.01	1.951	2.07	-0.976
12	2.1	2.07	1.429	2.09	0.476
13	2.2	2.22	-0.909	2.14	2.727
14	2.3	2.24	2.609	2.39	-3.913
15	2.4	2.48	-3.333	2.42	-0.833
16	2.5	2.49	0.4	2.46	1.6
17	2.6	2.62	-0.769	2.67	-2.692
18	2.7	2.66	1.481	2.68	0.741
19	2.8	2.83	-1.071	2.77	1.071
20	2.9	2.85	1.724	2.88	0.69

6.4.12 Test cases result in a comparison of ANN and RNN techniques: Reverse mapping for responses spindle speed, feed rate and depth of cut in terms of % deviation.

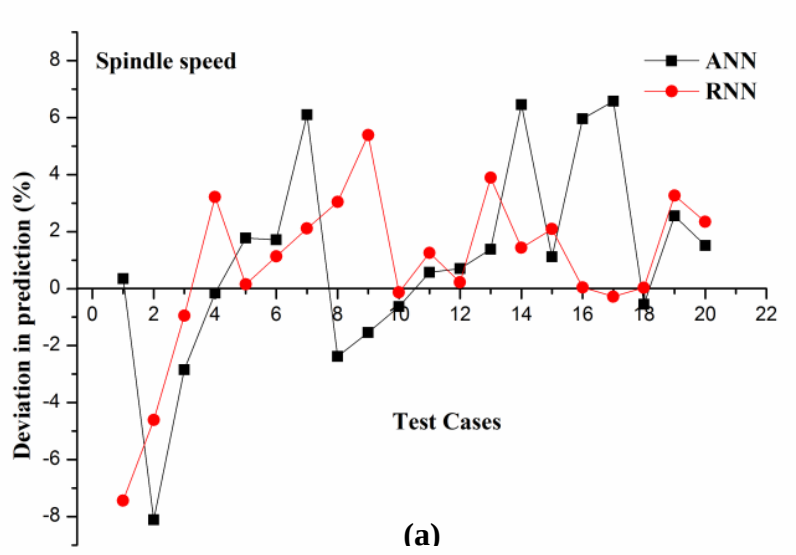

(a)

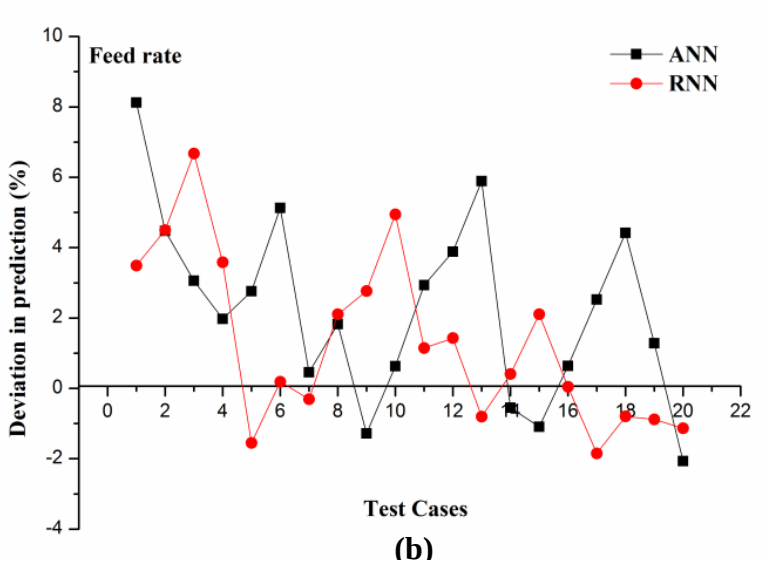

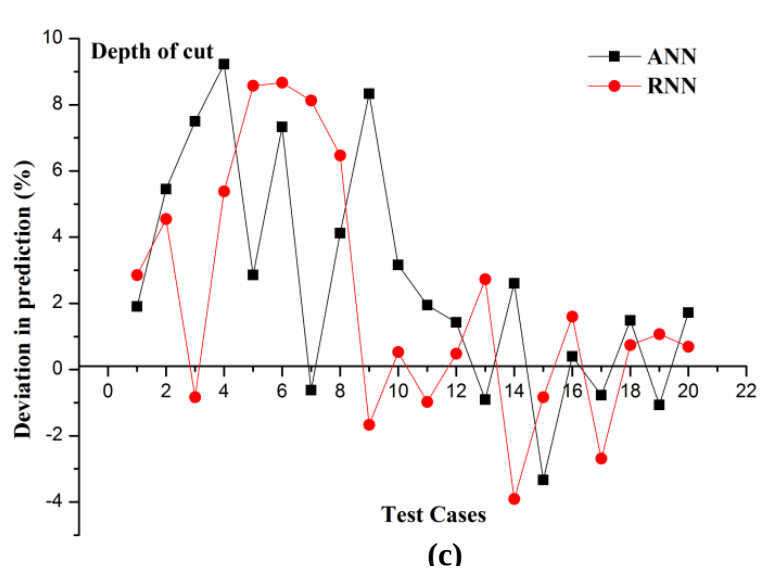

Figure 6.13 (a-c): Comparison of two models ANN and RNN in the mode of % deviation in the prediction of responses to the test cases in case of reverse mapping. (a) Prediction of response spindle speed, (b) prediction of response feed rate and (c) Prediction of response depth of cut.

6.4.13 Summarized results of forward and Reverse Mapping techniques in terms of Deviation and Average absolute deviation % for AA6061-4.5%Cu-5%SiCp

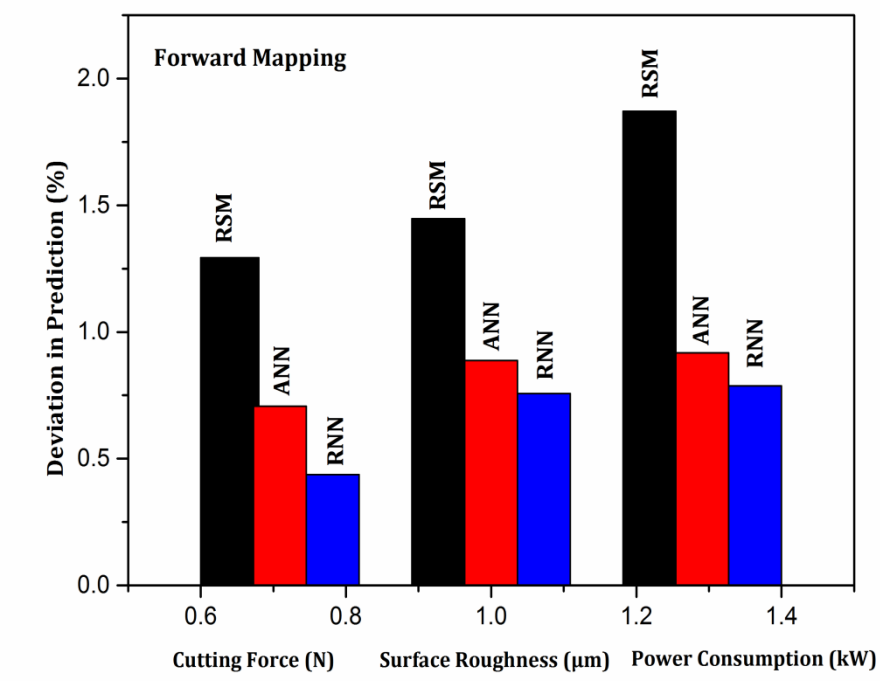

Figure 6.14: Forward Mapping: Comparison of RSM V/S ANN V/S RNN for AA6061-4.5%Cu-5%SiCp

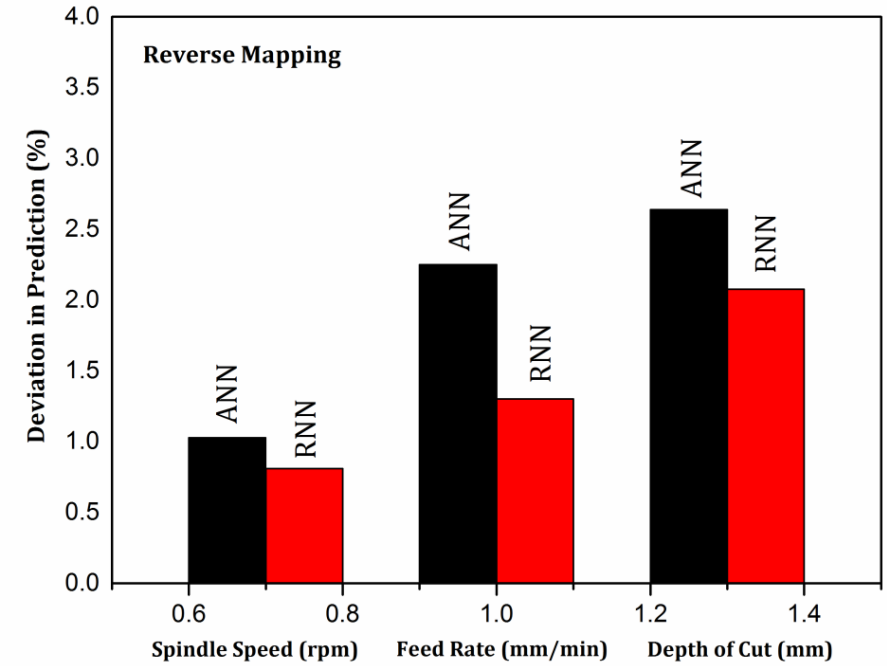

Figure 6.15: Reverse Mapping: Comparison of ANN V/S RNN for AA6061.

Figure 6.14 represents the comparision between the prediction models i.e. statistical method (RSM) with evolutionary prediction techniques (ANN, HRNN) for AA6061-4.5%Cu-5%SiCp. From the Figure 6.14 (a-b) it can be observed that the percentage of deviation attained through the RNN and ANN are within the range of ±5%. Thus indicate that the prediction accuracy is better compared to that of the RSM method.

From the Figure 6.15 represents the comparision between the ANN and RNN techniques in case of reverse mapping. From the Figure 6.15, it can be observed that the attained results through ANN and RNN are in well agreement with each other, the percentage of deviation lies within the acceptable range of ±10%. Thus indicate that the prediction accuracy is better compared to that of the RSM method.

Table 6.35, 6.36 summarizes the range of deviation % attained for CCD, ANN and RNN techniques in the mode of forward mapping. Similarly, in the mode of reverse mapping, the deviation % is achieved only through the neural network based approaches are indicated.The results tabulated in Table 6.37, 6.38 infer the average absolute deviation % in neural network based approaches i.e. ANN and RNN. The results obtained from ANN and RNN infers that both the techniques show comparable results.

Table 6.35: Summary Results of Forward Mapping in terms of deviation %

SL. No	**Responses**	**Methods - (Deviation %)**					
		CCD		ANN		RNN	
		Min	Max	Min	Max	Min	Max
1	Fx	-2.83	5.29	-1.864	2.376	-1.57	1.54
2	Ra	-1.64	5.32	-2.27	1.44	-1.42	1.42
3	Power Consumption	-4.29	5.83	-1.43	2.38	-2.14	1.43

Table 6.36: Summary Results of Reverse Mapping in terms of deviation %

SL. No	Responses	Methods - (Deviation %)			
		ANN		RNN	
		Min	Max	Min	Max
1	Spindle Speed	-8.112	6.58	-7.44	5.39
2	Feed Rate	-2.067	8.125	-1.85	6.675
3	Depth of cut	-3.333	9.231	-3.913	8.667

Table 6.37: Summary Results of Forward Mapping in terms of Average absolute deviation %

SL. No	Responses	Methods - (Average Absolute Deviation %)	
		ANN	RNN
1	FX	0.71	0.43
2	Ra	0.89	0.76
3	Power Consumption	0.92	0.79

- Summation of Average deviation % in ANN = 2.52
- Summation of Average deviation % in RNN = 1.98
- Mean absolute deviation % in ANN = 0.84
- Mean absolute deviation % in RNN = 0.66

Table 6.38: Summary Results of Reverse Mapping in terms of Average absolute deviation %

SL. No	Responses	Methods - (Average absolute Deviation %)	
		ANN	RNN
1	Spindle speed	2.648	2.151
2	Feed Rate	2.749	2.034
3	Depth of cut	3.310	3.168

- Summation of Average deviation % in ANN = 8.707
- Summation of Average deviation % in RNN = 7.353
- Mean absolute deviation % in ANN = 2.902
- Mean absolute deviation % in RNN = 2.451

6.5 GRAPHICAL USER INTERFACE DESIGN

The medium of graphics has revolutionised the user interface design. If used appropriately, it can harness the information assimilation, processing and dissemination capabilities of the user and allow for faster interaction with computer system. Graphical User Interface (GUI) has brought about a marked change in the world of computing in terms of use of computer systems across professions. A well designed GUI will help the user to interact with the system comfortably, in the sense, that it is easier to learn, more effective to use and does not cause vision fatigue when used for long periods. The fact that they are easy to use does not imply that they are easy to design. In fact the designing medium for GUIs in modern days is so rich with so many different options of architectures, colour combinations, facilities, metaphors, patterns available that one can create an excellent GUI for a given application. However, with so much flexibility available in terms of choices in design, there is every possibility of the designer going overboard and coming out with a mediocre, lacklustre design of GUI. Therefore designing a good GUI is a challenging task.

6.5.1 Objectives of Graphical User Interface Design

The user interface is a part of the computer system which connects the user with the internal system of the computer. In a typical information system or the systems used in offices, the user interface may include following.

- The components of the computer hardware with which the user can interact with the system such as, screen, mouse, keyboard, toggle switch, on/off switch etc.
- The images within the computer application software such as windows, task bars, pull down menus, pop ups, messages, help screens, etc.
- User documentations such as manuals, catalogues, reference cards

While the user operates on a GUI, he/she has no access to what is happening inside the computer system. The system will work in the background based on the

information provided by the user in the input section and provide him/her with the processed outputs. Therefore the user is more concerned with the interface, rather than what is happening in the background. Hence the objective of the GUI design is to make it as user friendly as possible, by increasing its usability. Usability here means, making the computer system adaptable to human beings who are going to use it, and has a lot of bearing on the psychological issues relating to human memory, perception, comprehension and conceptualization.

A good interface design is important as it is the only medium that allows the user to interact with the computer internals. A lacklustre design may not be attractive to the user and he may not use it. Further a wrongly designed GUI may confuse the user and there is every possibility that one may use it wrongly or stop using it. Actually, the interface is the front end of the computer system by which the designer represents the system to the user. A good user interface can result in increase of productivity while a poorly designed one may cause stress followed by fatigue and discomfort to the user. The flow of working of GUI is represented in Figures 6.16 – 6.21.

6.5.2 Development Of GUI

GUI has been designed using available API libraries which include three main modules, namely, material, method and test option. Each module has related sub modules.

- In material model there is a drop down list of materials used in the study (AA6061, AA6061-4.5%C-5%SiCp). In method module there is a choice of selecting offline (Prediction and Optimization sub modules) and online method (optimization module). In test option module for prediction (Forward and Reverse Sub Modules) there is list of approaches such as RSM, ANN,RNN and similarly for optimization (RSM and PSO).
- Prediction model has the sub components for prediction of cutting force, surface roughness and power consumption by forward mapping. Similarly in case of reverse mapping it predicts the spindle speed, feed rate and depth of cut.

- There is provision to obtain outputs by manually feeding the input values as well for plotting bar graphs by varying one parameter at a time, keeping other parameters constant.
- The GUI is also designed to generate bar plots by varying each input parameter at a time. Use of GUI is made in optimising the processing parameters for obtaining the best possible outcome for AA6061 alloy and Al-4.5%Cu-5%SiCp composite.
- The proposed ANN and RNN model along with the user friendly GUI designed for the purpose will serve as a useful tool for optimization of responses namely, cutting force, surface roughness and power consumption based on the parameters specified by the user.
- Graphical user interface (GUI) has been created for prediction and optimization models formulated, so that it creates a friendly environment for the user to obtain property predictions for different combinations of inputs, understand the variation of input – output relationship and achieve optimized process settings.

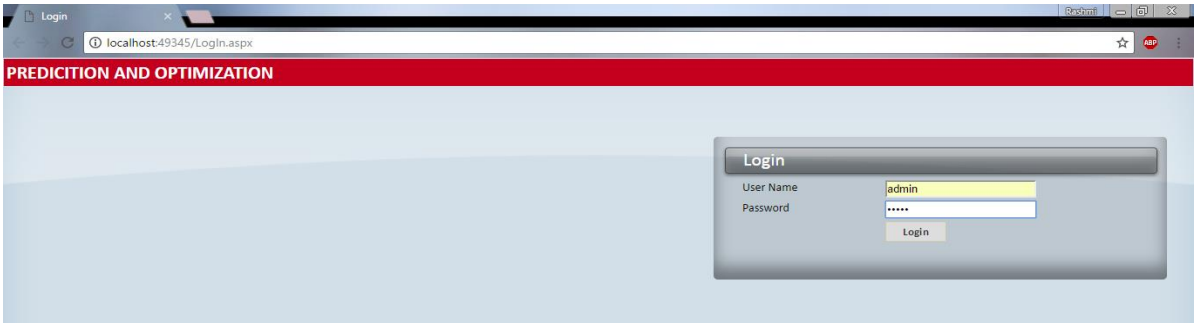

Figure 6.16: Login page

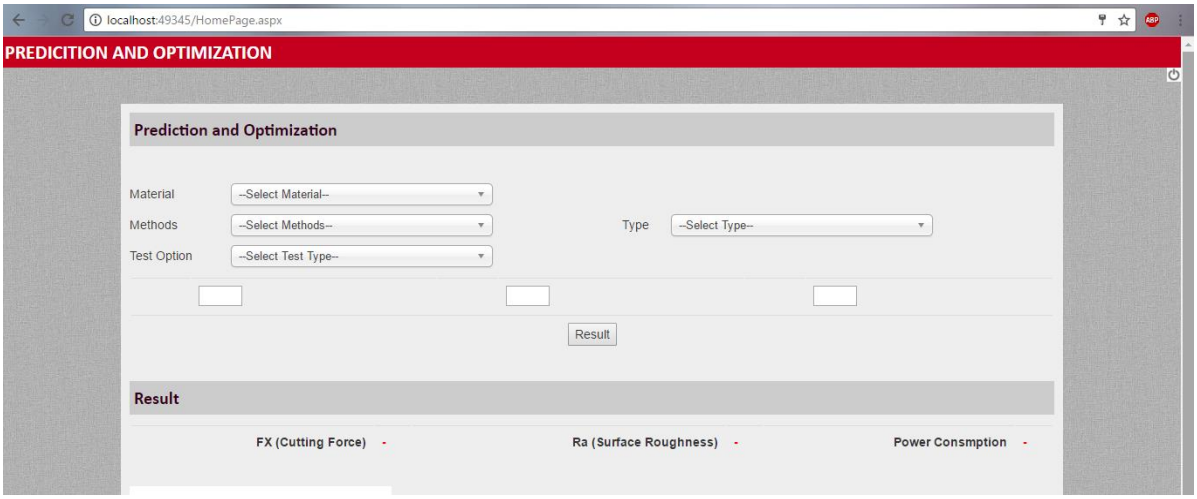

Figure 6.17: Selection of Method, Material and parameters.

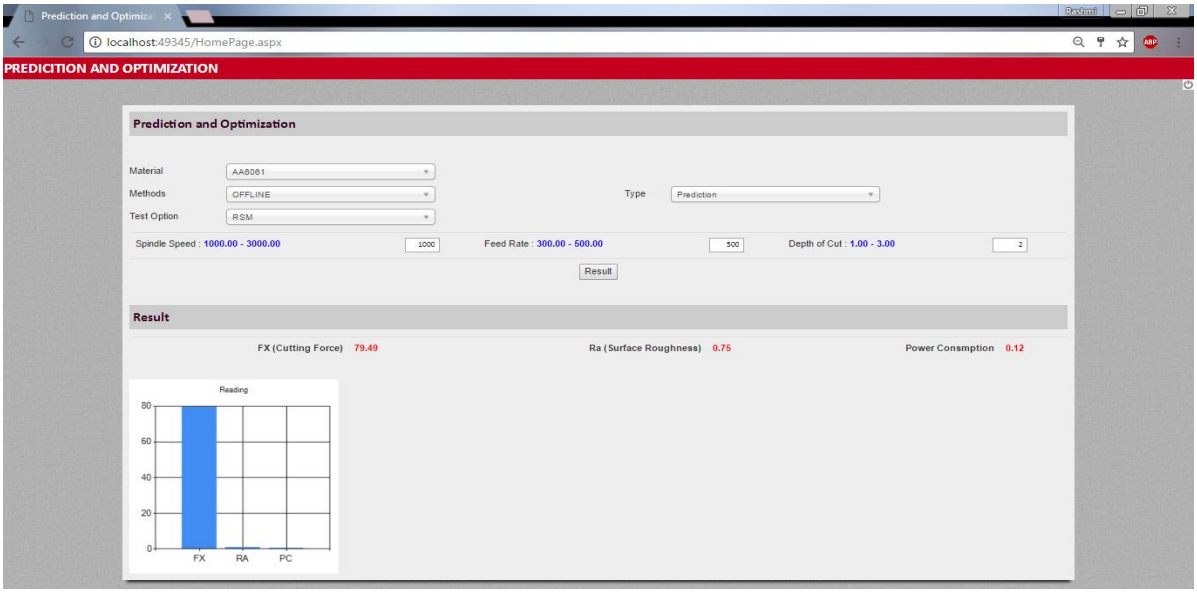

Figure 6.18: Output Graph of responses

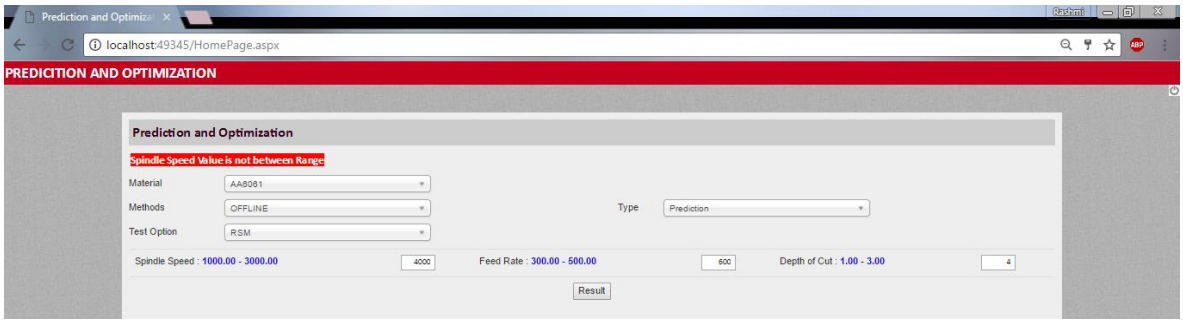

Figure 6.19: Warning Message

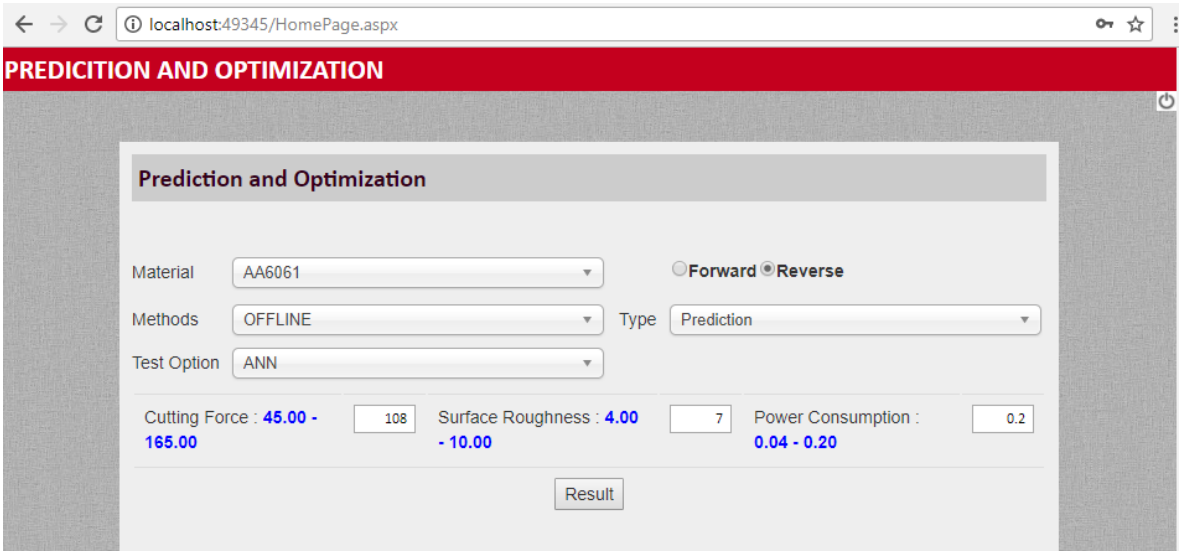

Figure 6.20: Selection of Reverse Mapping Approach

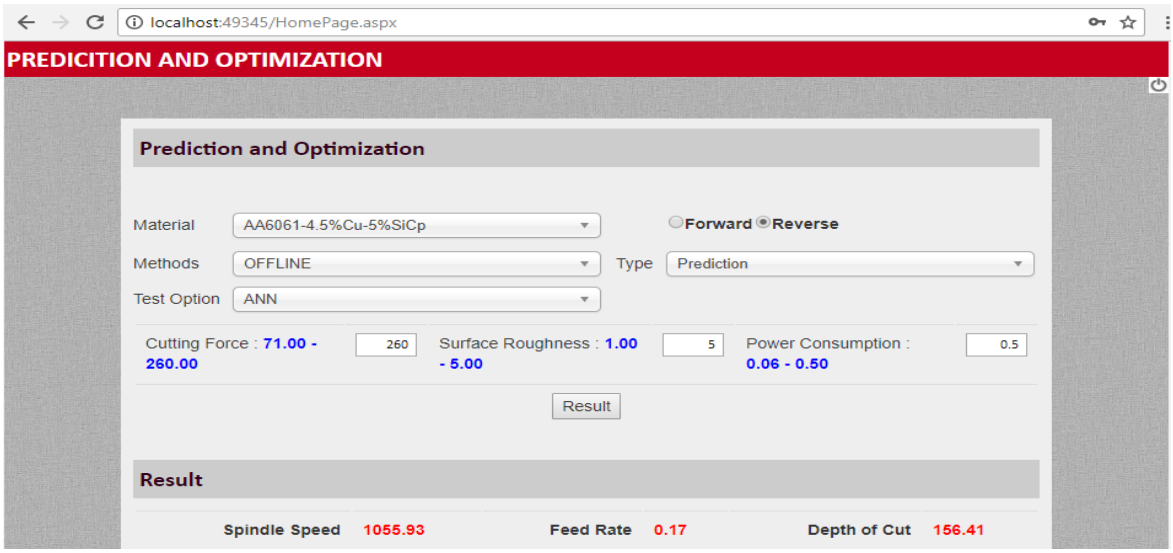

Figure 6.21: Reverse Mapping Approach Result

6.5.3 Concluding Remarks

- The ANN and RNN model successfully predict the values within an overall error of |5| percent for responses in case of forward mapping. However for majority of the predictions, the error is between ±3.6 percent. The proposed model is validated within a prediction error of |5.5 |percent within the bounds of data used for training the model.
- The ANN and RNN model successfully predict the values within an overall error of |10| percent for responses in case of reverse mapping. However for majority of the predictions, the error is between ±10 percent. The proposed model is validated within a prediction error of |8.5 |percent within the bounds of data used for training the model.
- The idea behind selecting various prediction techniques is to provide generic nature of the decision support system through development of GUI.
- Developed GUI utilizes both forward and reverse mapping approaches via ANN and RNN method to predict the responses.

IN Case of AA6061

- The statistical model CCD was shown to be a valuable approach, attains higher deviation % in case of forward mapping i.e. the range of responses deviation % lie -3.39 to 7.14. The accuracy of prediction attained by the statistical model is lesser as compared to ANN and RNN.
- The results attained in the case of forward mapping indicate that the neural network based approaches i.e. ANN and RNN attain greater predicting accuracy as compared to CCD statistical model.
- In the case of both forward and reverse mapping, the results attained from ANN and RNN infer that both technique results are comparable.
- In the case of forward mapping, it can be observed that the mean absolute deviation % in ANN is 1.7 which fall within the acceptable range.
- In the case of forward mapping, it can be observed that the mean absolute deviation % in RNN is 1.38 found to be within the range.
- In the case of reverse mapping, it can be observed that the mean absolute deviation % in ANN is 2.29 found to be within the acceptable range.

- In the case of reverse mapping, it can be observed that the mean absolute deviation % in RNN is 0.96 which is found to be within the range.
- In the case of reverse mapping, the results attained through ANN and RNN indicate that the RNN is better as compared to that of the ANN because due to the capability of the faster convergence of RNN compared to ANN.

IN Case of AA6061-4.5%Cu-5%SiCp

- The statistical model CCD was shown to be a valuable approach, attains higher deviation % in case of forward mapping i.e. the range of responses deviation % lie -3.39 to 7.14. The accuracy of prediction attained by the statistical model is lesser as compared to ANN and RNN.
- The results attained in the case of forward mapping indicate that the neural network based approaches i.e. ANN and RNN attain greater predicting accuracy as compared to CCD statistical model.
- In the case of both forward and reverse mapping, the results attained from ANN and RNN infer that both technique results are comparable.

So far, the prediction of process parameters and responses has been discussed, In industry, most of the concentration is towards minimizing the cost incurred during the process. Hence the optimization technique is a better approach to suggest the input parameters based on the desired responses. So, further chapter deals with incorporation of optimization techniques.

Related Airtcle: **Rashmi L Malghan, Karthik Rao, Arun Shettigar, Shrikantha S Rao and R J D'Souza** (2018) Forward and Reverse Mapping in Milling process using ANN, Data in Brief, Elsevier, 16, 114–121. Doi: 10.1016/j.dib.2017.10.069.

CHAPTER 7

RESULTS AND DISCUSSION (PART 3)

OPTIMIZATION

Finding an optimal solution for more than one objective functions is called multi-objective optimization (deals with more than one objective function). In most of the optimization problems, it involves multi objectives. A multiobjective function problem has number of objective functions which are to be minimized or maximized. All the objectives are important; a solution is may be extreme for one objective, in that situation compromise of other objective is required. Optimization is the technique to obtain best results for the given problems under given constraints. An investigation is done here to compare and arrive at the best optimization technique from among GRA, Desirability Approach and PSO.

7.1 EVOLUTIONARY ALGORITHM

Evolution algorithms (EAs) are imitative of natural evolutionary principles to constitute search and optimization procedure. Genetic algorithm (GA) is evolutionary algorithm and was introduced by John Holland (1975). These algorithm functions are to selection of the fittest to produce better approximation to solutions.

Particle swarm optimization algorithm (PSO) is a relatively new approach in modern heuristics for optimization, is one of the evolutionary protocol methods. PSO was first developed by Eberhart and Kennedy (1995) for continues function optimization. There are several stochastic algorithms such as genetic algorithms, differential evolution, Tabu search, simulated annealing, ant colony optimization and particle swarm optimization. These algorithms are used to find optimal solution for different objective function. The basic concept of PSO originated from the food hunting behaviour of birds. It was found that through the intelligent swarming behaviour, flocks of birds would always suddenly change the direction, scatter and gather. Behaviour of birds is also unpredictable but always consistent as whole, with individuals keeping the most suitable distance. Every swarm of PSO is a solution in

the solution space. It adjusts the fight according to its own and its companion flying experience.The goal of optimization is to minimize or maximize certain quantities such as life, mass, etc. In mathematical models, these goals are expressed as functions of certain variables. There are various methods available for solving these models towards minimization or maximization. The response equations attained through RSM model are further utilized as fitness function in implementation of PSO algorithm. The chapter deals with the implementation and comparison of both statistical and evolutionary optimization techniques and background of these optimization techniques are explained in chapter 3 (section 3.10). The foresaid optimization techniques are carried out to predict the optimum combinations of process parameters for the desired responses

7.2 GREY RELATIONAL ANALYSIS

The Grey relational analysis proposed by (Deng 1989), it is extensively used to estimate the degree of connection between sequences by grey relational grade. The Grey relational analysis technique is used by several researchers to optimize the process parameters comprising of multi-responses through grey relational grade grades (Chen et al. 2000, Balasubramanian et al. 2011, Lin et al. 2004).. Grey relation analysis is considered as black box technique which is generally used to identify the interior lacking information. In this technique, the consideration of information falls into two ways, the one with lack of information is considered to be black, whereas the other with full of information is considered as white. The grey is nothing but the one which is in between of these two black and white information. In other words, the information which is wavering and partial is regarded as Grey. Thus the system with partial information is considered as Grey system. In the Grey phenomenon Grey element, Grey number and Grey system are the three terms which are very important. Grey element is the element with partial information. The Grey number is one with incomplete information in the Grey system. Similarly the Grey relation is related with partial information. The black box is used to indicate a system lacking interior information. Generally the Grey relation technique is incorporated to determine and analyze the relational grade in the case of discrete sequences. Generally, the Grey

relation analysis requires less data, but it analyzes many factors, thus proving to be more advantageous as compared to that of the statistical method.

The algorithm of grey relational analysis coupled with principal analysis to determine the optimal combinations of the cutting parameters in milling operation is described step by step as follows:

(1) Convert the experimental data into respective S/N ratio values.
(2) Normalize the S/N ratio, i.e. the data pre - processing step is carried out.
(3) Next the Grey deviation sequence is computed.
(3) Further the corresponding Grey relational coefficients are computed.
(4) Determine the Grey relational grade using principal component analysis.
(5) Select the optimal levels of cutting parameters.
(6) Conduct confirmation experiments.

The explanation of the above steps mentioned in the algorithm is as follows:

Step 1: In the 1st step, the transformation of original or experimental values of S/N ratio values is performed. The transformation to S/N ratio is done to identify the desirable result through the smallest variance and finest performance. In order to transform to the S/N ratio values, the following equations are incorporated:

1) For smaller the better

$$\frac{\mathbf{S}}{\mathbf{N}} = -10\log\left(\frac{1}{n}\right)\sum Rij^2 \qquad \textbf{(7.1)}$$

2) For Larger the better

$$\frac{\mathbf{S}}{\mathbf{N}} = -10\log\left[\sum\frac{Rij^2}{n}\right] \qquad \textbf{(7.2)}$$

3) For Nominal is better

$$\frac{\mathbf{S}}{\mathbf{N}} = 10\log\left[\frac{1}{pm^2}\right] \qquad \textbf{(7.3)}$$

Where : Rij is the response value j in the i^{th} experiment condition, where i=1, 2, 3....n; j=1, 2, 3...k, and pm^2 are the sample mean and variance.

In the present study the equations (7.1) is considered for surface roughness and equation (7.2) for Cutting Force (FX) and Power Consumption.

Step 2: In this step data pre - processing is carried out. The data pre - processing is performed for normalizing the data for the purpose of analysis. Rij is normalized as L_{ij} ($0 \leq L_{ij} \leq 1$) by using the equation (7.4). This is for larger the better normalized response such as FX and Power Consumption in the current study. Similarly for the smaller the better response such as Ra the equation (7.5) holds good.

$$L_{ij} = \frac{Rij - \min(Rij,\ i=1,2..n)}{\max(Rij,\ i=1,2..n) - \min(Rij,\ i=1,2..n)} \quad \textbf{(7.4)}$$

$$L_{ij} = \frac{\max(Rij,\ i=1,2..n) - Rij}{\max(Rij,\ i=1,2..n) - \min(Rij,\ i=1,2..n)} \quad \textbf{(7.5)}$$

Step 3: The Grey Deviation sequence is computed as per the equation (7.7), later on the Grey relation coefficient is determined based on the equation (7.6) . The Grey coefficient helps in identifying the relationship between the actual and ideal normalized values.

$$E_i(k) = \frac{\Delta_{\min} + \zeta\Delta_{\max}}{\Delta_{oi}(k) + \zeta\Delta_{\max}} \quad \textbf{(7.6)}$$

$$\Delta_{oi}(k) = \| r_o(k) - r_i(k) \| \quad \textbf{(7.7)}$$
$$\Delta_{\min} = \min_{\forall j \in i} \min_{\forall k} \| r_o(k) - r_j(k) \|$$
$$\Delta_{\min} = \max_{\forall j \in i} \max_{\forall k} \| r_o(k) - r_j(k) \|$$

Where $\Delta_{oi}(k)$ represents the Grey deviation sequence for the responses, r_j (k) represents the comparability sequence, ζ denotes the discriminate.

Step 4 : The Grey relation grade (GRG) is useful in evaluating the multiple performance characteristics. Average of all obtained grey relation coefficient gives the grey relation grade. Equation (7.8) is used to compute the GRG Yi(p) and obtained results and GRG ranks were tabulated in Tables 7.1 and 7.6 respectively for AA6061 and AA6061-4.5%Cu-5%SiCp. The attained values of all the steps from 1 - 4 are depicted in Tables 7.1- 7.2.

$$Y_i(p) = \frac{1}{N}\Sigma_{i=0}^{N}[\omega p * E_i(k)] = \frac{1}{N}\Sigma_{i=0}^{N} E_i(k) \quad \textbf{(7.8)}$$

Where, N = No. of performance characteristics, ω = Weightage or importance of each performance characteristics, in this work it is assumed that all the performance

characteristics have equal importance, generally this value should be in between 0 and 1 ($0 < \omega i < 1$). The larger GRG represents how closer the corresponding experimental response to the ideal value. From the Table 7.2 and 7.7, first experiment with A1B1C1D1 combination has the highest grade among all the orthogonal experiments.

Table 7.1: Grey Relation Analysis for AA6061

	Responses						Data Preprocessing			Deviation Sequence			Grey Relational Co-efficient			Relational
Expt .No	FX	SNRA	Ra	SNRA	Power	SNRA	FX	Ra	Power	Delta-FX	Delta-Ra	Delta-Powe	FX	Ra	Power	Grade
1	45.50	33.16	0.70	3.10	0.04	-28.53	1.00	0.54	1.00	0.00	0.46	0.00	1.00	0.52	1.00	0.841
2	50.31	34.03	0.64	3.88	0.04	-27.48	0.92	0.42	0.94	0.08	0.58	0.06	0.86	0.46	0.89	0.738
3	56.69	35.07	0.63	4.01	0.05	-26.33	0.83	0.39	0.87	0.17	0.61	0.13	0.74	0.45	0.79	0.663
4	58.72	35.38	0.86	1.31	0.07	-23.42	0.80	0.84	0.70	0.20	0.16	0.30	0.72	0.76	0.62	0.699
5	63.42	36.05	0.76	2.38	0.07	-22.65	0.74	0.66	0.65	0.26	0.34	0.35	0.66	0.60	0.59	0.615
6	72.60	37.22	0.67	3.48	0.08	-21.47	0.64	0.48	0.58	0.36	0.52	0.42	0.58	0.49	0.54	0.538
7	73.27	37.30	0.96	0.35	0.11	-19.32	0.63	1.00	0.45	0.37	0.00	0.55	0.57	1.00	0.48	0.684
8	79.05	37.96	0.86	1.31	0.12	-18.64	0.57	0.84	0.41	0.43	0.16	0.59	0.54	0.76	0.46	0.586
9	83.56	38.44	0.68	3.35	0.13	-18.03	0.53	0.50	0.38	0.47	0.50	0.62	0.51	0.50	0.45	0.487
10	93.58	39.42	0.63	4.01	0.08	-21.61	0.44	0.39	0.59	0.56	0.61	0.41	0.47	0.45	0.55	0.491
11	100.01	40.00	0.61	4.29	0.09	-20.90	0.39	0.35	0.55	0.61	0.65	0.45	0.45	0.43	0.53	0.469
12	107.23	40.61	0.62	4.15	0.10	-20.29	0.33	0.37	0.51	0.67	0.63	0.49	0.43	0.44	0.51	0.459
13	110.22	40.84	0.73	2.73	0.13	-17.46	0.31	0.60	0.34	0.69	0.40	0.66	0.42	0.56	0.43	0.471
14	115.02	41.22	0.66	3.61	0.14	-17.03	0.28	0.46	0.32	0.72	0.54	0.68	0.41	0.48	0.42	0.438
15	119.84	41.57	0.62	4.15	0.15	-16.62	0.25	0.37	0.30	0.75	0.63	0.70	0.40	0.44	0.41	0.419
16	126.74	42.06	0.85	1.41	0.19	-14.26	0.20	0.82	0.16	0.80	0.18	0.84	0.39	0.74	0.37	0.499
17	134.22	42.56	0.71	2.97	0.20	-13.78	0.16	0.56	0.13	0.84	0.44	0.87	0.37	0.53	0.36	0.424
18	141.48	43.01	0.60	4.44	0.22	-13.31	0.12	0.32	0.10	0.88	0.68	0.90	0.36	0.42	0.36	0.381
19	143.30	43.12	0.52	5.68	0.13	-17.59	0.11	0.12	0.35	0.89	0.88	0.65	0.36	0.36	0.44	0.385
20	148.55	43.44	0.55	5.19	0.14	-17.29	0.08	0.20	0.33	0.92	0.80	0.67	0.35	0.38	0.43	0.388
21	150.52	43.55	0.56	5.04	0.14	-17.16	0.07	0.22	0.33	0.93	0.78	0.67	0.35	0.39	0.43	0.389
22	152.58	43.67	0.66	3.61	0.19	-14.56	0.06	0.46	0.17	0.94	0.54	0.83	0.35	0.48	0.38	0.401
23	153.29	43.71	0.58	4.73	0.19	-14.39	0.05	0.27	0.16	0.95	0.73	0.84	0.35	0.41	0.37	0.376
24	155.15	43.82	0.55	5.19	0.20	-14.20	0.04	0.20	0.15	0.96	0.80	0.85	0.34	0.38	0.37	0.366
25	158.30	43.99	0.71	2.97	0.25	-12.06	0.03	0.56	0.03	0.97	0.44	0.97	0.34	0.53	0.34	0.405
26	159.82	44.07	0.56	5.04	0.25	-11.88	0.02	0.22	0.01	0.98	0.78	0.99	0.34	0.39	0.34	0.355
27	164.21	44.31	0.48	6.38	0.26	-11.64	0.00	0.00	0.00	1.00	1.00	1.00	0.33	0.33	0.33	0.333

Related Airtcle: **Karthik Rao, Rashmi L Malghan, Arun Shettigar, Shrikantha S Rao and R J D'Souza** (2015). "Multiple Response Optimizations in Milling Using Taguchi and Grey Relational Analysis ." *International Journal of Applied Engineering Research, 10(1)* ISSN 0973-4562.

Table 7.2: Performance characteristics GRG, S/N ratio and its orders for AA6061

Expt. NO	Grey Relational Grade	S/N Ratio	Orders
1	0.841	-1.5034	1
2	0.738	-2.634	2
3	0.663	-3.5664	5
4	0.699	-3.108	3
5	0.615	-4.2185	6
6	0.538	-5.3836	8
7	0.684	-3.2974	4
8	0.586	-4.6461	7
9	0.487	-6.2521	11
10	0.491	-6.1837	10
11	0.469	-6.5738	13
12	0.459	-6.7663	14
13	0.471	-6.5468	12
14	0.438	-7.1773	15
15	0.419	-7.5647	17
16	0.499	-6.0377	9
17	0.424	-7.459	16
18	0.381	-8.3847	23
19	0.385	-8.2868	22
20	0.388	-8.2222	21
21	0.389	-8.2026	20
22	0.401	-7.9307	19
23	0.376	-8.5024	24
24	0.366	-8.7317	25
25	0.405	-7.8616	18
26	0.355	-8.9869	26
27	0.333	-9.5424	27

Table 7.3: Response table for GRG for AA6061

Level	Spindle Speed (rpm)	Feed Rate (mm/min)	Depth of Cut (mm)
1	-3.846	-5.771	-5.64
2	-6.966	-6.574	-6.491
3	-8.474	-6.941	-7.155
Delta	4.629	1.17	1.515
Rank	1	3	2

From the methodology it has been observed that, the multiple responses are converted to single response. So, now it will be treated as a single objective optimization problem. Further on, Taguchi method was utilized to optimize the attained GRG. Thus, Higher-the -better [as presented in equation (7.2)] option quality characteristic was involved in acquiring the S/N ratio for GRG. The attained S/N ratio values of RG for AA6061 and AA6061-4.5%Cu-5%SiCp are tabulated in Table 7.2 and 7.7. These attained values are computed from the equation (7.2). Later on, the means of GRG for individual level of the machining parameters of AA6061 and AA6061-4.5%Cu-5%SiCp were computed using software tool (Minitab 17.0) and are presented in Table 7.3 and 7.8 respectively. The results of GRG for each level of machining parameters, namely spindle speed, feed rate and depth of cut for AA6061 and AA6061-4.5%Cu-5%SiCp have been summarized and depicted in Table 7.3 and 7.8 respectively.

From the means analysis, the predicted optimum machining parameter combination is $A_1B_1C_1$. Therefore the optimum machining parameter levels are spindle speed at 1000 rpm, feed rate at 300mm/min and depth of cut 1 mm for both AA6061 and AA6061-4.5%Cu-5%SiCp. Generally the GRG for optimum machining parameters AA6061 and AA6061-4.5%Cu-5%SiCp is calculated as per the equation (7.9) and the achieved results are depicted in Table 7.4 and 7.9. The confirmatory results were compared with the data of the highest ranking orthogonal array No.1 ($A_1B_1C_1$). From the Table 7.4 for AA6061 and Table 7.9 for AA6061-4.5%Cu-5%SiCp it can be observed that improvement of the grey relation grade is by 16.2 % and 12.11% respectively. The results attained are well in agreement with the results of Ranganathan and senthivelan 2011, Tang et al. 2014, Senthilkumar et al 2014). Thus, from the results, it may be concluded that the improvement in the machining performance characteristics was obtained during machining of AA6061 and AA6061-4.5%Cu-5%SiCp with TGRA. The GRG is further analyzed with ANOVA for AA6061 and AA6061-4.5%Cu-5%SiCp as tabulated in Table 7.5 and 7.10 respectively to attain the effect of machining parameter on grey relation grade value. From the ANOVA as represented in Table 7.5 and 7.10, it can be concluded spindle speed (80.936, 77.578 %) has major contribution compared to the rest of the parameters. The attained R-Sq and R-Sq(adj)

for AA6061 are 99.8%, 99.3% respectively. Similarly the attained R-Sq and R-Sq(adj) for AA6061-4.5%Cu-5%SiCP is 99.7%, 99.1% respectively.

$$X_{Predicted} = X_m + \sum_{i=1}^{k}(X_o - X_m) \quad \textbf{(7.9)}$$

Where: X_m Average of total GRG, X_o The mean of the GRG at the optimal levels,

k Total number of the machining parameters.

Means of S/N rations of grey relation grades for AA6061

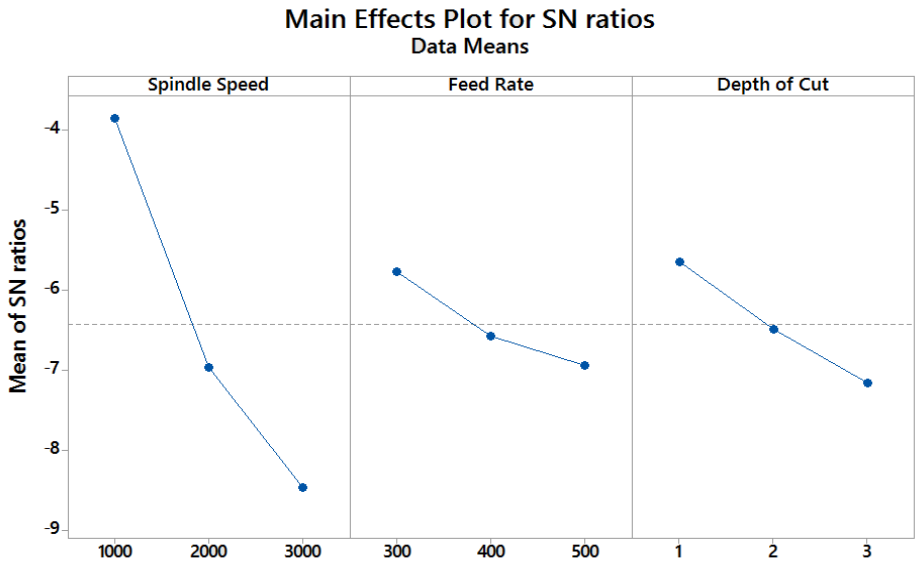

Figure 7.1: Means of S/N rations of grey relation grades for AA6061

Table 7.4 Results of cutting performance at conformation test for AA6061

	Orthogonal array No.1 process parameters	**Optimal process parameters using Taguchi-based grey relational analysis**
		Prediction
Level	$A_1B_1C_1$	$A_1B_1C_1$
Cutting Force	45.50	
Surface Roughness	0.70	
Power Consumption	0.04	
Grey Relation Grade	0.841	0.978
The improvement in GRG	0.137	
The % improvement in GRG	16.2%	

Table 7.5 ANOVA of grey relational grade for AA6061

Source	DF	Seq SS	Adj MS	F	P	% Contribution
Spindle Speed	2	100.31	50.155	1883.91	0	80.936
Feed Rate	2	6.443	3.222	121.01	0	5.199
DOC	2	10.386	5.193	195.07	0	8.38
Spindle Speed*Feed Rate	4	2.775	0.694	26.06	0	2.239
Spindle Speed*DOC	4	2.125	0.531	19.96	0	1.715
Feed Rate* DOC	4	1.686	0.421	15.83	0.001	1.36
Residual Error	8	0.213	0.027			
Total	26	123.938				

R-Sq = 99.8% R-Sq(adj) = 99.3%

Table 7.6: Grey Relation Analysis for AA6061-4.5%Cu-5%SiCp

	Responses						Data Preprocessing			Deviation Sequence			Grey Relational Co-efficient			Grey Relational
Expt .No	FX	SNRA	Ra	SNRA	Power	SNRA	FX	Ra	Power	Delta-FX	Delta-Ra	Delta-Power	FX	Ra	Power	Grade
1	71.28	37.06	3.24	-10.21	0.06	-24.50	1.00	-11.21	1.00	0.00	12.21	0.00	1.00	0.04	1.00	0.680
2	78.03	37.85	2.99	-9.51	0.07	-23.17	0.93	-0.26	0.92	0.07	1.26	0.08	0.88	0.28	0.87	0.677
3	87.64	38.85	2.35	-7.42	0.08	-22.06	0.84	-0.42	0.86	0.16	1.42	0.14	0.76	0.26	0.78	0.600
4	90.37	39.12	3.81	-11.62	0.11	-19.25	0.82	-0.09	0.70	0.18	1.09	0.30	0.73	0.31	0.63	0.557
5	109.45	40.78	3.39	-10.60	0.13	-17.74	0.67	-0.17	0.61	0.33	1.17	0.39	0.60	0.30	0.56	0.488
6	115.33	41.24	2.70	-8.63	0.14	-17.07	0.63	-0.32	0.58	0.37	1.32	0.42	0.57	0.27	0.54	0.463
7	120.39	41.61	4.35	-12.77	0.18	-14.81	0.59	0.00	0.45	0.41	1.00	0.55	0.55	0.33	0.48	0.453
8	134.79	42.59	3.99	-12.02	0.20	-13.84	0.51	-0.06	0.39	0.49	1.06	0.61	0.50	0.32	0.45	0.425
9	139.53	42.89	3.06	-9.71	0.21	-13.45	0.48	-0.24	0.37	0.52	1.24	0.63	0.49	0.29	0.44	0.407
10	144.91	43.22	2.00	-6.02	0.15	-16.67	0.45	-0.53	0.55	0.55	1.53	0.45	0.48	0.25	0.53	0.417
11	155.12	43.81	2.07	-6.32	0.15	-16.20	0.40	-0.51	0.53	0.60	1.51	0.47	0.45	0.25	0.51	0.406
12	176.66	44.94	1.77	-4.96	0.17	-15.37	0.30	-0.61	0.48	0.70	1.61	0.52	0.42	0.24	0.49	0.381
13	179.40	45.08	2.44	-7.75	0.23	-12.73	0.28	-0.39	0.33	0.72	1.39	0.67	0.41	0.26	0.43	0.368
14	182.50	45.23	2.29	-7.20	0.24	-12.48	0.27	-0.44	0.32	0.73	1.44	0.68	0.41	0.26	0.42	0.362
15	185.55	45.37	1.74	-4.81	0.24	-12.22	0.26	-0.62	0.30	0.74	1.62	0.70	0.40	0.24	0.42	0.352
16	187.34	45.45	2.82	-9.00	0.31	-10.07	0.25	-0.29	0.18	0.75	1.29	0.82	0.40	0.28	0.38	0.352
17	190.09	45.58	2.58	-8.23	0.32	-9.87	0.24	-0.36	0.17	0.76	1.36	0.83	0.40	0.27	0.37	0.347
18	194.46	45.78	1.94	-5.76	0.33	-9.56	0.22	-0.55	0.15	0.78	1.55	0.85	0.39	0.24	0.37	0.335
19	232.49	47.33	1.20	-1.58	0.24	-12.40	0.08	-0.88	0.31	0.92	1.88	0.69	0.35	0.21	0.42	0.328
20	241.82	47.67	1.40	-2.92	0.25	-12.10	0.05	-0.77	0.29	0.95	1.77	0.71	0.35	0.22	0.41	0.327
21	245.12	47.79	1.30	-2.28	0.25	-11.89	0.04	-0.82	0.28	0.96	1.82	0.72	0.34	0.22	0.41	0.323
22	247.98	47.89	1.21	-1.66	0.33	-9.61	0.03	-0.87	0.15	0.97	1.87	0.85	0.34	0.21	0.37	0.308
23	249.63	47.95	1.34	-2.54	0.34	-9.42	0.03	-0.80	0.14	0.97	1.80	0.86	0.34	0.22	0.37	0.308
24	250.16	47.96	1.14	-1.14	0.35	-9.24	0.03	-0.91	0.13	0.97	1.91	0.87	0.34	0.21	0.37	0.304
25	254.03	48.10	1.45	-3.23	0.44	-7.20	0.02	-0.75	0.01	0.98	1.75	0.99	0.34	0.22	0.34	0.299
26	257.86	48.23	1.35	-2.61	0.44	-7.05	0.00	-0.80	0.01	1.00	1.80	0.99	0.33	0.22	0.33	0.296
27	259.00	48.27	1.00	0.00	0.45	-6.95	0.00	-1.00	0.00	1.00	2.00	1.00	0.33	0.20	0.33	0.289

Table 7.7: Performance characteristics GRG, S/N ratio and its orders for AA6061-4.5%Cu-5%SiCP

Expt. No	Grey Relation Grade	S/N Ratio	Orders
1	0.68	-3.35265	1
2	0.677	-3.39045	2
3	0.6	-4.43434	3
4	0.557	-5.0812	4
5	0.488	-6.22572	5
6	0.463	-6.69278	6
7	0.453	-6.87029	7
8	0.425	-7.43014	8
9	0.407	-7.81433	10
10	0.417	-7.59654	9
11	0.406	-7.83763	11
12	0.381	-8.38707	12
13	0.368	-8.69338	13
14	0.362	-8.81657	14
15	0.352	-9.07689	16
16	0.352	-9.061	15
17	0.347	-9.19196	17
18	0.335	-9.49663	18
19	0.328	-9.68361	19
20	0.327	-9.71703	20
21	0.323	-9.81705	21
22	0.308	-10.2416	23
23	0.308	-10.2195	22
24	0.304	-10.3438	24
25	0.299	-10.4991	25
26	0.296	-10.5886	26
27	0.289	-10.7854	27

Table 7.8: Response table for GRG for AA6061-4.5%Cu-5%SiCp

Level	Spindle Speed (rpm)	Feed Rate (mm/min)	Depth of Cut (mm)
1	-5.699	-7.135	-7.898
2	-8.684	-8.377	-8.158
3	-10.211	-9.082	-8.539
Delta	4.512	1.947	0.641
Rank	1	2	3

Table 7.9: Results of cutting performance at conformation test for AA6061-4.5%Cu-5%SiCp

	Orthogonal array No.1 process parameters	Optimal process parameters using Taguchi-based grey relational analysis
		Prediction
Level	$A_1B_1C_1$	$A_1B_1C_1$
Cutting Force	71.28	
Surface Roughness	3.10	
Power Consumption	0.06	
Grey Relation Grade	0.680	0.824
The improvement in GRG	0.147	
The % improvement in GRG	12.11%	

Means of S/N rations of grey relation grades for AA6061-4.5%Cu-5%SiCp

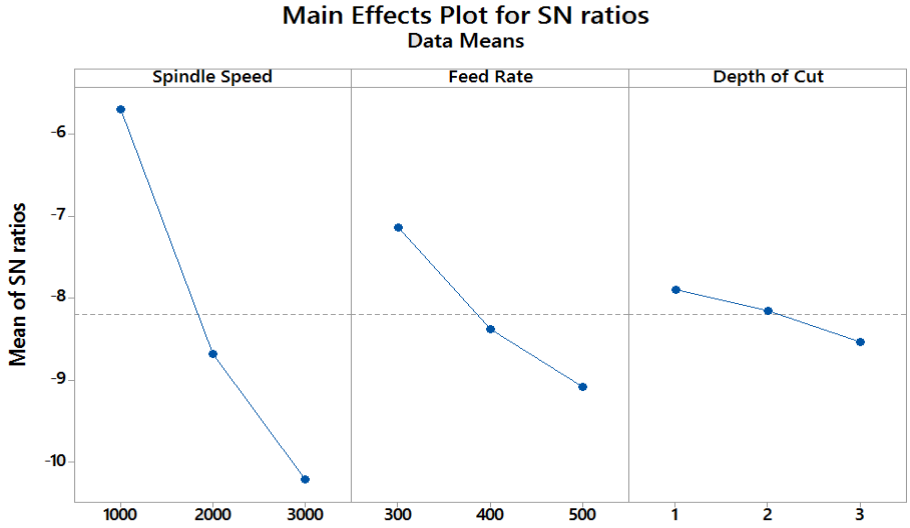

Figure 7.2: Means of S/N rations of grey relation grades AA6061-4.5%Cu-5%SiCp

Table 7.10: ANOVA of grey relational grade for AA6061-4.5%Cu-5%SiCp

Source	DF	Seq SS	Adj MS	F	P	% Contribution
Spindle Speed	2	94.785	47.392	1166.79	0	77.578
Feed Rate	2	17.487	8.743	215.26	0	14.312
DOC	2	1.871	0.936	23.03	0	1.531
Spindle Speed*Feed Rate	4	6.763	1.691	41.62	0	5.535
Spindle Speed* DOC	4	0.84	0.21	5.17	0.024	0.688
Feed Rate* DOC	4	0.11	0.028	0.68	0.626	0.09
Residual Error	8	0.325	0.041			
Total	26	122.18				

R-Sq = 99.7% R-Sq(adj) = 99.1%

7.3 DESIRABILITY APPROACH FOR OPTIMIZATION

The main purpose of optimization is to minimize the surface roughness. In the current study, it is observed that as the feed rate increases the cutting force indirectly increases due to the power consumed by the servo motor increases. Hence the power is considered as the major factor for optimization. The desirability was conducted for 2 materials. AA6061 and AA6061-4.5%Cu-5%SiCp.

In case 1:

The surface roughness value in the range from 0.48 to 0.96 microns with maximum cutting force 45.49 to 164.20 N was selected. The optimized surface roughness value (Ra) of 0.4906 microns is achieved with maximum cutting force (FX) of 165.8610 N and Maximum power consumption of 0.2642 at a spindle speed of 300rpm, feed rate of 500 mm/min and depth of cut of 3mm as depicted in Figure 7.3.

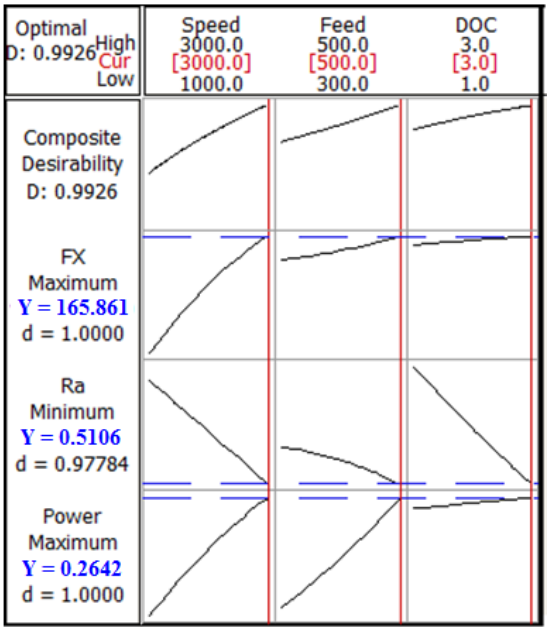

Figure 7.3: Desirability optimization for AA6061

In case 2:

The surface roughness value in the range from 1 to 4.35 microns with maximum cutting force 71.27 to 258.99 N was selected. The optimized surface roughness value (Ra) of 1.0141 microns is achieved with maximum cutting force (FX) of 259.0721 N and Maximum power consumption of 0.4512 at a spindle speed of 300rpm, feed rate of 500 mm/min and depth of cut of 3mm as depicted in Figure 7.4.

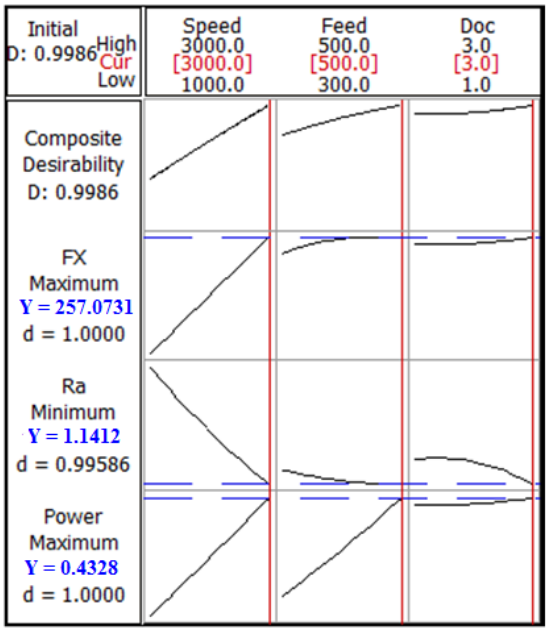

Figure 7.4: Desirability optimization for AA6061-4.5%Cu-5%SiCp

7.4 RESULTS OF PSO

The present study considers simultaneously multi objective optimization of cutting force, surface roughness and power consumption which are conflicting in nature. The mathematical models developed by RSM were used as a fitness function in PSO algorithm. The objective functions used for evaluation of fitness values are given (Garg et al. 2012). The objectives are as follows:

Objective (1) = cutting force (FX)

Objective (2) = Surface roughness (Ra)

Objective (3) = Power consumption

The second order regression models for cutting force, surface roughness and power consumption are obtained by using equations (3.3) and (3.5) (as represented in the earlier RSM Chapter) respectively. These regression models are used for multiobjective optimization using the PSO as fitness functions.

Table 7.11 clearly indicates projected model and signifies the parameters that play

a vital role in obtaining finer convergence characteristics of PSO and indicates the best operating parameters recommended for milling process of AA6061 and AA6061-4.5%Cu-5%SiCp. These parameters play a significant role in obtaining good convergence characteristics of PSO as depicted in Figure 7.5 and 7.6 for AA6061 and AA6061-4.5%Cu-5%SiCp respectively. If the number of parameters increases, the learning rate increases. In turn, the number of iterations increases in the search space. The outcome leads to a probability of getting a global optimum solution and leading the convergence to be accomplished in a smaller number of iterations. The PSO algorithm was implemented using software tool (MATLAB), and the maximum and minimum range of process parameters, which were employed as constraints inorder to evaluate the objective functions for AA6061 and AA6061-4.5%Cu-5%SiCp are as follows : Spindle speed (Min) = 1000rpm, Max = 3000 rpm, feed rate Min = 300mm/min, Max=500mm/min, depth of cut Min = 1mm, Max=3mm.

Table 7.11: Numerical elucidation of PSO

Number of parameters	3
Number of particles	100
Number of iterations	100
Learning rate	
C1 max = C2 max	1.4
C1 min = C2 min	1.8
C1=C2=Cmin+R*(Cmax-Cmin)	Where R = total iterations
$\mathbf{X_{ulim}}$	[1000, 300, 1]
$\mathbf{X_{llim}}$	[3000, 500, 3]

Related Airtcle: **Rashmi L Malghan, Karthik Rao, Arun Shettigar, Shrikantha S Rao and Mervin A Herbert (2018). "Machining** Parameters Optimization of AA6061 using Response Surface Methodology and Particle Swarm Optimization." *International Journal of precision Engineering and Manufacturing*, Springer

7.4.1 PSO Optimization for AA6061

Table 7.12: PSO Optimization for AA6061

SL. NO	Spindle Speed (rpm)	Feed Rate (mm/min)	Depth of Cut (mm)	FX (N)	Ra (µ)	Power Consumption (kW)
1	2.6294	0.3324	0.0023	185.767	0.4283	0.2596
2	1.6563	0.3359	0.0018	172.087	0.5221	0.2364
3	1.7763	0.4153	0.0017	174.956	0.5111	0.2462
4	2.9653	0.3082	0.002	187.411	0.3965	0.2616
5	2.7755	0.3604	0.0024	186.774	0.4138	0.2691
6	1.9713	0.3725	0.0025	198.148	0.4918	0.2487
7	1.7455	0.4473	0.003	174.57	0.5143	0.2477
8	1.6353	0.3359	0.0018	172.087	0.5221	0.2364
9	2.8408	0.3114	0.001	186.966	0.4084	0.2608
10	2.2042	0.4891	0.0014	182.105	0.4688	0.2641
11	2.5901	0.3427	0.0029	185.305	0.432	0.2598
12	2.3628	0.3121	0.001	183.225	0.4542	0.2531
13	2.8152	0.3099	0.0019	186.838	0.4109	0.2602
14	2.0347	0.4335	0.0028	149.87	0.4857	0.2552
15	1.6725	0.3313	0.001	172.39	0.5205	0.2366
16	1.8789	0.3873	0.0025	176.665	0.5008	0.2472
17	2.7923	0.3121	0.0021	186.729	0.413	0.2601
18	2.4352	0.3624	0.0027	184.192	0.4967	0.2584
19	1.1804	0.3118	0.0025	160.448	0.5674	0.2172
20	1.8408	0.3277	0.0029	175.644	0.5042	0.2415
21	2.7145	0.4294	0.0014	186.627	0.4186	0.2692
22	2.643	0.3246	0.0025	180.813	0.4731	0.2498
23	2.793	0.3752	0.0027	186.901	0.4118	0.2656
24	2.4899	0.4437	0.003	185.013	0.4406	0.2666
25	2.8674	0.3725	0.0026	187.23	0.4046	0.2663

Related Article: **Rashmi Malghan, Karthik Rao, Arun Shettigar, Shrikantha Rao and D'Souza** (2016). " Application Of Particle Swarm Optimization And Response Surface Methodology For Machining Parameters Optimization Of Aluminium Matrix Composites In Milling Operation." *Journal of the Brazilian Society of Mechanical Sciences and Engineering*, Springer, 39(9), 3541–3553.

7.4.2 PSO Optimization for AA6061-4.5%Cu-5%SiCp

Table 7.13: PSO Optimization for AA6061-4.5%Cu-5%SiCp

SL. NO	Spindle Speed (rpm)	Feed Rate (mm/min)	Depth of Cut (mm)	FX (N)	Ra (µm)	Power Consumption (kW)
1	2.6294	0.3324	0.0023	215.655	2.71	0.1817
2	1.6563	0.3359	0.0018	180.24	2.09	0.18
3	1.7763	0.4153	0.0017	185.62	2.24	0.2
4	2.9653	0.3082	0.002	258.93	1.45	0.45
5	2.7755	0.3604	0.0024	254.61	1.32	0.36
6	1.9713	0.3725	0.0025	194.06	2.21	0.31
7	1.7455	0.4473	0.003	183.32	2.36	0.29
8	1.6353	0.3359	0.0018	176.14	2.58	0.24
9	2.8408	0.3114	0.001	243.98	1.4	0.42
10	2.2042	0.4891	0.0014	198.06	2.18	0.33
11	2.5901	0.3427	0.0029	214.53	1.42	0.3
12	2.3628	0.3121	0.001	209.28	1.38	0.37
13	2.8152	0.3099	0.0019	257.3	1.42	0.41
14	2.0347	0.4335	0.0028	187.11	2.28	0.21
15	1.6725	0.3313	0.001	170.84	2.46	0.19
16	1.8789	0.3873	0.0025	173.02	2.15	0.17
17	2.7923	0.3121	0.0021	253.26	1.2	0.43
18	2.4352	0.3624	0.0027	227.31	1.38	0.34
19	1.1804	0.3118	0.0025	74.06	3.12	0.08
20	1.8408	0.3277	0.0029	126.23	1.38	0.26
21	2.7145	0.4294	0.0014	252.89	0.94	0.39
22	2.643	0.3246	0.0025	191.73	1.39	0.4
23	2.793	0.3752	0.0027	255.46	0.98	0.42
24	2.4899	0.4437	0.003	246.17	0.91	0.41
25	2.8674	0.3725	0.0026	258.09	1.68	0.44

Twenty Five solutions each for AA6061 and AA6061-4.5%Cu-5%SiCp out of 100 sets of iterations along with the subsequent parameter setting is represented in the Table 7.11 respectively. The optimal points for AA6061 and AA6061-4.5%Cu-5%SiCp are represented in 3D plot as shown in Figure 7.6 and 7.7 respectively. Even the considered twenty Five optimal points for both AA6061 and AA6061-4.5%Cu-5%SiCp have been reported in the Table 7.12 and 7.13 respectively. Based on the surface component requirements, the best solution can be selected. PSO optimal process parameters can be used as handy technology guidelines for optimal machining of AA6061 and AA6061-4.5%Cu-5%SiCp. Fitness evaluation function for AA6061 and AA6061-4.5%Cu-5%SiCp are represented in the Figures 7.5 (a-b).

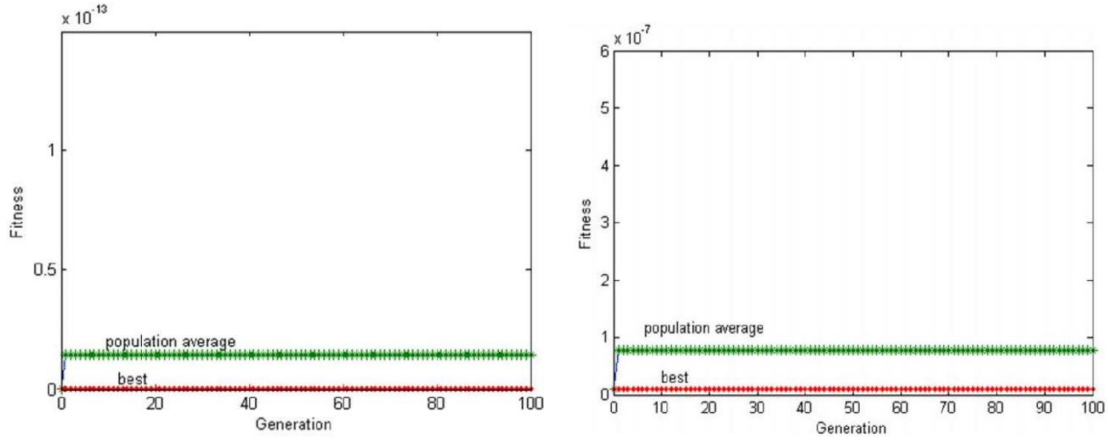

(a) **(b)**

Figure 7.5: Convergence characteristics of PSO for (a) AA6061 (b) AA6061-4.5%Cu-5%SiCp

7.4.3 Graphical Display of optimal points for AA6061 and AA6061-4.5%Cu-5%SiCp

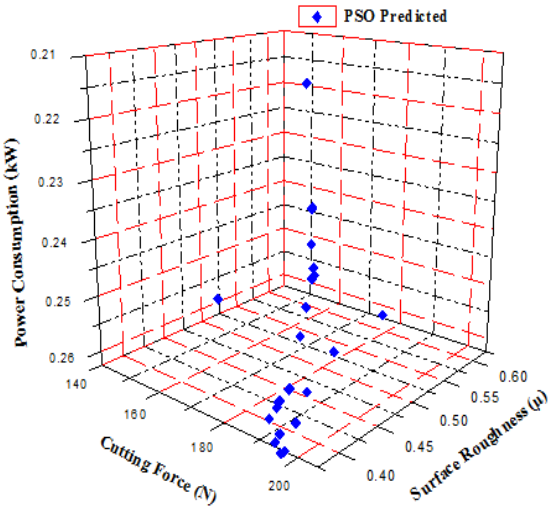

(a)

Figure 7.6: Optimal points for AA6061

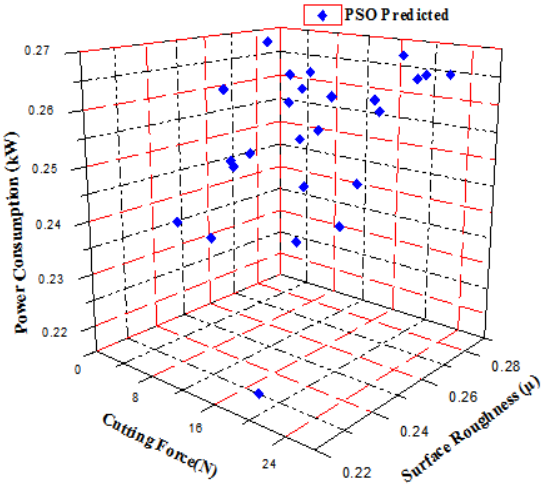

(b)

Figure 7.7: Optimal points for A6061-4.5%Cu-5%SiCp

7.4.4 Validation Of PSO Results

The PSO optimized values were experimentally evaluated for process parameter combination as confirmation experimentation. The responses precisely FX, Ra and Power consumption comparison of experimental and predicted values of AA6061 and AA6061-4.5%Cu-5%SiCp are depicted in Figure 7.8 (a-c)and

Figure 7.9 (a-c). From the Figures 7.8 (a-c) , 7.9 (a-c) it can be observed that, the predicted values are closely following the experimental values. The % of error attained is calculated based on the equation (7.10):

$$\% \text{ Error} = [\frac{E_{i,expt} - E_{i,pred}}{E_{i,expt}}] * 100 \qquad (7.10)$$

Where, E_i, expt is the experimental value for i^{th} trial and $Y_{i,}$ pred is the predicted by PSO for i^{th} trial. The error was calculated between the experimental and predicted value which is < 3% for FX, <2.8% for Ra and < 2.6% for power concumption for machining of AA6061. The error for FX is <2.5%, for Ra is <2.1% and for power consumption is <1.8% for machining of AA6061-4.5%Cu-5%SiCp. The Figures 7.8 (a-c) and 7.9 (a-c) clearly indicate that the PSO predicted values are having good agreement with the experimental values. Hence PSO can be applied as a tool to predict the machining parameters for AA6061-4.5%Cu-5%SiCp in milling effectively.

The RSM technique inorder to predict individual response it needs individual equation, thus at a single go only one response from its respective equation can be predicted. So, the multi objective optimization technique is suitable if more than one response is opted. Table 7.14 and 7.15 summarizes the optimal parameters attained through adopting different techniques for AA6061 and AA6061-4.5%Cu-5%SiCp respectively. Table 7.14 and 7.15 indicates the achieved optimized process parameters to attain the desired values of the respective responses and gives an indication that PSO technique gives accurate values as compared to that of the desirability approach and thus PSO has a better computational efficiency. PSO optimal process parameters can be used as handy technology guidelines for optimal machining of AA6061 and AA6061-4.5%Cu-5%SiCp material.

7.4.5 AA6061- Experimental V/S PSO Predicted

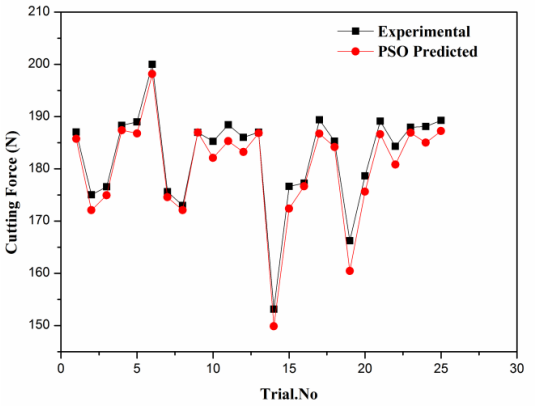

(a)

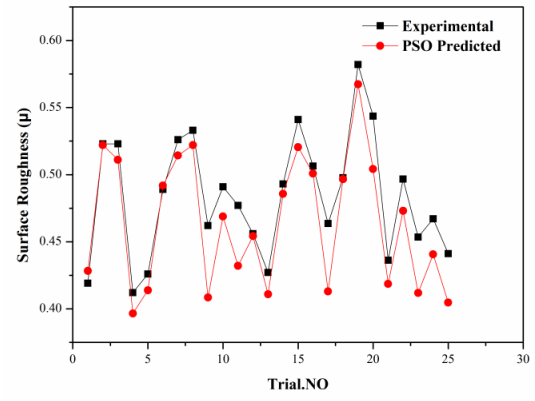

(b)

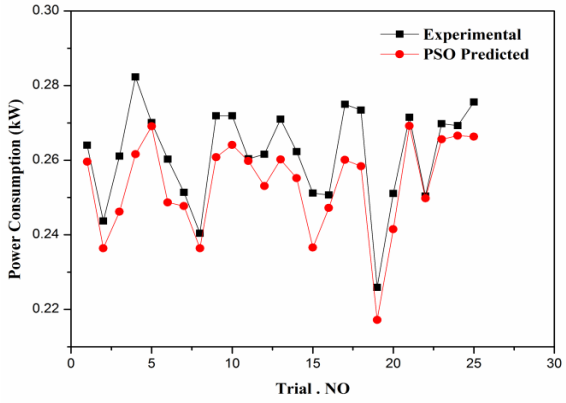

(c)

Figure 7.8 (a-c): Shows AA6061- Experimental V/S PSO Predicted (a) Cutting Force (b) Surface Roughness and (c) Power Consumption

7.4.6 AA6061-4.5%Cu-5%SiCp - Experimental V/S PSO Predicted

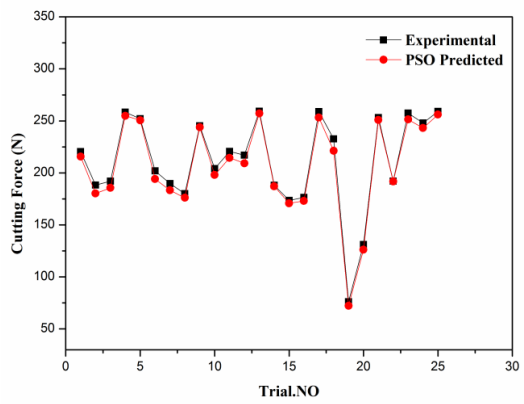

(a)

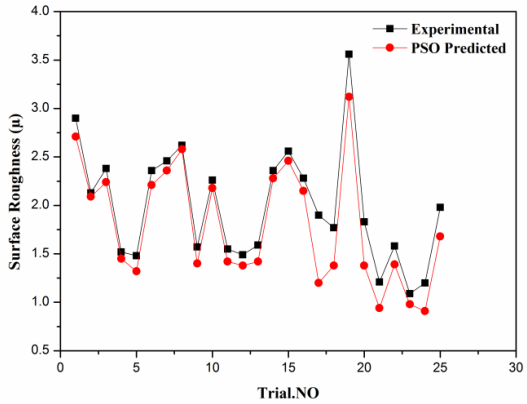

(b)

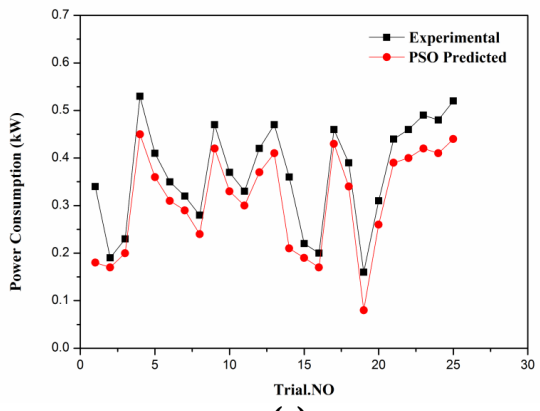

(c)

Figures 7.9 (a-c): Shows AA6061-4.5%Cu-5%SiCp- Experimental V/S PSO Predicted (a) Cutting Force (b) Surface Roughness and (c) Power Consumption

Table 7.14: Optimal process parameters for AA6061

Parameters	Spindle speed (rpm)	Feed rate (mm/min)	Depth of cut (mm)	Ra (µm)	FX (N)	Power Consumption (kW)
Desirability	3000	500	3	0.51	165.	0.264
PSO	3000	500	3	0.489	166.	0.263
Experiment	3000	500	3	0.48	164.	0.262

Table 7.15: Optimal process parameters for AA6061-4.5%Cu-5%SiCp

Parameters	Spindle speed (rpm)	Feed rate (mm/min)	Depth of cut (mm)	Ra (µm)	FX (N)	Power Consumption (kW)
Desirability	3000	500	3	1.14	257.	0.43
PSO	3000	500	3	1.03	259.	0.45
Experiment	3000	500	3	1.0	259.	0.45

7.5 SUMMARY

This section dealt with both traditional and non-traditional optimization algorithm, namely grey relational analysis, desirability approach and PSO technique. The working principle of grey relation and PSO technique were narrated. The mathematical models developed by RSM technique were utilized as a fitness function in PSO algorithm. In this chapter, cutting force (FX), surface roughness (Ra) and power consumption for AA6061 and AA6061-4.5%Cu-5%SiCp were analyzed through experiments. The quadratic regression model has been developed inorder to correlate the relation between input and the output machining parameters. The

developed models are utilized in PSO objective functions inorder to optimize the machining parameters. Based on the experimental analysis, the following conclusions are drawn:

- Optimized process parameters were developed based on the Desirability, GRA and PSO optimization technique.
- From the statistical (Desirability and GRA) and evolutionary (PSO) optimization techniques, it can be derived that PSO yields better results. PSO technique gives accurate values as compared to that of the desirability approach and thus PSO has a better computational efficiency.
- The computational results reveal that the PSO algorithm is competitive with or superior to the other optimization algorithms for the considered problem.
- The outcomes acquired through PSO are likewise compared with the customary desirability approach and it was found that PSO gives closer values compared to the results obtained with the desirability approach.
- The error was calculated between the experimental and predicted value which is < 3% for FX, <2.8% for Ra and < 2.6% for power consumption for machining of AA6061.
- The error for FX is <2.5%, for Ra is <2.1% and for power consumption is <1.8% for machining of AA6061-4.5%Cu-5%SiCp. The attained error percentage of predicted and experimental values was minimum for FX, Ra and power consumption. Hence it can be concluded that PSO technique is quite efficient and effective in optimization.
- The result of confirmation experiments shows the effectiveness of PSO in surface roughness, cutting force and power consumption prediction .
- Since PSO could able to obtain a global optimum solution within a reasonable execution time on a personal computer due to its faster convergence characteristic, the algorithms can be used on on-line systems for the selection of optimal cutting parameters.
- The method is completely generalized and problem independent, so that it can be easily modified to other machining operations such as drilling, grinding, non-traditional machining operations, etc.

CHAPTER 8

RESULTS AND DISCUSSION (PART 4)

DEVELOPMENT OF CONTROL STRATEGY

The proposed Adaptive controller is meant to minimize machining time during rough machining of raw material. The section discusses the modeling and simulation of control strategies in process of face milling using Software platform (Labview). The basic control design is based on the principle of 'Adaptive Control', where a process parameter controls one or more of control parameters to achieve desired output/result. Here, the system measures the cutting force by measuring spindle power during machining and controls the feed rate as (Control parameter). By this technique the power utilization of the spindle power is improved and machining time reduced thus increasing production. The proposed concept is used for on-line determination of optimal cutting conditions in face milling operation, but it is obvious that the system can be extended to other machines to improve cutting efficiency.

8.1 FLOW OF WORK

The planning of strategy (both online and offline) for milling is implemented using Proportional, Integral and Derivative logic (PID). PID is a control loop feedback mechanism. The flow of strategy is explained through flow chart as shown in Figure 8.1. Initially the input parameters are assigned in frame 1. In frame 2, based on input parameters the specific cutting force is calculated (i.e. by online or offline method). If it is offline than we need to provide manually the attained cutting force (X-axis, Y-xis, Z-axis) in order to calculate the specific cutting force. If it is online then suitable data acquisition component need to added so that it fetches the current signal and through these current signals the cutting force need to be calculated (as discussed in chapter 4). Now, the torque calculation needs to be done. In frame 3, based on the torque and specific cutting force the power utilization is calculated and compared with the rated machine capacity. So inorder to compensate the parameters (Speed and feed) based on the power utilization a PID logic is incorporated. Based on the PID logic the compensation of the parameters is set inorder to get the desired responses. Further on,

the same logic can be implemented using reverse mapping approach. Where the attained values from frame 3 can be fetched in excel sheet using C++ program. These fetched values can be further given for training. As the reverse mapping acts as advisory approach, the experimentation work can be reduced.

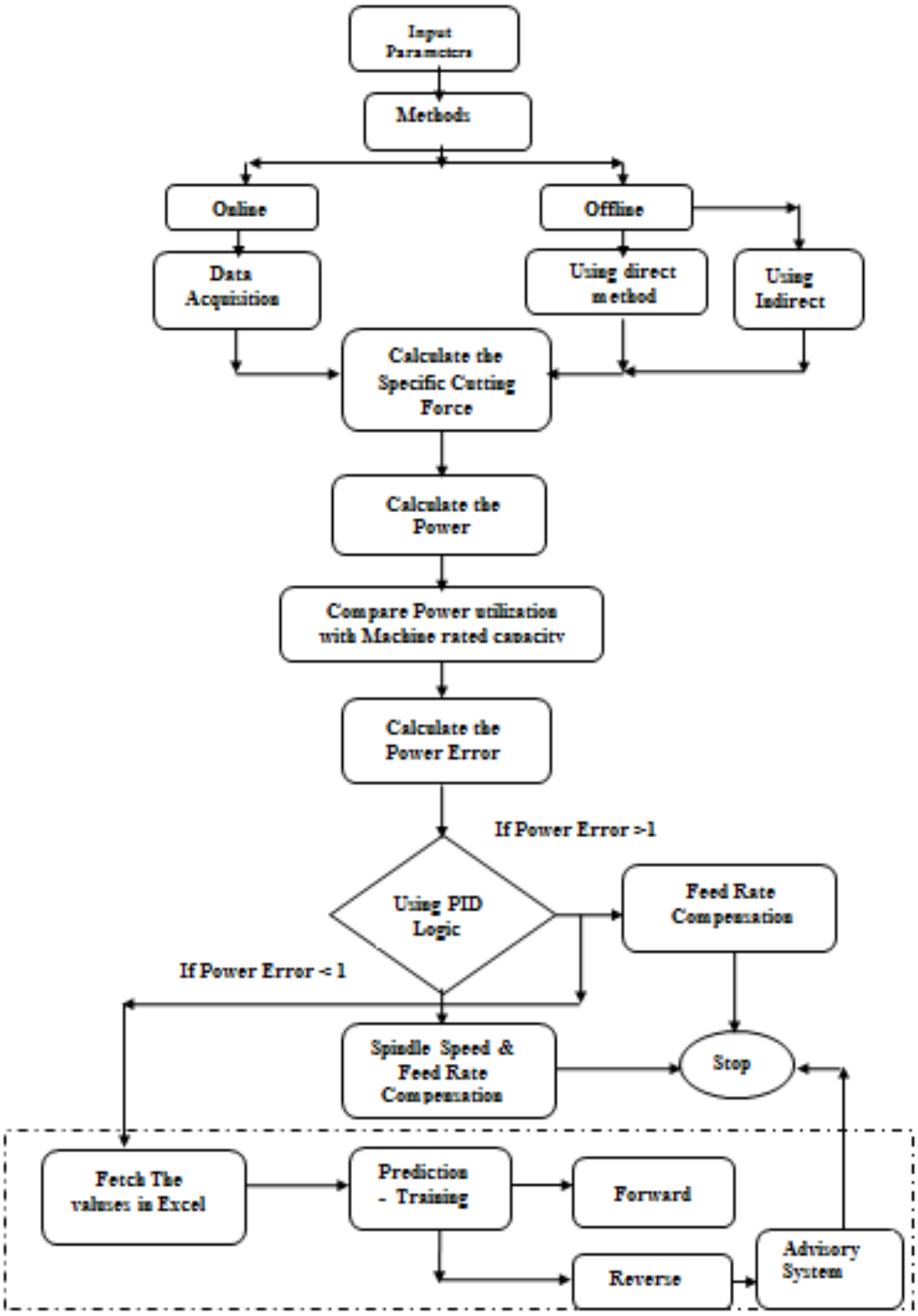

Figure 8.1 : Planning of Control Strategy

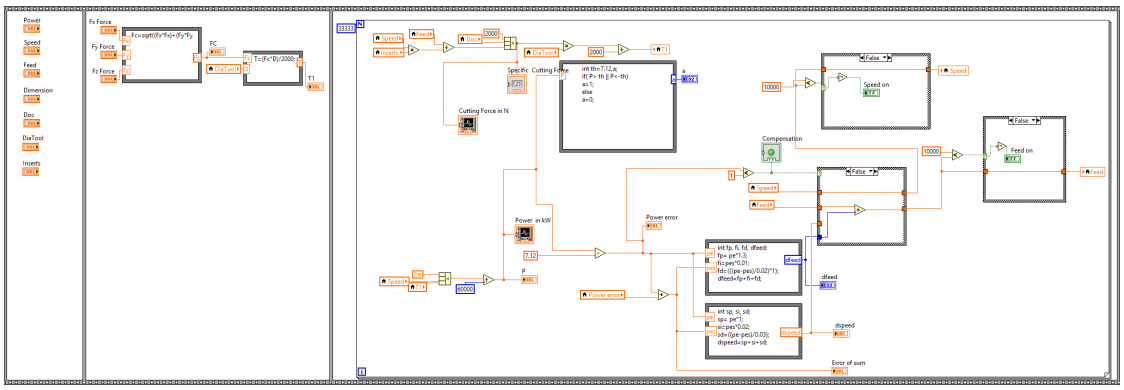

Figure 8.2 : Control Strategy Code

Figure 8.2 represents the control strategy code (LABVIEW code). Figure 8.3(a-b) shows the simulation diagram for maximization of power capacity of CNC milling machine by considering the input parameters. The working and controlling logics have been discussed below;

A. Frame 1:

In the frame 1 the user provides the input parameters, at initial stage the user has to provide the total power capacity of the machine (7.5Kw, Spark DTC 250) .The user can vary this in such a way that he can apply the same concept for other machines.

The Rotational Speed of Spindle: It is selected based on the characteristics of the spindle capacity similarly Feedrate also selected.

Dimension: In this part the user has to provide the Length, Width and Total Depth of Cut.

Depth of Cut: where the user has to provide the DOC for each pass.

Diameter of the Tool: Diameter of the tool has to be specified (Considered for 50mm).

Inserts: The number of Inserts has to be mentioned (5)

B. Frame2:

In this section each cutting force obtained from X, Y and Z axis are fed in to the frame 2, in order to calculate the specific cutting force. This specific cutting force further calculates the Torque of the spindle. In case of automatic control system

the data's (FX, FY and FZ) are directly fetched from the CNC system by using data acquisition system.

C. Frame 3:

In order to calculate the power the control logic has to be in run mode in order to achieve the desired value. The data's from the frame 1 and 2 are fed to the control system to calculate the power consumption of CNC machine during machining operation. The current power consumption during operation is compared with power capacity of CNC machine. In order to make use of the rated power utilization the following control logic has been adapted.

- **Selection of process parameters for maximization of the power consumption.**

  From the Taguchi analysis technique the most significant factors are DOC, Feed rate, Spindle Speed. Since DOC remains constant during machining operation therefore in the controlling algorithm we considered Feedrate and Spindle speed to achieve the maximum power consumption.

- **The Adaption of selecting the control variables : Based on PID Logic**

  The PID logic has been incorporated for the study to suggest a online and offline (feedback) strategy to compensate the spindle speed and feed rate.

Condition 1:

If error in the power is less than 1, speed and feed has to be compensated. This compensated speed and feed are calculated by PID control logic.

dfeed= fp+fi+fd;

dspeed=sp+si+sd;

Condition 2:

If error in the power is more than 1, only the feed has to be compensated to achieve the maximum power**. dfeed= fp+fi+fd;**

8.2 Simulation Performance using Software Tool

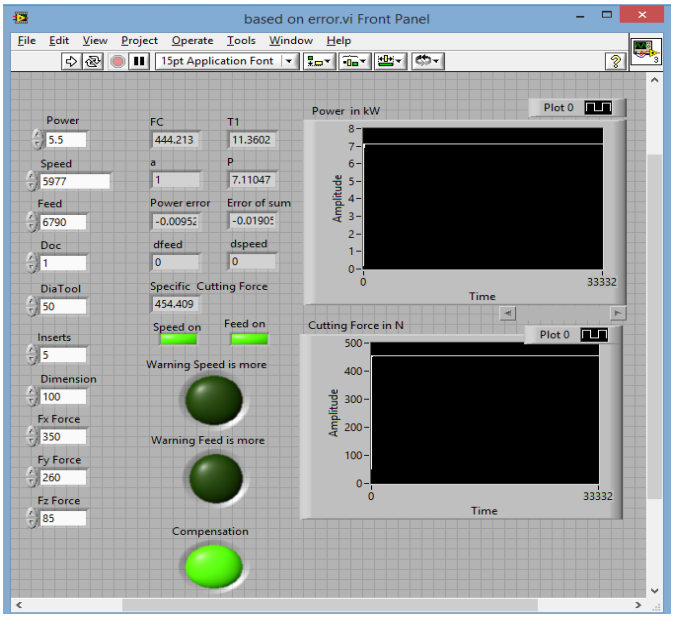

Figure 8.3 (a): Power and cutting force.

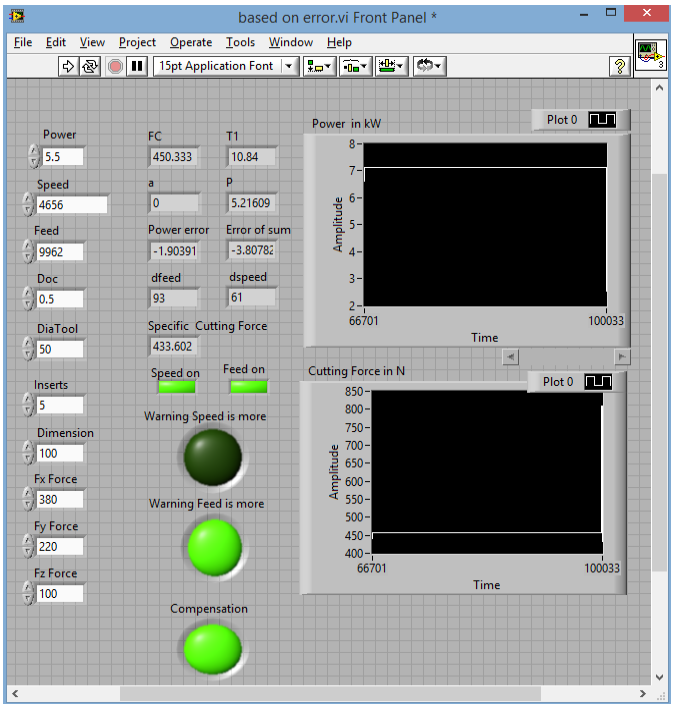

Figure 8.3 (b): Power and cutting force

The accuracy of simulation results clearly indicates the usefulness of the tool in facilitating a decision making system various combination of input parameters and the resulting system response in terms of measurable output can be tried to arrive at suitable recommendations to be adopted for the process. Simulated result for the

speed of 500 rpm, feed of 200 mm/min, depth of cut of 1 mm, cutting force in X direction as 350, Y direction as 260 and z direction as 85 N is shown in Figure 8.3(a). Result obtained from simulator was cutting force as 458 and Power raised to 7.5 indicating for the need of compensation. Similarly the Simulated result for the speed of 2000 rpm, feed of 400 mm/min, depth of cut of 0.5 mm, cutting force in X direction as 380, Y direction as 220 and z direction as 100 N is shown in Figure 8.3 (b). Result obtained from simulator was cutting force as 458 and Power raised to 7.5 indicating Feed rate is more and needs compensation. The built simulation model can be tried for different combinations of Spindle Speed, Feed Rate, and DOC.

8.3 CONCLUSION

The accuracy of simulation results clearly indicate the usefulness of tool in facilitating a decision making system for various combination of input parameters and the resulting system responses in terms of measurable output can be tried to attain a suitable recommendations to be adopted for the process.

- PID logic efficiently facilitates proper compensation of input parameters (speed and feed) based on the power constraint to attain desired response.
- Simulated result for the spindle speed of 500 rpm, feed rate of 200 mm/min, depth of cut of 1 mm, cutting force in X direction as 350N, Y direction as 260N and Z direction as 85 N, is shown in Figure 8.3(a). Attained simulator result for cutting force is 458N, Power raised to 7.5KW. Thus, indicating compensation need.
- Similarly the Simulated result for the speed of 2000 rpm, feed of 400 mm/min, depth of cut of 0.5 mm, cutting force in X direction as 380N, Y direction as 220N and Z direction as 100 N is shown in Figure 8.3(b).

Related Airtcle : **Rashmi L Malghan, Karthik Rao, Arun Shettigar, Shrikantha S Rao and R J D'Souza** (2015). "Adaptive Control System for CNC Machine." *International Engineering Symposium - IES 2015* , Kumamoto University, Japan.

CHAPTER 9

CONCLUSIONS AND SCOPE FOR FUTURE WORK

1. Comparative study of various soft computing techniques namely (RSM, ANN, RNN, Desirability and PSO were successfully formulated for optimized prediction of the responses of AA6061 alloy and AA6061-4.5%Cu-5%SiCp in CNC machining. PSO technique is effective in optimization and yields better results compared to that of Desirability approach.
2. The statistical study of errors indicates that the means of the errors in prediction of both the HRNN and ANN models calculated over target values are comparable and the statistical distribution of the two errors is equivalent. Thus the ANN and HRNN models are equivalent in terms of prediction capability, provided that the HRNN model is constructed from the parent ANN model having similar architecture as that of HRNN. The overall training time for an HRNN constructed by borrowing weights from a partially trained ANN is found to reduce significantly as compared to a fully trained ANN having the same prediction capability. The results attained in case of forward mapping indicate that the neural network based approaches i.e. ANN and RNN (HRNN) attain greater predicting accuracy as compared to RSM statistical model, In case forward mapping, the results attained from ANN and RNN (HRNN) infer that both technique results are comparable and error lies within |5%|.
3. In case of reverse mapping the results attained through ANN and RNN (HRNN) indicate that the RNN (HRNN) is better as compared to that of the ANN because due to the capability of the faster convergence of RNN compared to ANN and the error for ANN and HRNN lies within |10%|.
4. The prediction of the input and output responses using Forward and Reverse Mapping approach have been successfully obtained by incorporating the RSM, ANN and HRNN models with available API libraries as part of the developed Graphical user interface (GUI). The GUI comprises of modules for task management namely, material, method and test option, it also includes sub

components for prediction of cutting force, surface roughness and power consumption. The developed GUI will serve as a generic platform to predict responses based on the parameters specified by the user.

5. A control strategy has been developed by using PID logic with power as the constraint in software tool (Labview) for better machine utilization in milling operation.

The unique feature of the current research is the development of an HRNN model (Case: Forward and Reverse mapping) which performs faster predictions than corresponding FFNNs with same levels of accuracy. This HRNN model has been developed through a novel approach of borrowing weights from a partially trained FFNN model, to be fed into an extended Elman Simple Recurrent Neural Network.

9.1 Results and Purpose Of Incorporating Various Soft Computing Techniques

	TECHNIQUES	PURPOSE	OUTCOME
PREDICTION	RSM	Significance of the machining parameters on responses. Regression Equations = no. Of output parameters. Single objective at a time can be computed. Outside boundary limits cant be achieved.	Equations can be used for predicting the machining parameters. % of error is higher. Adequacy of model was tested using ANOVA.
	ANN Forward Mapping Reverse Mapping	To solve the nonlinear data Both mapping work on same architecture but the calling of data sets need to be altered in the function incorporated in programming **(Language: C++)**	Computational Time, Speed and efficiency. Attained error is < 5%
	HRNN Forward Mapping Reverse Mapping	**Dynamic in nature** **(Language: C++)**	Computational Time, speed and efficiency Attained error is < 5%
OPTIMIZATION	Desirability Approach	Multi response optimization It works within the assigned boundary limits.	Computational time moderate.
	Grey Relation Analysis	In Taguchi one parameter optimization can be achieved to overcome this GRA is implemented Statistical Optimization technique Multi response optimization	Multi response optimization
	PSO	Multi response optimization at a time Population based method	Computational Speed ,Time and Accurate results

9.2 DIRECTIONS FOR FUTURE WORK

The basic purpose of this thesis has been fulfilled by the contributions presented in the preceding chapters of this dissertation. However, there is still scope for further research which facilitates the enhancement of the performance of . Among them few possible future research topics have been outlined as follows:

1. The developed HRNN model can be tired for other materials to study the prediction accuracy in other machining process.
2. Reverse Mapping approach can be further extended to predict the responses and can be utilized as an advisory system in online feedback system.
3. Comparative study of various soft computing techniques can be formulated for optimized prediction of responses for other materials in different machining process.
4. Control strategy can be developed by using PID logic with other software tool for enhancement of productivity other machining process.

REFERENCES

Abellan, J.V., Romero, F., Siller, H.R., Estruch, A. and Vila (2008). "Adaptive Control Optimization of Cutting Parameters for High Quality Machining Operations Based on Neural Networks and Search Algorithms." *Systems Engineering*, 1–20.

Akshay Nigalye. (2013) . "Modelling And Validation Of Behaviour Of Mushy State Rolled Al-4.5cu-5tib2 Composite Using Neural Network Techniques." Department of Mechanical Engineering, NITK-Surathkal.

Al-Aomar, Raid, and Al-Okaily (200). "A GA-Based Parameter Design for Single Machine Turning Process with High-Volume Production." *Computers and Industrial Engineering*, 50 (3), 317–37. doi:10.1016/j.cie.2006.02.003.

Al-kindi Ghassan, and Bijan Shirinzadeh (2007). "An Evaluation of Surface Roughness Parameters Measurement Using Vision-Based Data." *International Journal of Machine Tools and Manufacture*, 47(3-4), 697–708, doi:10.1016/j.ijmachtools.2006.04.013.

Alauddin, Baradie and Hashmi (1995). "Computer-Aided Analysis of a Surface-Roughness Model for End Milling." Journal of Materials Processing Technology, 6 (1), 123-127.

Ashok Kumar, B., and Murugan, N. (2012). " Metallurgical and mechanical characterization of stir cast AA6061-T6–AlNp composite." Materials & Design, 40, 52-58.

Asilturk Ilhan, and Harun Akkus (2011). "Determining the Effect of Cutting Parameters on Surface Roughness in Hard Turning Using the Taguchi Method." *Measurement*, 44 (9), 1697–1704, doi:10.1016/j.measurement.2011.07.003.

Asokan, Baskar, P., Saravanan, and Prabhaharan (2005). "Optimization of Machining

Parameters for Milling Operations Using Non-Conventional Methods." *Int J Adv Manuf Technol*, 25, 1078–88, doi:10.1007/s00170-003-1939-9.

Astakhov Viktor , and Paulo Davim (2009). "Tools (Geometry and Material) and Tool Wear."

Badrinathan, K. S., and Karunamoorthy (2013). "Study of the Effect of Progressive Feed Rateon the Cutting Force in CNC End Milling of AISI 1045 Steel." *International Journal of Engineering and Technology* , 5 (6), 4741–51.

Bagci, Eyup, and Seref Aykut (2006). "A Study of Taguchi Optimization Method for Identifying Optimum Surface Roughness in CNC Face Milling of Cobalt-Based Alloy (Stellite 6)." *International Journal of Advanced Manufacturing Technology* , 29 (9–10), 940–47. doi:10.1007/s00170-005-2616-y.

Baji, Lela and Zivkovic (2008). "Modeling of machined surface roughness and optimization of cutting parameters in face milling." *Metallurgy*, 474, 331–334.

Baji, D., Jozi, S. and Podrug, S. (2010), "Design of experiment's application in the optimization of milling process".*Metalurgija*, 49 (2), 123-126.

Balasubramanian, Ganapathy (2011). "Grey Relational Analysis to determine optimum process parameters for Wire Electro Discharge Machining (WEDM)." *International journal of engineering Science and Technology*,3(1), 95-101.

Bayraktar, E., Masounave, J., Caplain, R., and Bathias, C. (2008). "Manufacturing and damage mechanisms in metal matrix composites." Journal of Achievements in Materials and Manufacturing Engineering, 31(2),294-300.

Benardos, and Vosniakos (2002). "Prediction of Surface Roughness in CNC Face Milling Using Neural Networks and Taguchi's Design of Experiments." *Robotics and Computer-Integrated Manufacturing*, 18 (5-6), 343–54.

Beruvides, Gerardo, Fernando Castano, Ramon Quiza, and Rodolfo Haber (2016). “Surface Roughness Modeling and Optimization of Tungsten-Copper Alloys in Micro-Milling Processes.” *Measurement: Journal of the International Measurement Confederation*, 86, 246–52, doi:10.1016/j.measurement.2016.03.002.

Bod, M. (2001). “A guide to recurrent neural networks and backpropagation.” 2, 1–10.

Bologna, Luca Leonardo, Valentina Pasquale, Matteo Garofalo, Mauro Gandolfo, Pieter Laurens Baljon, Alessandro Maccione, Sergio Martinoia, and Michela Chiappalone (2010). “Investigating Neuronal Activity by SPYCODE Multi-Channel Data Analyzer.” *Neural Networks*, 23 (6), 685–97, doi:10.1016/j.neunet.2010.05.002.

Bedini, Lisini, and Pinolti (1976). "Experiments on adaptive control,of a milling machine." T*rans. ASME Journal of Engineering for Industry*, 239-245.

Briceno, Jorge , Hazim El-Mounayri, and Snehasis Mukhopadhyay (2002). “Selecting an Artificial Neural Network for Efficient Modeling and Accurate Simulation of the Milling Process.” *International Journal of Machine Tools and Manufacture* , 42 (6), 663–74, doi:10.1016/S0890-6955(02)00008-1.

Chandrasekaran, M., Muralidhar, M., Murali Krishna, and Dixit (2010). “Application of Soft Computing Techniques in Machining Performance Prediction and Optimization: A Literature Review.” *International Journal of Advanced Manufacturing Technology*, 46, 445–64, doi:10.1007/s00170-009-2104-x.

Chandrasekaran, M., and Santosh Tamang (2014). “Desirability Analysis and Genetic Algorithm Approaches to Optimize Single and Multi Response Characteristics in Machining Al-SiCp MMC.” 1–6.

Chang, Hun-keun, Jin-hyun Kim, Il Hae, Dong Young, and Dong Chul (2007). "In-Process Surface Roughness Prediction Using Displacement Signals from Spindle Motion." *nternational Journal of Machine Tools and Manufacture*, 47(6), 1021–26, doi:10.1016/j.ijmachtools.2006.07.004.

Chawla, K. (2012). "Metal matrix Composites." Composite Materials, Springer, 197-248.

Chen, Lin, Chang and Ho (2000). "Grey relation for solving multi quality characteristics problems of Taguchi method."*Journal of Technology,* 15, 25-33.

Cheng, M. N., Cheung, Lee, To, and Kong (2008). "Theoretical and Experimental Analysis of Nano-Surface Generation in Ultra-Precision Raster Milling." *International Journal of Machine Tools and Manufacture*, 48(10), 1090–1102, doi:10.1016/j.ijmachtools.2008.02.006.

Chiou Richard, Michael Mauk, Yueh-ting Yang, Robin and Yongjin Kwon (2010). "On-Line Surface Roughness Measurement Using Labview And Vision Method For E-Quality Control." A*merican Society for Engineering Education*, 936 .

Ciurana, J., Arias, and Ozel (2009). "Neural Network Modeling and Particle Swarm Optimization (PSO) of Process Parameters in Pulsed Laser Micromachining of Hardened AISI H13 Steel." *Materials and Manufacturing Processes,* 24 (3), 358–68. doi:10.1080/10426910802679568.

Clerc, Maurice. "A Method to Improve Standard PSO." Technical report, 1–18.

Correa, M., Bielza, and Pamies-Teixeira (2009). "Comparison of Bayesian Networks and Artificial Neural Networks for Quality Detection in a Machining Process." *Expert Systems with Applications* 36, 7270–79. doi:10.1016/j.eswa.2008.09.024.

Cus Franci, and Joze Balic (2003). “Optimization of Cutting Process by GA Approach.” *Robotics and Computer IntegratedManufacturing*, 19, 113–21.

Das, S.,and Das, K. (2007). “Abrasive wear of zircon sand and alumina reinforced Al-4.5 wt% Cu alloy matrix composites - a comparative study.” Composite Science and Technology, 67, 746-751.

Datta, Saurav, Goutam Nandi, and Asish Bandyopadhyay (2009). “Application of Entropy Measurement Technique in Grey Based Taguchi Method for Solution of Correlated Multiple Response Optimization Problems: A Case Study in Welding.” *Journal of Manufacturing Systems*, 28 (2–3), 55–63. doi:10.1016/j.jmsy.2009.08.001.

Davim Paulo, Pedro Reis, and Conceicao (2004). “A Study on Milling of Glass Fiber Reinforced Plastics Manufactured by Hand-Lay up Using Statistical Analysis (ANOVA).”*Composite Structures*, 64, 493–500. doi:10.1016/j.compstruct.2003.09.054.

Demir Halil, and Suleyman Gunduz (2009). “ The Effects of Aging on Machinability of 6061 Aluminium Alloy.” *Materials and Design*, 30(5), 1480–83, doi:10.1016/j.matdes.2008.08.07.

Deng (1989) “Introduction to Grey System Theory.” Journal of Grey System, Vol. 1(2), 103-117.

Derringer, Suich (1980). " Simultaneous optimization of several response variables." *J Qual Technol*, 12(4),214–219.

Dhokia, Vimal, G., Sanjeev Kumar, Parag Vichare, and Stephen Newman (2008). “An Intelligent Approach for the Prediction of Surface Roughness in Ball-End Machining of Polypropylene.” *Robotics and Computer-Integrated Manufacturing*, 24 (6), 835–42, doi:10.1016/j.rcim.2008.03.019.

Ding, Tongchao, Song Zhang, Yuanwei Wang, and Xiaoli Zhu. 2010. “Empirical Models and Optimal Cutting Parameters for Cutting Forces and Surface Roughness in Hard Milling of AISI H13 Steel.” *International Journal of Advanced Manufacturing Technology* ,51 (1–4), 45–55, doi:10.1007/s00170-010-2598-2.

Eberhart, R., Kennedy, J. (1995). "Particle swarm optimization". *In Proceedings of IEEE international conference on neural networks piscataway*, NJ, 1942–1948

Elman, J. L. (1990). “Finding structure in time.” Cogn. Sci., 14(2), 179–211, 1990.

El-Sonbaty, Khashaba, Selmy, and Ali (2008). “Prediction of Surface Roughness Profiles for Milled Surfaces Using an Artificial Neural Network and Fractal Geometry Approach.” *Journal of Materials Processing Technology*, 200 (1–3), 271–78, doi:10.1016/j.jmatprotec.2007.09.006.

Erdik, Tarkan, and Zekai (2009). “Prediction of Tool Wear Using Regression and ANN Models in End-Milling Operation a Critical Review.” *International Journal of Advanced Manufacturing Technology* ,43 (7–8), 765–66, doi:10.1007/s00170-008-1758-0.

Erzurumlu, Tuncay, and Hasan Oktem (2007). “Comparison of Response Surface Model with Neural Network in Determining the Surface Quality of Moulded Parts.” *Materials & Design*, 28 (2), 459–65, doi:10.1016/j.matdes.2005.09.004.

Fadhel Ibraheem, Saad, Kareem Shather, and Kasim Khalaf (2008). “Prediction of Cutting Forces by Using Machine Parameters in End Milling Process.” J. *Eng.&Tech*, 26 (11), 1-4.

Farahnakian, Masoud, Mohammad Reza Razfar, Mahdi Moghri, and Mohsen Asadnia (2011). “The Selection of Milling Parameters by the PSO-Based Neural Network Modeling Method.” *International Journal of Advanced Manufacturing Technology*, 57 (1–4), 49–60, doi:10.1007/s00170-011-3262-1.

Felho, Csaba, Bernhard, and Janos Kundrak (2015). “Surface Roughness Modelling in Face Milling.” CIRP 15th Conference on Modelling of Machining Operations, *Procedia CIRP*, 31, 136–41, doi:10.1016/j.procir.2015.03.075.

Ficko, Brezocnik, and Balic (2004). “Designing the Layout of Single- and Multiple-Rows Flexible Manufacturing System by Genetic Algorithms.” *Journal of Materials Processing Technology* ,157–158 (SPEC. ISS.), doi:10.1016/j.jmatprotec.2004.09.012.

Franco, Estrems, and Faura (2008). “A Study of Back Cutting Surface Finish from Tool Errors and Machine Tool Deviations during Face Milling.” *International Journal of Machine Tools and Manufacture*, 48 (1), 112–23, doi:10.1016/j.ijmachtools.2007.07.001.

Ganesh, Muthusamy, Ramanathan, and Velukkudi Senthil Kumar (2017). “An Experimental Investigation and Numerical Simulation in SPF of AA 5083 Alloy Using Programming Logic Control Approach.” J*ournal of Mechanical Engineering*, 63, 255–64, doi:10.5545/sv-jme.2016.3721.

Ghani, Choudhury, and Hassan (2004). “Application of Taguchi Method in the Optimization of End Milling Parameters.” *Journal of Materials Processing Technology* ,145 (1), 84–92, doi:10.1016/S0924-0136(03)00865-3.

Gupta, Munish Kumar, Sood, and Vishal Sharma (2015). “Machining Parameters Optimization of Titanium Alloy Using Response Surface Methodology and Particle Swarm Optimization Under Minimum Quantity Lubrication Environment.” *Materials and Manufacturing Processes* ,doi:10.1080/10426914.2015.1117632.

Haber, Rodolfo, JoseR. Alique, Salvador Ros, and Clodeinir Peres (1996). “Fuzzy Supervisory Control of End Milling Process.” *Information Sciences,* 89 (1–2), 95–106, doi:http://dx.doi.org/10.1016/0020-0255(95)00222-7.

Haber, Rodolfo, Jose Jimenez, Ronei Peres, and Jose Alique (2004). "An Investigation of Tool-Wear Monitoring in a High-Speed Machining Process." *Sensors and Actuators, A: Physical* ,116 (3), 539–45, doi:10.1016/j.sna.2004.05.017.

Haque, Mohammed, and Sudhakar (2002). "ANN Back-Propagation Prediction Model for Fracture Toughness in Microalloy Steel." *International Journal of Fatigue,* 24 (9), 1003–10, doi:10.1016/S0142-1123(01)00207-9.

Ho, Wen-Hsien, Jinn-Tsong Tsai, Bor-Tsuen Lin, and Jyh-Horng Chou (2009). "Adaptive Network-Based Fuzzy Inference System for Prediction of Surface Roughness in End Milling Process Using Hybrid Taguchi-Genetic Learning Algorithm." *Expert Systems with Applications,* 36 (2), 3216–22, doi:10.1016/j.eswa.2008.01.051.

Hornik, Kurt, Maxwell, and Halbert White (1989). "Multilayer Feedforward Networks Are Universal Approximators." *Neural Networks,* 2 (5), 359–66, doi:10.1016/0893-6080(89)90020-8.

Huang, Sunan, Kok Tan, Geok Hong, and Yoke Wong (2007). "Cutting Force Control of Milling Machine." *Mechatronics,* 17 (10), 533–41, doi:10.1016/j.mechatronics.2007.07.005.

Huang Yunlin, and Juntang Yuan (2014). "High Speed Constant Force Milling Based on Fuzzy Controller and BP Neural Network." *International Journal of Control and Automation,* 7 (5), 143–52.

Huber, and Centner (1968). "Test Results with an Adaptively Controlled Milling Machine." *Asme Paper,* MS68-638.

Iqbal , He N, Dar NU, and Li (2007). "Comparison of fuzzy expert system based strategies of offline and online estimation of flank wear in hard milling process." *Exp Syst Appl ,* 33, 61–6.

Jenarthanan, and Jeyapaul (2013). “Optimisation of Machining Parameters on Milling of GFRP Composites by Desirability Function Analysis Using Taguchi Method.” *International Journal of Engineering, Science and Technology* ,5 (4), 23–36.

Jeyakumar, S., Marimuthu, and Ramachandran (2015). “Optimization of Machining Parameters of Al6061 Composite to Minimize the Surface Roughness Modelling Using RSM and ANN.” *Indian Journal of Engineering and Materials Sciences,* 22 (1), 29–37.

Kalla, Devi, Jamal Sheikh-Ahmad, and Janet Twomey (2010). “Prediction of Cutting Forces in Helical End Milling Fiber Reinforced Polymers.” *International Journal of Machine Tools and Manufacture,* 50 (10), 882–91, doi:10.1016/j.ijmachtools.2010.06.005.

Kadirgama, Noor, Zuki Rahman, Rejab, Daud, and Abou-El-Hossein (2008). “Optimization of surface roughness in end milling on mould aluminium alloys (AA6061-T6) using response surface method and radian basis function network.” *Jordan Journal of Mechanical and Industrial Engineering*, 2, 209- 214.

Karagiannis, Stefanos, Panagiotis, Christos Ziogas, and John Kechagias (2014). “Prediction of Surface Roughness Magnitude in Computer Numerical Controlled End Milling Processes Using Neural Networks , by Considering a Set of Influence Parameters : An Aluminium Alloy 5083 Case Study.” *Journal of Engineering Manufacture,* 228(2), 233–44, doi:10.1177/0954405413498582.

Karl Kainer, U. (2006). “Metal Matrix Composites.” Custom-made Materials for Automotive and Aerospace Engineering”, WILEY-VCH Verlag GmbH & Co. KGaA, Weinheim, ISBN: 3-527-31360-5.

Kaya, Bulent, Cuneyt Oysu, and Huseyin Ertunc (2011). "Force-Torque Based on-Line Tool Wear Estimation System for CNC Milling of Inconel 718 Using Neural Networks." *Advances in Engineering Software,* 42 (3),76–84, doi:10.1016/j.advengsoft.2010.12.002.

Kayacan Cengiz, Oguz Colak, and Cahit Kurbanog (2007). "Materials & Design Milling Surface Roughness Prediction Using Evolutionary Programming Methods." *Materials and Design,* 28, 657–666, doi:10.1016/j.matdes.2005.07.004.

Kennedy, James, and Russell Eberhart (1995). "Particle Swarm Optimization." 1942–48.

Kim, Kwon, and Chu (1999). "Indirect Cutting Force Measurement and Cutting Force Regulation Using Spindle Motor Current." *Int J Manufact Sci Technol,* 1, 46–54. http://www.eng.utoledo.edu/pmmc/paper06.htm.

Kim, Tae Yong, and Jongwon Kim (1996). "Adaptive Cutting Force Control for a Machining Center by Using Indirect Cutting Force Measurements." *International Journal of Machine Tools and Manufacture,* 36 (8), 925–37, doi:10.1016/0890-6955(96)00097-1.

Kim, Tae Yong, Joongwon Woo, Dongwon Shin, and Jongwon Kim (1999). "Indirect Cutting Force Measurement in Multi-Axis Simultaneous NC Milling Processes." *International Journal of Machine Tools and Manufacture,* 39 (11), 1717–31, doi:10.1016/S0890-6955(99)00027-9.

Korkut, Ihsan, Mustafa Kasap, Ibrahim and Ulvi Seker (2004). "Determination of Optimum Cutting Parameters during Machining of AISI 304 Austenitic Stainless Steel." *Materials and Design,* 25 (4), 303–5, doi:10.1016/j.matdes.2003.10.011.

Korosec, Balic, and Kopac (2005). “Neural Network Based Manufacturability Evaluation of Free Form Machining.” *International Journal of Machine Tools and Manufacture,* 45 (1),13–20. doi:10.1016/j.ijmachtools.2004.06.022.

Kalmanje Kumar, and JamesNeidhoefer (1997). “Immunised Neurocontrol.” *Expert Systems with Applications,*13 (3), 201–14.

Kumar Suresh, and Venkateswara (2005). “Selection of Optimum Tool Geometry and Cutting Conditions Using a Surface Roughness Prediction Model for End Milling.” I*nt J Adv Maanuf Technol,* 26, 1202–10, doi:10.1007/s00170-004-2110-y.

Lai Wen-Hsiang (2000). “Modeling of Cutting Forces in End Milling Operations.” *Tamkang Journl of Science and Engineering,* 3 (1),15–22.

Lajis, Mustafizzul, Nurul Amin, Hafiz, Turnad, (2008). “Prediction of tool life in end milling of hardened steel AISI D2.” *Eur. J. Sci. Res*, 21(4), 592–602.

Lamikiz, López De Lacalle, Sanchez, and Salgado (2004). “Cutting Force Estimation in Sculptured Surface Milling.” *International Journal of Machine Tools and Manufacture* , 44 (14), 1511–26, doi:10.1016/j.ijmachtools.2004.05.004.

Lee, and Chen (2003). “On-Line Surface Roughness Recognition System Using Artificial Neural Networks System in Turning Operations.” *International Journal of Advanced Manufacturing Technology,* 22 (7–8), 498–509, doi:10.1007/s00170-002-1511-z.

Lee, Zheng, and Ponnambalam (2012). “Optimisation of Multipass Turning Operations Using PSO and GA-AIS Algorithms.” *International Journal of Production Research,* 50 (22), 6499–6518.

Li (2001). “Real-Time Prediction of Workpiece Errors for a CNC Turning Centre, Part 3. Cutting Force Estimation Using Current Sensors.” *The International Journal of Advanced Manufacturing*, 17 (9), 659–64.

Li, Venuvinod, and Chen (2000). “Feed Cutting Force Estimation from the Current Measurement with Hybrid Learning.” *International Journal of Advanced Manufacturing Technology* ,16 (12), 859–62, doi:10.1007/s001700070002.

Li, Yawei, and Steven Liang (1999). “Cutting Force Analysis in Transient State Milling Processes.” *International Journal of Advanced Manufacturing Technology*, 15 (11), 785–90, doi:10.1007/s001700050132.

Li, Zhang, and Zheng (2004). “Feedrate Optimization for Variant Milling Process Based on Cutting Force Prediction.” *International Journal of Advanced Manufacturing Technology*, 24 (7–8), 541–52, doi:10.1007/s00170-003-1700-4.

Lin (2004). “Use of the Taguchi Method and Grey Relational Analysis to Optimize Turning Operations with Multiple Performance Characteristics.” *Materials and Manufacturing Processes*, 19(2),209 – 220.

Liu, N., Wang, Zhang, and Lu (2016). “A Novel Approach to Predicting Surface Roughness Based on Specific Cutting Energy Consumption When Slot Milling Al-7075.” *International Journal of Mechanical Sciences*, 118, 13–20. doi:10.1016/j.ijmecsci.2016.09.002.

Lo Ship-Peng (2003). “An Adaptive-Network Based Fuzzy Inference System for Prediction of Workpiece Surface Roughness in End Milling.” *Journal of Materials Processing Technology*, 142, 665–75, doi:10.1016/S0924-0136(03)00687-3.

Valluru Rao (1995), C++ Neural Networks and Fuzzy Logic:Preface.

Lou, Mike, Joseph Chen, and Caleb (1999). "Surface Roughness Prediction Technique For CNC End-Milling Surface Roughness Prediction Technique For CNC End-Milling." *Journal of Industrial Technology*, 15 (1), 1–6.

Lu, and Tsai (2007). "Generalized Predictive Control Using Recurrent Fuzzy Neural Networks for Industrial Processes." *Journal of Process Control,* 17 (1), 83–92. doi:10.1016/j.jprocont.2006.08.003.

Lu, Chen, and Chung (2008). "The Optimal Cutting Parameter Design of Rough Cutting Process in Side Milling." *Journal of Achievements in Materials and Manufacturing Engineering*, 29 (2), 183–86.

Luo, Tao, Wen Lu, Krishnamurthy, and Bruce McMillin (1998). "A Neural Network Approach for Force and Contour Error Control in Multi-Dimensional End Milling Operations." *International Journal of Machine Tools and Manufacture,* 38 (10–11), 1343–59, doi:10.1016/S0890-6955(97)00061-8.

Ma, Yuan, Pingfa Feng, Jianfu Zhang, Zhijun Wu, and Dingwen (2016). "Prediction of Surface Residual Stress after End Milling Based on Cutting Force and Temperature." *Journal of Materials Processing Technology,* 235, 41–48, doi:10.1016/j.jmatprotec.2016.04.002.

Malghan, Rashmi Laxmikant, Karthik Rao, Arun Kumar, Shrikantha Rao, and D'Souza (2016). "Application of Particle Swarm Optimization and Response Surface Methodology for Machining Parameters Optimization of Aluminium Matrix Composites in Milling Operation." *Journal of the Brazilian Society of Mechanical Sciences and Engineering*, 39(9), 3541-3553, doi:10.1007/s40430-016-0675-7.

Manjunath, P., Chandrashekarappa, G., Krishna, P., and Parappagoudar, M. B. (2014). "Forward and Reverse Process Models for the Squeeze Casting Process Using Neural Network Based Approaches." Applied Computational Intelligence and Soft Computing, http://dx.doi.org/10.1155/2014/293976.

Mathias, R., (1968). "An effective system for adaptive control of the milling process." *ASTME*, MS68-202.

Michalik, Peter, Jozef Zajac, Michal Hatala, Dusan Mital, and Veronika Fecova (2014). "Monitoring Surface Roughness of Thin-Walled Components from Steel C45 Machining down and up Milling." *Measurement*, 58, 416–28, doi:10.1016/j.measurement.2014.09.008.

Ming Han, Miao Changyun and Zhu Guangyu (2012). "Design and Application of Multi-Axis Automatic Control System Based on LabVIEW." *Proceedings of 2012 International Conference on Mechanical Engineering and Material Science (MEMS 2012)* ,280–82.

Mohd Adnan, Azlan Mohd Zain, and Habibollah Haron (2011). "Consideration of Fuzzy Components for Prediction of Machining Performance: A Review." *Procedia Engineering*, 24, 754–58, doi:10.1016/j.proeng.2011.11.2731.

Monostori, Viharos, and Markos (2000). "Satisfying Various Requirements in Different Levels and Stages of Machining Using One General ANN-Based Process Model." *Journal of Materials Processing Technology*, 107 (1–3), 228–35, doi:10.1016/S0924-0136(00)00698-1.

Montgomery (2008). "Design and analysis of experiments".Wiley, New York

Mukherjee, Indrajit, and Pradip Kumar (2006). "A Review of Optimization Techniques in Metal Cutting Processes."*Computers & Industrial Engineering*, 50 (1-2), 15–34, doi:10.1016/j.cie.2005.10.001.

Munoz-Escalona, Patricia, and Paul (2010). "Artificial Neural Networks for Surface Roughness Prediction When Face Milling Al 7075-T7351." *Journal of Materials Engineering and Performance*, 19 (2), 185–93. doi:10.1007/s11665-009-9452-4.

Muthukrishnan, and Davim (2009). “Optimization of machining parameters of Al/SiC–MMC with ANOVA and ANN analysis.” *J. Mater. Process. Technol*, 209, 225–232.

Nee, Ong, Chryssolouris, and Mourtzis (2012). “Augmented Reality Applications in Design and Manufacturing.” *CIRP Annals - Manufacturing Technology* , 61 (2), 657–79, doi:10.1016/j.cirp.2012.05.010.

Nimase, and Khodke (2015). “Effect of Machining Parameters on Surface Roughness of Al-7075 Alloy in End Milling.” *International Research Journal of Engineering and Technology*, 2 (3),1505–8, doi:10.1177/0954405413506417.

Tunde Ogedengbe, Robert and Srichand (2011). “Feasibility of Tool Condition Monitoring on Micro-Milling Using Current Signals.” *University Journal*, 14 (3), 161–72.

Oktem, Erzurumlu, and Kurtaran (2005). “Application of Response Surface Methodology in the Optimization of Cutting Conditions for Surface Roughness.” *Journal of Materials Processing Technology*, 170 (1–2), 11–16, doi:10.1016/j.jmatprotec.2005.04.096.

Omar, El-Wardany and Elbestawi (2007). “An Improved Cutting Force and Surface Topography Prediction Model in End Milling.” *International Journal of Machine Tools and Manufacture*, 47 (7-8), 1263–75, doi:10.1016/j.ijmachtools.2006.08.021.

Ozcelik, Babur, Hasan Oktem, and Hasan Kurtaran (2005). “Optimum Surface Roughness in End Milling Inconel 718 by Coupling Neural Network Model and Genetic Algorithm.” *International Journal of Advanced Manufacturing Technology*, 27 (3–4), 234–41, doi:10.1007/s00170-004-2175-7.

Ozturk, Erdem, and Erhan Budak. “Tool Orientation Effects on the Geometry of 5-Axis Ball-End Milling.” *Proceedings of the 36th International MATADOR Conference*, 243-246

Phadke (1989). "Quality engineering using robust design".Prentice Hall, New Jersey

Palanisamy, Rajendran, and Shanmugasundaram (2007). “Optimization of Machining Parameters Using Genetic Algorithm and Experimental Validation for End-Milling Operations.” *International Journal of Advanced Manufacturing Technology*, 32 (7–8), 644–55, doi:10.1007/s00170-005-0384-3.

Patwari Anayet, Nurul Amin and Arif (2011). “Optimization of Surface Roughness in End Milling of Medium Carbon Steel by Coupled Statistical Approach with Genetic Algorithm.” *International Journal of the Computer, the Internet and Management*,19, 1–5.

Peklenik. J, (1970). " Geometric adaptive control of manufacturing systems." *Annals of the CIRP*, 18. (I), 265-212.

Peng, Tao, and Xun Xu (2017). “An Interoperable Energy Consumption Analysis System for CNC Machining.” *Journal of Cleaner Production*, 140, 1828–41, doi:10.1016/j.jclepro.2016.07.083.

Pervaiz, Rashid, Deiab and Nicolescu (2014). “Influence of tool materials on machinability of titanium and nickel-based alloys: a review.” *Materials and Manufacturing Processes*, 29 (3), 219–252.

Pomares, Jorge, Ivan Perea, Carlos , Gabriel Garcia, and Fernando (2013). “Dynamic Visual Servo Control of a 4-Axis Joint Tool to Track Image Trajectories during Machining Complex Shapes.” *Robotics and Computer-Integrated Manufacturing*, 29, 261–70, doi:10.1016/j.rcim.2013.01.008.

Porter. B. and Summers (1969). "Adaptive machine-tool control--The state of the art", *Machinery.*

Prakasvudhisarn, Chakguy, Siwaporn Kunnapapdeelert, and Pisal Yenradee (2009). "Optimal Cutting Condition Determination for Desired Surface Roughness in End Milling." *International Journal of Advanced Manufacturing Technology,* 41 (5–6), 440–51, doi:10.1007/s00170-008-1491-8.

Radhakrishnan, and Uday Nandan (2005). "Milling Force Prediction Using Regression and Neural Networks." *Journal of Intelligent Manufacturing,* 16 (1), 93–102, doi:10.1007/s10845-005-4826-4.

Ranjit Roy (2001). "Design of Experiments Using The Taguchi Approach: 16 Steps to Product and Process Improvement." Wiley Publications, ISBN: 978-0-471-36101-5

Ramanujam, Lohithaksha Maiyar, Venkatesan, and Mithun Vasan (2014). "Multi-Response Optimization Using Anova and Desirability Function Analysis: A Case Study in End Milling of Inconel Alloy." *ARPN Journal of Engineering and Applied Sciences* , 9 (4), 457–63.

Ramesh, Palanikumar, and Hemachandra Reddy (2013). "Mechanical Property Evaluation of Sisal Jute Glass Fiber Reinforced Polyester Composites." *Composites - Part B,* 48, 1–9, doi:10.1016/j.compositesb.2012.12.004.

Reddy, Prasada Rao, Chakraborty, and Murty (2005). "Prediction of Grain Size of Al–7Si Alloy by Neural Networks." *Materials Science and Engineering A,*391 (1–2), 131–40, doi:10.1016/j.msea.2004.08.042.

Ripley (1996). "Pattern recognition and neural networks. Cambridge." UK: Cambridge University Press. Samson.

Risbood, Dixit, and Sahasrabudhe (2003). “Prediction of Surface Roughness and Dimensional Deviation by Measuring Cutting Forces and Vibrations in Turning Process.” *Journal of Materials Processing Technology*, 132, 203–214.

Ross, P.,J. (1996). "Taguchi techniques for quality engineering." McGraw-Hill, New York

Sahoo, and Pal (2007). “Tribological performance optimization of electroless Ni–P coatings using the Taguchi method and grey relational analysis.” *Triboletters,* 28, 191–201.

Samarasinghe, Sandhya (2007). “Neural Networks for Applied Sciences and Engineering: From Fundamentals to Complex Pattern Recognition.” Auerbach Publications,1-582.

Sarah, Anitha, Jeya Daisy, and Roshini Varghese (2010). “Optimization of Process Parameters Using Genetic Algorithm and PSO.” *International Conference on Communication and Computational Intelligence (INCOCCI).*

Sarikaya, Murat, and Abdulkadir (2014). “Taguchi Design and Response Surface Methodology Based Analysis of Machining Parameters in CNC Turning under MQL.” *Journal of Cleaner Production,* 65, 604–16, doi:10.1016/j.jclepro.2013.08.040.

Savas, Vedat, and Cetin Ozay (2008). “The Optimization of the Surface Roughness in the Process of Tangential Turn-Milling Using Genetic Algorithm.” *International Journal of Advanced Manufacturing Technology*, 37 (3-4),335–40, doi:10.1007/s00170-007-0984-1.

Savas, Vedat, Cetin Ozay, Esme, Yung Kuang , Jie Ren Shie, Cheng Huang, Christ, Bonanno, MAlkinson, Rubin (2010). "Application of Response Surface Methodology in the Optimization of Cutting Conditions for Surface Roughness." *International Journal of Advanced Manufacturing Technology,* 37 (2), 1697–1704, doi:10.1016/j.measurement.2011.07.003.

Seeman, Ganesan, Karthikeyan, and Velayudham (2010). "Study on Tool Wear and Surface Roughness in Machining of Particulate Aluminum Metal Matrix Composite-Response Surface Methodology Approach." *International Journal of Advanced Manufacturing Technology* ,48 (5–8), 613–24, doi:10.1007/s00170-009-2297-z.

Selaimia, Abdel-ali, Mohamed Athmane, Hamza Bensouilah, Ikhlas Meddour, and Riad Khattabi (2017). "Modeling and Optimization in Dry Face Milling of X2CrNi18-9 Austenitic Stainless Steel Using RMS and Desirability Approach." *Measurement* 107, 53–67, doi:10.1016/j.measurement.2017.05.012.

Seyab, and Yi Cao (2008). "Differential Recurrent Neural Network Based Predictive Control." *Computers & Chemical Engineering*, 32(7), 1533–45, doi:10.1016/j.compchemeng.2007.07.007.

Shunmugam (2015). "Machining Challenges: Macro to Micro Cutting." *Journal of The Institution of Engineers (India): Series C*, 2250-0545, doi:10.1007/s40032-015-0182-0.

Soleimanjahi, Nategh, and Falahi (2009). "A Performance Appraisal of Neural Networks Developed for Response Prediction across Heterogeneous Domains." *World Academy of Science, Engineering and Technology*, 52, 263–68.

Sukumar, Venkata Ramaiah, and Nagarjuna (2014). "Optimization and Prediction of Parameters in Face Milling of Al-6061 Using Taguchi and ANN Approach." *Procedia Engineering*, 97,365–71, doi:10.1016/j.proeng.2014.12.260.

Surappa, M. (2003). "Aluminium matrix composites: challenges and opportunities." Sadhana, 28, 319-334.

Suresh, Venkateswara Rao, and Deshmukh (2002). "A Genetic Algorithmic Approach for Optimization of Surface Roughness Prediction Model." *International Journal of Machine Tools & Manufacture,* 42, 675–80, doi:10.1016/S0890-6955(02)00005-6.

T Sadasiva Rao, Rajesh, and Venu Gopal (2012). "Taguchi Based Grey Relational Analysis to Optimize Face Milling Process with Multiple Performance Characteristics." International Conference on Trends in Industrial and Mechanical Engineering (ICTIME'2012) March 24-25, Dubai,166–70.

Tamiloli, Venkatesan, and Vijaya Ramnath (2016). "A Grey-Fuzzy Modeling for Evaluating Surface Roughness and Material Removal Rate of Coated End Milling Insert." *Measurement*, 84, 68–82, doi:10.1016/j.measurement.2016.02.008.

Tandon and El-Mounayri (2001). "A Novel Artificial Neural Networks Force Model for End Milling." *The International Journal of Advanced Manufacturing Technology,18(10),* 693–700.

Tansel, Ozcelik, Bao, Chen, Rincon, Yang, and Yenilmez (2014). "Selection of Optimal Cutting Conditions by Using GONNS." *Journal of the International Measurement Confederation,*48, 306-313, doi:10.1016/j.ijmachtools.2005.04.012.

Tsai, Nan-chyuan, Din-chang Chen, Rong-mao Lee, and Bai-lu Wang (2010). "Milling Chatter Prevention by Adaptive Spindle Speed Tuning." *World Academy of Science, Engineering and Technology*, 4, 597–602.

Tsai Yu-Hsuan, Chen Joseph and Lou Shi-Jer (1999). "An in-process surface recognition system based on neural networks in end milling cutting operations." *Int J MachTools Manuf*, 39, 583–605.

Turnad Ginta, Nurul Amin, Mohd Lajis, Mustafizul Karim, and Mohd Radzi (2009). "Improved Tool Life in End Milling Ti-6Al-4V Through Workpiece Preheating." *European Journal of Scientific Research*, 27 (3),384-391.

Venkata Rao and Pawar (2010). "Parameter Optimization of a Multi-Pass Milling Process Using Non-Traditional Optimization Algorithms." *Applied Soft Computing Journal*, 10 (2), 445–56, doi:10.1016/j.asoc.2009.08.007.

Venkata Rao, and Kalyankar (2011). "Parameter Optimization of Machining Processes Using a New Optimization Algorithm." *Materials and Manufacturing Processes*, 27 (9), 978–85, doi:10.1080/10426914.2011.602792.

Volos, Kyprianidis, Stouboulos, Tlelo-Cuautle, and Vaidyanathan (2015). "Adaptive control of mechatronic machine-tool equipment." *Journal of Engineering Science and Technology Review*, 8 (6),188–92.

Wang, Ming-Yung, and Hung-Yen Chang (2004). "Experimental Study of Surface Roughness in Slot End Milling AL2014-T6." *International Journal of Machine Tools and Manufacture*, 44 (1), 51–57, doi:10.1016/j.ijmachtools.2003.08.011.

Wong, Shaw Voon, Wong, and Hamouda (2003). "Machinability Data Representation with Artificial Neural Network." *Journal of Materials Procesisng Technology*, 138, 538-544, doi:10.1016/S0924-0136(03)00143-2.

Yang Lieh-dai, and Joseph Chen (1999). "An In-Process Surface Roughness Recognition System in End Milling Operations." *Journal of Technology Studies*, 98–103.

Yang, Wen-an, Yu Guo, and Wen-he Liao (2011a). “Optimization of Multi-Pass Face Milling Using a Fuzzy Particle Swarm Optimization Algorithm.” *The International Journal of Advanced Manufacturing Technology*, 54 (1–4), 45–57, doi:10.1007/s00170-010-2927-5.

Yang, Wen-an, Yu Guo, and Wenhe Liao (2011b). “Multi-Objective Optimization of Multi-Pass Face Milling Using Particle Swarm Intelligence.” *The International Journal of Advanced Manufacturing Technology*, 56 (5–8), 429–43, doi:10.1007/s00170-011-3187-8.

Yang, Yung Kuang, Jie Ren Shie, and Cheng Huang (2006). “Optimization of Dry Machining Parameters for High-Purity Graphite in End-Milling Process.” *Materials and Manufacturing Processes*, 21 (8), 832–37, doi:10.1080/03602550600728141.

Yilmaz, O., and Buytoz, S. (2001). “Abrasive Wear of Al2O3-Reinforced Aluminum- Based MMCs.” Composite Science and Technology, 61, 2381–2392.

Yoon, Hae Sung, Jang Lee, Min Soo Kim, and Sung Ahn (2014). “Empirical Power-Consumption Model for Material Removal in Three-Axis Milling.” *Journal of Cleaner Production* 78, 54–62, doi:10.1016/j.jclepro.2014.03.061.

Yoram Koren (1989). " Adaptive Control Systems for Machining." *ASME* ,Manufacturing Review, 2(1),6-15.

Yusup, Norfadzlan, Azlan Mohd Zain, and Siti Zaiton Mohd Hashim (2012a). “Evolutionary Techniques in Optimizing Machining Parameters: Review and Recent Applications (2007-2011).”*Expert Systems with Applications*, 39 (10), 9909–27, doi:10.1016/j.eswa.2012.02.109.

Yusup, Norfadzlan, Zain, Azlan Mohd, Hashim, Siti Zaiton Mohd (2012b). “Overview of PSO for Optimizing Process Parameters of Machining.” *Procedia Engineering*, 29, 914–23, doi:10.1016/j.proeng.2012.01.064.

Zahedi, Fatemeh (1991). “An Introduction to Neural Networks and a Comparison with Artificial Intelligence and Expert System." *Interfaces,* 21(2), 25–38. http://www.jstor.org/stable/25061463%5Cnhttp://about.jstor.org/terms.

Zain, Azlan Mohd, Habibollah Haron, Sultan Qasem, and Safian (2012). “Regression and ANN Models for Estimating Minimum Value of Machining Performance.” *Applied Mathematical Modelling,* 36 (4), 1477–92, doi:10.1016/j.apm.2011.09.035.

Zain, Azlan Mohd, Habibollah Haron, and Safian Sharif (2010a). “Application of GA to Optimize Cutting Conditions for Minimizing Surface Roughness in End Milling Machining Process.”*Expert Systems with Applications,*37(6), 4650–59, doi:10.1016/j.eswa.2009.12.043.

Zain, Azlan Mohd, Haron, Habibollah, Sharif, Safian (2010b). “Prediction of Surface Roughness in the End Milling Machining Using Artificial Neural Network.” *Expert Systems with Applications* 37 (2), 1755–68, doi:10.1016/j.eswa.2009.07.033.

Zarei, Fesanghary, Farshi, Jalili, Saffar, and Razfar (2008). “Optimization of Multi-Pass Face-Milling via Harmony Search Algorithm.” *Journal of Materials Processing Technology*, 209, 2386–2392, doi:10.1016/j.jmatprotec.2008.05.029.

Zhang, Julie Z, Joseph Chen, and Daniel Kirby (2007). “Surface Roughness Optimization in an End-Milling Operation Using the Taguchi Design Method." *Journal of Materials Processing Technology*, 184, 233–39, doi:10.1016/j.jmatprotec.2006.11.029.

Zhang, Lei, and Li Zheng (2005). “Prediction of Cutting Forces in End Milling of Pockets.” *International Journal of Advanced Manufacturing Technology,* 25 (3–4), 281–87, doi:10.1007/s00170-003-1841-5.

Zhao, Mei, Du, Tao, and Jiang (2012). “Online Evaluation Method of Machining Precision Based on Built in Signal Testing Technology.” *Procedia CIRP* 3 (1), 144–48, doi:10.1016/j.procir.2012.07.026.

Zhou, Jinhua, Junxue Ren, and Changfeng Yao (2017). “Multi-Objective Optimization of Multi-Axis Ball-End Milling Inconel 718 via Grey Relational Analysis Coupled with RBF Neural Network and PSO Algorithm.” *Measurement: Journal of the International Measurement Confederation*, 102, 271–85, doi:10.1016/j.measurement.2017.01.057.

Zuperl, Cus, and Gecevska (2007). “Optimization of the Characteristic Parameters in Milling Using the PSO Evolution Technique.” *Strojniski Vestnik-Journal of Mechanical Engineering*, 53 (6), 354–68.

BIO-DATA

1	Name	RASHMI LAXMIKANT MALGHAN
2	Father's Name	Laxmikant S Malaghan
3	Date of Birth	October 16, 1987
4	Nationality	Indian
5	Permanent Address	#206 (2A-2B), Near Laxmi Temple Behind Aishwarya Hotel, Srinagar, Gokak, Dist: Belgaum, 591307, Karnataka, India
6	Mobile Number	+91-9742739015
7	Email Id	rashmi.malghan@gmail.com

8 **Education Qualification:**

Sl. No.	Qualification	University	College	Period	Performance
1	**PhD**	National Institute of Technology Karnataka	National Institute of Technology Karnataka	Dec 2012-Dec 2017	8.95
2	**M.Tech,** Engineering Management	Visvesvariah Technology University	Dayananda Sagar College Of Engg, Bangalore	2009-2011	82.85%
3	**B.E,** Computer Science	Visvesvariah Technology University	B.V.Bhoomraddi Engg College , Hubli	2005-2009	65.68%

9 Work Experience

Name of the Organization	Duration	Position
National Institute Of Technology Karnataka	2011-2012	Assistant Lecturer
Yellamma Dasappa Institute of Technology	2010	Assistant Lecturer

I declare that above information is true and correct to best of my knowledge.

(Rashmi laxmikant Malghan)

APPENDIX I
PREDICTION PROGRAM

```
main()
{

        cout << "      Prediction of responses of Milling of AA6061 andAA6061-
        4.5%Cu-5%SiCp " << endl;

        cout << "      Forward and Reverse Mapping technique through Artificial
Neural
                Network and Recuurent Neural Networks " << endl;

        cout << "                        by" << endl;

        cout << "       Rashmi L Malghan [ME12F07]" << endl;

        cout << "       National Institute of Technology Karnataka, Surathkal"
<<endl;

cout << endl;

        cout << endl << "Enter your Network preference" << endl;

        cout << "1. Feed Forward Neural Network" << endl;

        cout << "2. Recurrent Neural Network" << endl;

        fchoise = getch();

        if (fchoise != '1' && fchoise != '2' ) { return 0; }

        else  for(;;) {

                char choice;

                cout << endl << "Enter the Training or Prediction preference" <<
        endl;

                cout << "1. load data" << endl;

                cout << "2. learn from data" << endl;

                cout << "3. compute output pattern" << endl;

                cout << "4. make new data file" << endl;

                cout << "5. save data" << endl;
```

```
		cout << "6. print data" << endl;

		cout << "7. change learning rate and momentum factor" << endl;

		cout << "8. exit" << endl << endl;

		cout << "Enter your choice (1-8)";
```

// HIDDEN1 -> HIDDEN2

```
for(y=0; y<hidden_array_2_size; y++) {

	for(x=0; x<hidden_array_1_size; x++)

	{

		temp += (hidden1[x] * weight_h_h[x][y]);

	}
	hidden2[y] = (1.0 / (1.0 + exp(-1.0 * (temp + bias[y
+hidden_array_1_size]))));

	temp = 0;
}
```

// HIDDEN2 -> OUTPUT

```
	for(y=0; y<output_array_size; y++) {

		for(x=0; x<hidden_array_2_size; x++)
		 {
			temp += (hidden2[x] * weight_h_o[x][y]);
		}
		output[pattern][y] = (1.0 / (1.0 + exp(-1.0 * (temp + bias[y +
		hidden_array_1_size + hidden_array_2_size]))));

		temp = 0;
	 }

	return;
}

void backward_pass(int pattern)
{
```

```
 register int x, y;

register double dweight_h_o = 0.0 , dweight_h_h = 0.0, dweight_i_h = 0.0,
temp = 0.0;


// COMPUTE ERRORSIGNAL FOR OUTPUT UNITS

for(x=0; x<output_array_size; x++)

{

errorsignal_output[x] = ((target[pattern][x] - output[pattern][x]) *
output[pattern][x] * (1- output[pattern][x])) ; }
```

// ADJUST WEIGHTS OF CONNECTIONS FROM HIDDEN LAYER 2 TO OUTPUT UNITS

```
for(x=0; x<hidden_array_2_size; x++) {

        for(y=0; y<output_array_size; y++) {

                dweight_h_o = weight_h_o[x][y] - oldweight_h_o[x][y];

                weight_h_o[x][y] += ((learning_rate * errorsignal_output[y] *
        hidden2[x]) + (momentum * dweight_h_o));

        }

}

        for(x=0; x<hidden_array_2_size; x++)

                for(y=0; y<output_array_size; y++)

                        oldweight_h_o[x][y] = weight_h_o[x][y];
```

// ADJUST BIASES FOR OUTPUT UNITS

```
        for(x=(hidden_array_1_size+hidden_array_2_size); x<bias_array_size;
x++) {

        bias[x] += (learning_rate * errorsignal_output[x]);
         }
```

```
// COMPUTE ERRORSIGNAL FOR HIDDEN LAYER 2 UNITS

for(x=0; x<hidden_array_2_size; x++) {

        for(y=0; y<output_array_size; y++) {

                temp += (errorsignal_output[y] * weight_h_o[x][y]);
}

errorsignal_hidden2[x] = hidden2[x] * (1-hidden2[x]) * temp;


temp = 0.0;

}

// ADJUST WEIGHTS OF CONNECTIONS FROM HIDDEN LAYER 2 TO
HIDDEN LAYER 1

        for(x=0; x<hidden_array_1_size; x++) {

                for(y=0; y<hidden_array_2_size; y++) {

                        dweight_h_h = weight_h_h[x][y] - oldweight_h_h[x][y];

                        weight_h_h[x][y] += ((learning_rate *
                        errorsignal_hidden2[y] * hidden1[x]) + (momentum *
                        dweight_h_h));
                }

        }

        for(x=0; x<hidden_array_1_size; x++)

                for(y=0; y<hidden_array_2_size; y++)

                        oldweight_h_h[x][y] = weight_h_h[x][y];


// ADJUST BIASES OF HIDDEN LAYER 2 UNITS

        for(x=hidden_array_1_size; x<(bias_array_size-hidden_array_2_size); x++)
{

        bias[x] += (learning_rate * errorsignal_hidden2[x]);

}
```

```
// COMPUTE ERRORSIGNAL FOR HIDDEN LAYER 1 UNITS
        for(x=0; x<hidden_array_1_size; x++) {
                for(y=0; y<hidden_array_2_size; y++) {
                temp += (errorsignal_hidden2[y] * weight_h_h[x][y]);
        }
        errorsignal_hidden1[x] = hidden1[x] * (1-hidden1[x]) * temp;
        temp = 0.0;
}
```

Development of GUI

```
using System;
using System.Collections.Generic;
using System.Linq;
using System.Web;
using System.Web.UI;
using System.Web.UI.WebControls;
using iBL;
using System.Data;
using System.Web.UI.DataVisualization.Charting;

namespace PandO
{
   public partial class HomePage : System.Web.UI.Page
   {
      DataTable dtMethods;
      DataTable dtMaterial;
      DataTable dtTestType;
```

```
    Methods objMethods = new Methods();
    CMaterial objMaterial = new CMaterial();
    CValidationcs objValidate = new CValidationcs();
    protected void Page_Load(object sender, EventArgs e)
    {
        ScriptManager.RegisterStartupScript(this, this.GetType(), "ddlMet",
"$('#ddlMethods').chosen();", true);
        ScriptManager.RegisterStartupScript(this, this.GetType(), "ddlType",
"$('#ddlType').chosen();", true);
        ScriptManager.RegisterStartupScript(this, this.GetType(), "ddlMaterial",
"$('#ddlMaterial').chosen();", true);
        ScriptManager.RegisterStartupScript(this, this.GetType(), "ddlTestType",
"$('#ddlTestType').chosen();", true);
        lblHeader.Text = "Prediction and Optimization";
        if (!IsPostBack)
        {
            fillMethodList();
            fillMaterialList();
            fillTestType();
        }
    }
    public void fillMethodList()
    {
        dtMethods = objMethods.getMethodListforCombo();
        if (dtMethods != null)
        {
            foreach (DataRow _objRow in dtMethods.Rows)
            {
```

```
            ddlMethods.Items.Add(new
ListItem(_objRow.Field<string>("MethodName"),
Convert.ToString(_objRow.Field<Int32>("MethodId"))));
        }
        ddlMethods.Items.Add(new ListItem("--Select Methods--", "0"));
        ddlMethods.SelectedValue = "0";
      }
      else
      {
        ddlMethods.Items.Add(new ListItem("--Select Methods--", "0"));
        ddlMethods.SelectedValue = "0";
      }
       ddlType.Items.Clear();
      ddlType.Items.Add(new ListItem("--Select Type--", "0"));
      ddlType.SelectedValue = "0";
    }
    public void fillTestType()
    {
      dtTestType = objMaterial.getTestTypeListforCombo();
      if (dtTestType != null)
      {
        foreach (DataRow _objRow in dtTestType.Rows)
        {
          ddlTestType.Items.Add(new
ListItem(_objRow.Field<string>("TypeNM"),
Convert.ToString(_objRow.Field<Int32>("TypeId"))));
        }
        ddlTestType.Items.Add(new ListItem("--Select Test Type--", "0"));
        ddlTestType.SelectedValue = "0";
```

```
        }
        else
        {
            ddlTestType.Items.Add(new ListItem("--Select Test Type--", "0"));
            ddlTestType.SelectedValue = "0";
        }
    }
    public void fillMaterialList()
    {

        dtMaterial = objMaterial.getMaterialListforCombo();
        if (dtMaterial != null)
        {
            foreach (DataRow _objRow in dtMaterial.Rows)
            {
                ddlMaterial.Items.Add(new
ListItem(_objRow.Field<string>("MaterialName"),
Convert.ToString(_objRow.Field<Int32>("MaterialId"))));
            }
            ddlMaterial.Items.Add(new ListItem("--Select Material--", "0"));
            ddlMaterial.SelectedValue = "0";
        }
        else
        {
            ddlMaterial.Items.Add(new ListItem("--Select Material--", "0"));
            ddlMaterial.SelectedValue = "0";
        }
        //ddlType.Items.Clear();
```

```
        //ddlType.Items.Add(new ListItem("--Select Type--", "0"));
        //ddlType.SelectedValue = "0";
    }
    protected void ddlMethods_SelectedIndexChanged(object sender, EventArgs
e)
    {
        MethodType objMethodType = new MethodType();
        objMethodType.MethodId = int.Parse(ddlMethods.SelectedValue);
        string ID = Convert.ToString(objMethodType.MethodId);
        DataTable dt = objMethodType.getListofMethodType(ID);
        //if (ddlMethods.SelectedValue != "0")
        //{
```

DEVELOPMENT OF GUI (Home Page): FORWARD & REVERSE

```
using System;
using System.Collections.Generic;
using System.Linq;
using System.Web;
using System.Web.UI;
using System.Web.UI.WebControls;
using iBL;
using System.Data;
using System.Web.UI.DataVisualization.Charting;
namespace PandO
{
  public partial class HomePage : System.Web.UI.Page
  {
```

```
    DataTable dtMethods;
    DataTable dtMaterial;
    DataTable dtTestType;
    Methods objMethods = new Methods();
    CMaterial objMaterial = new CMaterial();
    CValidationcs objValidate = new CValidationcs();
    protected void Page_Load(object sender, EventArgs e)
    {
        ScriptManager.RegisterStartupScript(this, this.GetType(), "ddlMet",
"$('#ddlMethods').chosen();", true);
        ScriptManager.RegisterStartupScript(this, this.GetType(), "ddlType",
"$('#ddlType').chosen();", true);
        ScriptManager.RegisterStartupScript(this, this.GetType(), "ddlMaterial",
"$('#ddlMaterial').chosen();", true);

        ScriptManager.RegisterStartupScript(this, this.GetType(), "ddlTestType",
"$('#ddlTestType').chosen();", true);

        lblHeader.Text = "Prediction and Optimization";
        if (!IsPostBack)
        {
            fillMethodList();
            fillMaterialList();
            fillTestType();
        }
    }

    public void fillMethodList()
    {
```

```
        dtMethods = objMethods.getMethodListforCombo();
        if (dtMethods != null)
        {
           foreach (DataRow _objRow in dtMethods.Rows)
           {
              ddlMethods.Items.Add(new
ListItem(_objRow.Field<string>("MethodName"),
Convert.ToString(_objRow.Field<Int32>("MethodId"))));
           }
           ddlMethods.Items.Add(new ListItem("--Select Methods--", "0"));
           ddlMethods.SelectedValue = "0";
        }
        else
        {
           ddlMethods.Items.Add(new ListItem("--Select Methods--", "0"));
           ddlMethods.SelectedValue = "0";
        }

        ddlType.Items.Clear();
        ddlType.Items.Add(new ListItem("--Select Type--", "0"));
        ddlType.SelectedValue = "0";
     }
    public void fillTestType()
     {
        dtTestType = objMaterial.getTestTypeListforCombo();
        if (dtTestType != null)
        {
           foreach (DataRow _objRow in dtTestType.Rows)
```

```
            {
                ddlTestType.Items.Add(new
ListItem(_objRow.Field<string>("TypeNM"),
Convert.ToString(_objRow.Field<Int32>("TypeId"))));
            }
            ddlTestType.Items.Add(new ListItem("--Select Test Type--", "0"));
            ddlTestType.SelectedValue = "0";
        }
        else
        {
            ddlTestType.Items.Add(new ListItem("--Select Test Type--", "0"));
            ddlTestType.SelectedValue = "0";
        }
    }
    private void SplineChartExample_AISH11()
    {
        this.Chart1.Series.Clear();
        this.Chart1.Titles.Add("Reading");

        Series series = this.Chart1.Series.Add("Reading");
        series.ChartType = SeriesChartType.Column;

        //series.Points.AddY(objMaterial.FX_Cutting_Force);
        //series.Points.AddY(objMaterial.Ra_Surface_Roughness);
        //series.Points.AddY(objMaterial.Power_Consmption);

        series.Points.AddXY("FX", objMaterial.FX_Cutting_Force_AISH11);
        series.Points.AddXY("RA", objMaterial.Ra_Surface_Roughness_AISH11);
```

```
        series.Points.AddXY("PC", objMaterial.Power_Consmption_AISH11);
    }
    protected void RadioForward_SelectedIndexChanged(object sender,
EventArgs e)
    {
        if (RadioForward.SelectedItem.Text == "Forward")
        {
            objMaterial.MaterialId = int.Parse(ddlMaterial.SelectedValue);
            if (objMaterial.GetMaterialDetails())
            {
                lblSpindleSpeed.Text = "Spindle Speed : <B> <font color='blue'> " +
objMaterial.SpindleSpeed_low.ToString() + " - " +
objMaterial.SpindleSpeed_High.ToString() + "</font></B>";
                lblFeedRate.Text = "Feed Rate : <B> <font color='blue'> " +
objMaterial.FeedRate_Low.ToString() + " - " +
objMaterial.FeedRate_High.ToString() + "</font></B>";
                lblDepthOfCut.Text = "Depth of Cut : <B> <font color='blue'> " +
objMaterial.Depth_of_Cut_Low.ToString() + " - " +
objMaterial.Depth_of_Cut_High.ToString() + "</font></B>";

                lblFXR.Text = "FX-Cutting Force";
                lblRAR.Text = "RA-Surface Roughness";
                lblPC.Text = "Power Consumption";
            }
            else
            {
            }
        if (RadioForward.SelectedItem.Text == "Reverse")
        {
            objMaterial.MaterialId = int.Parse(ddlMaterial.SelectedValue);
```

```
        if (objMaterial.GetMaterialDetailsReverse())

        {

            lblSpindleSpeed.Text = "Cutting Force : <B> <font color='blue'> " +
objMaterial.SpindleSpeed_low.ToString() + " - " +
objMaterial.SpindleSpeed_High.ToString() + "</font></B>";

            lblFeedRate.Text = "Surface Roughness : <B> <font color='blue'> " +
objMaterial.FeedRate_Low.ToString() + " - " +
objMaterial.FeedRate_High.ToString() + "</font></B>";

            lblDepthOfCut.Text = "Power Consumption : <B> <font color='blue'> "
+ objMaterial.Depth_of_Cut_Low.ToString() + " - " +
objMaterial.Depth_of_Cut_High.ToString() + "</font></B>";

            lblFXR.Text = "Spindle Speed";

            lblRAR.Text = "Feed Rate";

            lblPC.Text = "Depth of Cut";

        }

        else

        {

}
```

RESPONSE EQUATIONS : (CMaterial)

```
 public DataTable getMaterialListforCombo()
    {
      DataTable dtTeams = null;
      string strSql = string.Format("SELECT MaterialId,MaterialName  FROM
MaterialMaster");
      if (objDB.selQueryDataset(strSql))
      {
        dtTeams = objDB.resultDataset.Tables[0];
      }
      return dtTeams;
    }

    public DataTable getMaterialList(string MeterialId)
    {
      DataTable dtTeams = null;
      string strSql = string.Format("SELECT MaterialId,MaterialName, from
MaterialMaster Where MethodId=" + MeterialId);
      if (objDB.selQueryDataset(strSql))
      {
        dtTeams = objDB.resultDataset.Tables[0];
      }
      return dtTeams;
    }

    public DataTable getTestTypeListforCombo()
    {
      DataTable dtTeams = null;
      string strSql = string.Format("SELECT TYpeId,TypeNM FROM
TypeMaster");
      if (objDB.selQueryDataset(strSql))
      {
        dtTeams = objDB.resultDataset.Tables[0];
      }
      return dtTeams;       }
public bool Get_RSM_FX_Cutting_Force_AA6061_45()
    {
      try  {
        decimal Var1 = Convert.ToDecimal(-215.06991);
        decimal Var2 = Convert.ToDecimal(0.10846);
        decimal Var3 = Convert.ToDecimal(0.83246);
        decimal Var4 = Convert.ToDecimal(10.39903);
        decimal Var5 = Convert.ToDecimal(8.19703E-005);
        decimal Var6 = Convert.ToDecimal(2.23735E-003);
```

```
        decimal Var7 = Convert.ToDecimal(6.21407E-004);
_FX_Cutting_Force_AA6061_45 = Var1 + (Var2 * _SpindleSpeed_Input) + (Var3 *
_FeedRate_Input)
              + (Var4 * _Depth_of_Cut_Input ) - (Var5 * _SpindleSpeed_Input *
_FeedRate_Input)
              - (Var6 * _SpindleSpeed_Input * _Depth_of_Cut_Input) - (Var7 *
_FeedRate_Input * _FeedRate_Input);
           return true;
        }
        catch (Exception e)
        {
           _errorMessage = e.Message;
           return false;
        }
 }

public bool Get_RSM_FX_Cutting_Force_AA6061_45()  {

 try         {

           decimal Var1 = Convert.ToDecimal(-215.06991);

           decimal Var2 = Convert.ToDecimal(0.10846);

           decimal Var3 = Convert.ToDecimal(0.83246);

           decimal Var4 = Convert.ToDecimal(10.39903);

           decimal Var5 = Convert.ToDecimal(8.19703E-005);

           decimal Var6 = Convert.ToDecimal(2.23735E-003);

           decimal Var7 = Convert.ToDecimal(6.21407E-004);

           _FX_Cutting_Force_AA6061_45 = Var1 + (Var2 * _SpindleSpeed_Input) +
(Var3 * _FeedRate_Input)

              + (Var4 * _Depth_of_Cut_Input ) - (Var5 * _SpindleSpeed_Input *
_FeedRate_Input)

              - (Var6 * _SpindleSpeed_Input * _Depth_of_Cut_Input) - (Var7 *
_FeedRate_Input * _FeedRate_Input);

           return true;         }

        catch (Exception e)       {  _errorMessage = e.Message;   return false;       }
}
```

********** **The End** **********

APPENDIX II - Machine Specifications

DTC- 250/Spark [Drill Tap Machining Center, Vertical]

I. Feed Slide - Z Axis (Vertical)

- **a.** Type of Feed : A. C. Servo drive with ball screw and pre-loaded nut.
- **b.** Feed range : 1 mm/min. to 10,000 mm/min.
- **c.** Rapid Traverse :15000 mm/min.
- **d.** Motor torque : 7 Nm.
- **e.** Max working Stroke : 250 mm.
- **f.** Axial Thrust : 350 kg.

II. Feed Slide - X Axis (Horizontal)

- **a.** Type of Feed : A. C. Servo drive with ball screw and pre-loaded nut.
- **b.** Feed range : 1 mm/min. to 10,000 mm/min.
- **c.** Rapid Traverse : 20000 mm/min.
- **d.** Motor torque : 3.5 Nm.
- **e.** Max working Stroke : 300 mm.
- **f.** Axial Thrust : 180 kg.

III. Feed Slide - Y Axis (Horizontal)

- **a.** Type of Feed : A. C. Servo drive with ball screw and pre-loaded nut.
- **b.** Feed range : 1 mm/min. to 10,000 mm/min.
- **c.** Rapid Traverse : 20000 mm/min.
- **d.** Motor torque : 3.5 Nm.
- **e.** Max working Stroke : 250 mm.
- **f.** Axial Thrust : 180 kg.

IV. Spindle Drive

- **a.** No. of Spindles : 1.
- **b.** Speed Range : 60 to 6000rpm as std, 80 to 8000 rpm as optional.
- **c.** Type of Motor : A.C. Motor with Transistor (PWM) Control.

d. Constant Power range : 5.5 kw max at 30 min. of Continuous Running, 3.7 kw

Continuous Running.

e. Tool Holder Taper : BT 30.

V. Electrical Supply Condition

a. Machine : 415V+ 5%, 5o Cycle/Minute, 3Phase, 4 wire.

b. Controls : 24 Volts, DC. Necessary Transformer for Conversion is provided.

c. Tool Connected Load : 15 KVA Std.

VI. Automated Tool Changer

a. Tool Storage Capacity : 6Nos.

b. Max Tool Weight : 2.5 kg.

c. Max Tool Length : 200mm.

d. Max Tool Dia : 80mm.

APPENDIX III

G codes

G00 - Positioning at rapid speed

G01 - Linear interpolation (machining a straight line)

G02 - Circular interpolation clockwise (machining arcs)

G03 - Circular interpolation, counter clockwise

G04 - Dwell

G09 - Exact stop

G10 - Setting offsets in the program

G12 - Circular pocket milling, clockwise

G13 - Circular pocket milling, counter-clockwise

G17 - X-Y plane for arc machining

G18 - Z-X plane for arc machining

G19 - Z-Y plane for arc machining

G20 - Inch units

G21 - Metric units

G27 - Reference return check

G28 - Automatic return through reference point

G29 - Move to location through reference point

G31 - Skip function

G32 - Thread cutting

G33 - Thread cutting

G40 - Cancel diameter offset

G41 - Cutter compensation left

G42 - Cutter compensation right

G43 - Tool length compensation

G44 - Tool length compensation cancel

G50 - Set coordinate system and maximum RPM

G52 - Local coordinate system setting

G53 - Machine coordinate system setting

G54~G59 - Workpiece coordinate system settings

G61 - Exact stop check

G65 - Custom macro call

G70 - Finish cycle

G71 - Rough turning cycle

G72 - Rough facing cycle

G73 - Irregular rough turning cycle

G73 - Chip break drilling cycle

G74 - Left hand tapping

G74 - Face grooving or chip break drilling

G75 - OD groove pecking

G76 - Fine boring cycle

G76 - Threading cycle

G80 - Cancel cycles

G81 - Drill cycle

G82 - Drill cycle with dwell

G83 - Peck drilling cycle

G84 - Tapping cycle

G85 - Bore in, bore out

G86 - Bore in, rapid out

G87 - Back boring cycle

G90 - Absolute programming

G91 - Incremental programming

G92 - Reposition origin point

G92 - Thread cutting cycle

G94 - Per minute feed

G95 - Per revolution feed

G96 - Constant surface speed control

G97 - Constant surface speed cancel

G98 - Per minute feed

G99 - Per revolution feed

M codes

M00 - Program stop

M01 - Optional program stop

M02 - Program end

M03 - Spindle on clockwise

M04 - Spindle on counter-clockwise

M05 - Spindle off

M06 – Tool change

M08 - Coolant on

M09 - Coolant off

M10 - Chuck or rotary table clamp

M11 - Chuck or rotary table clamp off

M19 - Orient spindle

M30 - Program end, return to start

M97 - Local sub-routine call

M98 - Sub-program call

M99 - End of sub program

List of Publications based on PhD Research Work

Sl. No.	Title of the paper	Authors (in the same order as in the paper. Underline the Research Scholar's name)	Name of the Journal/ Conference, Vol., No., Pages	Month, Year of Publication	Category *
1.	Machining Parameters Optimization of AA6061 using Response Surface Methodology and Particle Swarm Optimization	Rashmi L Malghan, Karthik Rao, Arun Shettigar, Shrikantha S Rao and Mervin A Herbert	International Journal of precision Engineering and Manufacturing, Springer	November 2017 (Accepted) [SCI]	1
2.	Implementation of Forward and Reverse Mapping in Milling process using RNN	Rashmi L Malghan, Karthik Rao, Arun Shettigar, Shrikantha S Rao and R J D'Souza	Journal of Mechanical Engineering Strojniski vestnik	Revisions Submitted [SCI]	1
3.	Forward and Reverse Mapping in Milling process using ANN	Rashmi L Malghan, Karthik Rao, Arun Shettigar, Shrikantha S Rao and R J D'Souza	Data in Brief, Elsevier	November 2017 (Published) [SCI]	1
4.	Investigation of Cutting Force via Indirect Approach and Evaluation of machining characteristics of AA6061	Rashmi L Malghan, Karthik Rao, Arun Shettigar, Shrikantha S Rao and R J D'Souza	Materials and Manufacturing Processes Taylor and Francis	October 2017 (Published) [SCI]	1
5.	Application Of Particle Swarm Optimization And Response Surface Methodology For Machining Parameters Optimization Of Aluminium Matrix Composites In Milling Operation	Rashmi L Malghan, Karthik Rao, Arun Shettigar, Shrikantha S Rao and R J D'Souza	Journal of the Brazilian Society of Mechanical Sciences and Engineering, Springer, Volume 39, Issue 9, pp 3541–3553.	November 2016 (Published) [SCI]	1
6.	Development of a Prediction Model for Optimized Surface Roughness in Face Milling Operation Using Recurrent Neural Network Technique	Rashmi L Malghan, Karthik Rao, Arun Shettigar, Shrikantha S Rao and R J D'Souza	International Journal of Applied Engineering Research ISSN 0973-4562 Volume 10, Number 11 (2015)	April 2015 (Published) [Scopus]	1
7.	Multiple Response Optimizations in Milling Using Taguchi and Grey Relational Analysis	Karthik Rao, Rashmi L Malghan, , Arun Shettigar, Shrikantha S Rao and R J D'Souza	International Journal of Applied Engineering Research ISSN 0973-4562 Volume 10, Number 11 (2015)	April 2015 (Published) [Scopus]	1

8	A Review of Developments in Web Based manufacturing	Rashmi L Malghan, Shrikantha S Rao and R J D'Souza	International Journal of Engineering Research and Development Volume 8, Issue 2, PP. 08-18.	August (Published) 2013	1
9.	Adaptive Control System for CNC Machine	Rashmi L Malghan, Karthik Rao, Arun Shettigar, Shrikantha S Rao and R J D'Souza	4th International Engineering Symposium - IES 2015 , Kumamoto University, Japan	May 2015	4
10.	An Artificial Intelligence Approach for Forward and Reverse Mapping of AA6061: Modeling of Milling process	Rashmi L Malghan, Karthik Rao, Arun Shettigar, Shrikantha S Rao and R J D'Souza	Journal of the Brazilian Society of Mechanical Sciences and Engineering, Springer, [Revisions Completed] (Communicated), BMSE-D-17-00916R1	Revisions Submitted [SCI]	1
11.	Evolution of Hybrid Recurrent Neural Networks: Via Partially Trained ANN of AA6061-4.5%Cu-5%SiCp in Milling	Rashmi L Malghan, Karthik Rao, Arun Shettigar, Shrikantha S Rao and Mervin A Herbert	Modelling and Simulation in Materials Science and Engineering	Communicated [SCI]	1
12.	Application of GAMLPNN and PSO in Milling	Rashmi L Malghan, Karthik Rao, Arun Shettigar, Shrikantha S Rao and Mervin A Herbert	Journal of Cleaner Production	Communicated [SCI]	1
13.	Hybrid Recurrent Neural Networks: Via Partially Trained ANN of AA6061 in Milling	Rashmi L Malghan, Karthik Rao, Arun Shettigar, Shrikantha S Rao and Mervin A Herbert	International Journal of Computational Methods	Communicated [SCI]	1
14.	Reverse Mapping as an Advisory System for CNC Milling	Rashmi L Malghan, Karthik Rao, Arun Shettigar, Shrikantha S Rao and R J D'Souza	Soft Computing	Communicated [SCI]	1
15.	Development Of An Integrated Platform for Process Modeling using NN approach	Rashmi L Malghan, Karthik Rao, Arun Shettigar, Shrikantha S Rao and R J D'Souza	Applied Soft Computing	Communicated [SCI]	1

* Category: 1: Journal paper, full paper reviewed 2: Journal paper, Abstract reviews 3: Conference/Symposium paper, full paper reviewed
4: Conference/Symposium paper, abstract reviewed 5: others (including papers in Workshops, NITK Research Bulletins, Short notes etc.)

(Rashmi L Malghan)

Research Scholar
Name & Signature, with Date

(Dr. Shrikantha S Rao)

Research Guide
Name & Signature, with Date

(Dr.R J D'Souza)

Research Guide
Name & Signature, with Date